

CHARACTERIZATION OF D-BOROALA AS A NOVEL BROAD-SPECTRUM
ANTIBACTERIAL AGENT TARGETING D-ALA-D-ALA LIGASE
&
DESIGNER LINKERS: MODEL REACTIONS AND LINEAR FREE ENERGY
RELATIONSHIPS IN THE REACTIVITY AND DESIGN OF SOLID-PHASE
LINKERS

A DISSERTATION IN
Pharmaceutical Sciences
and Pharmacology

Presented to the Faculty of University
of Missouri-Kansas City in partial fulfillment of
the requirements for the degree

DOCTOR OF PHILOSOPHY

by

SANDEEP PUTTY

MS, Western Illinois University, 2005

Kansas City, Missouri

2014

CHARACTERIZATION OF D-BOROALA AS A NOVEL BROAD-SPECTRUM
ANTIBACTERIAL AGENT TARGETING D-ALA-D-ALA LIGASE
&
DESIGNER LINKERS: MODEL REACTIONS AND LINEAR FREE ENERGY
RELATIONSHIPS IN THE REACTIVITY AND DESIGN OF SOLID-PHASE
LINKERS

Sandeep Putty, Candidate for the Doctor of Philosophy Degree
University of Missouri-Kansas City, 2014

ABSTRACT

Bacterial infections were the major cause of death and morbidity prior to the development of modern antibiotics, and the increasing resistance of pathogenic bacteria to commonly used antibacterial agents is a major public health concern. During our efforts to develop transition-state analog inhibitors for bacterial cell wall-synthesizing enzymes, we observed that D-boroAlanine (D-Ala with the -COOH group replaced with a -B(OH)₂ group) had effective antibacterial activity. In the first part of this dissertation, we describe the antibacterial properties of D-boroAla, structure-activity correlation among several D-boroAla homologs, and determination of the biochemical mechanism for D-boroAla's antibacterial activity. This study

demonstrates that D-boroAla has broad-spectrum antibacterial activity and targets D-Ala-D-Ala ligase (DDL) in the alanine branch of bacterial cell wall biosynthesis.

Vancomycin exerts its antibacterial effect by binding to the D-Ala-D-Ala termini of pentapeptide peptidoglycan precursors, thereby interfering with the last steps of bacterial cell wall biosynthesis. In the most clinically common resistance mechanisms in VRE, the terminal D-Ala-D-Ala moiety of peptidoglycan precursors is replaced by D-Ala-D-Lac. The middle section of the dissertation deals with developing an LC-MS/MS assay for detection and quantitation of D-Ala-D-Lac, the key intermediate for most types of vancomycin resistance. This assay was validated and then used to demonstrate the effect of vancomycin induction on alanine branch metabolites – including D-Ala-D-Lac, in VRE.

Considerable research has been done on the synthesis of peptides and peptide mimetics using classical solid-phase peptide synthesis (SPPS) in the classical C-to-N direction. However, this strategy is not generally useful for preparing C-terminally modified peptide derivatives, which are of high interest as bioactive agents and drugs. SPPS in the N-to-C direction inverse SPPS (ISPPS) would provide the synthetically versatile C-terminal carboxyl group for further elaboration. Prior studies in our laboratory established the feasibility of performing ISPPS using readily available amino acid OtBu esters. In the last section of this dissertation, described efforts to develop a backbone amide attachment linkers with the appropriate chemical stability for ISPPS i.e. stable to 25% TFA/DCM treatment and cleavable with 5% HBr/TFA. Candidate linkers were then loaded onto aminomethylated polystyrene resin to demonstrate an effective method for ISPPS

using amino acid t-butyl esters. Chemical sensitivity to different capping groups on sensitivity to cleavage was demonstrated and several tripeptides were synthesized using this approach.

APPROVAL PAGE

The faculty listed below, appointed by the Dean of School of Graduate Studies have examined the dissertation titled “Characterization of D-BoroAla as a novel broad spectrum antibacterial agent targeting D-Ala-D-Ala ligase” & “Designer linkers: Model reactions and linear free energy relationships in the reactivity and design of solid-phase linkers” presented by Sandeep Putty, candidate for the Doctor of Philosophy degree, and certify that in their opinion it is worthy of acceptance.

Supervisory Committee

William G. Gutheil, Ph.D., Committee Chair

Department of Pharmaceutical Sciences

Simon H. Friedman, Ph.D.

Department of Pharmaceutical Sciences

Kun Cheng, Ph.D.

Department of Pharmaceutical Sciences

Santosh Kumar, Ph.D.

Department of Pharmacology and Toxicology

Nathan A. Oyler, Ph.D.

Department of Chemistry

CONTENTS

ABSTRACT	iii
LIST OF ILLUSTRATIONS	x
LIST OF TABLES.....	xix
ACKNOWLEDGEMENTS	xxi
Chapter	
Part I	
1. INTRODUCTION	1
Good bacteria	1
Bad bacteria	2
Bacteria Classification	3
History of antibacterial agents	6
Mechanism of action of antibacterial agents.....	10
Bacteria Resistance mechanisms to antibiotics	12
2. IDENTIFICATION OF D-BOROALA AS A NOVEL ANTIBACTERIAL AGENT	15
3. CHARACTERIZATION OF D-BOROALA AS A NOVEL BROAD-SPECTRUM ANTIBACTERIAL AGENT TARGETING D-ALA-D-ALA LIGASE.....	21
Introduction and Rationale.....	21
Materials and Methods	24
Compound Synthesis	24
Antibacterial Properties Characterization.....	42
Results.....	46
Discussion	53

Conclusions and Future Directions.....	58
4. AN LC-MS/MS ASSAY FOR D-ALA-D-LAC: A KEY INTERMEDIATE FOR VANCOMYCIN RESISTANCE IN VANCOMYCIN-RESISTANT ENTEROCOCCUS	81
Introduction and Rationale.....	81
Materials and Methods	84
Results and Discussion	89
Part II	
5. DESIGNER LINKERS: MODEL REACTIONS AND LINEAR FREE ENERGY RELATIONSHIPS IN THE REACTIVITY AND DESIGN OF SOLID-PHASE LINKERS	103
Introduction.....	103
Overview of Boc and Fmoc approaches.....	104
Resins for Boc SPPS (Figure 46)	105
Resins for Fmoc SPPS (Figure 46)	106
Anchoring.....	108
Side chain protecting groups.....	108
Coupling reactions	109
Cleavage from the resin.....	112
Methods which allow for the synthesis of C-terminally modified peptides	113
Overview of peptide derived agents (PDAs).....	115
Hammett equation and constants.....	119
Overall Rationale.....	121

Experimental.....	123
Solution phase model reactions and kinetics of liners	124
Preparation of solid phase attached linker	129
Loading of linker onto resin and demonstration of ISPPS	130
Results and Discussion	134
6. SUMMARY.....	170
APPENDIX.....	173
REFERENCES	178
VITA.....	205

LIST OF ILLUSTRATIONS

Figure	Page
1. A) Gram Postive bacterial cell wall; B) Gram negative bacterial cell wall. adapted from micro.digitalproteus.com	5
2. Timeline of antibiotic classes inventions. Adapted from M.A. Fischbach and C.T.Walsh 2010.	8
3. Main classes of marketed antibiotics. Adapted from A.R. Coates et. al. 2011.	9
4. Antibiotic targets and mechanisms of resistance. Adapted from G.D. Wright 2010.	11
5. Bacterial cell wall biosynthesis reactions catalyzed by the PBPs in most Gram negative bacteria. Adapted from Bobba et. al. 2011.	15
6. TLC of crude Boc-L-Lys(Cbz)-D-boroAla and the zone of inhibition of the TLC resolved compounds on <i>S. aureus</i>	18
7. Transition state analogues synthesized in our lab. Adapted from Pechenov et., al 2003.....	19
8. Substrate specificity and corresponding transition state analogues for serine proteases and related enzymes. The four transition state analogue classes shown at the bottom can form tetrahedral adducts with the active site serine. Adapted from Pechenov et., al 2003.	20
9. Bacterial cell wall biosynthesis pathway in <i>E.Coli</i> . Adapted from Jamindar et. al. 2009.....	23
10. Synthetic scheme for the synthesis of D-boro amino acid analogs	39
11. Synthetic scheme for L-boroAla-(+)Pd	40

12. Synthetic scheme for D-boroAla (6a).	41
13. Synthetic scheme for boroGly pinacol (9).	41
14. Synthetic scheme for Acetyl-D-boroAla(-)-pinanediol (10).....	41
15. Zone of inhibition of D-boroAla(-)-Pd, L-boroAla(-)-Pd and pure pinanediol.	46
16. Marfey's reagent and reactions to give adducts with L-Ala, D-Ala and D-Ala-D-Ala. Adapted from Jamindar et. al. 2010.....	51
17. Sample MRM chromatogram for an untreated E. coli extract. The top panel represents the LC–MS/MS chromatogram specific for the Marfey's derivatives of β -Ala (peak at 5.6 min), L-Ala (peak at 8.2 min), and D-Ala (peak at 9.6 min). The center panel represents Marfey's derivative of $^{13}\text{C}_3$ -D-Ala used as an internal standard and the bottom panel represents Marfey's derivative of D-Ala-D-Ala (peak at 8.7 min). Adapted from Jamindar et. al. 2010.	52
18. Levels of L-Ala, D-Ala, and D-Ala-D-Ala in E. coli as a function of added agents.	56
19. Levels of L-Ala, D-Ala, and D-Ala-D-Ala in S. aureus as a function of no added D-boroAla(-)-Pd (control) and 4x MIC of added D-boroAla(-)-Pd. This experiment was performed as described for E. coli in the main text, with the exception that since S. aureus is fastidious it was necessary to grow in Mueller Hinton Broth. Because of background levels of amino acids in Mueller Hinton Broth, cells were washed 3x in ice cold minimal media prior to lysis and metabolite analysis.	57
20. NMR spectrum of Diisopropyl-(1-methyl)-1-borate (1a)	60
21. NMR spectrum of Diisopropyl-(1-ethyl)-1-borate (1b)	61
22. NMR spectrum of Diisopropyl-(1-isopropyl)-1-borate (1c)	62

23. NMR spectrum of (-)-Pinanediol-(1-methyl)-1-boronate (2a)	63
24. NMR spectrum of (-)-Pinanediol-(1-ethyl)-1-boronate (2b)	64
25. NMR spectrum of (-)-Pinanediol-(1-isopropyl)-1-boronate (2c).....	65
26. NMR spectrum of (+)-Pinanediol-(1-methyl)-1-boronate (2d)	66
27. NMR spectrum of (-)-Pinanediol (1R)-(1-chloroethyl)-1-boronate (3a).....	67
28. NMR spectrum of (-)-Pinanediol (1R)-(1-chloro-1-propyl)-1-boronate (3b)	68
Figure 29. NMR spectrum of (-)-Pinanediol (1R)-(1-chloro-1-isobutyl)-1-boronate (3c)	69
30. NMR spectrum of (+)-Pinanediol (1S)-(1-chloroethyl)-1-boronate (3d)	70
31. NMR spectrum of (-)-Pinanediol (1S)-(1-hexamethyldisilazaneaminoethyl)-1- boronate (4a)	71
32. NMR spectrum of (-)-Pinanediol (1S)-(1-hexamethyldisilazaneamino-1-propyl)-1- boronate (4b)	72
33. NMR spectrum of (-)-Pinanediol (1S)-(1-hexamethyldisilazaneamino-1-isobutyl)- 1-boronate (4c)	73
34. NMR spectrum of (+)-Pinanediol (1R)-(1-hexamethyldisilazaneamino-1-ethyl)-1- boronate (4d)	74
35. (-)-Pinanediol (1S)-(1-aminoethyl)-1-boronate (D-boroAla-(-)-pinanediol) (5a) ..	75
36. (-)-Pinanediol (1S))-1-amino-1-methylethyl-1-boronate (D-boroVal-(-)-pinanediol) (5b)	76
37. (-)-Pinanediol (1S))-1-amino-1methyisopropyl-1-boronate (5c).....	77
38. NMR spectrum of (+)-Pinanediol (1R)-(1-aminoethyl)-1-boronate (L-boroAla-(+)- pinanediol) (5d).....	78

39. NMR spectrum of (1S)-(1-aminoethyl)-1-boronate (D-boroAla) (6a)	79
40. NMR spectrum of (1R)-(1-aminoethyl)-1-boronate (L-boroAla) (6d)	80
41. Cell wall intermediate biosynthesis pathway in VRE. Cell wall biosynthesis intermediates and enzymes specific to the vancomycin resistance pathway are shown in italicized bold text. NAM=N-acetylmuramic acid.	83
42. Measured levels of γ -aminobutyric acid (GABA) during washing. Error bars represent the standard error (n = 4) for each measurement.	93
43. Representative LC–MS/MS chromatograms of Marfey’s derivatized metabolites extracted from VRE. Peak identities were verified using standards. Top panel: LC–MS/MS chromatogram detected at m/z 342.2/297.2 (Q1/Q3), which is specific for the Marfey’s adduct of L-Ala (12.4 min) and D-Ala (13.8 min). Middle panel: Analogous data for m/z 413.2/368.2, which is specific for the Marfey’s adduct of D-Ala-D-Ala (12.5 min). Bottom panel: Analogous data for m/z 414.2/369.2, which is specific for the Marfey’s adduct of D-Ala-D-Lac (peak at 16.2 min). A peak for the +1 isotopomer of D-Ala-D-Ala is also seen (12.5 min), but this peak is well resolved chromatographically from D-Ala-D-Lac (16.2 min) and does not interfere with quantitation of D-Ala-D-Lac.....	94
44. Standard curves for L-Ala, D-Ala, D-Ala-D-Ala, and D-Ala-D-Lac serially diluted in water (left panel) and VRE extract (right panel), derivatized with Marfey’s reagent, and quantitated using the developed LC–MS/MS method. Because VRE has background levels of these metabolites, blank values were subtracted before plotting the values in the right panel. Each point represents the average of four	

determinations. Diamonds (◆), Mar-D-Ala; squares (■), Mar-L-Ala; triangles (▲), Mar-D-Ala-D-Ala; circles (●), Mar-D-Ala-D-Lac.	95
45. Measured levels of $^{13}\text{C}_3$ -D-Ala (internal standard), L-Ala, D-Ala, D-Ala-D-Ala, and D-Ala-D-Lac from extracts of VRE grown at different levels of vancomycin. Each data point is from the extract of 7.0 μg dry cells.....	96
46. Data for D-Ala, D-Ala-D-Ala, and D-Ala-D-Lac in Figure 44 normalized to corresponding levels of L-Ala in Figure 44	97
47. Standard resins for Boc and Fmoc SPPS.	107
48. Structure of Bacitracin A. Adapted from Toscano et.al 1982.	117
49. Structure of Capreomycin IA and IB. Adapted from DeMong D.E. et. al. 2003.	117
50. Structure of Kahalalide F. Adapted from Hamann M.T et. al. 2001.....	118
51. Structure of Alpha-Amanitin. Adapted from Bushnell D.A. et. al. 2002.	118
52. Ionization of benzoic acids.	119
53. Hydrolysis of t-cumyl chlorides.....	120
54. Scheme for loading acetate and butyrate linker onto benzaldehyde compounds	125
55. Scheme for loading H-Phe-OtBu-HCl and capping with acetic anhydride.	126
56. Vial setup for performing kinetics on model compounds with 5%HBr/TFA.	128
57. Scheme for saponification of ester group on the linker.	129
58. Scheme for loading 2-methyl-4-(5-oxyvaleric acid)benzaldehyde linker onto the amino methyl polystyrene resin.	130
59. Scheme for amino acid t-butyl ester based ISPPS.	131
60. Scheme of solution phase model cleaving reaction	136

61. Plot between observed k value and predicted k value for different linkers, and consensus best line.	140
62. Plot between σ^+ and $\log(k_{obs})$ for calculating Rho value.	141
63. Mass spectrum of N-Acetyl-[4-(5-oxy-methylbutyrate)benzyl]-L-phenylalanine (Cmp. No. 1).	149
64. HPLC chromatogram of N-Acetyl-[4-(5-oxy-methylbutyrate)benzyl]-L- phenylalanine (Cmp. No. 1).	149
65. Mass spectrum of N-Acetyl-[4-(5-oxy-ethylvalerate)benzyl]-L-phenylalanine (Cmp. No. 2).	150
66. HPLC chromatogram of N-Acetyl-[4-(5-oxy-ethylvalerate)benzyl]-L-phenylalanine (Cmp. No. 2).	150
67. Mass spectrum of N-Acetyl-[4-methoxybenzyl]-L-phenylalanine (Cmp. No. 3).	151
68. HPLC chromatogram of N-Acetyl-[4-methoxybenzyl]-L-phenylalanine (Cmp. No. 3).	151
69. Mass spectrum of N-Acetyl-[2-methyl-4-methoxybenzyl]-L-phenylalanine (Cmp. No. 4).	152
70. HPLC chromatogram of N-Acetyl-[2-methyl-4-methoxybenzyl]-L-phenylalanine (Cmp. No. 4).	152
71. Mass spectrum of N-Acetyl-[2-methyl-4-(5-oxy-ethylvalerate)benzyl]-L- phenylalanine (Cmp. No. 5).	153
72. HPLC chromatogram of N-Acetyl-[2-methyl-4-(5-oxy-ethylvalerate)benzyl]-L- phenylalanine (Cmp. No. 5).	153

73. Mass spectrum of N-Acetyl-[2,6-dimethyl-4-(5-oxy-methylbutyrate)benzyl]-L-phenylalanine (Cmp. No. 6).	154
74. HPLC chromatogram of N-Acetyl-[2,6-dimethyl-4-(5-oxy-methylbutyrate)benzyl]-L-phenylalanine (Cmp. No. 6).	154
75. Mass spectrum of N-Acetyl-[2,6-dimethyl-4-(5-oxy-ethylvalerate)benzyl]-L-phenylalanine (Cmp. No. 7).	155
76. HPLC chromatogram of N-Acetyl-[2,6-dimethyl-4-(5-oxy-ethylvalerate)benzyl]-L-phenylalanine (Cmp. No. 7).	155
77. Mass spectrum of N-Acetyl-[2-methoxy-4-(5-oxy-methylbutyrate)benzyl]-L-phenylalanine (Cmp. No. 8).	156
78. HPLC chromatogram of N-Acetyl-[2-methoxy-4-(5-oxy-methylbutyrate)benzyl]-L-phenylalanine (Cmp. No. 8).	156
79. Mass spectrum of N-Acetyl-[2-methoxy-4-(5-oxy-ethylvalerate)benzyl]-L-phenylalanine (Cmp. No. 9).	157
80. HPLC chromatogram of N-Acetyl-[2-methoxy-4-(5-oxy-ethylvalerate)benzyl]-L-phenylalanine (Cmp. No. 9).	157
81. Mass spectrum of N-Acetyl-[2-methoxy-4-methoxylbenzyl]-L-phenylalanine (Cmp. No. 10).	158
82. HPLC chromatogram of N-Acetyl-[2-methoxy-4-methoxylbenzyl]-L-phenylalanine (Cmp. No. 10).	158
83. Mass spectrum of N-Acetyl-[2,6-dimethoxy-4-(5-oxy-methylbutyrate)benzyl]-L-phenylalanine (Cmp. No. 11).	159

84. HPLC chromatogram of N-Acetyl-[2,6-dimethoxy-4-(5-oxy-methylbutyrate)benzyl]-L-phenylalanine (Cmp. No. 11).	159
85. Mass spectrum of N-Acetyl-[2,6-dimethoxy-4-(5-oxy-ethylvalerate)benzyl]-L-phenylalanine (Cmp. No. 12).	160
86. HPLC chromatogram of N-Acetyl-[2,6-dimethoxy-4-(5-oxy-ethylvalerate)benzyl]-L-phenylalanine (Cmp. No. 12).	160
87. Mass spectrum of N-Acetyl-[4-(5-oxy-methylbutyrate)naphthyl]-L-phenylalanine (Cmp. No. 13).	161
88. HPLC chromatogram of N-Acetyl-[4-(5-oxy-methylbutyrate)naphthyl]-L-phenylalanine (Cmp. No. 13).	161
89. Mass spectrum of N-Acetyl-[4-(5-oxy-ethylvalerate)naphthyl]-L-phenylalanine (Cmp. No. 14).	162
90. HPLC chromatogram of N-Acetyl-[4-(5-oxy-ethylvalerate)naphthyl]-L-phenylalanine (Cmp. No. 14).	162
91. Mass spectrum of Ac-Phe-Ala-Gly.	163
92. HPLC chromatogram of Ac-Phe-Ala-Gly.....	163
93. Mass spectrum of Ac-Phe-Leu-Val.	164
94. HPLC chromatogram of Ac-Phe-Leu-Val.	164
95. Mass spectrum of Ac-Phe-Ala-Gly.	165
96. HPLC chromatogram of Ac-Phe-Ala-Gly.....	165
97. Mass spectrum of Benzoyl-Phe.	166
98. HPLC chromatogram of Benzoyl-Phe.	166
99. Mass spectrum of Tolyoyl-Phe.....	167

100. HPLC chromatogram of Tolyoyl-Phe.	167
101. Mass spectrum of Ac-Phe.....	168
102. HPLC chromatogram of Ac-Phe.....	168
103. Mass spectrum of Isovaleryl -Phe.....	169
104. HPLC chromatogram of Isovaleryl -Phe.....	169

LIST OF TABLES

Table	Page
1. Summary of optimized parameters for MS/MS detection of Marfey's adducts	45
2. Structure/activity correlation of different analogues of D-boroAla	47
3. Spectrum of activity: MICs for D-boroAla-(-)-pinanediol, D-boroAla (no pinanediol), and control antibiotics.	49
4. MICs and MBCs for D-boroAla-(-)-pinanediol against several bacterial strains. ..	49
5. Summary of optimized parameters for MS/MS detection of Marfey's adducts	92
6. Analyte sensitivity and linearity characteristics in water and VRE extract (matrix).	98
7. Side chain protected amino acids suitable for Boc or Fmoc chemistry	111
8. Some Hammett σ^+_p and σ_m constants from published standard tables.....	120
9. List of X,Y,Z substituents for the model compounds in Figure 55	126
10. Amino acid t-butyl ester based ISPPS protocol.....	132
11. Molecular weight confirmation and yields of linkers synthesized.	137
12. Half-lives and rate constants of the linkers under 5%HBr/TFA treatment.	138
13. σ^+ values of individual substituents	139
14. σ^+ values for different benzaldehyde linkers synthesized	139
15. N-Acetyl-[2-methyl-4-(5-oxy-ethylvalerate)benzyl]-L-phenylalanine linker's cleavage rate for different acid treatments.....	143
16. Molecular weight confirmation, purities, and yields of the synthesized peptides.	146

17. Molecular weight confirmation of different capping groups and % cleavage during deprotection step.	146
-------------------------------------------------------------------------------------------------------------	-----

ACKNOWLEDGEMENTS

I would like to thank my advisor, Dr. William Gutheil for his guidance, support and constant encouragement throughout my PhD program. He has been very helpful in teaching me all the experimental techniques, experimental designing, troubleshooting the instruments and problem solving. I am very thankful for his support during my visa renewal process. I am thankful to Drs. Simon Friedman, Kun Cheng, Santosh Kumar, and Nathan Oyler for serving on my supervisory committee and for their time and valuable inputs.

I want to thank my current and former lab mates Ramakrishna Sasubelli, Darshan Jamindar, Jian Wang, Sudheer Bobba, and Harika Shetty Vemula for their help and support in my research. I am thankful to my former lab mates Alex Pechanov and Aman Rai for establishing the synthesis of D-boro-Ala-pinacol in our lab. I am thankful to P. Pagano, C.L. Quinn, T. Mima, and H.P. Schweitzer for their help in determining the frequency of resistance and bactericidal/bacteriostatic activity of D-boroAla. I am thankful to Dr. Ekaterina N. Kadnikova for allowing me to use her GC/MS instrument and Dr. Keith R. Buszek for allowing me to use his microwave reactor. I am thankful to Department of Chemistry, UMKC for allowing me to use their NMR facility. I am thankful to Connie Mahone, Joyce Johnson, Sharon Self, and Nancy Hoover for their help with administrative work.

I would like to thank all my teachers who taught me, made me to think and learn new things. I am very much thankful to all my friends who helped me a lot during tough times. I am indebted to their love, support, concern and positive criticism which helped me to evolve and keep moving forward. I would like to

express my sincere thanks to my mother, father and brother for their unconditional love and encouragement.

DEDICATED TO MY LOVING FAMILY

CHAPTER 1

INTRODUCTION

Bacteria are single celled microscopic organisms. They are one of the oldest living organisms on earth and are omnipresent. Bacteria are abundantly present in the air we breathe, the food we eat, the water we drink, the human body, plants, animals, and the surfaces we touch. There is virtually no place on earth without the presence of bacteria.

Most people have the prejudice that bacteria are always harmful, but only 1% are harmful. Early in the 20th century, Elli Metchnikoff, a Russian Nobel laureate, discovered that some bacteria present in our bodies are useful in several internal processes. These bacteria are called 'probiotics'. Examples of good and bad bacteria are given below.

Good bacteria

Lactobacilli species are found in the mouth, intestine and vagina of humans and animals and are also present in milk, dairy products and fermented foods. They convert sugar and lactose into lactic acid. They are used in preparation of fermented foods, and yogurt from milk. They are known to relieve lactose intolerance, gastrointestinal problems, and vaginal yeast infections in mammals. *Bifidobacterium* present in the gastrointestinal tract of humans prevents the growth of pathogenic bacteria in the intestine by altering the pH levels upon production of lactic acid. *Escherichia coli* (*E. coli*) is present in small and large intestines, and helps in digestion by breaking down of monosaccharide sugars. They are also known to produce vitamin K and biotin which are vital nutrients. *Streptomyces*

present in soil, water and decaying matter are useful in decomposing the organic matter present in soil. Several bacterial species like *Rhizobium etli*, *Azorhizobium spp*, *Bradyrhizobium spp*, and many others are useful in fixing nitrogen from the atmosphere and convert it into usable compounds for plants. *Methanotrophs* metabolize the greenhouse gas methane. *Alcanivorax* feeds on petroleum, and is used in cleaning petroleum spills.

Bad bacteria

Enterococci bacteria are often found in human intestines and the female genital tract are naturally resistant to many antibiotics and cause systemic infections. Vancomycin is the drug of choice to treat infections caused by *enterococci*. Vancomycin-resistant *enterococci*, first reported in late 1980s [1], are now widespread and can cause infections to the urinary tract, bloodstream and wounds associated with catheters or surgical procedures [2]. *Staphylococcus aureus*, frequently found in the human respiratory tract and on the skin, can cause skin infections, respiratory disease and food poisoning. Methicillin-resistant *Staphylococcus aureus* (MRSA) is a strain of *S. aureus* that is resistant to many β -lactam antibiotics. In a hospital setting MRSA can cause life threatening bloodstream infections, pneumonia and surgical site infections. Typhoid fever common in the developing countries is caused by bacterium *salmonella Typhi*. Each year around 21.5 million people are affected by typhoid fever. *E. coli* normally live in the human as well as animal intestine and are usually harmless. But certain strains of *E. coli* can cause diarrhea, urinary tract infections, respiratory illness and pneumonia. Shigellosis is an infectious disease caused by a group of bacteria called *shigella*.

People infected with *shigella* develop diarrhea, fever and stomach cramps. *P. aeruginosa* is one of the most common Gram-negative bacteria found in nosocomial infections and can cause infections of the blood, skin, eye, gut, respiratory and genitourinary tract in patients suffering from AIDS, cancer, surgery, cytotoxic drugs or burn wounds [3]. Infections caused by *P. aeruginosa* kill several thousand individuals each year and 10% of all hospital acquired nosocomial infections are accounted to *P. aeruginosa* [4]. Melioidosis, also known as Whitmore's, disease is caused by the bacterium *Burkholderia pseudomallei*. Common symptoms include pain in chest, bones, or joints, cough, skin infections and pneumonia.

Bacteria Classification

Bacteria taxonomy was started by Ferdinand and Cohn in 1872 and classified bacteria as members of plants based upon their morphology [5]. Besides morphology, growth requirements and pathogenic potential became the most important taxonomic markers between 1880 and 1900 [5]. The history of the classification of bacteria changed with the availability of new techniques. Physiological and biochemical data were used, along with morphology for the classification and identification between 1900 and 1960. In the later years chemo taxonomy, numerical taxonomy, DNA-DNA hybridization, genotypic analysis, multilocus sequence analyses, average nucleotide identity, and whole genome analysis were used as markers for the classification of bacteria [6-11].

Of all the classification systems, the Gram stain technique developed by H.C. Gram in 1884 remains an important and useful technique to this day. It classifies a large proportion of bacteria as either Gram positive or negative based on their

differential staining properties. In this technique bacteria are stained with crystal violet and iodine, and then washed and counter-stained with safranin red dye. Gram positive bacteria retain the original crystal violet stain and Gram negative bacteria lose the crystal violet stain during washing step and will retain the counterstain safranin red [12]. Gram positive bacterial cell walls consists of a thick layer of peptidoglycan that holds teichoic and lipoteichoic acids. Gram negative bacterial cell walls consists of a thin layer of peptidoglycan and an outer membrane that comprises lipopolysaccharide, phospholipids and proteins. The periplasmic space between the cytoplasmic and outer membranes holds transport, degradative, and cell wall synthetic proteins. The outer membrane is attached to the peptidoglycan by lipoprotein links and is joined to the cytoplasmic membrane at adhesion points

Figure 1. The difference in retaining stains is mainly due to the difference in the peptidoglycan layer in the cell wall structure of the bacteria.

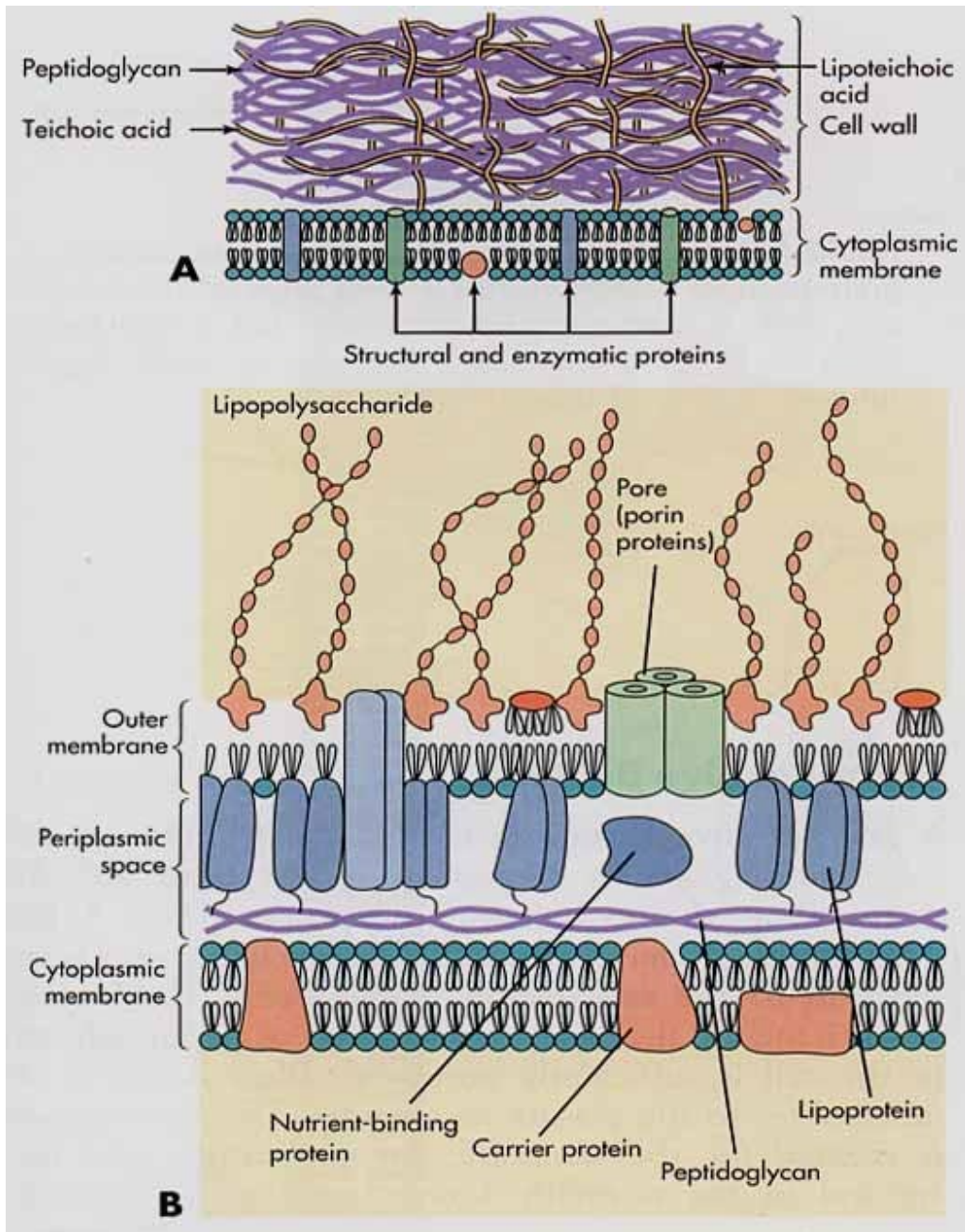


Figure 1. A) Gram Postive bacterial cell wall; B) Gram negative bacterial cell wall.

adapted from micro.digitalproteus.com

History of antibacterial agents

Van Leeuwenhoek's invention of the microscope in 1670s led to the identification of the first bacteria. The possibility that bacteria might be responsible for disease was widespread in nineteenth century after Pasteur demonstrating that specific bacterial strains were crucial for fermentation [13]. This possibility became a fact in latter half of the nineteenth century, when scientists such as Koch were able to identify the bacteria responsible for diseases such as tuberculosis, cholera, and typhoid. This led to efforts to find effective antibacterial agents. Paul Ehrlich who won a Nobel prize for his contribution to immunology, later changed his area of research to a new area which he defined as chemotherapy. Ehrlich's 'Principle of Chemotherapy' popularly known as the 'magic bullet', was that specific chemical bullets which could destroy the microorganism without adversely affecting the host. By 1910, Ehrlich successfully developed first synthetic antimicrobial drug Salvarsan, an arsenic-containing compound used to treat syphilis. Over the next two decades efforts in finding antibacterial agents were futile, until the introduction of proflavine in 1934. Proflavine is a yellow colored aminoacridine structure effective against bacterial infections in deep surface wounds. Although proflavine was successful in treating certain kind of bacterial infections but was not effective against bacterial infections in bloodstream, urgent need was there to find agents that could fight these kind of infections. A red dye called prontosil was discovered in 1935 and found to be effective against *streptococcal* infections *in vivo*. Later it was recognized as a prodrug to a new class of antibacterial agents sulfonamides. These were effective against bacterial infections carried in the bloodstream, and were the only available drugs

until penicillin became available in early 1940s. Although Fleming discovered penicillin in 1928, an effective means of isolating it was developed only in 1940 by Florey & Chain. This revolutionized the fight against bacterial infection, and was even more effective than sulfonamides. Despite penicillin's success, it was not effective against all types of infections and the need for new antibacterial agents still remained. Streptomycin, the first example of series of antibiotics known as the aminoglycoside antibiotics was discovered from soil organisms in 1944. Efforts to find new antibiotics led to the discovery of series of antibiotics, such as bacitracin a peptide antibiotic in 1945, chloramphenicol in 1947, chlortetracycline a tetracycline antibiotic in 1948, erythromycin a macrolide antibiotic in 1952, cycloserine a cyclic peptide antibiotic in 1955, cephalosporin C a second major group of β -lactam antibiotics in 1955, and vancomycin a glycopeptide in 1956. Synthetic agents such as isoniazid a pyridine hydrazide structure, and nalidixic acid the first quinolone antibacterial agent, were discovered in 1952 and 1962 respectively [13].

From 1960s to 2000, all antibiotics approved for clinical use were synthetic derivatives of existing scaffolds. Around 73% of antibacterial agents, new chemical entities filed between 1981 and 2005 are just from four scaffolds - cephalosporins, penicillins, quinolones, and macrolides [14]. Around 20 new classes of antibiotics were identified between 1930 and 1960, but since then only three new classes of antibiotic oxazolidinones, lipopeptides, and mutilins, were developed **Figure 2** [15-19]. Antibiotics and their respective analogues that are developed so far are listed in **Figure 3**. Analogue development was more successful for cephalosporins, penicillins and quinolones as there are sites in the scaffolds for easy modification [20].

Eventually analogue development based on the core structure will become too difficult or too expensive to make especially with new antibiotic resistance mechanisms. So there is an urgent need for development of new class of antibacterial agents that act by novel mechanisms and for which mechanisms of resistance are not yet known [21].

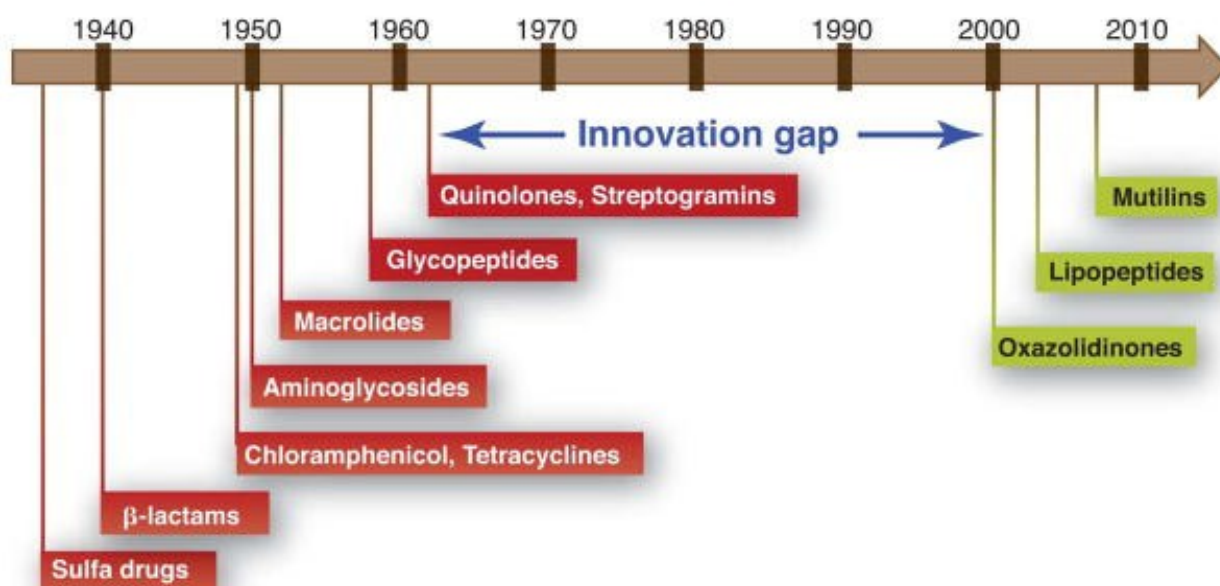


Figure 2. Timeline of antibiotic classes inventions. Adapted from M.A. Fischbach and C.T.Walsh 2010.

Class examples
<p>β-Lactams</p> <p>Penicillins</p> <p>Penicillin G, penicillin V, methicillin, oxacillin, cloxacillin, dicloxacillin, nafcillin, ampicillin, amoxicillin, carbenicillin, ticarcillin, mezlocillin, piperacillin, azlocillin, temocillin</p> <p>Cephalosporins</p> <p><i>First generation</i> Cephalothin, cephalirin, cephradine, cephaloridine, cefazolin</p> <p><i>Second generation</i> Cefamandole, cefuroxime, cephalexin, cefprozil, cefaclor, loracarbef, cefoxitin, cefmetazole</p> <p><i>Third generation</i> Cefotaxime, ceftizoxime, ceftriaxone, cefoperazone, ceftazidime, cefixime, cefpodoxime, ceftibuten, cefdinir</p> <p><i>Fourth generation</i> Cefpirome, cefepime</p> <p><i>Fifth generation¹</i> Ceftaroline², ceftobiprole³</p> <p>Carbapenems</p> <p>Imipenem, meropenem, doripenem</p> <p>Monobactams</p> <p>Aztreonam</p> <p>β-Lactamase inhibitors</p> <p>Clavulanate, sulbactam, tazobactam</p> <p>Aminoglycosides</p> <p>Streptomycin, neomycin, kanamycin, paromomycin, gentamicin, tobramycin, amikacin, netilmicin, spectinomycin, sisomicin, dibekacin, isepamicin</p> <p>Tetracyclines</p> <p>Tetracycline, chlortetracycline, demeclocycline, minocycline, oxytetracycline, methacycline, doxycycline, tigecycline</p> <p>Rifamycins</p> <p>Rifampicin (also called rifampin), rifapentine, rifabutin, bezoxazinorifamycin, rifaximin</p> <p>Macrolides</p> <p>Erythromycin, azithromycin, clarithromycin</p> <p>Ketolides</p> <p>Telithromycin</p> <p>Lincosamides</p> <p>Lincomycin, clindamycin</p> <p>Glycopeptides</p> <p>Vancomycin, telcoplanin, telavancin</p> <p>Lipopeptides</p> <p>Daptomycin</p> <p>Streptogramins</p> <p>Quinupristin, dalfopristin, pristinamycin</p> <p>Sulphonamides</p> <p>Sulphanilamide, <i>para</i>-aminobenzoic acid, sulfadiazine, sulfisoxazole, sulfamethoxazole, sulfathalidine</p> <p>Oxazolidinones</p> <p>Linezolid</p> <p>Quinolones</p> <p>Nalidixic acid, oxolinic acid, norfloxacin, pefloxacin, enoxacin, ofloxacin/levofloxacin, ciprofloxacin, temafloxacin, lomefloxacin, fleroxacin, grepafloxacin, sparfloxacin, trovafloxacin, clinafloxacin, gatifloxacin, moxifloxacin, sitafloxacin</p> <p>Others</p> <p>Metronidazole, polymyxin B, colistin, trimethoprim</p>

¹Spectrum combines third generation gram-negatives with methicillin resistant *Staphylococcus aureus* (MRSA) and multidrug-resistant *Streptococcus pneumoniae*.

²Pending Federal Drugs Administration review.

³Marketed in Canada and Switzerland; now withdrawn.

Figure 3. Main classes of marketed antibiotics. Adapted from A.R. Coates et. al. 2011.

Mechanism of action of antibacterial agents

Antibacterial agents act selectively on vital bacterial functions with nominal effects or without affecting host functions. The mechanism of action of antibacterial agents can be categorized based on how they affect the bacterial physiology or biochemistry **Figure 4**. There are five general modes of action:

- 1) Inhibition of cell wall synthesis
- 2) Inhibition of protein synthesis
- 3) Inhibition of nucleic acid synthesis
- 4) Inhibition of folate metabolism
- 5) Inhibition of cell membrane function

Antibacterial agents that inhibit cell wall synthesis include β -lactams, such as penicillins, cephalosporins, carbapenems, monobactams, and glycopeptides, such as vancomycin and teicoplanin [22-23]. β -lactams interfere with the enzymes required for the synthesis of peptidoglycan layer thereby inhibiting the synthesis of the bacterial cell wall [22]. Glycopeptides binds to the terminal D-alanine residues of the nascent peptidoglycan chain, thereby inhibiting the cross-linking steps required for cell wall synthesis [22].

Antibacterial agents that inhibit protein synthesis include aminoglycosides, tetracyclines, macrolides, chloramphenicol, streptogramins, and oxazolidinones [22-23]. Aminoglycoside and tetracyclines bind to the 30s subunit of the ribosome, whereas macrolides, chloramphenicol, and clindamycin binds to the 50s subunit [24].

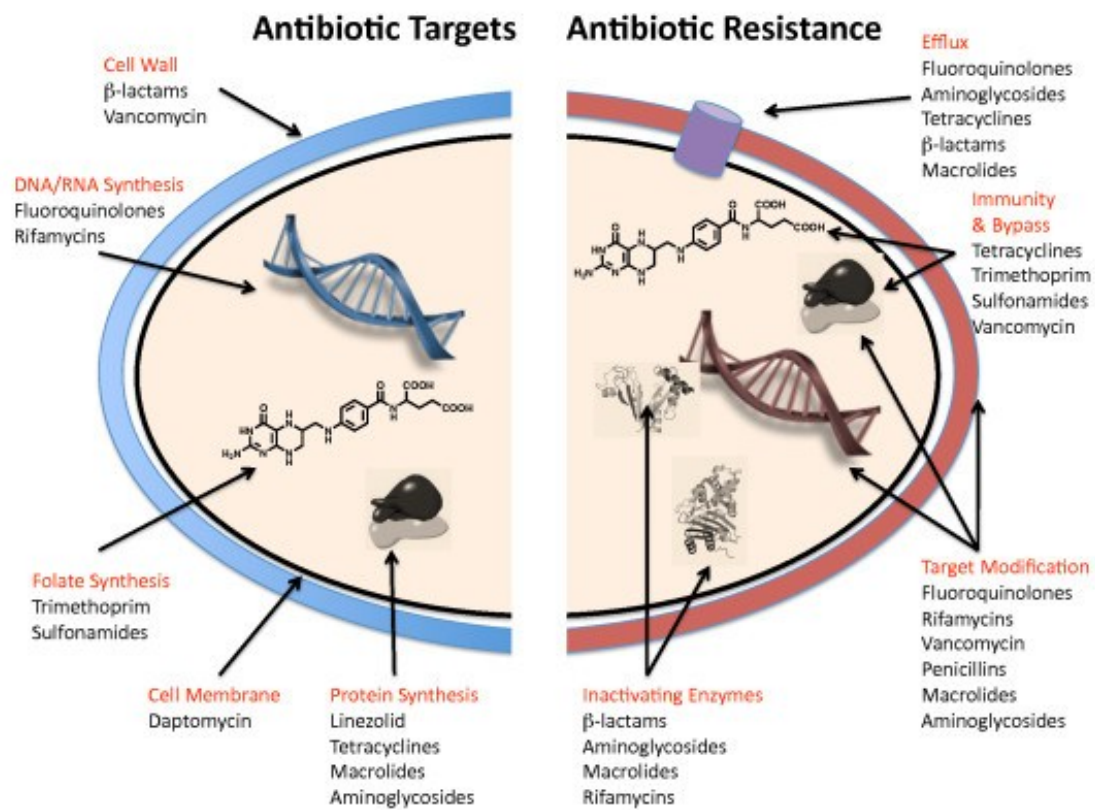


Figure 4. Antibiotic targets and mechanisms of resistance. Adapted from G.D. Wright 2010.

Fluoroquinolones exert their antibacterial effects by selectively inhibiting topoisomerase ligase domain causing DNA fragmentation during DNA replication [25]. Rifamycins exert their antibacterial activity by selectively binding to bacteria's RNA polymerase thereby blocking RNA synthesis [26-27]. Sulfonamides and trimethoprim exert their antibacterial activity by inhibiting two enzymatic steps dihydropteroate synthetase and dihydrofolate reductase respectively, thereby inhibiting the synthesis of folic acid, an important metabolite in DNA synthesis. Trimethoprim, a folic acid analogue plus, sulfamethoxazole, a para-aminobenzoic acid (PABA) analogue, are used in combination for their synergistic effects. They inhibit in the bacterial folate synthesis pathway [28-29]. Polymyxins exert their inhibitory effects by binding to lipopolysaccharide (LPS) present on the outer membrane of Gram-negative bacteria, causing membrane damage and leakage of bacterial contents [30]. Daptomycin a cyclic lipopeptide exerts its antibacterial activity by inserting its lipid tail into the bacterial cell membrane, causing rapid membrane depolarization and eventual death of the bacterium [31].

Bacteria Resistance mechanisms to antibiotics

The four main mechanisms by which bacteria exhibit resistance to antibacterial agents are inactivating enzymes, target modification, alteration of metabolic pathway, and efflux. The major mechanism of β -lactam resistance is due to enzyme mediated antibiotic degradation. Three classes of enzymes namely β -lactamases, acylases, and esterases hydrolyze β -lactam antibiotics resulting in

degradation of β –lactam nucleus [32-34]. Aminoglycoside resistance is due to enzyme mediated antibiotic modification. Aminoglycoside-modifying enzymes inactivate aminoglycoside antibiotics by catalyzing acetylation, nucleotidylation or phosphorylation reactions at either amino or hydroxyl groups on aminoglycoside antibiotics [35-38]. Similarly chloramphenicol acetyltransferase inactivates chloramphenicol by acetylation [39-41]. In vancomycin-resistant enterococcus, resistance to vancomycin was achieved by replacing the terminal D-Ala-D-Ala moiety of peptidoglycan precursors with D-Ala-D-Lac [42-43]. Bacteria developed resistance to trimethoprim either by producing an altered dihydrofolate reductase that lacks the capacity to bind trimethoprim or by over producing the normal dihydrofolate reductase, the latter is particularly in *E. coli* and *Klebsiella pneumonia* [44-49]. Sulfonamides resistance was due to the production of plasmid-encoded dihydropteroate synthetase which has a decreased affinity for sulfonamides [48, 50-51]. Macrolide resistance is either due to post-transcriptional methylation of the 23S ribosomal RNA or production of active ATP-dependent efflux proteins that transport drug outside of the cell [52-53]. Tetracycline resistance is either due to ribosomal protection proteins that dislodge tetracycline from the ribosome and allowing the translation or due to efflux pumps that transport the tetracycline outside of the cell [54-56].

Some strains of bacteria have developed resistance to all commonly available agents. Among gram positive strains methicillin resistant *Staphylococcus aureus* (MRSA) needs a special mention. MRSA is not only resistant to methicillin but usually also to aminoglycosides, macrolides, tetracycline, chloramphenicol, and

lincosamides [57]. Among gram negative strains multidrug-resistant carbapenemase-producing *Klebsiella pneumonia*, *Pseudomonas aeruginosa*, *Burkholderia* sp. and *Acinetobacter* spp. developed resistance to all currently available antibacterial agents or remain susceptible to potentially more toxic agents such as the polymyxins [58-60]. These bacteria have developed resistance by accumulation of resistance plasmids or transposons, of genes with each coding for resistance to specific agent, and/or by multidrug efflux pumps, which can pump out more than one drug type [57].

We are totally dependent on antibiotics for the treatment of infectious diseases. Antibiotics are also critical for the success of many surgical procedures. Resistant bacteria have created an enormous clinical and financial burden on health care systems. At present it seems likely that bacteria resistant to essentially all the commonly used antibiotics will soon emerge. Further heightening concern about existing and emerging bacterial drug resistance is the fact that, only three new class of antibacterial agents have been introduced into clinical practice in the last 50 years. Therefore, there is an urgent need to identify new classes of antibacterial agents, especially agents that act through novel mechanisms and for which mechanisms of resistance are not yet known [21].

CHAPTER 1

IDENTIFICATION OF D-BOROALA AS A NOVEL ANTIBACTERIAL AGENT

Penicillin-binding proteins (PBPs) [61] are ubiquitous bacterial enzymes whose physiological function is to form and modulate the crosslinks important to bacterial cell wall integrity [61-64]. PBPs can be broadly divided into two groups: the low molecular mass (LMM) PBPs with molecular mass ranging from 20-50 kDa, and the high molecular mass (HMM) PBPs with molecular mass ranging from 50-120 kDa. In most Gram negative bacteria the reactions catalyzed by the PBPs are shown in **Figure 5**.

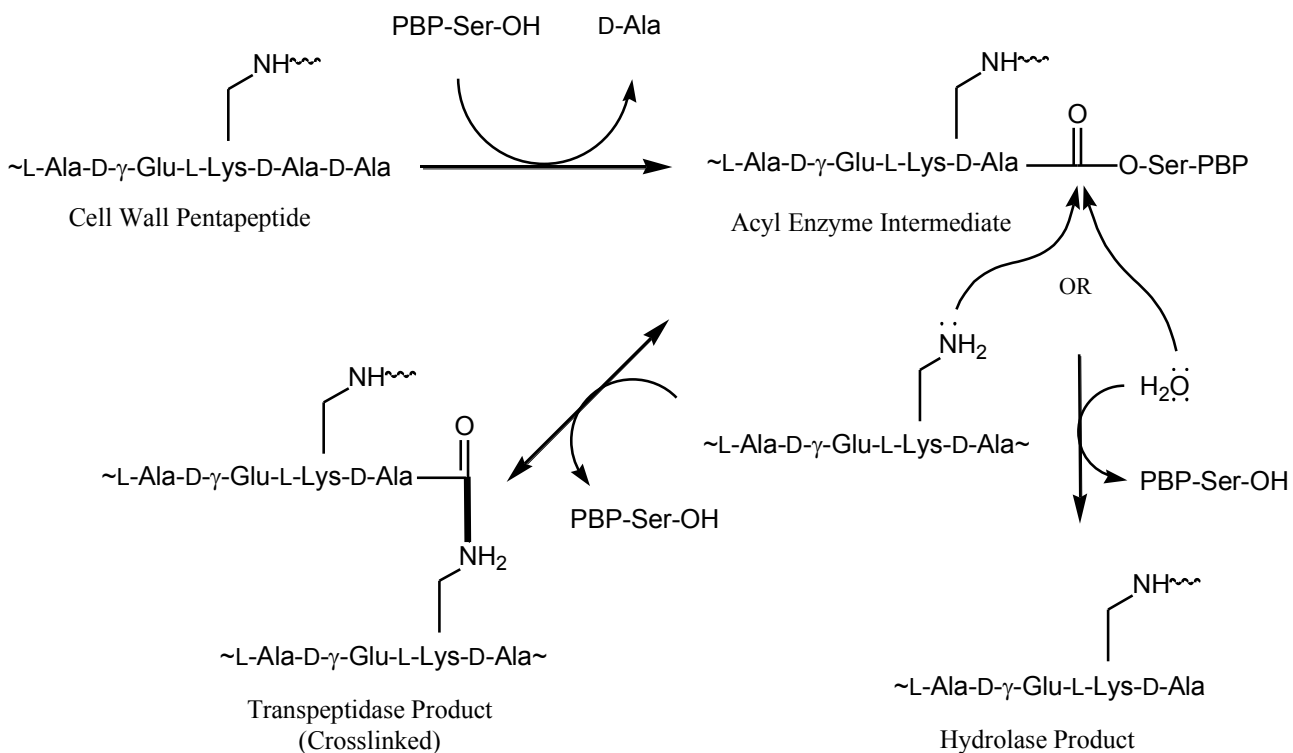


Figure 5. Bacterial cell wall biosynthesis reactions catalyzed by the PBPs in most Gram negative bacteria. Adapted from Bobba et. al. 2011.

The active site serine of the PBPs reacts with the D-Ala-D-Ala moiety, its pentapeptide substrate to form an acyl-enzyme complex, releases the C-terminal D-Ala. This acyl-enzyme intermediate can then either undergo hydrolysis resulting in a tetrapeptide (carboxypeptidase product) or transpeptidation by forming a cross link with amino group of another pentapeptide (transpeptidase product). The cross linked product can also be cleaved by PBPs (endopeptidase activity).

The active site serine involved in the acyl transfer reaction is the target of the β -lactam antibiotics, which inhibit the PBPs by acting as substrate analogs of D-Ala-D-Ala to form a stable acyl enzyme complex resistant to subsequent hydrolysis [65-67]. Bacteria were developed resistance to β -lactam antibiotics primarily by two mechanisms: producing β -lactam hydrolyzing enzymes known as β -lactamases [68], and acquiring mutations in their HMM PBP targets that make them less susceptible to β -lactam antibiotics [63, 69].

Transition state analogues (TSAs) are compounds that mimic the transition state of enzyme-catalyzed reactions and are the potent inhibitors for that particular enzyme [70-71]. There are several well-known classes of such inhibitors for the serine proteases, including peptide chloromethyl ketones [72-73], peptide boronic acids [74-75], peptide aldehydes [76], and peptide tri- and di-fluoromethyl ketones [77-78]. In an effort to combat β -lactam resistant bacteria, TSAs have been developed for β -lactamases, including boronic acids [79-83], and phosphonates [84-86], but potent inhibitors have not emerged from these studies [87].

In an effort to develop new non β -lactam inhibitors for the PBPs that could provide a basis for new antibacterial agents, a series of potential TSA inhibitors for

the PBPs were synthesized in our lab [88]. The classes of agents synthesized were peptide aldehydes, peptide trifluoromethyl ketones, peptide chloromethyl ketones, and peptide boronic acids **Figure 7**. These compounds were tested as inhibitors against a set of LMM PBPs: *Escherichia coli* (EC) PBP 5, *Neisseria gonorrhoeae* (NG) PBP 3, and NG PBP 4. Peptide boronic acids were found to be the most effective in the series of compounds synthesized. The lowest K_i of 370 nM was obtained for NG PBP 3 inhibition by Boc-L-Lys(Cbz)-D-boroAla. These compounds were subsequently tested for their antibacterial activity using filter disc assays. It was observed that Boc-L-Lys(Cbz)-D-boroAla had antibacterial activity. However, the antibacterial activity observed in different preparations was variable. The crude compound was resolved on a TLC plate, and the TLC plate was tested for antibacterial activity. Two halos were observed on the petri dish, one at the top of the plate, and the other at the bottom of the plate **Figure 6**. The halo at the bottom of the TLC plate is much bigger than that at the top. We identified that the compound at the bottom of the TLC as D-boroAla by running all the reagents used for the reaction, crude Boc-L-Lys(Cbz)-D-boroAla, and purified Boc-L-Lys(Cbz)-D-boroAla on TLC. This identified D-boroAla as the active compound, pure D-boroAla was tested for antibacterial activity using filter disc assay, and confirmed as the active agent **Figure 6**.

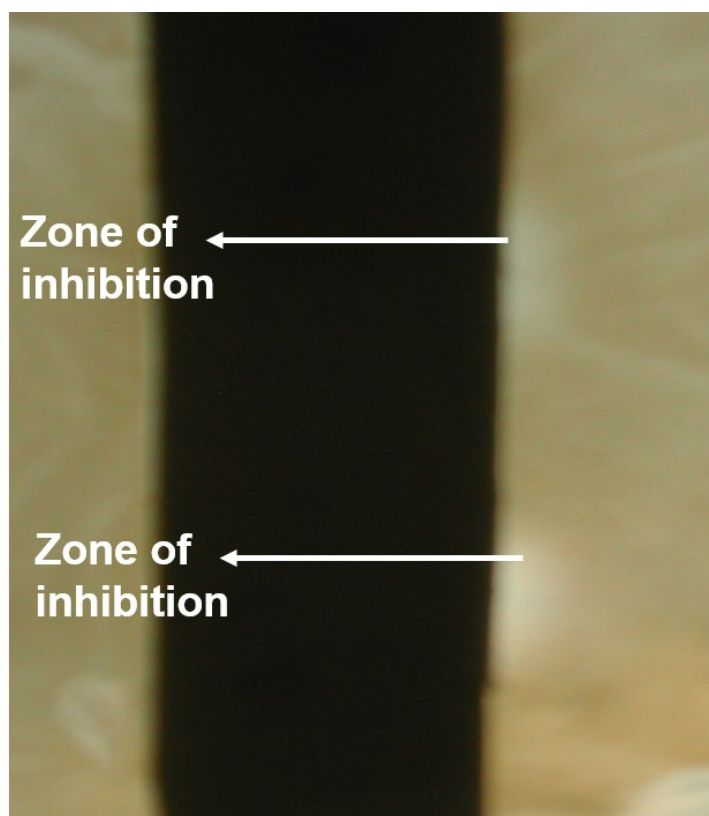
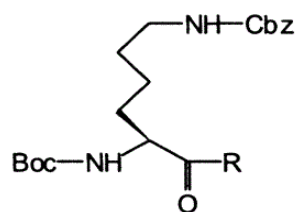
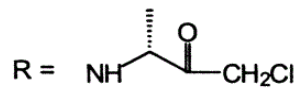


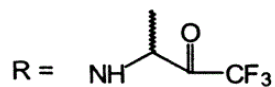
Figure 6. TLC of crude Boc-L-Lys(Cbz)-D-boroAla and the zone of inhibition of the TLC resolved compounds on *S. aureus*.



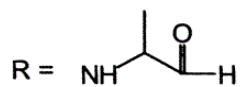
Boc-L-Lys(Cbz)-R



Boc-L-Lys(Cbz)-D-Ala-CH₂Cl

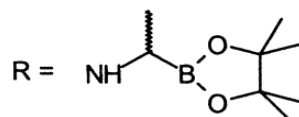


Boc-L-Lys(Cbz)-DL-Ala-CF₃

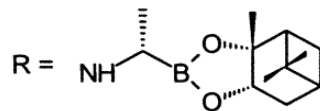


Boc-L-Lys(Cbz)-D-Ala-H

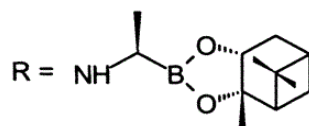
Boc-L-Lys(Cbz)-L-Ala-H



Boc-L-Lys(Cbz)-DL-boroAla-pinacol



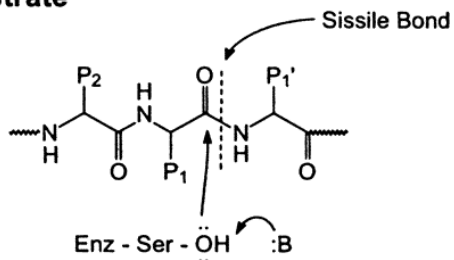
Boc-L-Lys(Cbz)-D-boroAla-(-)-pinanediol



Boc-L-Lys(Cbz)-L-boroAla-(+)-pinanediol

Figure 7. Transition state analogues synthesized in our lab. Adapted from Pechenov et., al 2003.

Substrate



Transition State Analogs

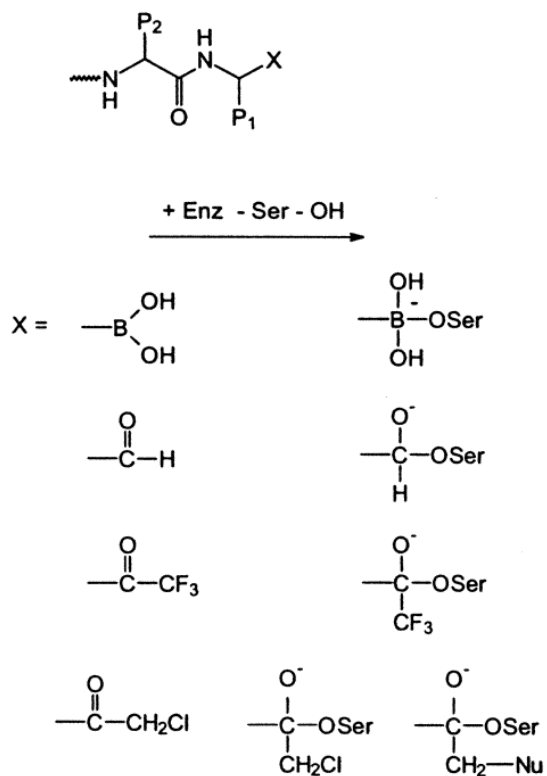


Figure 8. Substrate specificity and corresponding transition state analogues for serine proteases and related enzymes. The four transition state analogue classes shown at the bottom can form tetrahedral adducts with the active site serine. Adapted from Pechenov et., al 2003.

CHAPTER 2

CHARACTERIZATION OF D-BOROALA AS A NOVEL BROAD-SPECTRUM ANTIBACTERIAL AGENT TARGETING D-ALA-D-ALA LIGASE.

Introduction and Rationale

Bacterial infections were the major cause of death and morbidity prior to the development of modern antibiotics, and the increasing resistance of pathogenic bacteria to commonly used antibacterial agents is of major public health concern. Methicillin-resistant *Staphylococcus aureus* (MRSA) and several Gram-negative pathogens such as *Pseudomonas aeruginosa*, *Burkholderia* sp., *Acinetobacter baumannii*, and *Klebsiella pneumoniae* are of particular concern [21, 89-94]. Further heightening concern about existing and emerging bacterial drug resistance is the fact that, although a number of new antibacterial agents from known antibacterial classes are under development, only two new class of antibacterial agents have been introduced into clinical practice in the last 40 years – the oxazolidinones as represented by linezolid [95] and the lipopeptides as represented by daptomycin [96-97]. There is therefore an urgent need to identify new classes of antibacterial agents, especially agents that act through novel mechanisms and for which mechanisms of resistance are not yet known [21].

During our efforts to develop transition-state analog inhibitors for bacterial cell wall-synthesizing enzymes [88, 98], we observed that D-boroAlanine (D-Ala with the -COOH group replaced with a -B(OH)₂ group) had effective antibacterial activity. While D-boroAla has previously been described as an inhibitor of alanine racemase and D-Ala-D-Ala ligase (DDL) [99], it has not previously – to our knowledge – been

reported as an antibacterial agent. In this report, we describe the antibacterial properties of D-boroAla, structure–activity correlation among several D-boroAla homologs, and determination of the biochemical mechanism for D-boroAla’s antibacterial activity. This study demonstrates that D-boroAla has broad-spectrum antibacterial activity and targets DDL in the alanine branch of bacterial cell wall biosynthesis **Figure 9**.

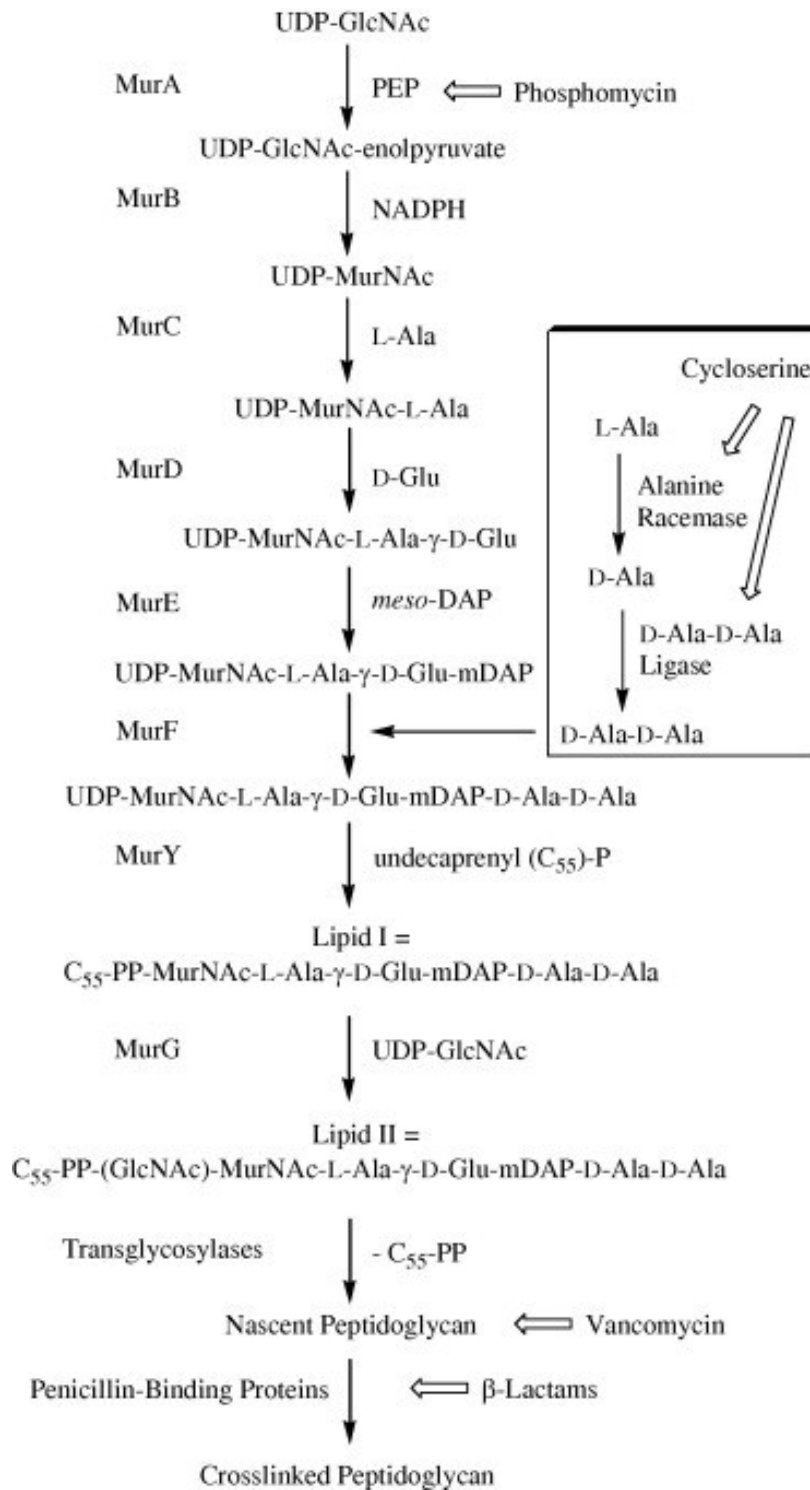


Figure 9. Bacterial cell wall biosynthesis pathway in *E. coli*. Adapted from Jamindar et. al. 2009.

Materials and Methods

General: D-Ala, L-Ala, D-Ala-D-Ala, $^{13}\text{C}_3$ -D-Ala, D-cycloserine, and ampicillin were purchased from Sigma–Aldrich (St. Louis, MO, USA). C18 silica gel was obtained from Sep-Pak Cartridges (Waters, Milford, MA, USA). Marfey's reagent (1-fluoro-2,4-dinitrophenyl-L- 5-alanine amide) was purchased from Novabiochem (a division of EMD Chemicals, Gibbstown, NJ, USA). Other reagents were obtained from standard sources and were reagent grade or better. M9 minimal medium, consisting of Na_2HPO_4 (6 g/L), KH_2PO_4 (3 g/L), NH_4Cl (1 g/L), NaCl (0.5 g/L), $\text{MgSO}_4 \cdot 7\text{H}_2\text{O}$ (1 mM), $\text{FeSO}_4 \cdot 7\text{H}_2\text{O}$ (3 mg/L), vitamin B1 (thiamine, 0.5 mg/L), and glycerol (20%, as carbon source), was prepared following standard procedures. LC–MS/MS was performed on an Applied Biosystems Sciex (ABI) 2000 QTrap LC–MS/MS mass spectrometer equipped with an Agilent 1100 HPLC system. All chromatographic separations were performed on a Nucleodur 100-3 C8 column (125 x 2.0 mm, Macherey–Nagel, Bethlehem, PA, USA). All centrifuge operations were performed on a Sorvall RT 6000 refrigerated centrifuge. Minimum inhibitory concentration (MIC) measurements were performed in 96-well microtiter plates and read with a Tecan Spectrafluor Plus spectrofluorometer. Klett measurements of cultures were performed at 600 nm using a BioMate 3 Thermo Spectronic spectrometer.

Compound Synthesis

General. The synthesis strategy used for alkyl side chain D-boro-amino acid analogs, adapted from the general procedure describe for L-boro analogs as

described by Matteson, Kettner, and coworkers [99-101]; is outlined in **Figure 10** and **Figure 11**.

Diisopropyl-(1-methyl)-1-borate (1a): Triisopropylborate (160 mmol, 30 g) was dissolved in 500 mL of dry ether cooled to – 72 °C in an isopropanol/dry ice bath. Methyl lithium (160 mmol, 100 mL) was added slowly over a 30 min period, and the reaction left to warm to room temperature overnight. The reaction mixture was cooled to 0 °C and quenched with 1 M HCl in ether (160 mmol). The precipitate was removed by filtration, the ether distilled off and the product is collected by distillation at atmospheric pressure at 110 °C. The yield was 13.6 g (59%) of product as a clear oil. ¹H NMR (400 MHz, CDCl₃): δ 4.41-4.31 (Heptet, J=6.15 Hz, 2 H), 1.18-1.15 (d, J=5.89 Hz, 12H), 0.24 (s, 3H) **Figure 20**.

Diisopropyl-(1-ethyl)-1-borate (1b): Triisopropylborate (160 mmol, 30 g) was dissolved in 500 mL of dry ether cooled to – 72 °C in an isopropanol/dry ice bath. Ethyl lithium (160 mmol, 100 mL) was added slowly over a 30 min period, and the reaction left to warm to room temperature overnight. The reaction mixture was cooled to 0 °C and quenched with 1 M HCl in ether (160 mmol). The precipitate was removed by filtration, the ether distilled off and the product is collected by distillation at atmospheric pressure at 230 °C. The yield was 15.4 g (61%) of product as a clear oil. ¹H NMR (400 MHz, CDCl₃): δ 4.39-4.29 (Heptet, J=6.55 Hz, 2H), 1.16-1.14 (d, J=5.72 Hz, 6H), 1.14-1.11 (d, J=6.06 Hz, 6H), 0.94-0.89 (T, J=7.77 Hz, 3H), 0.76-0.68 (Q, J=7.44 Hz, 2H) **Figure 21**.

Diisopropyl-(1-isopropyl)-1-borate (1c): Triisopropylborate (160 mmol, 30 g) was dissolved in 500 mL of dry ether cooled to – 72 °C in an isopropanol/dry ice

bath. Isopropyl lithium (160 mmol, 100 mL) was added slowly over a 30 min period, and the reaction left to warm to room temperature overnight. The reaction mixture was cooled to 0 °C and quenched with 1 M HCl in ether (160 mmol). The precipitate was removed by filtration, the ether distilled off and the product is collected by distillation at atmospheric pressure at 175-184 °C. The yield was 14.1 g (51%) of product as a clear oil. ¹H NMR (400 MHz, CDCl₃): δ 4.39-4.29 (Heptet, J=6.55 Hz, 2H), 1.16-1.14 (d, J=5.72 Hz, 6H), 1.14-1.11 (d, J=6.06, 6H), 1.02-0.99 (d, J=6.85 Hz, 6H), 0.94-0.89 (T, J=7.77 Hz, 3H), 0.76-0.68 (Q, J=7.44 Hz, 2H) **Figure 22**.

(-)-Pinanediol-(1-methyl)-1-boronate (2a): (1R, 2R, 3S, 5R)-(-)-pinanediol (29.36 mmol, 5 g) was dissolved in diisopropyl-(1-methyl)-borate (**1a**) (24.47 mmol, 3.53 g) at room temperature and stirred overnight. The reaction mixture was distilled at atmospheric pressure and the product was collected at 98 – 103 °C. The yield was 4.2 g (88%) of product as a clear oil. ¹H NMR (400 MHz, CDCl₃): δ 4.28-4.24 (dd, J=2.1 Hz, 1H), 2.37-2.29 (m, 1H), 2.26-2.19 (m, 1H), 2.06-2.02 (T, J=4.76 Hz, 1H), 1.94-1.89 (m, 1H), 1.88-1.82 (dQ, 1H), 1.39 (S, 3H), 1.29 (S, 3H), 0.85 (S, 3H), 0.29 (S, 3H) **Figure 23**.

(-)-Pinanediol-(1-ethyl)-1-boronate (2b): (1R, 2R, 3S, 5R)-(-)-pinanediol (29.36 mmol, 5 g) was dissolved in diisopropyl-(1-ethyl)-borate (**1b**) (24.47 mmol, 3.87 g) at room temperature and stirred overnight. The reaction mixture was distilled at 15 mm of Hg aspirator pressure and the product was collected at 107 – 110 °C. The yield was 3.4 g (67%) of product as a clear oil. ¹H NMR (400 MHz, CDCl₃): δ 4.28-4.24 (dd, J=2.1 Hz, 1H), 2.37-2.29 (m, 1H), 2.26-2.19 (m, 1H), 2.06-2.02 (T, J=4.76 Hz, 1H), 1.94-1.89 (m, 1H), 1.88-1.82 (dQ, 1H), 1.39 (S, 3H), 1.29 (S, 3H),

1.14-1.08 (d, J=10.83 Hz, 1H), 1.01-0.94 (Q, J=8.19 Hz, 2H), 0.85 (S, 3H) **Figure 24.**

(-)-Pinanediol-(1-isopropyl)-1-boronate (2c): (1R, 2R, 3S, 5R)-(-)-pinanediol (29.36 mmol, 5 g) was dissolved in diisopropyl-(1-isopropyl)-borate (**1c**) (24.7 mmol, 4.25 g) at room temperature and stirred overnight. The reaction mixture was distilled at 15 mm of Hg aspirator pressure and the product was collected at 195 – 198 °C. The yield was 5.3 g (96%) of product as a clear oil. ¹H NMR (400 MHz, CDCl₃): δ 4.28-4.24 (dd, J=2.1 Hz, 1H), 2.37-2.29 (m, 1H), 2.26-2.19 (m, 1H), 2.06-2.02 (T, J=4.76 Hz, 1H), 1.94-1.89 (m, 1H), 1.88-1.82 (dQ, 1H), 1.39 (S, 3H), 1.29 (S, 3H), 1.14-1.08 (d, J=10.83 Hz, 1H), 1.02-0.99 (Q, J=6.85 Hz, 6H), 0.85 (S, 3H) **Figure 25.**

(+)-Pinanediol-(1-methyl)-1-boronate (2d): (1R, 2R, 3S, 5R)-(-)-pinanediol (29.36 mmol, 5 g) was dissolved in diisopropyl-(1-methyl)-borate (**1a**) (26.8 mmol, 3.86 g) at room temperature and stirred overnight. The reaction mixture was distilled at atmospheric pressure and the product was collected at 103 – 116 °C. The yield was 4.61 g of product as a clear oil. and the product was collected at 195 – 198 °C. The yield was 5.1 g (98%) of product as a clear oil. ¹H NMR (400 MHz, CDCl₃): δ 4.28-4.24 (dd, J=2.1 Hz, 1H), 2.37-2.29 (m, 1H), 2.26-2.19 (m, 1H), 2.06-2.02 (T, J=4.76 Hz, 1H), 1.94-1.89 (m, 1H), 1.88-1.82 (dQ, 1H), 1.39 (S, 3H), 1.29 (S, 3H), 0.85 (S, 3H), 0.29 (S, 3H) **Figure 26.**

(-)-Pinanediol (1R)-(1-chloroethyl)-1-boronate (3a): Anhydrous methylene chloride (30.24 mmol, 2.75 mL) was placed in 100 mL round bottom flask, freshly distilled THF was transferred into the reaction vessel, and the mixture cooled to – 100 °C using a methanol/nitrogen slush bath. 2.5M n-butyl lithium (23.76 mmol, 9.5

mL) solution in hexane was slowly added along the cold walls of the reaction vessel using a canula, and the mixture stirred for 10 min. (-)-Pinanediol-(1-methyl)-1-boronate (**2a**) (21.6 mmol, 4.185 g) in 20 mL anhydrous ether was slowly added to the reaction mixture along the cold walls of the reaction vessel. Anhydrous zinc chloride (15.12 mmol, 2.06 g) was dried under high vacuum, and then added to the reaction mixture. The reaction mixture was warmed to room temperature overnight. 75 mL of petroleum ether was added, and the reaction mixture quenched with 40 mL of saturated ammonium chloride. The reaction was extracted, with three times with ethyl ether, and the organic phase was dried over MgSO₄, filtered and rotovap to give crude product as an oil. The pure product was collected at 150 – 159 °C by distillation at 30 mm of Hg. The yield was 2.5 g (47%) of product as a light yellow oil. ¹H NMR (400 MHz, CDCl₃): δ 4.39-4.35 (dd, J=2.1 Hz, 1H), 3.61-3.54 (Q, J=7.64 Hz, 1H), 3.52-3.32 (m, 1H) 1.6-1.56 (d, J=7.7 Hz, 3H), 1.43 (s, 3H), 1.3 (s, 3H), 1.19-1.14 (m, 1H), 0.95-0.89 (m, 2H), 0.85 (s, 3H) **Figure 27**.

(-)-Pinanediol (1R)-(1-chloro-1-propyl)-1-boronate (3b): Anhydrous methylene chloride (23.04 mmol, 1.5 mL) was placed in 100 mL round bottom flask, freshly distilled THF was transferred into the reaction vessel, and the mixture cooled to – 100 °C using a methanol/nitrogen slush bath. 2.5M n-butyl lithium (18.1 mmol, 7.25 mL) solution in hexane was slowly added along the cold walls of the reaction vessel using a canula, and the mixture stirred for 10 min. (-)-Pinanediol-(1-ethyl)-1-boronate (**2b**) (16.45 mmol, 3.43 g) in 20 mL anhydrous ether was slowly added to the reaction mixture along the cold walls of the reaction vessel. Anhydrous zinc chloride (15.12 mmol, 2.06 g) was dried under high vacuum, and then added to the

reaction mixture. The reaction mixture was warmed to room temperature overnight. 75 mL of petroleum ether was added, and the reaction mixture quenched with 40 mL of saturated ammonium chloride. The reaction was extracted, with three times with ethyl ether, and the organic phase was dried over MgSO_4 , filtered and rotovap to give crude product as an oil. The pure product was collected at 166 °C by distillation at 18 mm of Hg . The yield was 1.9 g (45%) of product as a clear oil. ^1H NMR (400 MHz, CDCl_3): δ 4.28-4.24 (dd, $J=2.1$ Hz, 1H), 3.46-3.41 (t, $J=6.32$ Hz, 1H), 3.52-3.32 (m, 1H) 1.6-1.56 (d, $J=7.7$ Hz, 3H), 1.43 (s, 3H), 1.3 (s, 3H), 1.19-1.14 (m, 1H), 0.95-0.89 (m, 2H), 0.85 (s, 3H) **Figure 28**.

(-)-Pinanediol (1R)-(1-chloro-1-isobutyl)-1-boronate (3c): Anhydrous methylene chloride (30.24 mmol, 2.75 mL) was placed in 100 mL round bottom flask, freshly distilled THF was transferred into the reaction vessel, and the mixture cooled to – 100 °C using a methanol/nitrogen slush bath. 2.5M n-butyl lithium (23.76 mmol, 9.5 mL) solution in hexane was slowly added along the cold walls of the reaction vessel using a canula, and the mixture stirred for 10 min. *(-)-Pinanediol-(1-isopropyl)-1-boronate (2c)* (24.53 mmol, 5.45 g) in 20 mL anhydrous ether was slowly added to the reaction mixture along the cold walls of the reaction vessel. Anhydrous zinc chloride (15.12 mmol, 2.06 g) was dried under high vacuum, and then added to the reaction mixture. The reaction mixture was warmed to room temperature overnight. 75 mL of petroleum ether was added, and the reaction mixture quenched with 40 mL of saturated ammonium chloride. The reaction was extracted, with three times with ethyl ether, and the organic phase was dried over MgSO_4 , filtered and rotovap to give crude product as an oil. The pure product was

collected at 166 °C by distillation at 18 mm of Hg. The yield was 4.5 g (68%) of product as a clear oil. ¹H NMR (400 MHz, CDCl₃): δ 4.28-4.24 (dd, J=2.1 Hz, 1H), 3.35-3.32 (d, J=6.34 Hz, 2H), 3.52-3.32 (m, 1H) 1.6-1.56 (d, J=7.7 Hz, 3H), 1.43 (s, 3H), 1.3 (s, 3H), 1.19-1.14 (m, 1H), 1.02-0.99 (d, J=6.85 Hz, 6H), 0.95-0.89 (m, 2H), 0.85 (s, 3H) **Figure 29**.

(+)-Pinanediol (1S)-(1-chloroethyl)-1-boronate (3d): Anhydrous methylene chloride (33.2 mmol, 2.13 mL) was placed in 100 mL round bottom flask, freshly distilled THF was transferred into the reaction vessel, and the mixture cooled to – 100 °C using a methanol/nitrogen slush bath. 2.5 M butyl lithium (26.07 mmol, 10.43 mL) solution in hexane was slowly added along the cold walls of the reaction vessel using a canula, and the mixture stirred for 10 min. (-)-Pinanediol-(1-methyl)-1-boronate (**2d**) (23.7 mmol, 4.6 g) in 20 mL anhydrous ether was slowly added to the reaction mixture along the cold walls of the reaction vessel. Anhydrous zinc chloride (15.12 mmol, 2.06 g) was dried under high vacuum, and then added to the reaction mixture. The reaction mixture was warmed to room temperature overnight. 75 mL of petroleum ether was added, and the reaction mixture quenched with 40 mL of saturated ammonium chloride. The reaction was extracted, with three times with ethyl ether, and the organic phase was dried over MgSO₄, filtered and rotovap to give crude product as an oil. The pure product was collected at 160 – 163 °C by distillation at 30 mm of Hg. The yield was 3.2 g (56%) of product as a light yellow oil. ¹H NMR (400 MHz, CDCl₃): δ 4.39-4.35 (dd, J=2.1 Hz, 1H), 3.61-3.54 (Q, J=7.64 Hz, 1H), 3.52-3.32 (m, 1H) 1.6-1.56 (d, J=7.7 Hz, 3H), 1.43 (s, 3H), 1.3 (s, 3H), 1.19-1.14 (m, 1H), 0.95-0.89 (m, 2H), 0.85 (s, 3H) **Figure 30**.

(-)-Pinanediol (1S)-(1-hexamethyldisilazaneaminoethyl)-1-boronate (4a): 20 mL of freshly distilled THF over sodium/benzophenone was placed in a round bottom flask and cooled to -78 °C using nitrogen/isopropanol slush bath. 1,1,1,3,3,3-hexamethyl disilazane (11.7 mmol, 2.44 mL) was slowly added along the cold walls of the reaction vessel using a canula, then 2.5 M butyl lithium (11.7 mmol, 4.7 mL) was added. The reaction mixture was warmed to room temperature for 10 min, then cooled to -78 °C. *(-)-Pinanediol (1R)-(1-chloroethyl)-1-boronate (3a)* (9.14 mmol, 2.5 g) was added to the reaction mixture and warmed to room temperature and kept the reaction vessel in desiccator for 4 days. THF was distilled off at aspirator vacuum and the product was collected at 105 – 115 °C by distillation at 50 µm of Hg. The yield was 2.2 g (66%) of product as a light yellow oil. ¹H NMR (400 MHz, CDCl₃): δ 4.32-4.28 (dd, J=1.75 Hz, 1H), 2.76-2.68 (Q, J=8.06 Hz, 1H), 2.36-2.28 (m, 1H), 2.24-2.16 (m, 1H), 2.06-2.01 (T, J=5.68 Hz, 1H), 1.92-1.87 (m, 1H), 1.87-1.8 (m, 1H), 1.38 (s, 3H), 1.28 (s, 3H), 1.19-1.16 (d, J=7.91 Hz, 3H), 0.84 (s, 3H), 0.1 (s, 18H) **Figure 31**.

(-)-Pinanediol (1S)-(1-hexamethyldisilazaneamino-1-propyl)-1-boronate (4b): 20 mL of freshly distilled THF over sodium/benzophenone was placed in a round bottom flask and cooled to -78 °C using nitrogen/isopropanol bath. 1,1,1,3,3,3-hexamethyl disilazane (8.7 mmol, 2.44 mL) was slowly added along the cold walls of the reaction vessel using a canula, then 2.5 M butyl lithium (8.7 mmol, 3.5 mL) was added. The reaction mixture was warmed to room temperature for 10 min, then cooled to -78 °C. *(-)-Pinanediol (1R)-(1-chloro-1-propyl)-1-boronate (3b)* (7.25 mmol, 1.86 g) was added to the reaction mixture and warmed to room temperature

and kept the reaction vessel in desiccator for 4 days. THF was distilled off at aspirator vacuum and the product is collected at 120 – 139 °C by distillation at 50 μ m of Hg. The yield was 1.1 g (40%) of product as a light yellow oil. ^1H NMR (400 MHz, CDCl_3): δ 4.32-4.28 (dd, $J=1.75$ Hz, 1H), 2.76-2.68 (Q, $J=8.06$ Hz, 1H), 2.36-2.28 (m, 1H), 2.24-2.16 (m, 1H), 2.06-2.01 (T, $J=5.68$ Hz, 1H), 1.92-1.87 (m, 1H), 1.87-1.8 (m, 1H), 1.79-1.68 (dT, $J=7.36$ Hz, 2H), 1.38 (s, 3H), 1.28 (s, 3H), 1.19-1.16 (d, $J=7.91$ Hz, 3H), 0.84 (s, 3H), 0.1 (s, 18H) **Figure 32**.

(-)-Pinanediol (1S)-(1-hexamethyldisilazaneamino-1-isobutyl)-1-boronate (4c): 20 mL of freshly distilled THF over sodium/benzophenone was placed in a round bottom flask and cooled to -78 °C using nitrogen/isopropanol bath. 1,1,1,3,3,3-hexamethyl disilazane (19.72 mmol, 4.1 mL) was slowly added along the cold walls of the reaction vessel using a canula, then 2.5M butyl lithium (19.72 mmol, 7.7 mL) was added. The reaction mixture was warmed to room temperature for 10 min, then cooled to -78 °C. *(-)-Pinanediol (1R)-(1-chloro-1-isobutyl)-1-boronate (3c)* (16.43 mmol, 4.45 g) was added to the reaction mixture and warmed to room temperature and kept the reaction vessel in desiccator for 4 days. THF was distilled off at aspirator vacuum and the product is collected at 135 – 145 °C by distillation at 50 μ m of Hg. The yield was 2.1 g (33%) of product as a light yellow oil. ^1H NMR (400 MHz, CDCl_3): δ 4.32-4.28 (dd, $J=1.75$ Hz, 1H), 2.76-2.68 (Q, $J=8.06$ Hz, 1H), 2.36-2.28 (m, 1H), 2.24-2.16 (m, 1H), 2.06-2.01 (T, $J=5.68$ Hz, 1H), 1.92-1.87 (m, 1H), 1.87-1.8 (m, 1H), 1.38 (s, 3H), 1.28 (s, 3H), 1.19-1.16 (d, $J=7.91$ Hz, 3H), 1.01-0.96 (d, $J=5.84$ Hz, 6H), 0.84 (s, 3H), 0.1 (s, 18H) **Figure 33**.

(+)-Pinanediol (1R)-(1-hexamethyldisilazaneamino-1-ethyl)-1-boronate (4d):

20 mL of freshly distilled THF over sodium/benzophenone was placed in a round bottom flask and cooled to -78 °C using nitrogen/isopropanol bath. 1,1,1,3,3,3-hexamethyl disilazane (15.9 mmol, 3.35 mL) was slowly added along the cold walls of the reaction vessel using a canula, then 2.5 M butyl lithium (14.5 mmol, 5.8 mL) was added. The reaction mixture was warmed to room temperature for 10 min, then cooled to -78 °C. (-)-Pinanediol (1R)-(1-chloroethyl)-1-boronate (**3d**) (13.2 mmol, 3.6 g) was added to the reaction mixture and warmed to room temperature and kept the reaction vessel in desiccator for 4 days. THF was distilled off at aspirator vacuum and the product is collected at 120 – 124 °C by distillation at 50 µm of Hg. The yield was 2.2 g (45%) of product as a yellow color oil. ¹H NMR (400 MHz, CDCl₃): δ 4.32-4.28 (dd, J=1.75 Hz, 1H), 2.76-2.68 (Q, J=8.06 Hz, 1H), 2.36-2.28 (m, 1H), 2.24-2.16 (m, 1H), 2.06-2.01 (T, J=5.68 Hz, 1H), 1.92-1.87 (m, 1H), 1.87-1.8 (m, 1H), 1.38 (s, 3H), 1.28 (s, 3H), 1.19-1.16 (d, J=7.91 Hz, 3H), 0.84 (s, 3H), 0.1 (s, 18H) **Figure 34.**

(-)-Pinanediol (1S)-(1-aminoethyl)-1-boronate (D-boroAla-(-)-pinanediol HCl salt) (5a) : (-)-Pinanediol (1S)-(1-hexamethyldisilazaneaminoethyl)-1-boronate (**4a**) (0.27 mmol, 100 mg) was placed in a round bottom flask and cooled to -10 °C using an ice/NaCl bath, 1M HCl/ether (2 mmol, 2 mL) was added drop wise and stirred for 1 hr. The solvent was removed using nitrogen flush and then by high vacuum system. The yield was 68 mg (97%) of product as a light yellow solid [88]. ¹H NMR (400 MHz, CDCl₃): δ 4.32-4.28 (dd, J=1.75 Hz, 1H), 2.92-2.88 (m, 1H), 2.76-2.68 (Q, J=8.06 Hz, 1H), 2.36-2.28 (m, 1H), 2.24-2.16 (m, 1H), 2.06-2.01 (T, J=5.68 Hz, 1H),

1.92-1.87 (m, 1H), 1.87-1.8 (m, 1H), 1.38 (s, 3H), 1.28 (s, 3H), 1.19-1.16 (d, J=7.91 Hz, 3H), 0.84 (s, 3H) **Figure 35**.

(-)-Pinanediol (1S))-1-amino-1-propyl -1-boronate (D-boroVal(-)-pinanediol HCl salt) (**5b**): (-)-Pinanediol (1S)-(1-hexamethyldisilazaneamino-1-propyl)-1-boronate (**4b**) (0.27 mmol, 100 mg) was placed in a round bottom flask and cooled to – 10 °C using an ice/NaCl bath, and 1M HCl/ether (2 mmol, 2 mL) was added drop wise and stirred for 1 hr. The solvent was removed using nitrogen flush and then by high vacuum system. The yield was 69 mg (93%) of product as a light yellow solid [102]. ¹H NMR (400 MHz, CDCl₃): δ 4.32-4.28 (dd, J=1.75 Hz, 1H), 2.76-2.68 (dT, J=6.08 Hz, 1H), 2.36-2.28 (m, 1H), 2.24-2.16 (m, 1H), 2.06-2.01 (T, J=5.68 Hz, 1H), 1.92-1.87 (m, 1H), 1.87-1.8 (m, 1H), 1.79-1.68 (dT, J=7.36 Hz, 2H), 1.38 (s, 3H), 1.28 (s, 3H), 1.19-1.16 (d, J=7.91 Hz, 3H) **Figure 36**.

(-)-Pinanediol (1S))-1-amino-1-isobutyl-1-boronate HCl salt (**5c**): (-)-Pinanediol (1S)-(1-hexamethyldisilazaneamino-1-isobutyl)-1-boronate (**4c**) (0.27 mmol, 100 mg) was placed in a round bottom flask and cooled to – 10 °C using an ice/NaCl bath, 1M HCl/ether (2 mmol, 2 mL) was added drop wise and stirred for 1 Hr. The solvent was removed using nitrogen flush and then by high vacuum system. The yield was 72 mg (93%) of product as a yellow color solid [75]. ¹H NMR (400 MHz, CDCl₃): δ 4.32-4.28 (dd, J=1.75 Hz, 1H), 2.76-2.68 (dT, J=5.84 Hz, 1H), 2.36-2.28 (m, 1H), 2.24-2.16 (m, 1H), 2.06-2.01 (T, J=5.68 Hz, 1H), 1.92-1.87 (m, 1H), 1.87-1.8 (m, 1H), 1.38 (s, 3H), 1.28 (s, 3H), 1.19-1.16 (d, J=7.91 Hz, 3H), 1.01-0.96 (d, J=5.84 Hz, 6H), 0.84 (s, 3H) **Figure 37**.

(+)-Pinanediol (1R)-(1-aminoethyl)-1-boronate (L-boroAla-(+)-pinanediol HCl salt) (**5d**) : (-)-(+)-Pinanediol (1R)-(1-hexamethyldisilazaneamino-1-ethyl)-1-boronate (**4d**) (0.27 mmol, 100 mg) was placed in a round bottom flask and cooled to – 10 °C using an ice/NaCl bath, 1M HCl/ether (2 mmol, 2 mL) was added drop wise and stirred for 1 Hr. The solvent was removed using nitrogen flush and then by high vacuum system. The yield was 68 mg (97%) of product as a yellow solid. ¹H NMR (400 MHz, CDCl₃): δ 4.32-4.28 (dd, J=1.75 Hz, 1H), 2.92-2.88 (m, 1H), 2.76-2.68 (Q, J=8.06 Hz, 1H), 2.36-2.28 (m, 1H), 2.24-2.16 (m, 1H), 2.06-2.01 (T, J=5.68 Hz, 1H), 1.92-1.87 (m, 1H), 1.87-1.8 (m, 1H), 1.38 (s, 3H), 1.28 (s, 3H), 1.19-1.16 (d, J=7.91 Hz, 3H), 0.84 (s, 3H) **Figure 38**.

(1S)-(1-aminoethyl)-1-boronate (D-boroAla) (**6a**): D-boroala(-)Pd (**5a**) (0.39 mmol, 88 mg) was dissolved in 2 mL of 1:1 ether/water solution and phenylboronic acid (0.78 mmol, 96 mg) was added followed by 1M HCl (0.08 mmol, 78 µL) and stirred for 1 Hr. The reaction mixture was extracted 2 times with ether to remove phenyl boronic acid and pinanediol. The product is obtained by lyophilizing the water layer. The yield was 32 mg (92%) of product as a yellow color solid. ¹H NMR (400 MHz, CDCl₃): δ 3.46-3.39 (Q, J=6.31 Hz, 1H), 2.85-2.77 (Q, J=6.31 Hz, 1H), 2.7-2.62 (Q, J=6.31 Hz, 1H), 1.13-1.09 (d, J=7.78 Hz, 3H), 1.06-1.01 (T, J=7.48 Hz, 1H), 0.97-0.92 (T, J=6.73 Hz, 1H) **Figure 39**.

(1R)-(1-aminoethyl)-1-boronate (L-boroAla) (**6d**): D-boroala(+)Pd (**5d**) (0.39 mmol, 88 mg) was dissolved in 2 mL of 1:1 ether/water solution and phenylboronic acid (0.78 mmol, 96 mg) was added followed by 1M HCl (0.08 mmol, 78 µL) and stirred for 1 Hr. The reaction mixture was extracted 2 times with ether to remove

phenyl boronic acid and pinanediol. The product is obtained by lyophilizing the water layer. The yield was 31 mg (89%) of product as a yellow color solid. ^1H NMR (400 MHz, CDCl_3): δ 3.46-3.39 (Q, $J=6.31$ Hz, 1H), 2.85-2.77 (Q, $J=6.31$ Hz, 1H), 2.7-2.62 (Q, $J=6.31$ Hz, 1H), 1.13-1.09 (d, $J=7.78$ Hz, 3H), 1.06-1.01 (T, $J=7.48$ Hz, 1H), 0.97-0.92 (T, $J=6.73$ Hz, 1H) **Figure 40**.

Pinacol aminomethylboronate hydrochloride (boroGly-pinacol): The synthesis strategy used for boroGly-pinacol is outlined in **Figure 13**.

Pinacol-1-(chloromethyl)-1-boronate (7): Diisopropyl (chloromethyl)boronate was synthesized following the procedure of Sadhu and Matteson, and converted in situ to the pinacol ester [89]. Briefly, 19.2 mL (48 mmol) of 2.5 M nBuLi in hexanes was added dropwise down the cold reaction vessel wall to a stirred mixture of 3.8 mL of ClCH_2I (52 mmol) and 12 mL (51 mmol) $\text{B}(\text{OiPr})_3$ in 60 mL of dry THF at -78°C under argon. After 1 h the reaction mixture was allowed to warm to 10°C and stirred for an additional 30 min. The diisopropyl (chloromethyl)boronate was converted to the pinacol ester *in situ* by first titrating the reaction mixture containing diisopropyl (chloromethyl)boronate with HCl/ether to the methyl orange endpoint, and then adding 6.03 g (51 mmol) of pinacol. The mixture was stirred overnight under argon, and the product isolated by distillation, first by removing volatile components (THF, iPrOH) by distillation at atmospheric pressure, and then rapid fractional distillation through a short Vigreux column under vacuum, where the product distilled over at $85\text{-}100^\circ\text{C}$ at 5 mm Hg to provide 8.98 g (48% overall) of the pure product as a clear oil. ^1H NMR for (7) was as described previously.

Pinacol bis-(trimethylsilyl)aminomethylboronate (pinacol N,N-bis-(trimethylsilyl)-boroGlycine) (8): This reaction was performed following the general procedure of Matteson and Sadhu. Briefly 20 mL of freshly distilled THF over sodium/benzophenone was taken in a round bottom flask and cooled to -78 °C using nitrogen/isopropanol bath. 1,1,1,3,3,3-hexamethyl disilazane (61 mmol, 2.44 mL) was added to the reaction vessel, then 2.5 M butyl lithium (61 mmol, 3.5 mL) was added along the cold walls. The reaction mixture was warmed to room temperature for 10 min, then cooled to – 78 °C. Pinacol-1-(chloromethyl)-1-boronate (**7**) (50.9 mmol, 8.98 g) was added to the reaction mixture and allowed to warm to room temperature and the reaction vessel kept in desiccator for 4 days. THF was distilled off at aspirator vacuum and the product is collected at 90 – 95 °C by distillation at 50 µm of Hg. The yield was 2.25 g of product as a yellow oil.

BoroGly-pinacol. (9): To a solution of 2.25 g of *Pinacol bis-(trimethylsilyl)aminomethylboronate (8)* (7.14 mmol) in 10 mL of ether at -80 °C was added 11 mL (22 mmol) of a 2 M solution of hydrogen chloride in ether. The reaction mixture was allowed to warm to room temperature and diluted with 25 mL of hexane. The precipitate formed upon hexane addition was filtered, washed with hexane, and dried to give 1.46 g (7.07 mmol, 99%) of a white crystalline solid. ¹H NMR: δ 1.279 (s, 12H, pinacolyl), 1.506 (d, J) 7.5 Hz, 3H, CH₃CHB), 2.92-3.10 (br s, 1H, CH₃CHB), 8.10-8.35 (br s, 3H, NH₃⁺) [103].

Acetyl-D-boroAla-(-)-pinanediol (10): Acetyl-D-boroAla-(-)-pinanediol was synthesized from D-boroAla-(-)-pinanediol as described previously [88]. D-boroAla-(-)-pinanediol hydrochloride (**5a**) (0.15 mmol, 40 mg) was dissolved in 3 mL of DCM at

–10 °C. To this TEA (0.45 mmol, 63 μ L) was added followed by acetyl chloride (0.23 mmol, 17 μ L). After 1 hr the reaction mixture was diluted with 7 mL of DCM and quenched with 3 mL of 1M hydrochloric acid, back extracted with 3 mL of water, 3 mL of saturated sodium bicarbonate solution, and 3 mL of water. The organic layer was dried over anhydrous magnesium sulfate and evaporated to dryness to give the product as a white solid. Yield 38 mg.

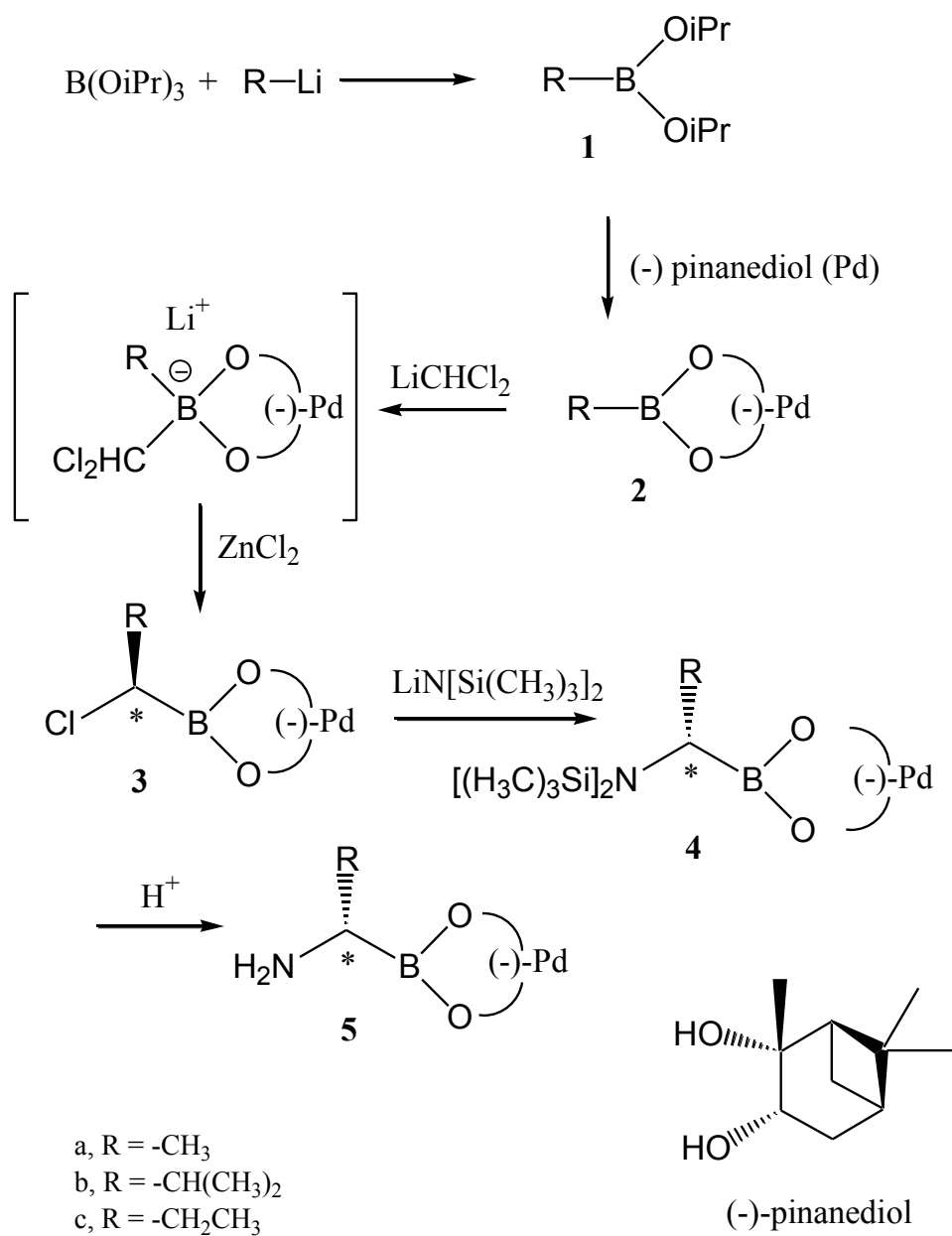


Figure 10. Synthetic scheme for the synthesis of D-boro amino acid analogs

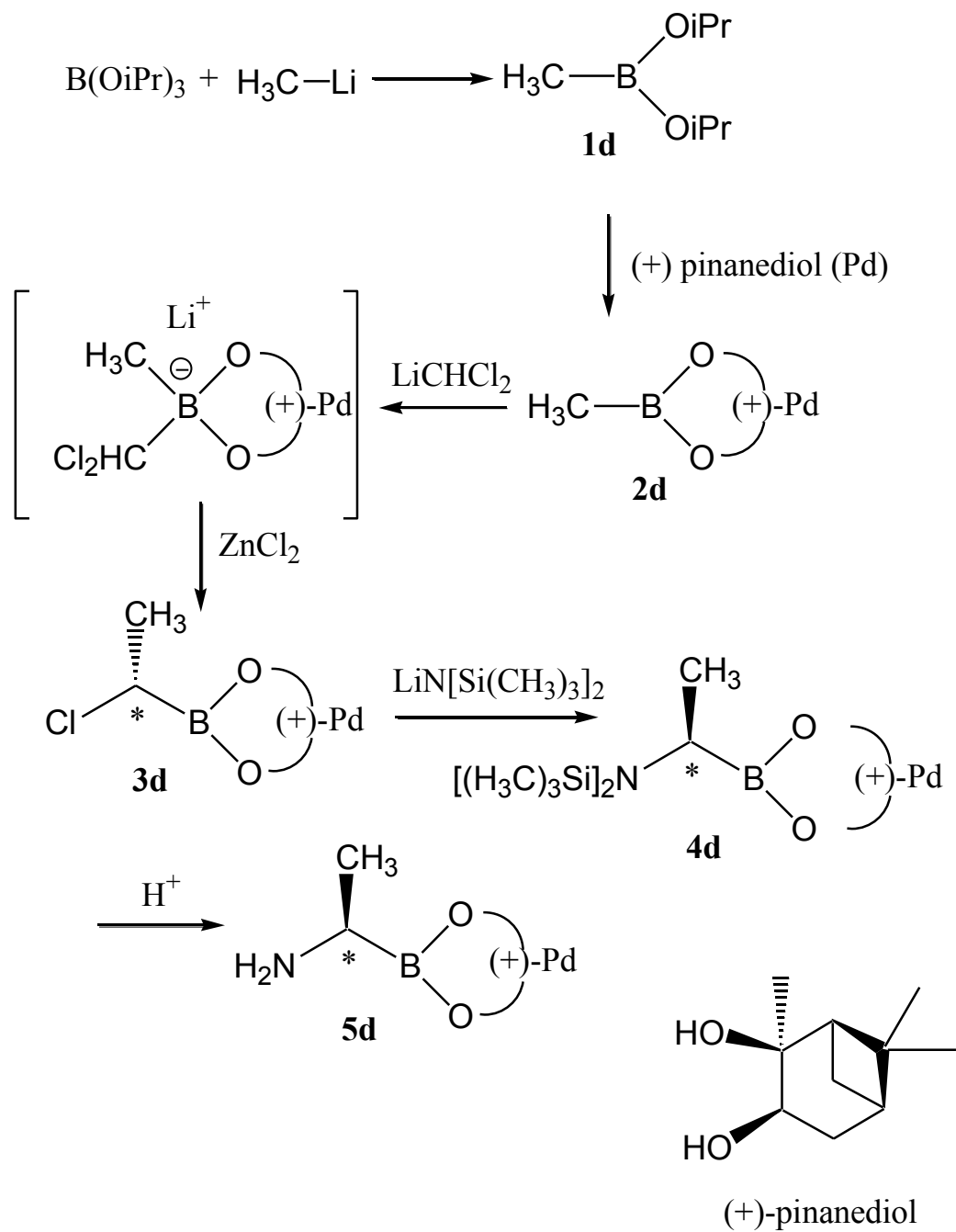


Figure 11. Synthetic scheme for L-boroAla-(+)Pd



Figure 12. Synthetic scheme for D-boroAla (**6a**).

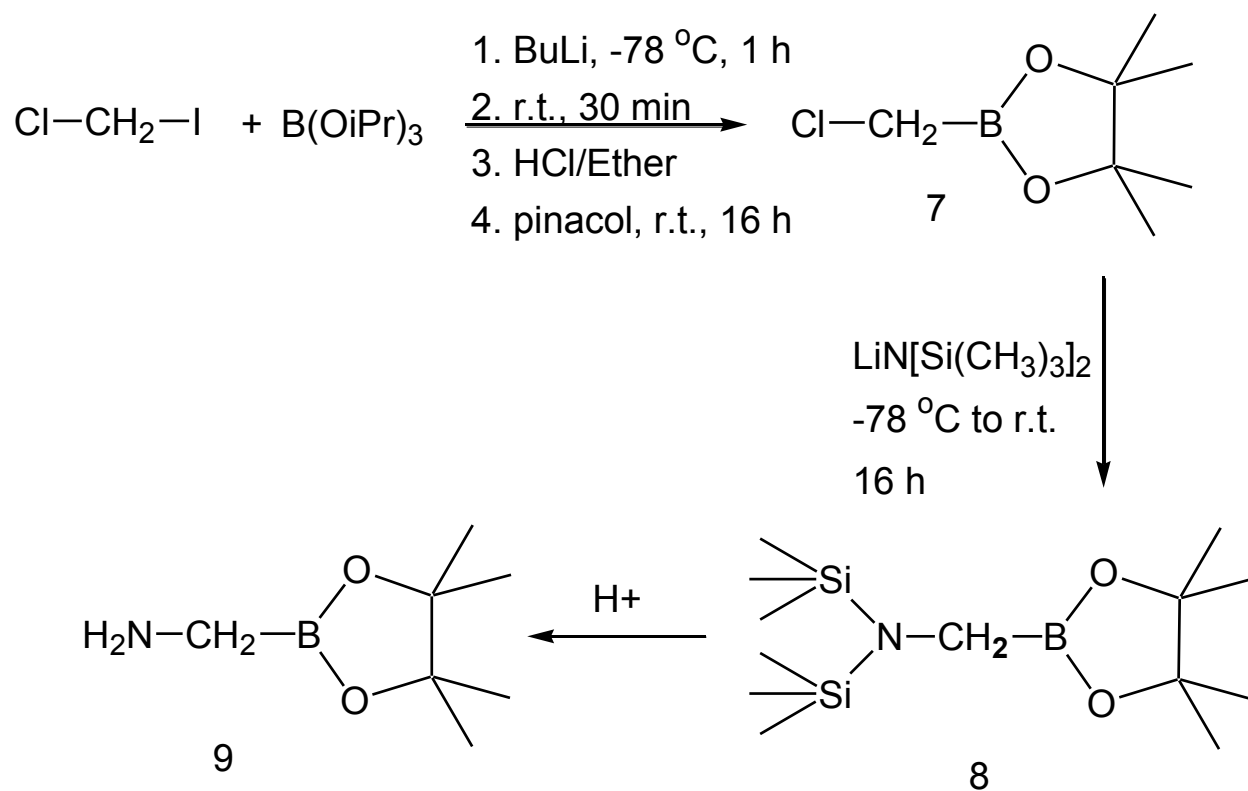


Figure 13. Synthetic scheme for boroGly pinacol (**9**).

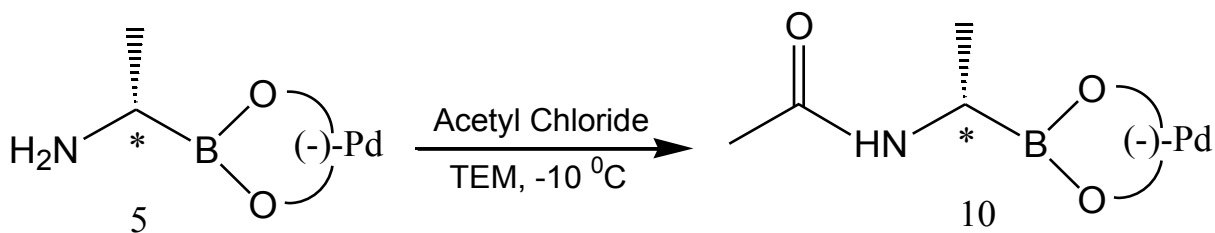


Figure 14. Synthetic scheme for Acetyl-D-boroAla-(-)-pinanediol (**10**)

Antibacterial Properties Characterization

Spectrum of activity: MICs were determined against several bacterial pathogens (**Table 3**), including both Gram-positive and Gram-negative organisms.

Minimal inhibitory concentrations (MICs): MICs were determined by broth microdilution generally following CLSI guidelines (Clinical and Laboratory Standards Institute, formerly National Committee for Clinical Laboratory Standards) [104]. Two-fold serial dilutions of test agents were prepared in 100 μ L of Mueller Hinton Broth (Difco) in the wells of microtiter plates. Wells were inoculated with $\sim 1 \times 10^4$ cfu of the test bacteria, and plates incubated for 16-20 hrs at 35 °C. The plates were read for turbidity either visually or at 600 nm in a Tecan SpectroFluor Plus microtiter plate reader. The MIC was read as the lowest concentration of test compound for which no turbidity is apparent (Transmittance >90% of a media control well). Each determination was performed in triplicate.

Minimal bactericidal concentrations (MBCs): MBCs were performed by plating serially diluted inhibited samples from the MIC determination onto agar media. After overnight (24 hrs) incubation at 35 °C, colonies were counted and used to calculate cfu's of the samples. The MBC was defined as the lowest concentration of drug which killed 99.9% (log3 reduction) of the original inoculum.

Frequency of resistance against D-boroAla: A clinical isolate of methicillin-sensitive *S. aureus* (MSSA) was grown for 16 hours at 35 °C in 100 mL Mueller Hinton Broth, with shaking at 250 rpm. Bacterial cells were concentrated from 50 mL of this saturated overnight culture by centrifugation at 3000 rpm for 15 minutes and reconstituted into a volume of 5 mL media. Volumes of 0.4 mL ($\sim 1 \times 10^9$ cfu) were

plated onto 150-mm agar plates containing 75 mL of media with D-boroAla-(-)-pinanediol at concentrations of 2x and 4x MIC. As a reference, the cfu of the reconstituted culture was also determined. At each concentration, 3-4 plates were used. Inoculated plates were incubated for 48 hours at 35 °C and each plate visually screened for growth of single colonies. Representative subsets of observed colonies were selected using a sterile inoculating loop and restreaked onto fresh media containing compound (at selection concentration). Colonies that did not grow on fresh media containing test D-boroAla against were not considered resistant. The frequency of resistance was calculated by dividing the number of resistant colonies by the total number of cfu's plated.

Determination of in vivo L-Ala, D-Ala, and D-Ala-D-Ala levels in response to D-boroAla-(-)-pinanediol (5a): Levels of L-Ala, D-Ala, and D-Ala-D-Ala were determined as described in detail previously [105]. Bacteria (*Escherichia coli* K12 or MRSA (clinical isolate)) were grown to an OD at 600 nm of 0.6 in either minimal media (*E. coli*) or Mueller Hinton broth (MRSA). To a test culture was added D-boroAla-(-)-pinanediol (**5a**) to 4x MIC, and to control cultures were added no antibiotic, or one of two control antibiotics (tetracycline or vancomycin) at 4x their respective MICs. Growth inhibition was observed within 15 min. Once growth inhibition was apparent cultures were rapidly cooled in an ice/water bath, 4 samples of 10 mL were moved from each flask to ice-cold 15-ml centrifuge tubes, and the cells were pelleted by centrifuge at 3000 rpm for 10 min at 2 °C. Cell pellets (~50 µL) were resuspended in 100 µL of ice-cold M9 minimal medium and treated with 200 µL of ice-cold 80% acetone spiked with 20 µM ¹³C₃-D-Ala as an internal standard. Tubes were kept on

ice with occasional vortexing for 5 min. These tubes were again centrifuged, and supernatants were collected into fresh ice-cold microcentrifuge tubes. Samples (15 μ l) were derivatized with Marfey's reagent, and analyzed by LC-MS/MS.

Marfey's derivatization reactions: Marfey's derivatization was performed as described previously [105], briefly 15 μ L of the culture extract was added to 15 μ L of 10 mM Marfey's reagent (w/v in acetone) and then 5 μ L of 1 M triethylamine. The contents were mixed by vortexing and incubated at 37 °C for 150 min. The derivatization reaction was quenched by adding 5 μ L of 1 M HCl, and the sample was diluted to 200 μ L using 75% H₂O/25% acetonitrile + 0.1% formic acid and analyzed by LC-MS/MS.

Chromatographic conditions: Chromatography was performed at a flow rate of 300 μ l/min, with 75% solvent A (100% H₂O and 0.1% formic acid) and 25% solvent B (70% acetonitrile/30% H₂O + 0.1% formic acid) for the first minute, followed by a linear gradient to 50% solvent A/50% solvent B in 11 min and then a gradient to 100% solvent C (100% acetonitrile + 0.1% formic acid) in 1 min.

Mass spectrometer conditions: An LC/MS/MS (MRM) separation and quantitation method was set up and used for quantitation of Marfey's adducts of D-Ala, L-Ala and D-Ala-D-Ala using the parameters detailed in **Table 1**.

Table 1. Summary of optimized parameters for MS/MS detection of Marfey's adducts

MS Parameters	
DP (V)	60
EP (V)	6
CEP (V)	Instrument Default
MS/MS Parameters	
CE (V)	20
CXP (V)	4
CAD (Arb)	5
ESI Parameters	
TEM (°C)	175
CUR (Arb)	30
GS1 (Arb)	40
GS2 (Arb)	50

Abbreviations; Arb=Arbitrary instrument based setting; DP=declustering potential; EP=entrance potential; CEP=collision cell exit potential; CE=collision energy; CXP=collision cell exit potential; CAD=collisionally activated dissociation; TEM=temperature; CUR=curtain gas setting; GS1 and GS2, gas spray 1 and 2 settings, respectively.

Results

Structure-activity correlation: A summary of MICs against MSSA (clinical isolate), MRSA (clinical isolate), and *E. coli* K12 is given in **Table 2**. D-boroAla-(-)-pinanediol (**5a**) has the most potent activity in this series. D-boroHomoAla-(-)-pinanediol (**5b**), D-boroVal-(-)-pinanediol (**5c**), and boroGly-(-)-pinacol (**9**) were found to have worse (higher) MIC values than D-boroAla-(-)-pinanediol (**5a**). Removal of the pinanediol group also reduced antibacterial effectiveness, which is presumably due to the lipophilic pinanediol group facilitating transport across the bacterial membrane. Acetyl-D-boroAla-(-)-pinanediol (**11**) was completely inactive, indicating that a positively charged amino group is required for antibacterial activity. Finally, L-boroAla-(+)-Pd (**5d**) [88] (the opposite enantiomer of **5a**), had very weak activity. Filter disc assay was done on D-boroAla-(-)-pinanediol (**5a**), L-boroAla-(+)-Pd (**5d**) and pinanediol and was shown in **Figure 15**.

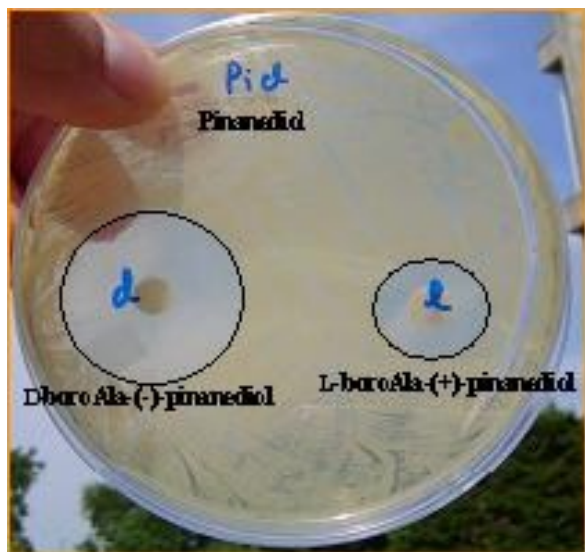


Figure 15. Zone of inhibition of D-boroAla-(-)-Pd, L-boroAla-(-)-Pd and pure pinanediol.

Table 2. Structure/activity correlation of different analogues of D-boroAla

Cmpd	MIC: μM and ($\mu\text{g/mL}$)		
	MSSA	MRSA	<i>E. coli</i>
	(clinical)	(clinical)	(K12)
5a	50 (10)	50 (10)	100 (20)
5b	200 (50)	1000 (250)	1000 (250)
5c	5000 (1250)	5000 (1250)	5000 (1250)
5d	1000 (250)	ND ¹	400 (100)
6a	200 (25)	200 (25)	400 (50)
9	Weak Activity	ND ¹	NA ¹
10	NA ¹	NA ¹	NA ¹
¹ ND – not determined, NA – no activity.			

Minimal inhibitory concentrations: MICs were determined against several bacterial pathogens, that include Gram-positive bacteria like *Enterococcus faecium* (VRE, clinical), MRSA (clinical), MSSA (clinical), and Gram-negative bacteria like *Salmonella typhi* (clinical), *Escherichia coli* K12, *Shigella sonnei* (clinical), *Pseudomonas aeruginosa* (ATCC 27853), *Burkholderia pseudomallei* (strain 1026b), to determine spectrum of activity. MICs were determined for compounds D-boroala(-)Pd (**5a**), D-boroAla (**6a**) and compared with commercially available antibiotics like D-cycloserine, vancomycine, tetracycline, ampicillin, and cefoxitin. The results were tabulated in **Table 3**. All MICs determinations were performed in triplicate.

Bactericidal activity. D-boroAla(-)-pinanediol (**5a**) was bactericidal against *S. aureus* and *Bacillus subtilis* at 1x MIC, and against *E. coli* and *Salmonella enterica* Serovar Typhimurium at 4x MIC. Results are tabulated in **Table 4**.

Frequency of Resistance. A frequency of resistance determination was performed for D-boroAla(-)-pinanediol (**5a**) against MSSA (clinical) at 2x and 4x MIC (16 and 32 µg/mL respectively). At 2x MIC a frequency of resistance of 1×10^{-6} was observed whereas at 4x MIC a frequency of resistance of 8×10^{-8} was observed.

Table 3. Spectrum of activity: MICs for D-boroAla-(-)-pinanediol, D-boroAla (no pinanediol), and control antibiotics.

Strain		MIC ($\mu\text{g/mL}$)						
		D-boroAla-(-)-Pd (6a)	D-boroAla (8)	Control antibiotics ^a				
				D-Cycloser	Vanc	Tet	Amp	Cefoxitin
<i>Enterococcus faecium</i> (VRE, clinical)	G+	16	>128	32	>512	8	128	>256
MRSA (clinical)	G+	16	64	16	1	0.125	128	>256
MSSA (clinical)	G+	8	64	8	2	0.0625	32	4
<i>Salmonella typhi</i> (clinical)	G–	8	32	64	>512	0.5	8	2
<i>Escherichia coli</i> K12	G–	32	256	8	>256	0.5	8	2
<i>Shigella sonnei</i> (clinical)	G–	64	>128	32	>512	16	2	2
<i>Pseudomonas aeruginosa</i> (ATCC 27853)	G–	128	ND ^b	ND ^b	ND ^b	ND ^b	ND ^b	ND ^b
<i>Burkholderia pseudomallei</i> (strain 1026b)	G–	64	ND ^b	ND ^b	ND ^b	ND ^b	ND ^b	ND ^b

^aD-Cycloser, D-cycloserine; Vanc, vancomycin; Tet, tetracycline; Amp, ampicillin.

^bND, not determined.

MRSA, methicillin-resistant *Staphylococcus aureus*; MSSA, methicillin-sensitive *S. aureus*; MIC, minimal inhibitory concentrations.

Table 4. MICs and MBCs for D-boroAla-(-)-pinanediol against several bacterial strains.

Strain		MIC	MBC
		($\mu\text{g/mL}$)	
<i>Staphylococcus aureus</i> (ATCC 29213)	G+	16	16
<i>Salmonella enterica</i> Seroovar Typhimurium (ATCC 14028)	G–	32	>128
<i>Bacillus subtilis</i> (ATCC 6633)	G–	16	16
<i>Escherichia coli</i> (K12)	G–	32	>128

Marfey's derivatization reactions: L-Ala, D-Ala, and D-Ala-D-Ala are small hydrophilic molecules that are not retained on reverse phase high-performance liquid chromatography (HPLC) media and are too small to give quantifiable ions by multiple reaction monitoring (MRM), which is the generally used method for quantitation in LC–MS/MS. Therefore, it is necessary to derivatize them for LC–MS/MS analysis. Also, L-Ala and D-Ala are enantiomers with the same mass and, therefore, will need to be separated chromatographically for quantitation by LC–mass spectrometry (MS)-based methods. Marfey's reagent is a chiral analog of Sanger's reagent that allows D- and L-amino acids to be separated by HPLC for quantitation [106-107, 109]. Marfey's adducts formed after Marfey's derivatization of L-Ala, D-Ala and D-Ala-D-Ala are shown in **Figure 16**. After Marfey's derivatization of L-Ala and D-Ala have become diastereomers which are easily separable on HPLC column. A sample MRM chromatogram for an untreated *E. coli* extract was shown in **Figure 17**. The top panel represents the LC–MS/MS chromatogram detected at m/z 342.2/297.2 (Q1/Q3), which is specific for the Marfey's derivatives of β -Ala (left peak at 5.6 min), L-Ala (center peak at 8.2 min, 15 pmol), and D-Ala (right peak at 9.6 min, 10 pmol). The center panel represents analogous data at m/z 345.2/200.2, which is specific for the Marfey's derivative of $^{13}\text{C}_3$ -D-Ala used as an internal standard (20 pmol), and the bottom panel represents analogous data for m/z 413.2/358.2, which is specific for the Marfey's adduct of D-Ala-D-Ala (peak at 8.7 min, ~3 pmol).

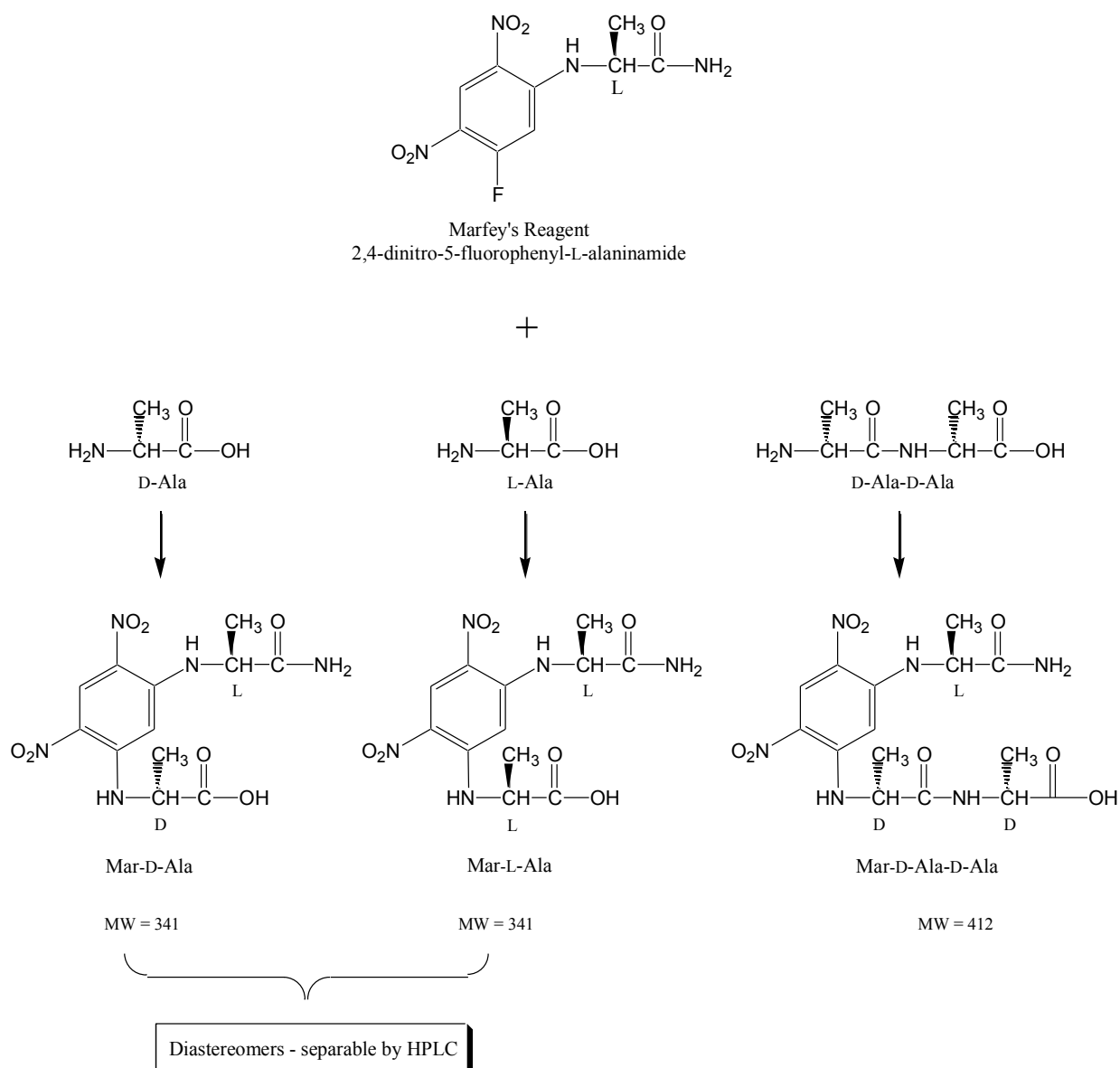


Figure 16. Marfey's reagent and reactions to give adducts with L-Ala, D-Ala and D-Ala-D-Ala. Adapted from Jamindar et. al. 2010.

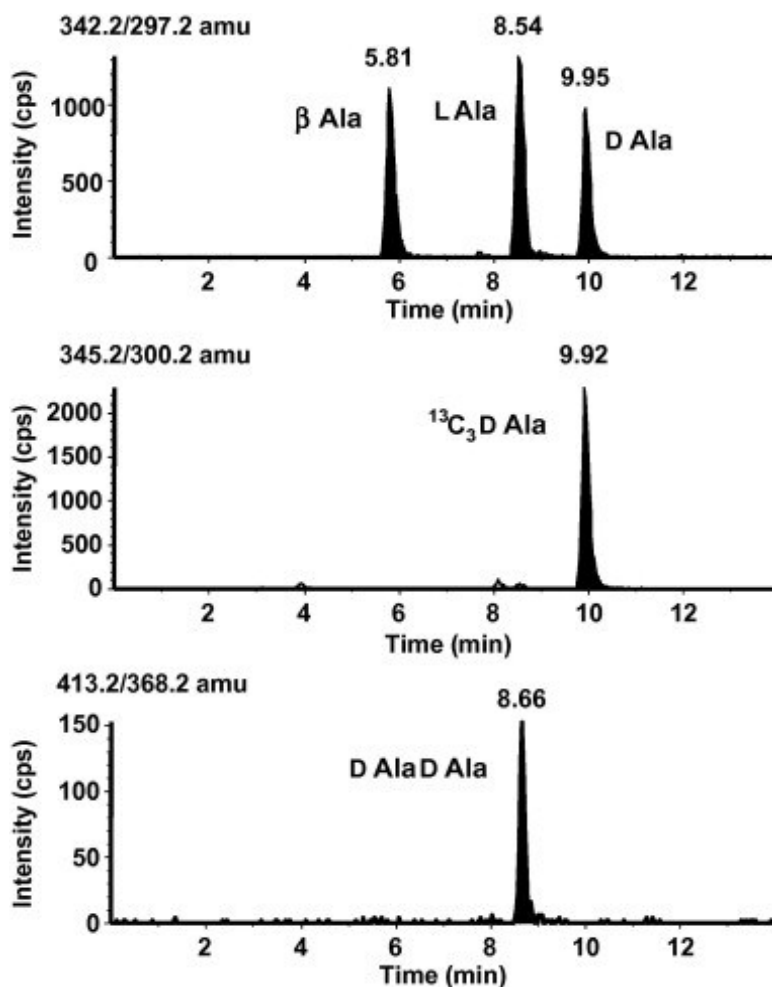


Figure 17. Sample MRM chromatogram for an untreated *E. coli* extract. The top panel represents the LC–MS/MS chromatogram specific for the Marfey's derivatives of β-Ala (peak at 5.6 min), L-Ala (peak at 8.2 min), and D-Ala (peak at 9.6 min). The center panel represents Marfey's derivative of ¹³C₃-D-Ala used as an internal standard and the bottom panel represents Marfey's derivative of D-Ala-D-Ala (peak at 8.7 min). Adapted from Jamindar et. al. 2010.

Discussion

Previous biochemical studies [99] have identified D-boroAla as an effective inhibitor of both alanine racemase (saturable time dependent inhibition with $K_i = 20$ mM and $k_{inact} = 0.35 \text{ min}^{-1}$) and D-Ala-D-Ala ligase (K_i under intracellular conditions against the *S. Typhimurium* enzyme of 18 μM). There have however been no previous reports on the antibacterial activity of D-boroAla. During the course of our investigations on peptide-D-boroAla derivatives as inhibitors of the penicillin-binding proteins [88] we observed antibacterial activity in some crude peptide-D-boroAla preparations which was lost on purification of the peptide-D-boroAla derivative. A filter disc test of D-boroAla (**6a**) for antibacterial activity revealed surprisingly good activity for D-boroAla-(-)-Pd (**5a**) against both *E. coli* and *S. aureus* indicating possible broad spectrum activity, and it seemed worthwhile to further characterize the antibacterial activity of D-boroAla and its homologs.

A structure-activity study was first performed by synthesizing a series of D-boroAla homologs. Three features of D-boroAla were examined including; 1) the length of the side chain alkyl group, 2) the effect of N-acylation, and 3) the effect of the presence or absence of the pinanediol protecting group. Pinanediol protecting groups are used in amino boronic acid syntheses to control the stereochemical outcome of the product [75, 110-111]. In aqueous solutions the boro-pinanediol ester is in equilibrium with the free boronic acid and pinanediol. A control test of racemic pinanediol revealed no antibacterial activity (data not shown). Among the compounds tested in this study, D-boroAla-(-)-pinanediol was the most active, with MICs against *E. coli* and *S. aureus* in the 8 to 32 $\mu\text{g/mL}$ range **Table 2** and **Table 3**.

Removal of the pinanediol group resulted in higher MICs, likely due to the lipophilic pinanediol group facilitating membrane permeability. L-boroAla showed much lower antibacterial activity, demonstrating stereospecificity of the antibacterial activity. This observation indicates that D-boroAla likely acts on a specific macromolecular target, and not simply as a non-specific membrane disrupting agent. Longer and shorter side chain homologs of D-boroAla (e.g. boroGly, D-boroHomoAla, and D-boroVal) demonstrated greatly reduced antibacterial activity. Acetylation of D-boroAla to give acetyl-D-boroAla abolished activity, demonstrating that a positively charged amine group is required for antibacterial activity.

Activity of D-boroAla was then tested against several Gram negative and Gram positive pathogenic bacteria to determine spectrum of activity **Table 3**. Broad spectrum activity against both Gram-positive and Gram-negative bacteria was observed, with MICs ranging from 8 to 128 µg/mL. Bactericidal activity was apparent at 1x MIC against *S. aureus* and *B. subtilis*, and at 4x MIC against *S. Typhimurium* and *E. coli* **Table 4**.

The frequency of resistance at 4x MIC was 8×10^{-8} . This is comparable to or lower than rifampicin resistance frequency in several bacterial strains [112-113] and falls at the lower end of the weakly hypermutable range (4×10^{-8} to 4×10^{-7}), and just above the normomutable range (8×10^{-9} to 4×10^{-8}) [114-115]. These are generally favorable characteristics, except for the frequency of resistance which is somewhat on the high side for a prospective antibacterial agent. Given these observations, an obvious question was: what is the molecular target of D-boroAla? Several lines of

evidence suggested that D-boroAla would act in the alanine branch of the bacterial cell wall biosynthesis pathway **Figure 9**, including that bacterial cell wall biosynthesis is unique in its requirement for D-Alanine, that the antibacterial activity in this series of compounds is correspondingly specific to D-boroAlanine **Table 2**, and that D-boroAla has previously been described as an inhibitor of both alanine racemase and D-Ala-D-Ala ligase [99] – the two enzymes catalyzing the reactions in the alanine branch **Figure 9**. We have recently developed an assay for the intermediates (L-Ala, D-Ala, and D-Ala-D-Ala) in the alanine branch of bacterial cell wall biosynthesis [105]. This assay was used to determine whether D-boroAla had a significant impact on the early cell wall intermediates in both *E. coli* and *S. aureus* and demonstrate that D-boroAla has a substantial effect on the level of D-Ala-D-Ala above its MIC in both *E. coli* **Figure 18** and *S. aureus* **Figure 19**. This effect is centered on the MIC for D-boroAla **Figure 18** –D-boroAla exhibits little effect on D-Ala-D-Ala levels below its MIC, but a pronounced effect above its MIC. It is also notable that the control antibiotic cycloserine exerts its effect on both D-Ala and D-Ala-D-Ala levels, consistent with its known mechanism of action as an alanine racemase inhibitor. From these observations, we conclude that D-boroAla exerts its antibacterial activity through inhibition of DDL. As a further test of biochemical mechanism, it is known that in *S. aureus* that the addition of D-Ala can antagonize the antibacterial action of cycloserine [116-117] which targets alanine racemase. We have also observed that D-Ala at 2.5 mM antagonizes the antibacterial activity of cycloserine at 2× and 4× MIC, but does not antagonize the antibacterial activity of D-

boroAla at 2× and 4× MIC, which is an observation also consistent with DDL as the molecular target of D-boroAla.

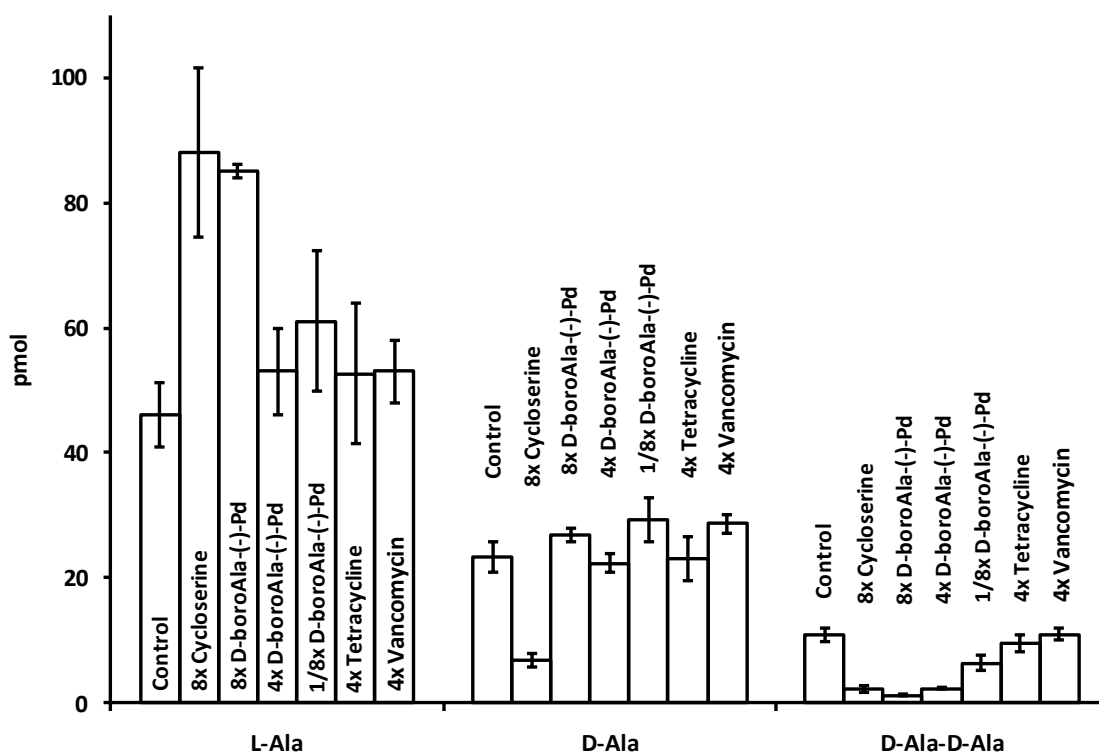


Figure 18. Levels of L-Ala, D-Ala, and D-Ala-D-Ala in *E. coli* as a function of added agents.

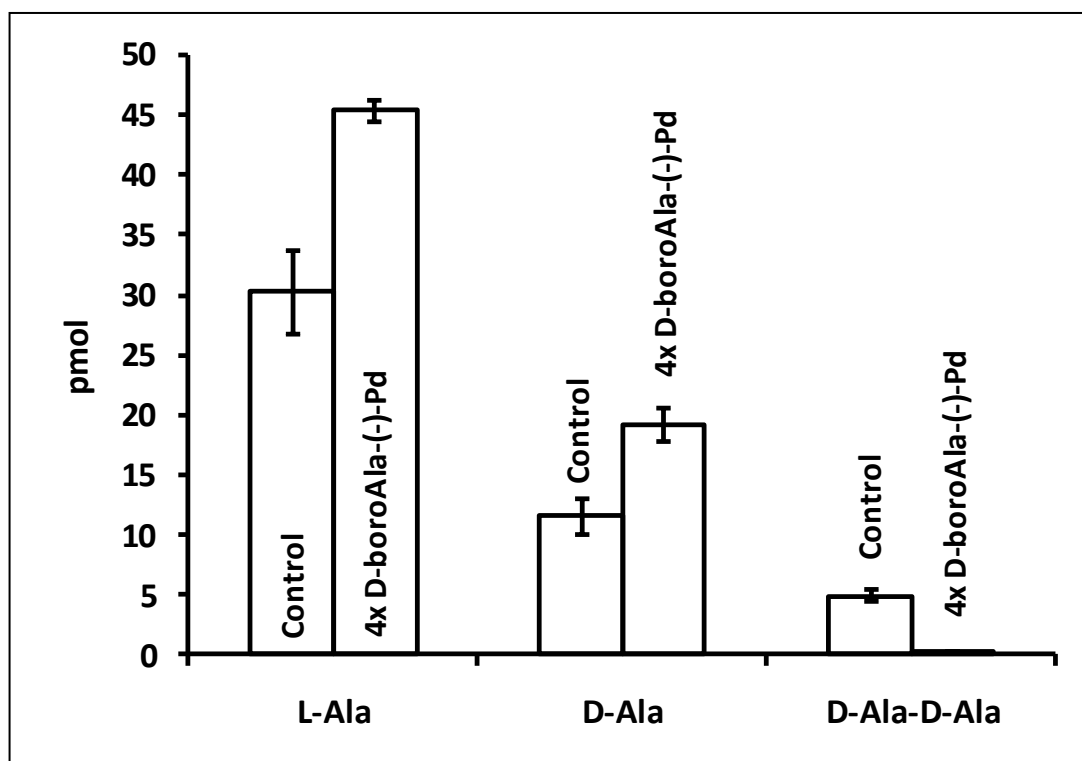


Figure 19. Levels of L-Ala, D-Ala, and D-Ala-D-Ala in *S. aureus* as a function of no added D-boroAla-(-)-Pd (control) and 4x MIC of added D-boroAla-(-)-Pd. This experiment was performed as described for *E. coli* in the main text, with the exception that since *S. aureus* is fastidious it was necessary to grow in Mueller Hinton Broth. Because of background levels of amino acids in Mueller Hinton Broth, cells were washed 3x in ice cold minimal media prior to lysis and metabolite analysis.

The identification of DDL as the molecular target of D-boroAla's antibacterial activity can be used to rationalize the MBC/MIC ratios observed against several bacterial strains **Table 4**. The difference in MBC/MIC ratio between bacterial strains appears correlated with the number of copies of DDL in the genomes of these organisms (1 in *S. aureus* and *B. subtilis*, and 2 in *E. coli* and *S. Typhimurium*). Our working hypothesis is that at 1x MIC D-boroAla inhibits the one DDL in *S. aureus* and *B. subtilis*, and is bactericidal. However, against *E. coli* and *S. Typhimurium* which have two copies of DDL, 1x MIC D-boroAla inhibits only one of the two DDLs which inhibits growth, while the other DDL appears capable of keeping these organisms viable. At higher D-boroAla concentrations (4x MIC) both DDLs in *E. coli* and *S. Typhimurium* are inhibited by D-boroAla, which then causes cell death.

Conclusions and Future Directions

This study demonstrates that D-boroAla has effective broad spectrum antibacterial activity, is bactericidal, and acts on D-Ala-D-Ala ligase. There has recently been considerable interest in D-Ala-D-Ala ligase as a potential target for antibacterial agent development [118], and the observations reported here further support D-Ala-D-Ala ligase as a viable target for the development of novel antibacterial agents. Future studies directed towards characterizing D-boroAla against the two DDL variants found in *E. coli* and *S. Typhimurium* will be of interest to determine which of these DDLs is of lower and higher affinity, and their correlation with D-boroAla's in vivo activity. This study also raises the question of why do some bacteria have two copies of DDL. One explanation is that two different DDL

enzymes with different kinetic properties may be required to allow efficient bacterial cell growth or survival under different growth condition, for example under nutrient rich or nutrient starved conditions. D-boroAla and gene knockout experiments could be used to address this question.

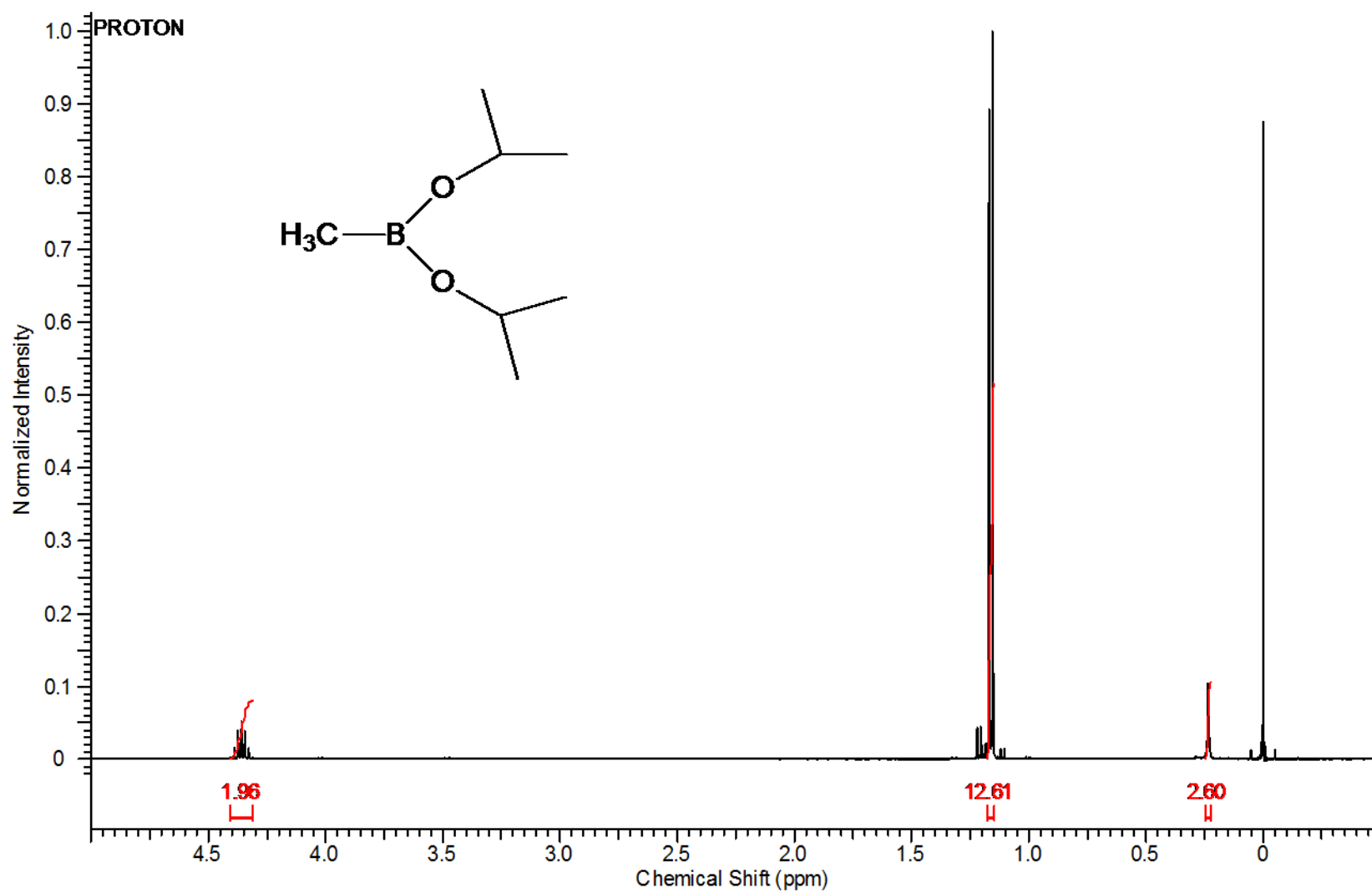


Figure 20. NMR spectrum of Diisopropyl-(1-methyl)-1-borate (**1a**)

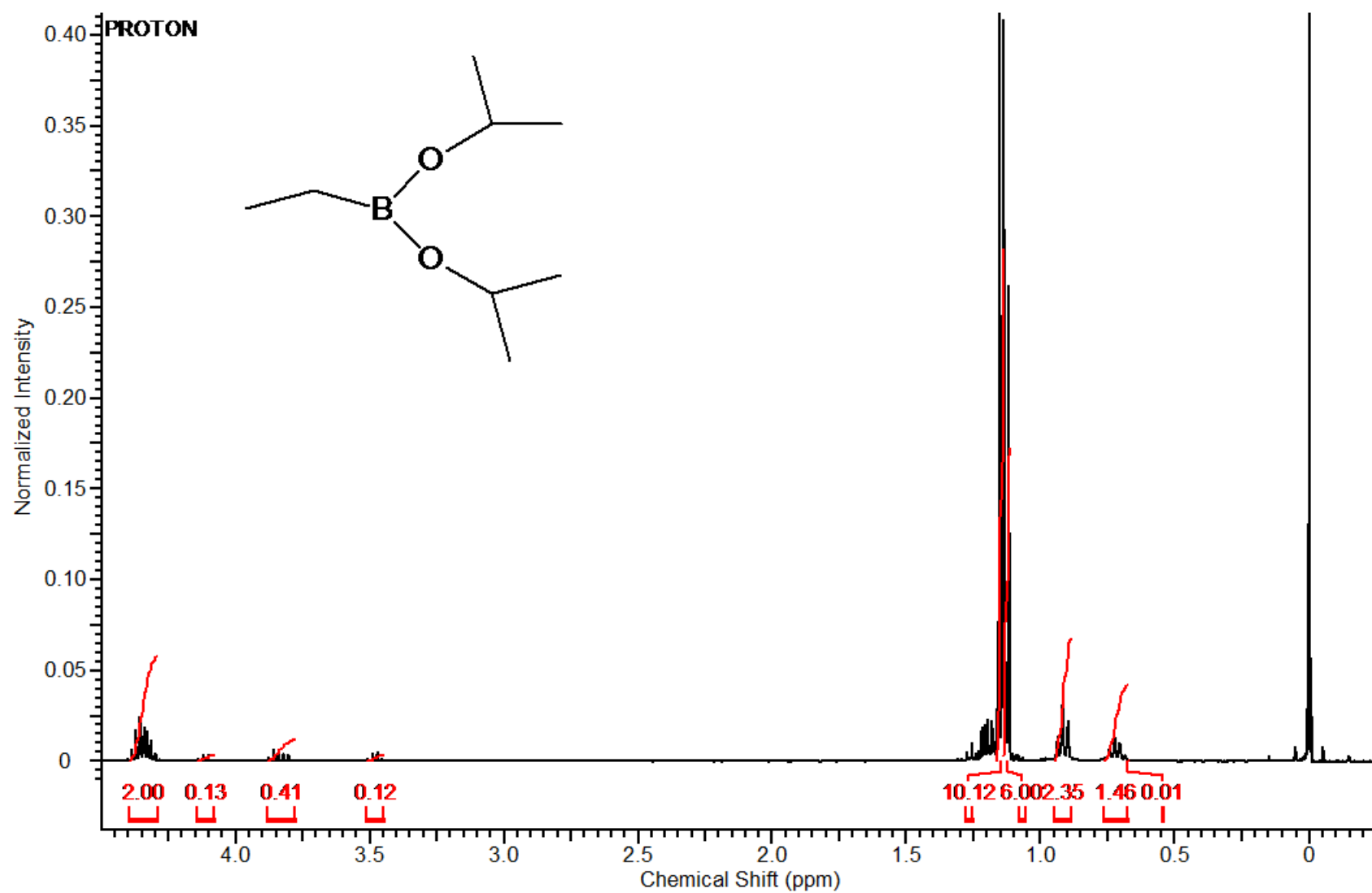


Figure 21. NMR spectrum of Diisopropyl-(1-ethyl)-1-borate (**1b**)

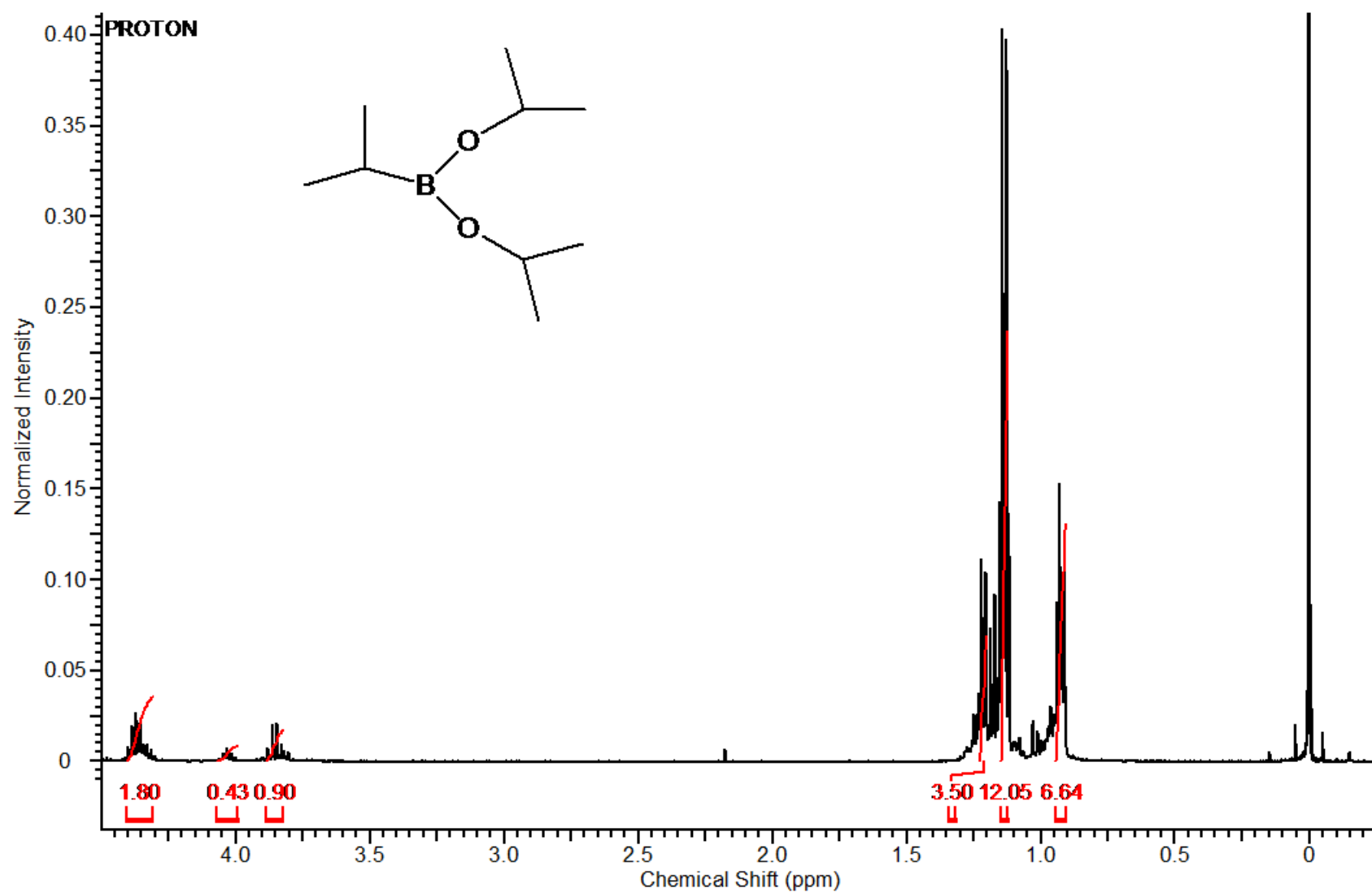


Figure 22. NMR spectrum of Diisopropyl-(1-isopropyl)-1-borate (**1c**)

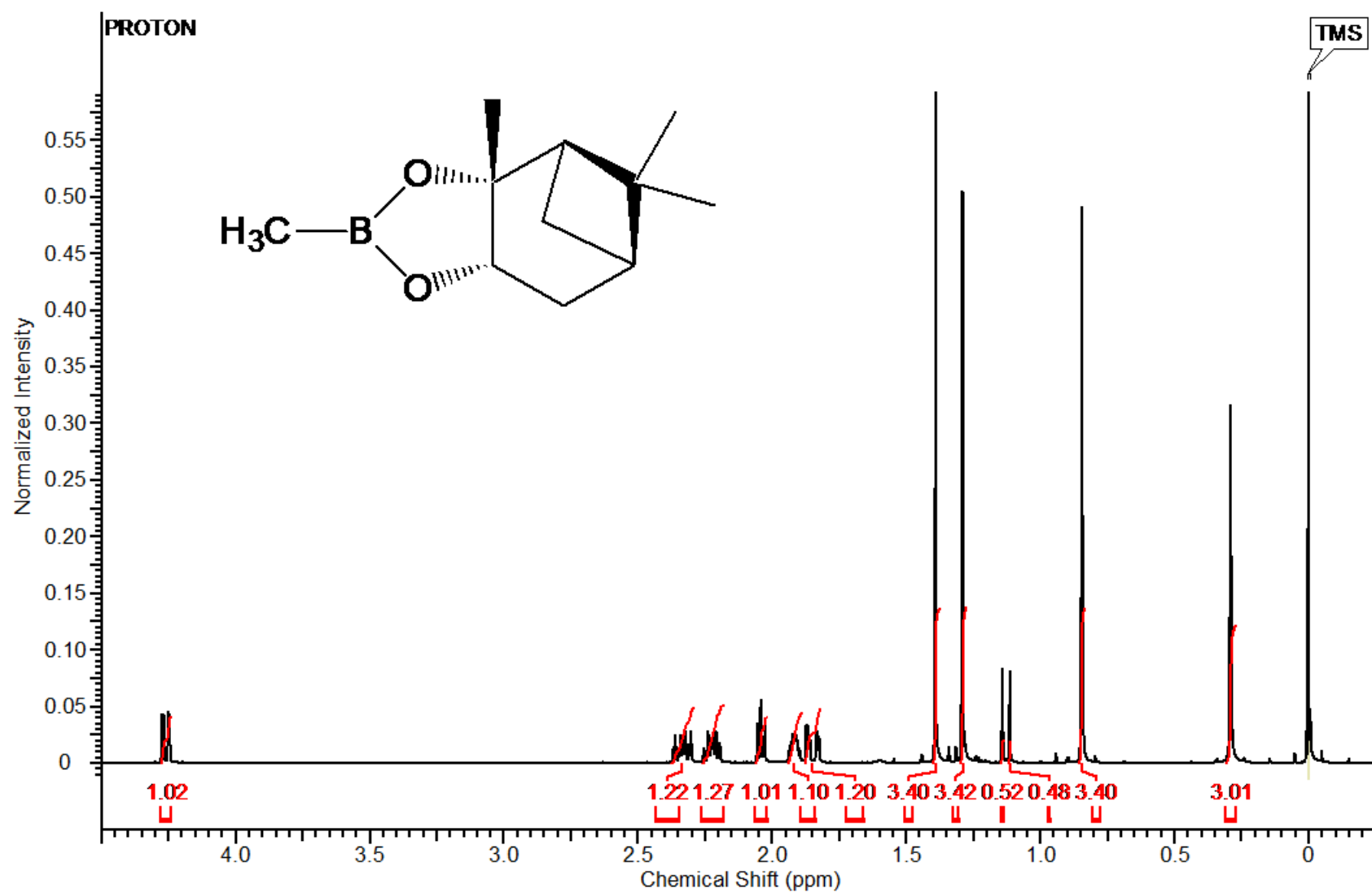


Figure 23. NMR spectrum of (-)-Pinanediol-(1-methyl)-1-boronate (**2a**)

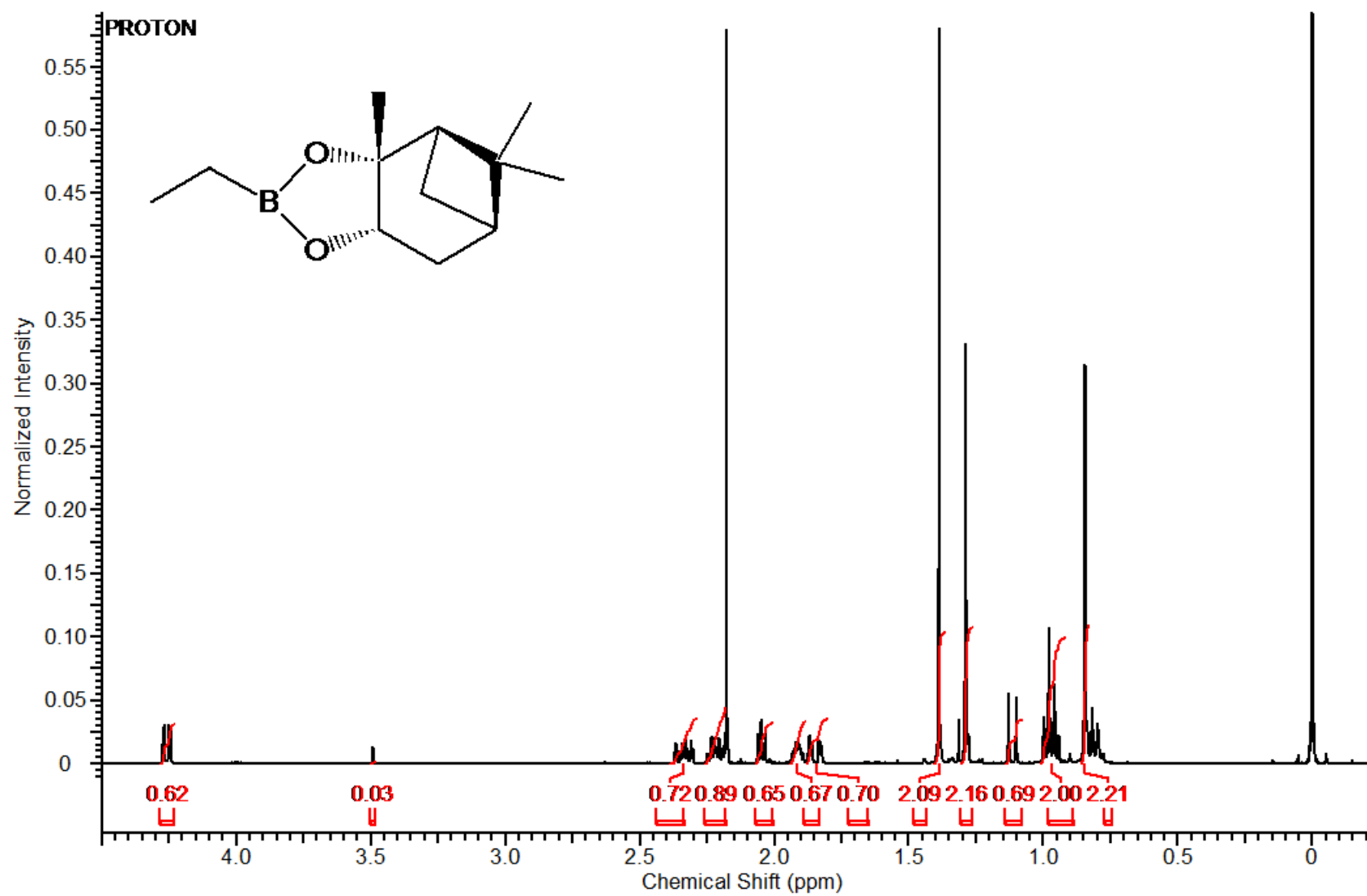


Figure 24. NMR spectrum of (-)-Pinanediol-(1-ethyl)-1-boronate (**2b**)

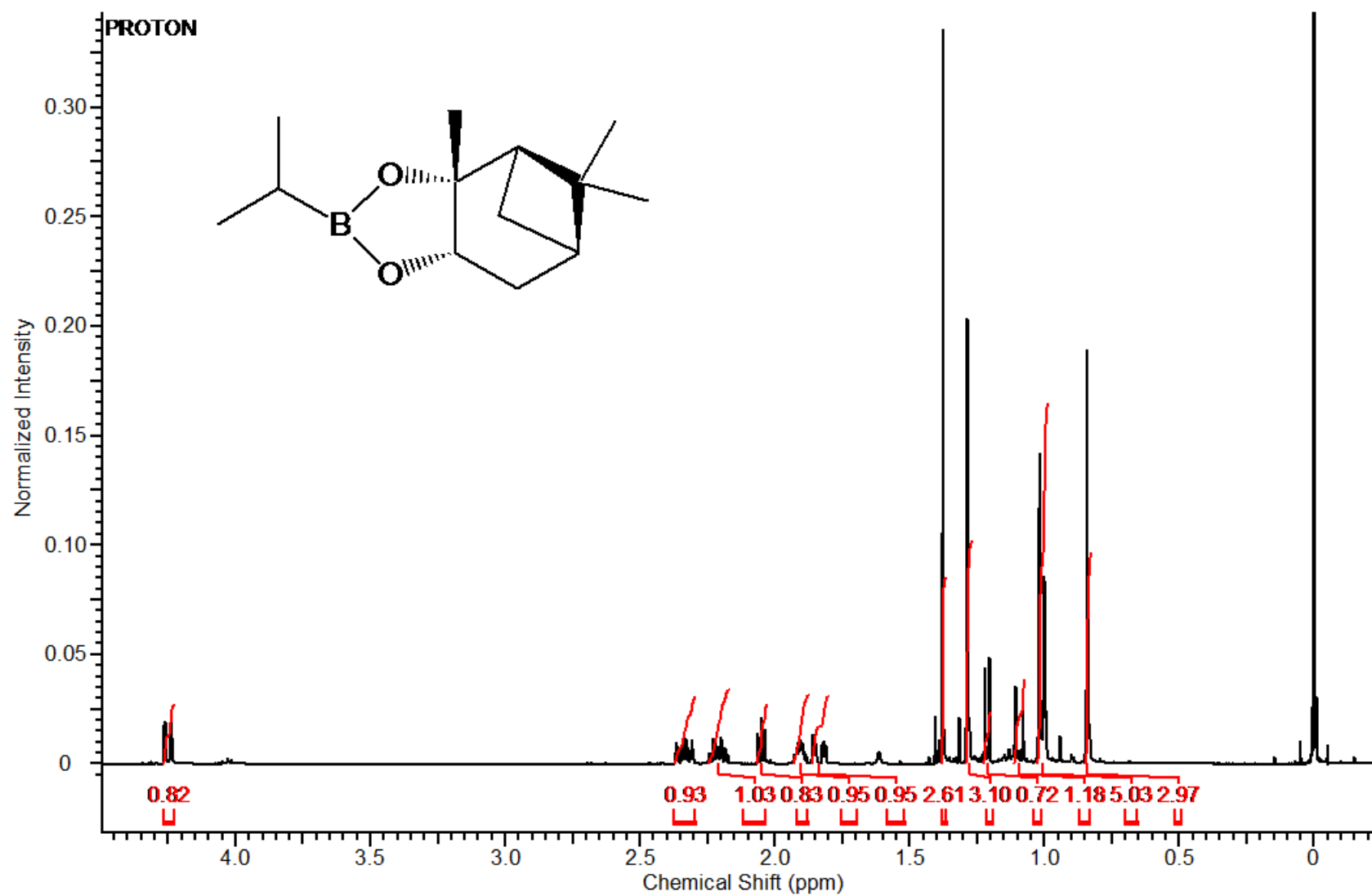


Figure 25. NMR spectrum of (-)-Pinanediol-(1-isopropyl)-1-boronate (**2c**)

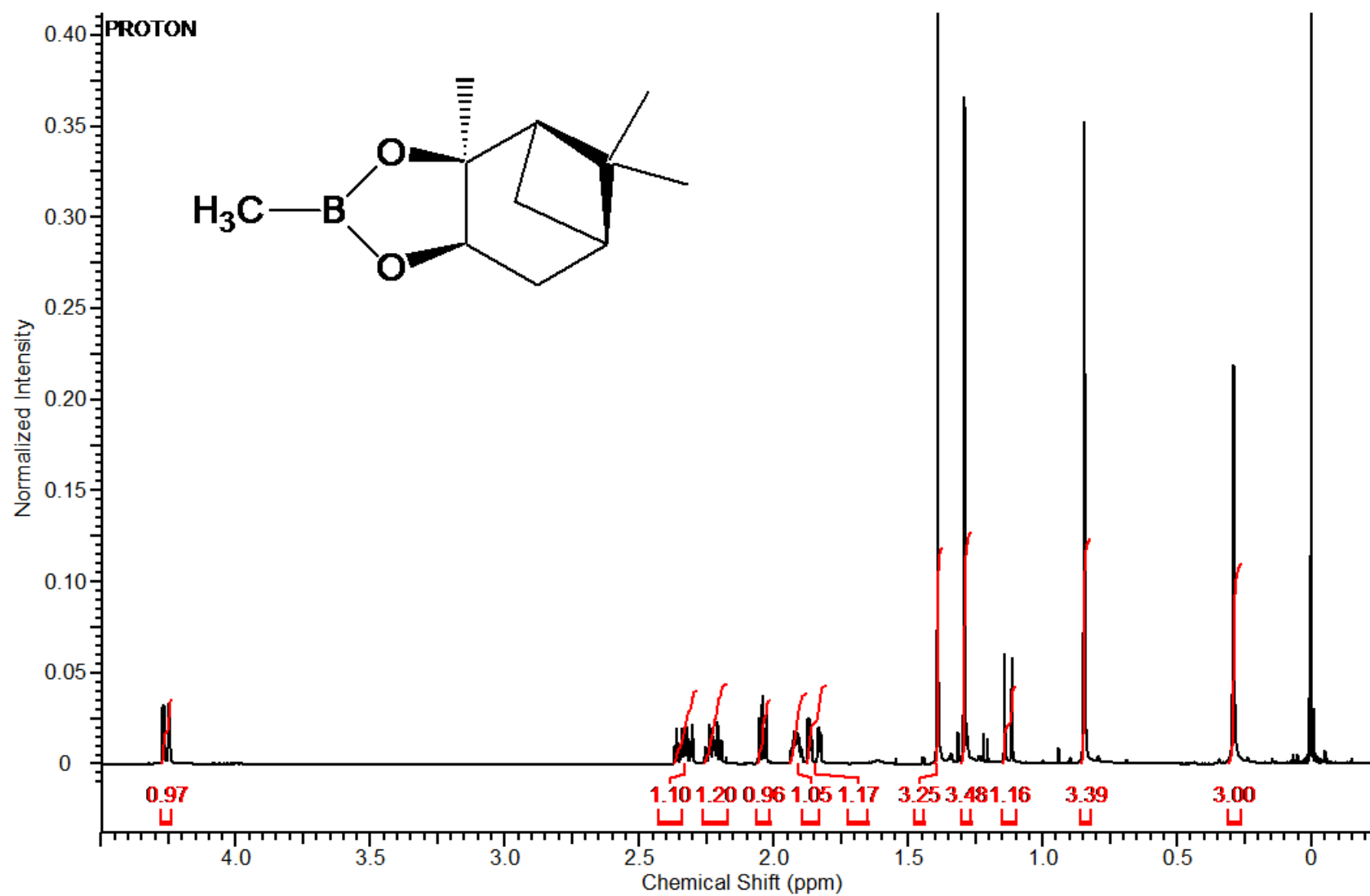


Figure 26. NMR spectrum of (+)-Pinanediol-(1-methyl)-1-boronate (**2d**)

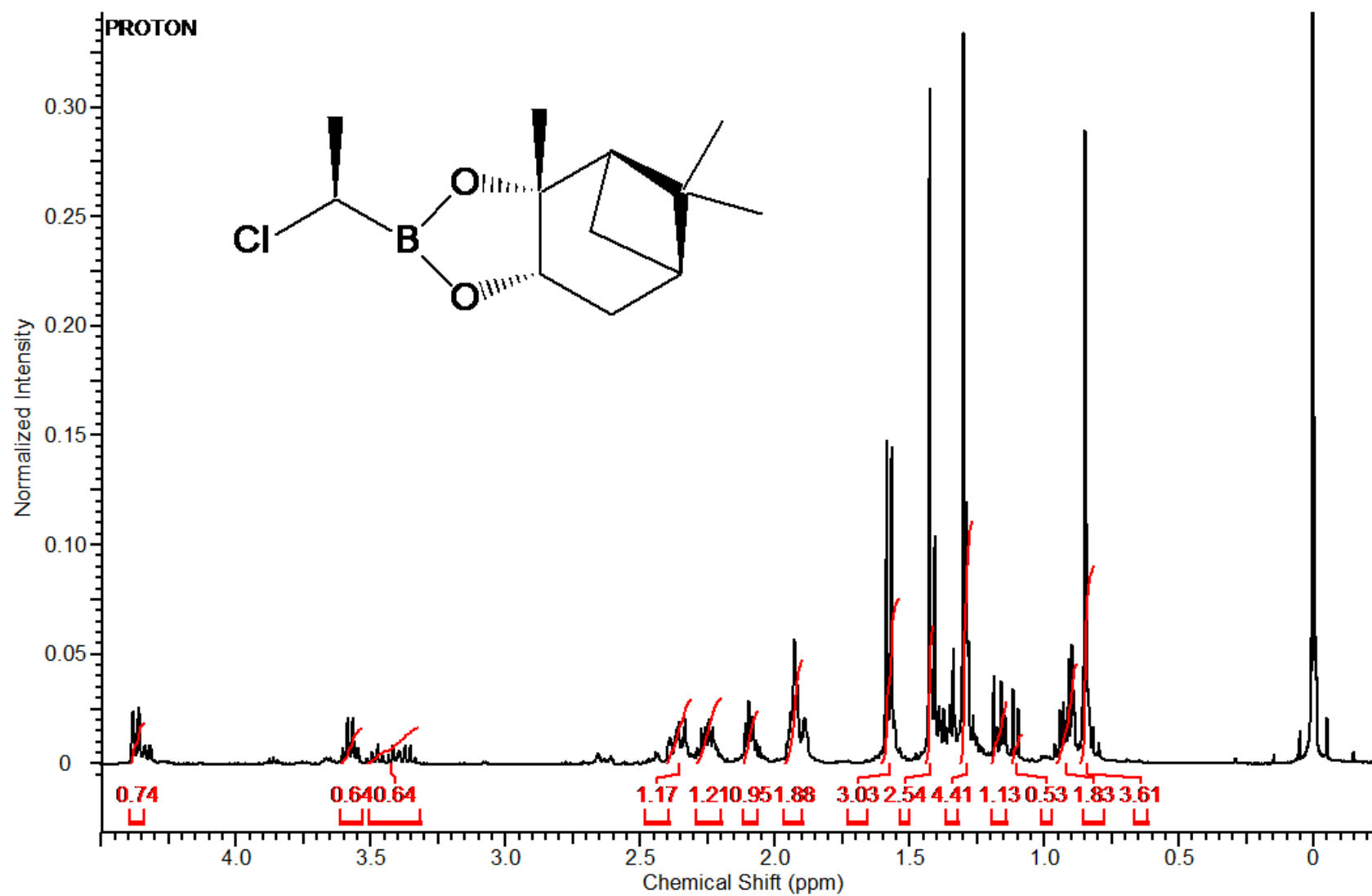


Figure 27. NMR spectrum of (-)-Pinanediol (1R)-(1-chloroethyl)-1-boronate (**3a**)

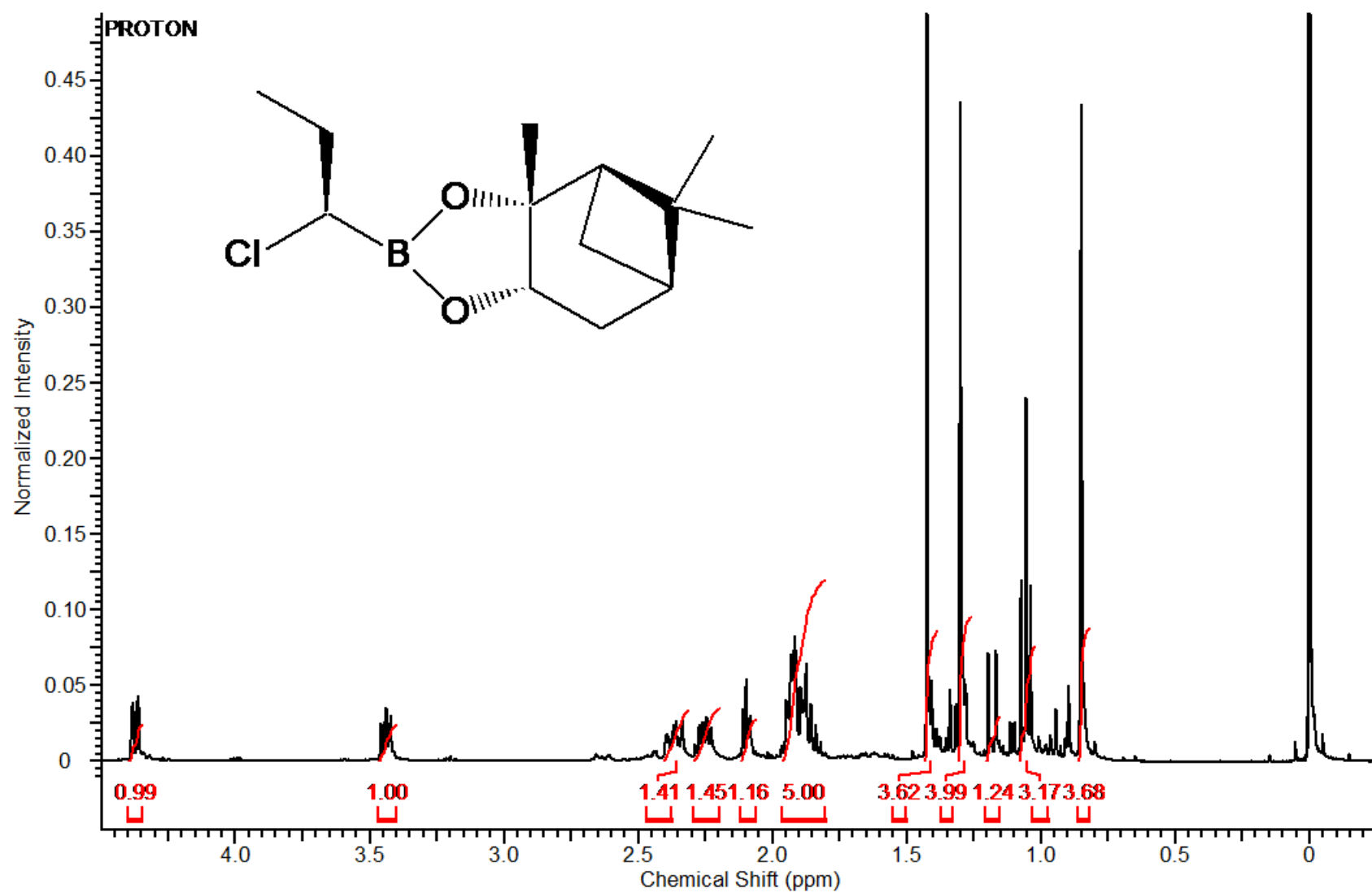


Figure 28. NMR spectrum of (-)-Pinanediol (1R)-(1-chloro-1-propyl)-1-boronate (**3b**)

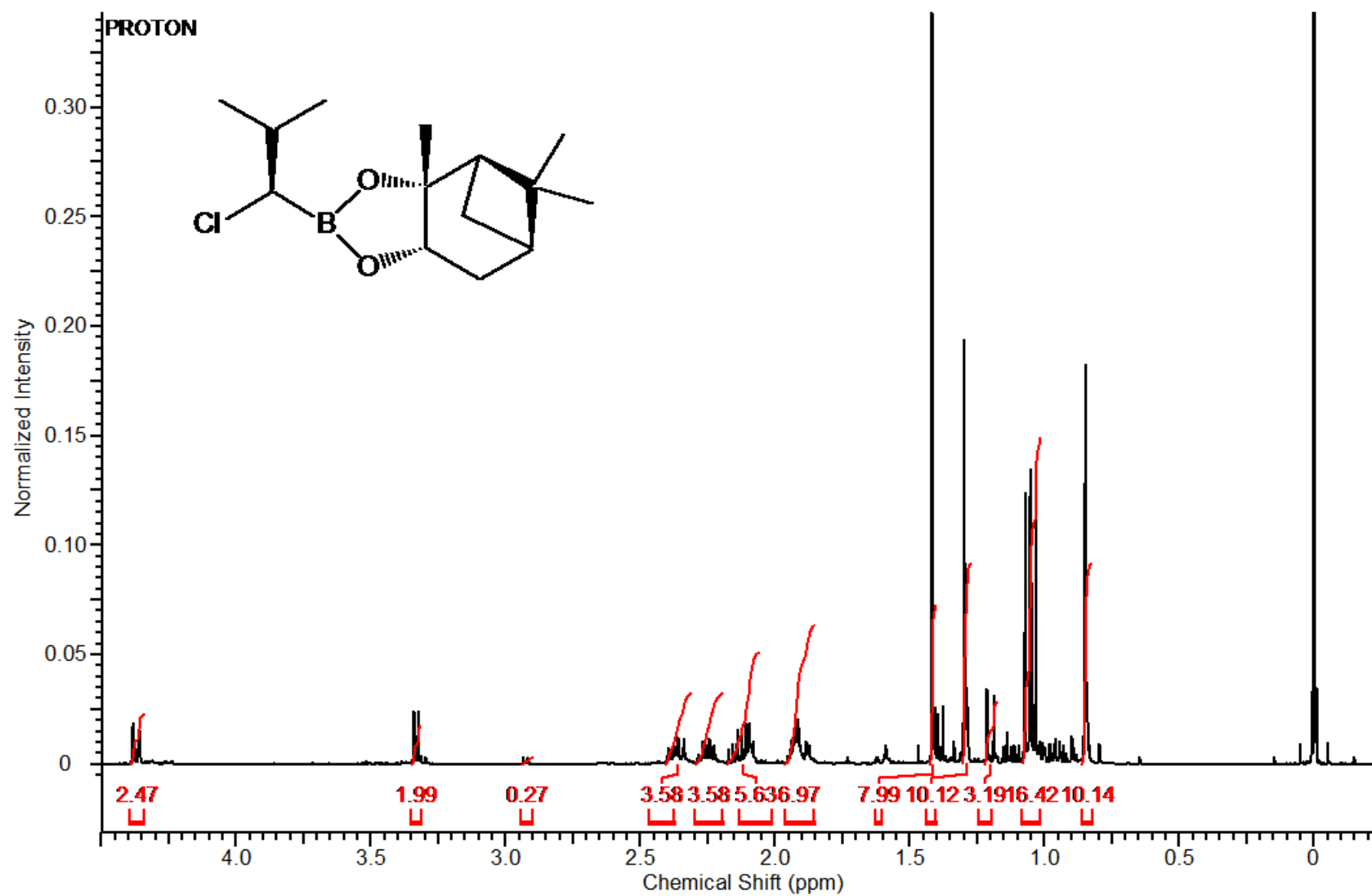


Figure 29. NMR spectrum of (-)-Pinanediol (1R)-(1-chloro-1-isobutyl)-1-boronate (**3c**)

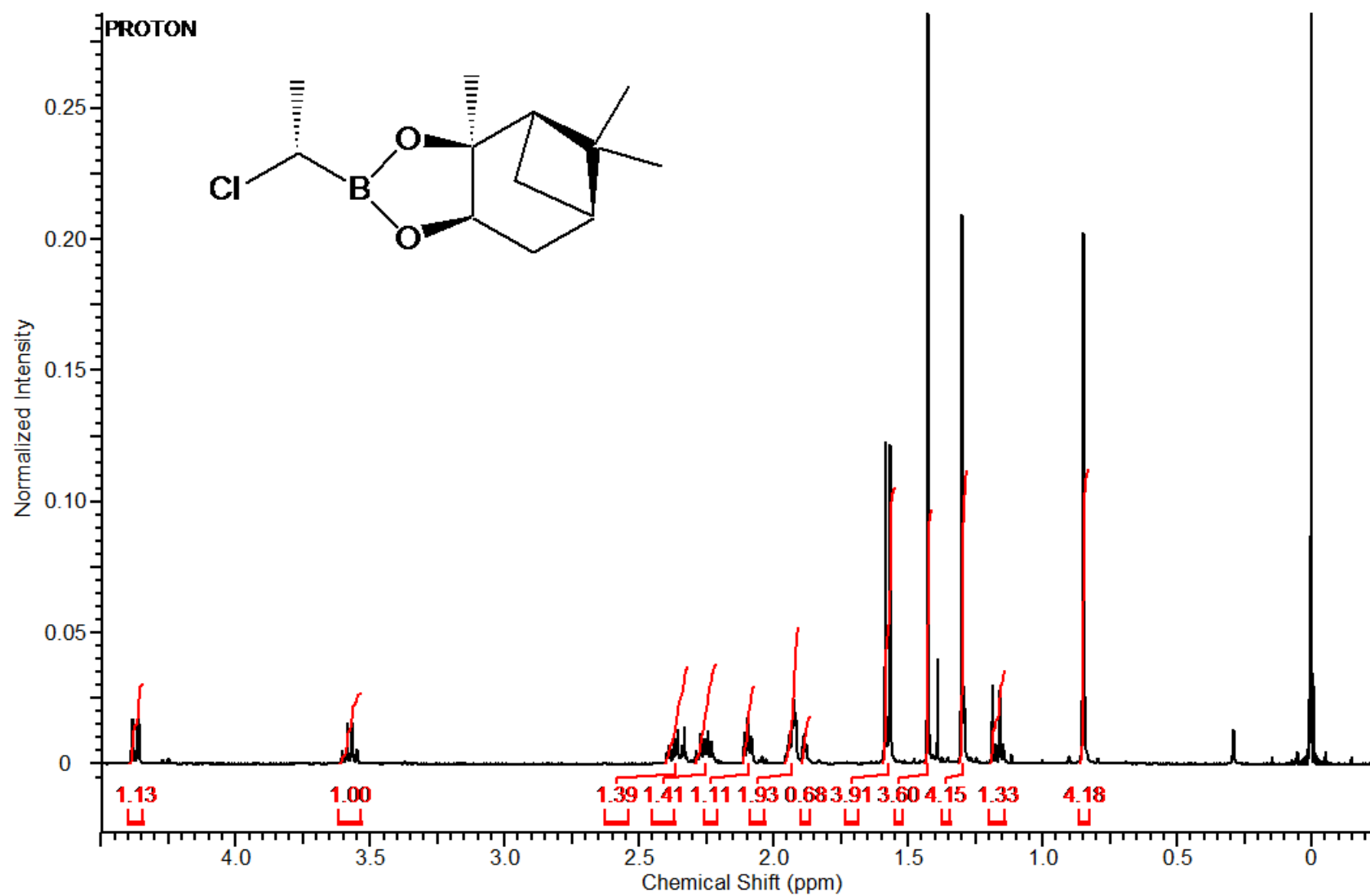


Figure 30. NMR spectrum of (+)-Pinanediol (1S)-(1-chloroethyl)-1-boronate (**3d**)

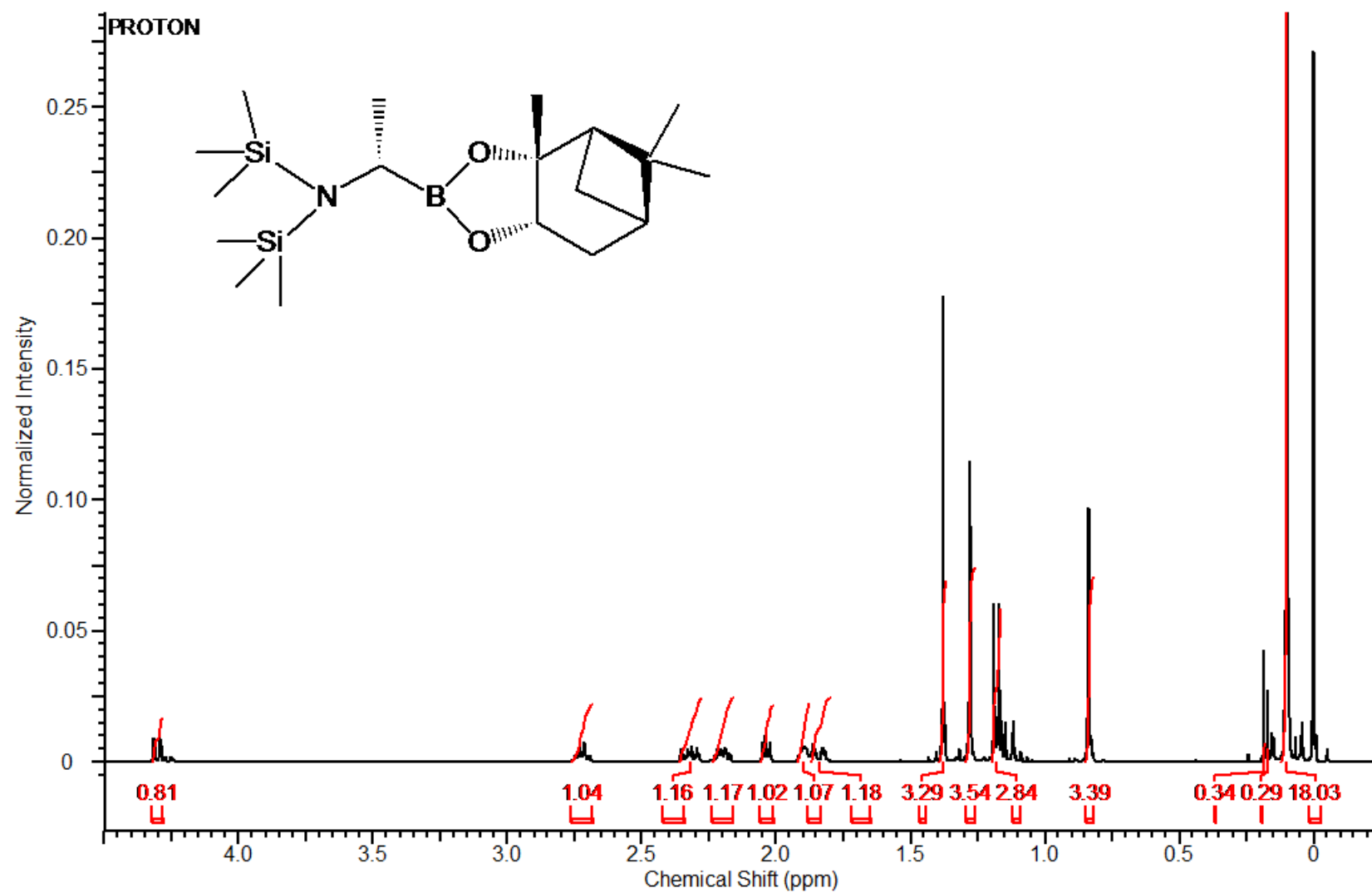


Figure 31. NMR spectrum of (-)-Pinanediol (1S)-(1-hexamethyldisilazaneaminoethyl)-1-boronate (**4a**)

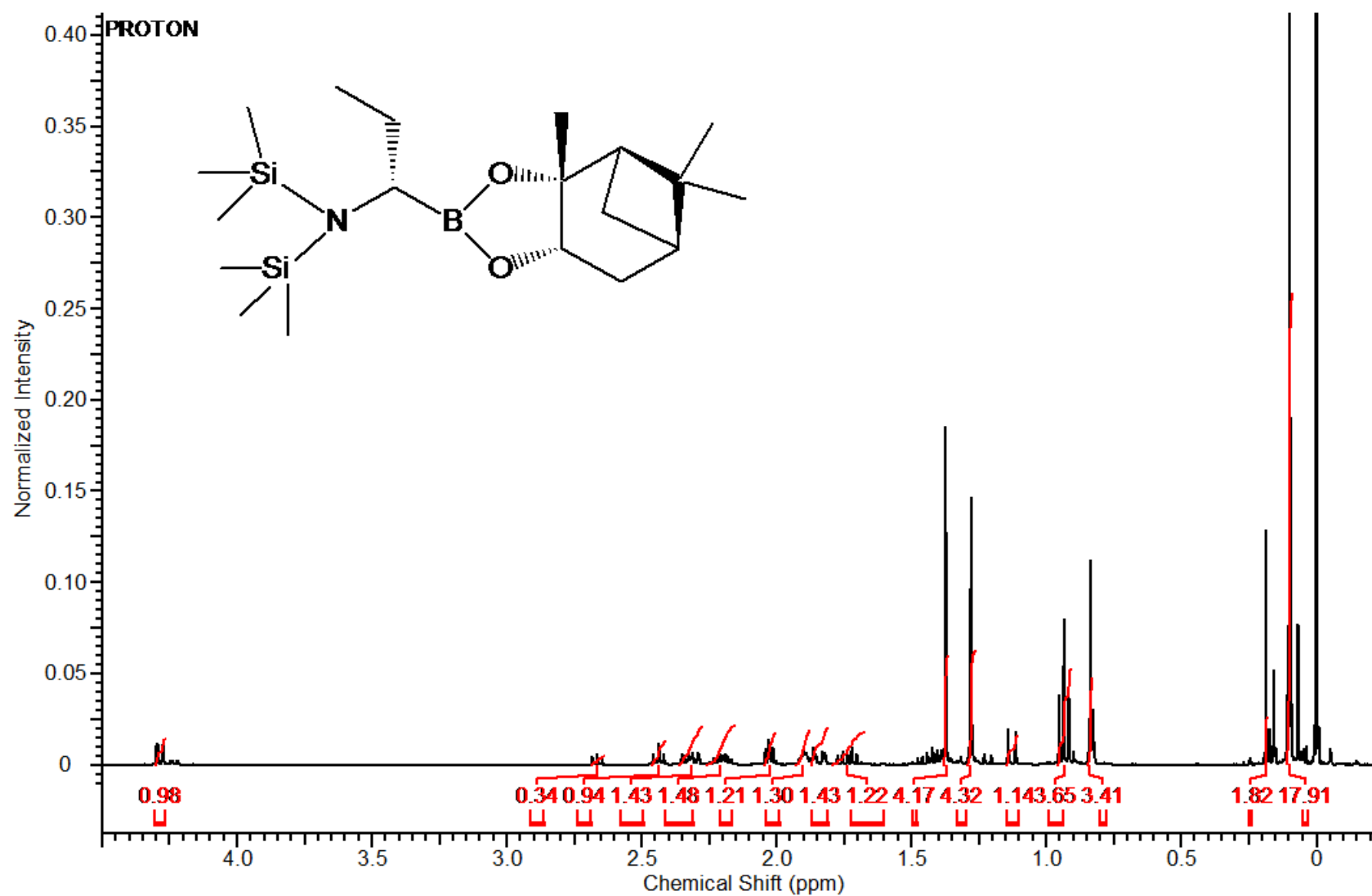


Figure 32. NMR spectrum of (-)-Pinanediol (1S)-(1-hexamethyldisilazaneamino-1-propyl)-1-boronate (**4b**)

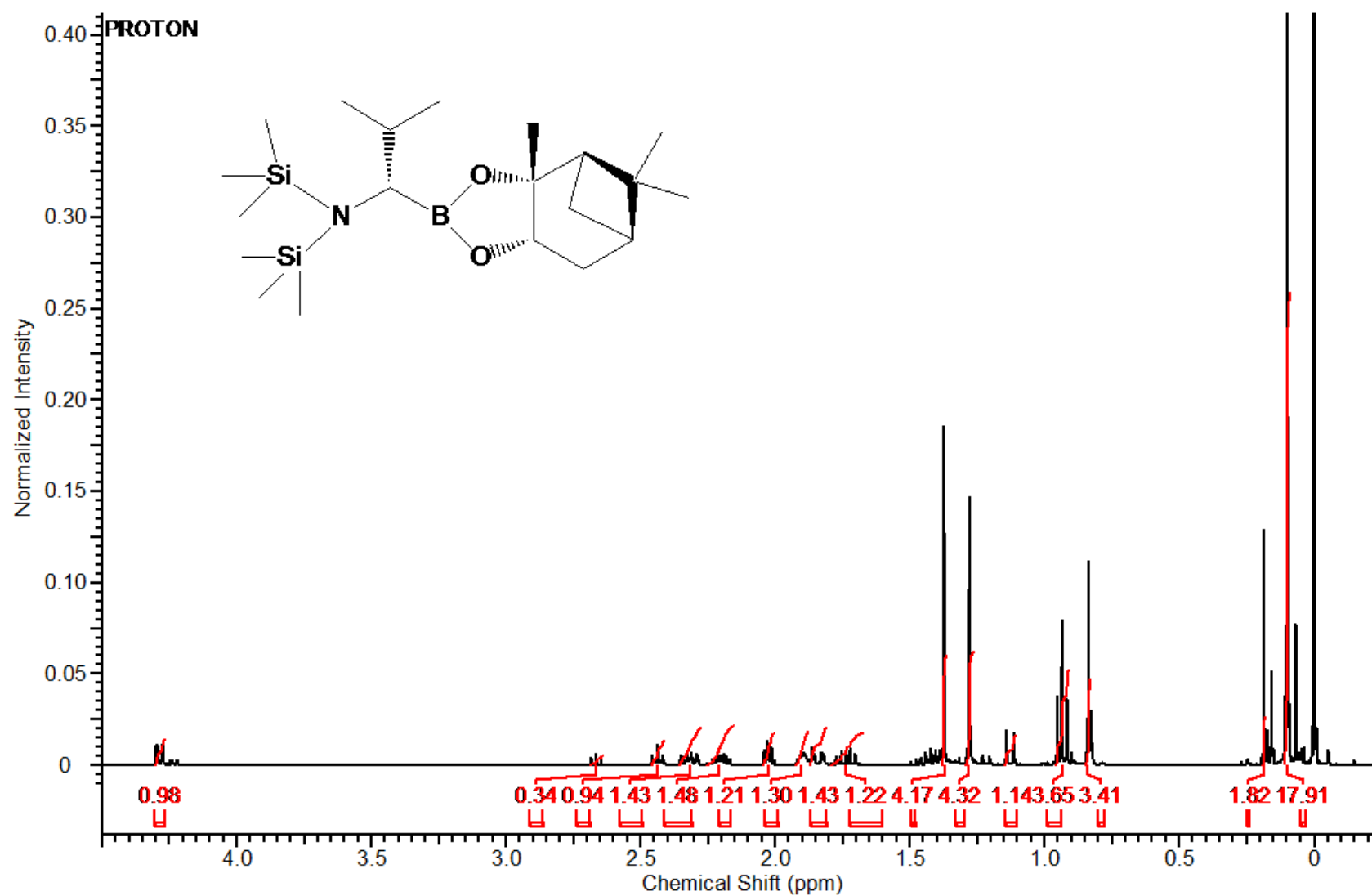


Figure 33. NMR spectrum of (-)-Pinanediol (1S)-(1-hexamethyldisilazaneamino-1-isobutyl)-1-boronate (**4c**)

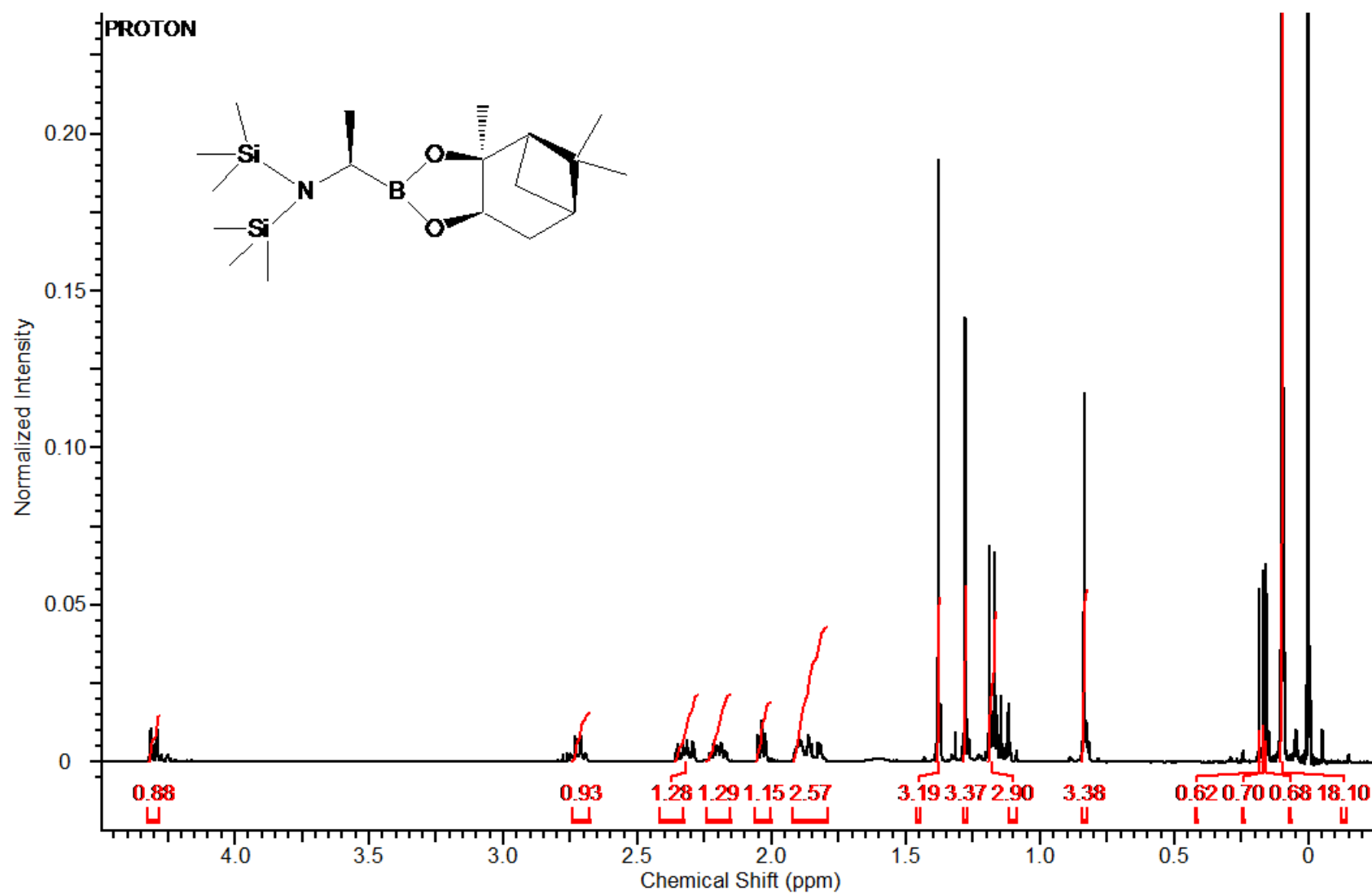


Figure 34. NMR spectrum of (+)-Pinanediol (1R)-(1-hexamethyldisilazaneamino-1-ethyl)-1-boronate (**4d**)

Figure 35. (-)-Pinanediol (1S)-(1-aminoethyl)-1-boronate (D-boroAla-(-)-pinanediol) (**5a**)

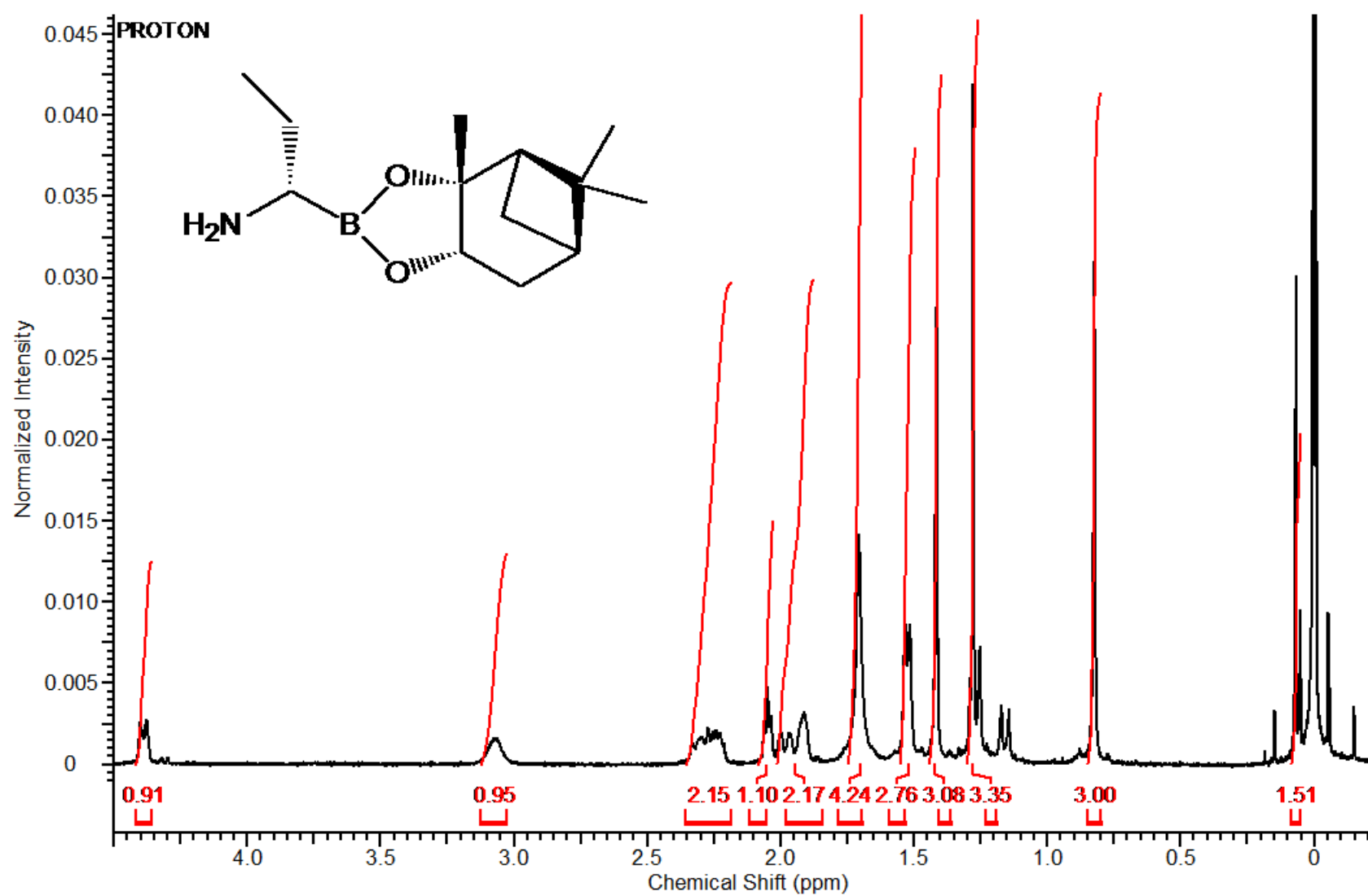


Figure 36. (-)-Pinanediol (1S))-1-amino-1-methylethyl-1-boronate (D-boroVal-(-)-pinanediol) (**5b**)

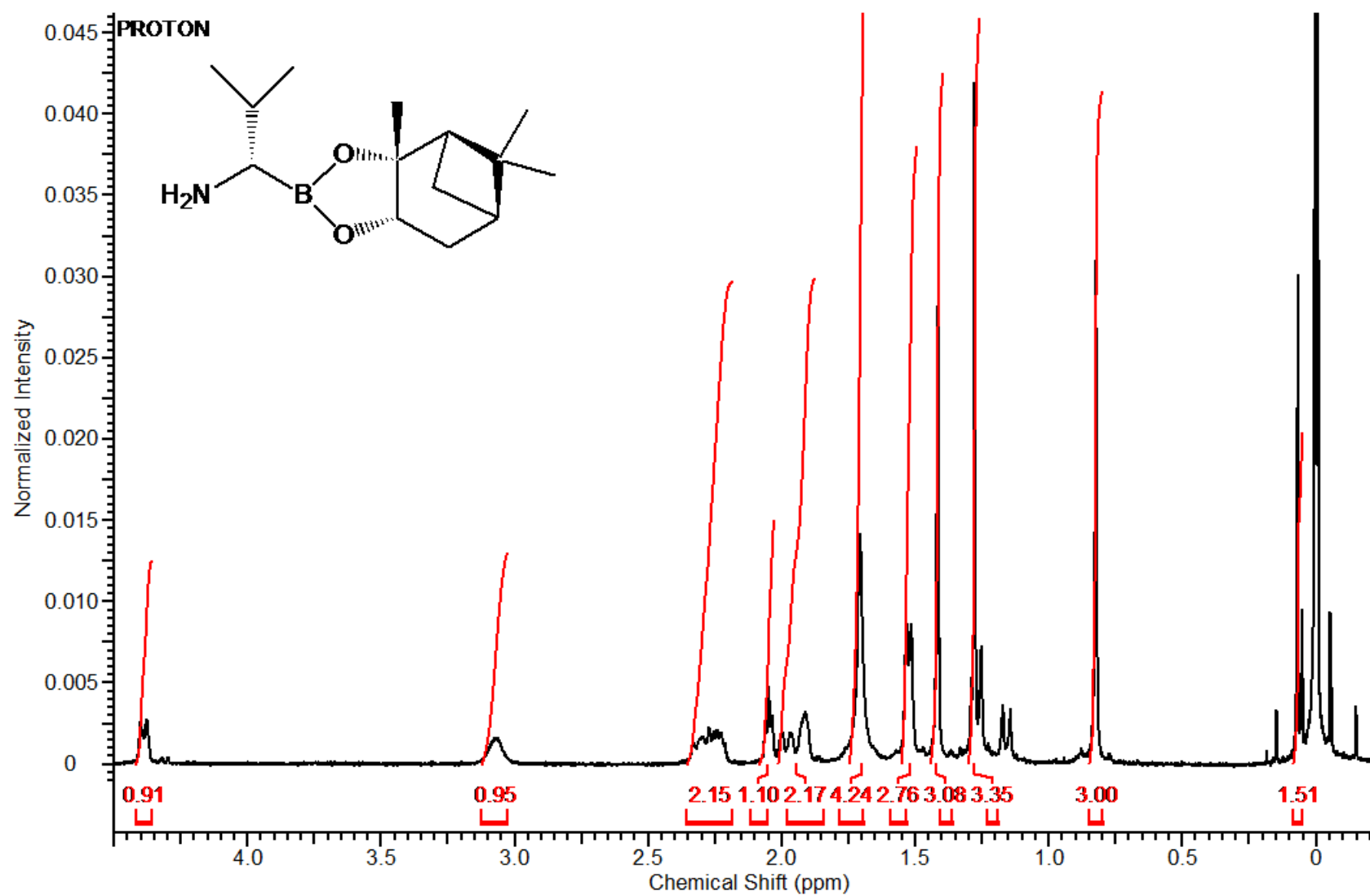


Figure 37. (-)-Pinanediol (1S)-1-amino-1methylisopropyl-1-boronate (5c)

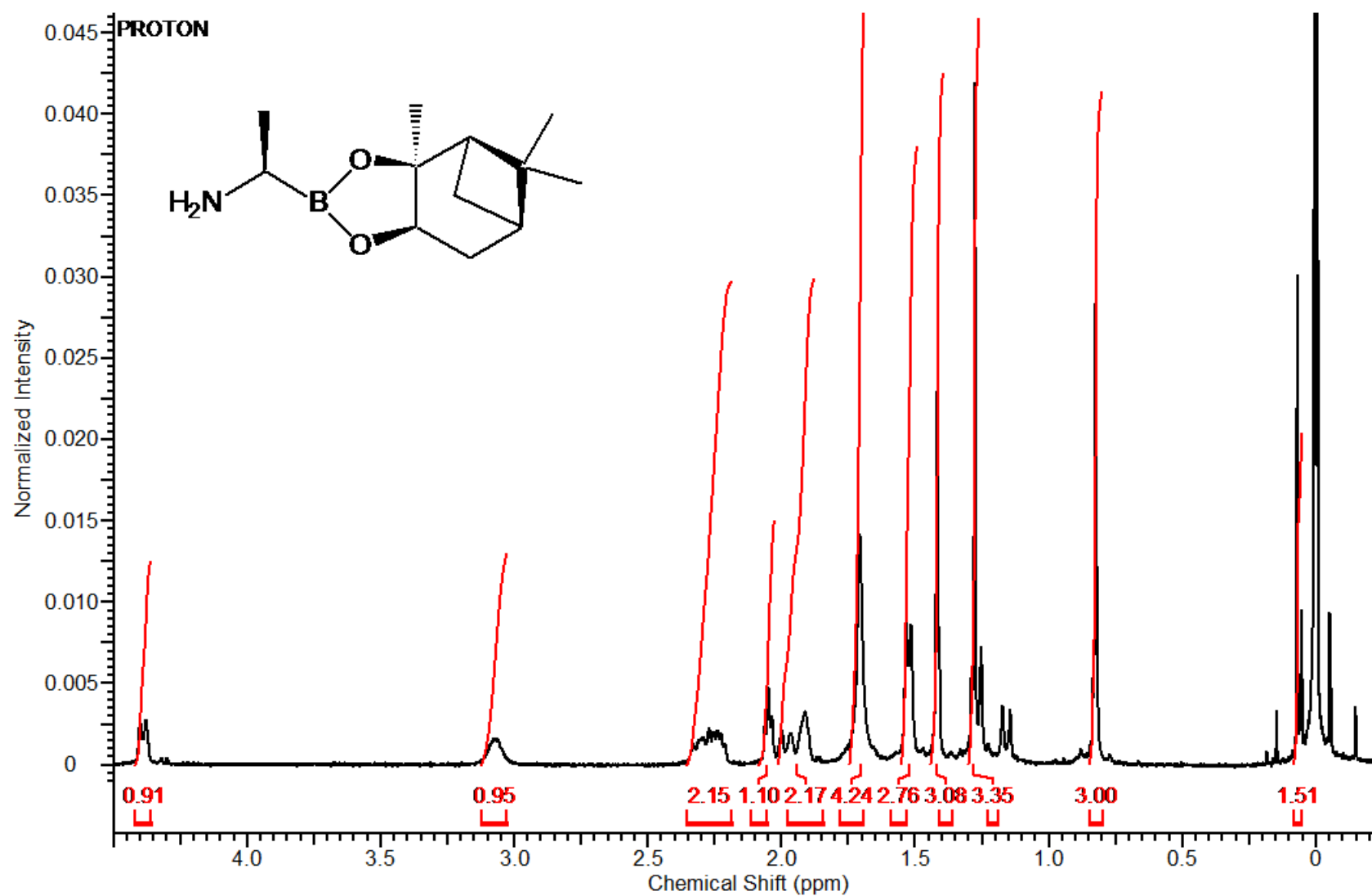


Figure 38. NMR spectrum of (+)-Pinanediol (1R)-(1-aminoethyl)-1-boronate (L-boroAla-(+)-pinanediol) (**5d**)

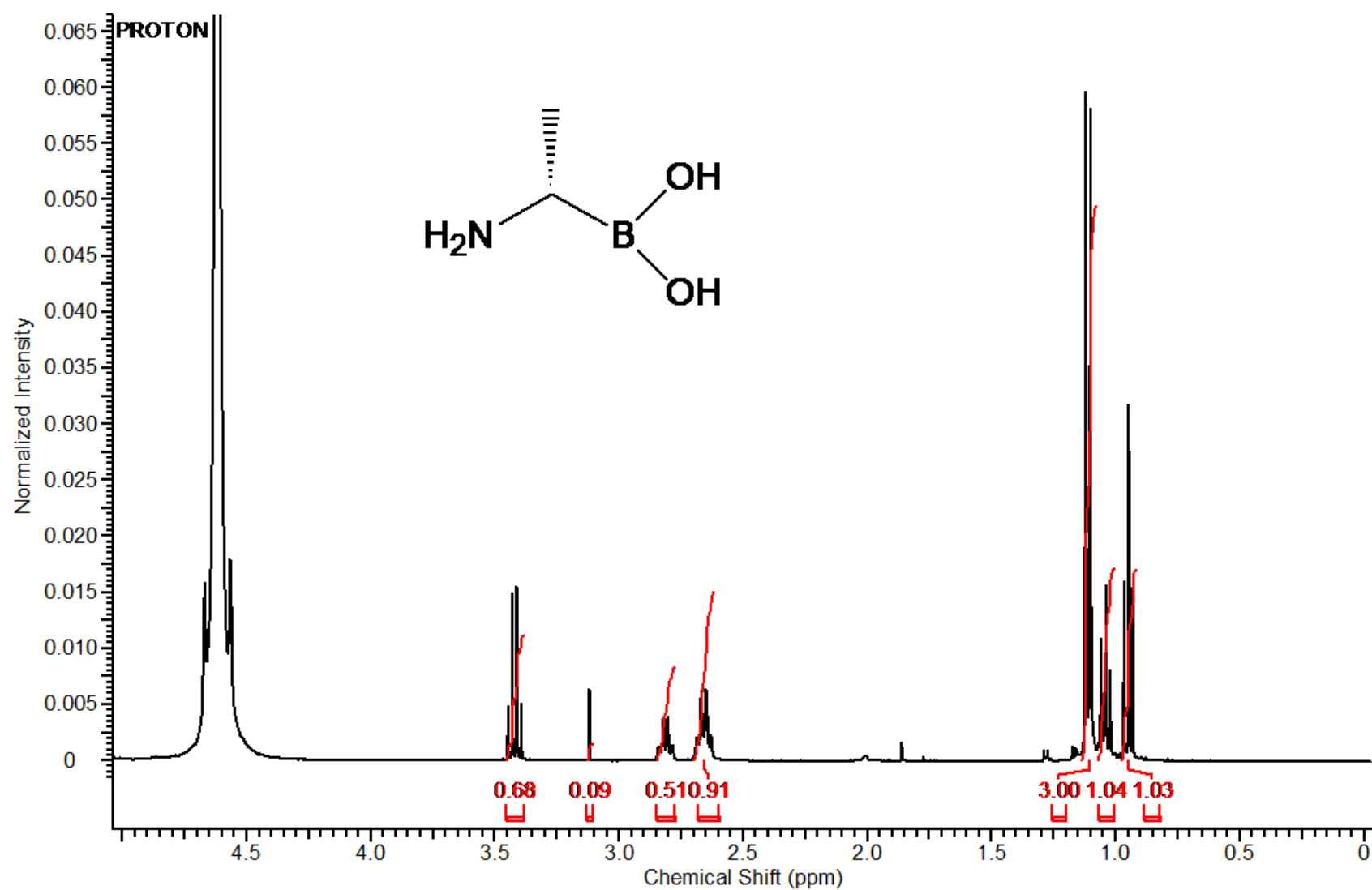


Figure 39. NMR spectrum of (1S)-(1-aminoethyl)-1-boronate (D-boroAla) (**6a**)

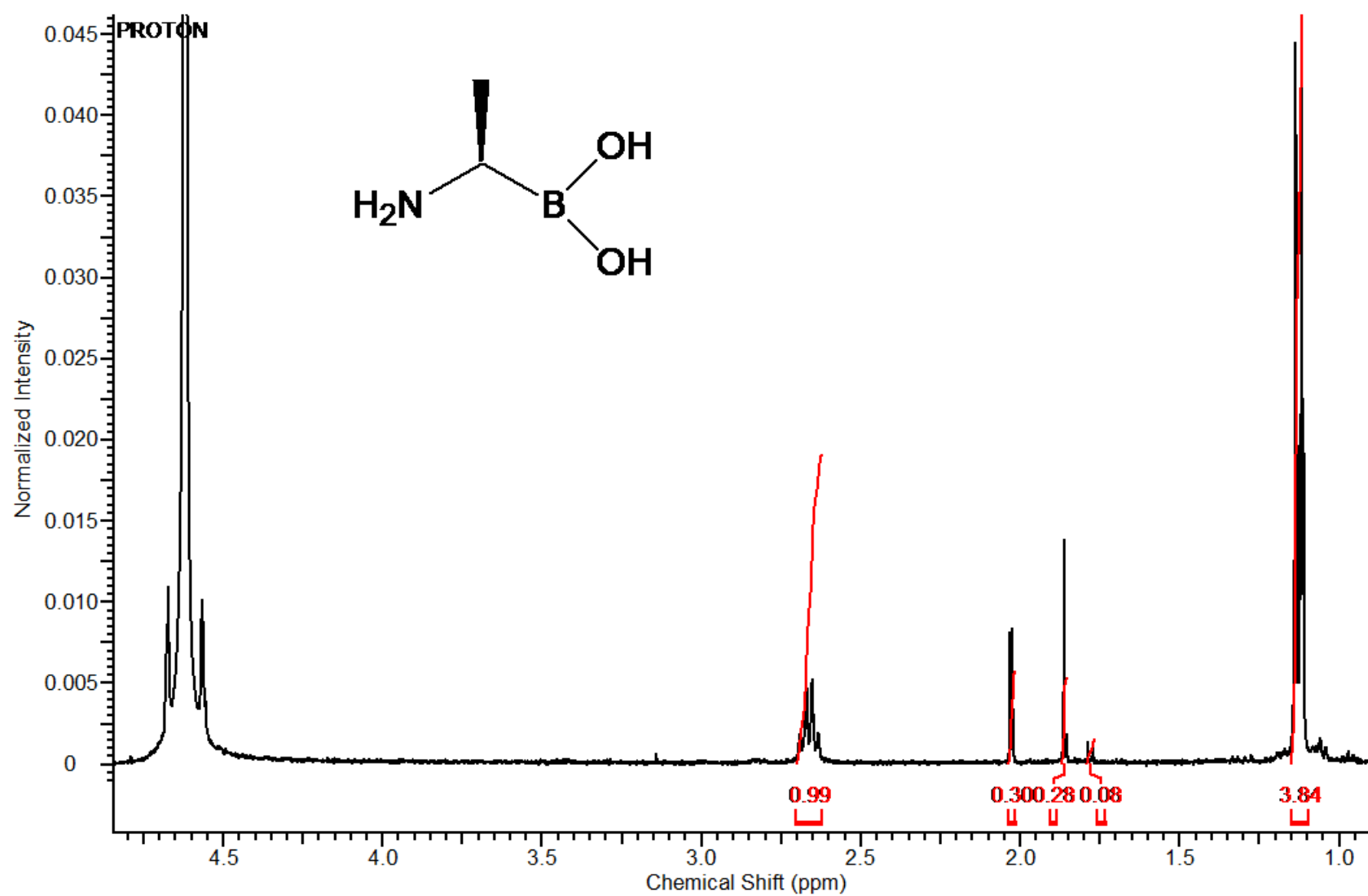


Figure 40. NMR spectrum of (1R)-(1-aminoethyl)-1-boronate (L-boroAla) (**6d**)

CHAPTER 3

AN LC-MS/MS ASSAY FOR D-ALA-D-LAC: A KEY INTERMEDIATE FOR VANCOMYCIN RESISTANCE IN VANCOMYCIN-RESISTANT ENTEROCOCCUS

Introduction and Rationale

Enterococcus spp. are commensal bacteria of the intestine in humans and animals, which can cause problematic infections of the gastrointestinal tract and soft tissues [119-120]. Vancomycin (Vm), a glycopeptide antibiotic, is one of the most important antibacterial agents for the treatment of Gram-positive bacterial infections resistant to most other antibacterial agents, including Vm sensitive enterococcal (VSE) and MRSA infections [121-123]. Vancomycin-resistance enterococci (VRE), first reported in late 1980s [1], are now widespread and a common cause of nosocomial infections [2]. Given resistance to most alternative classes of antibacterial agents, treatment options for VRE are limited [120, 124].

Cell wall biosynthesis is a biochemically unique bacterial pathway, which is the target of a number of antibacterial agents. This pathway is complex, and has both highly conserved elements between bacterial species, as well as important differences [64, 125-132]. Vancomycin exerts its antibacterial effect by binding to the D-Ala-D-Ala termini of pentapeptide peptidoglycan precursors [42, 133-136], thereby interfering with the last steps of bacterial cell wall biosynthesis. In the most clinically common resistance mechanisms in VRE, the terminal D-Ala-D-Ala moiety of peptidoglycan precursors is replaced by D-Ala-D-Lac [42-43]. This alternative pathway requires 4 enzymes to synthesize D-Ala-D-Lac (VanH and VanA), and to degrade D-Ala-D-Ala intermediates before they can be incorporated into nascent

peptidoglycan (VanX and VanY) **Figure 41**. Alanine branch metabolites (L-Ala, D-Ala, D-Ala-D-Ala), and D-Ala-D-Lac in particular, are key intermediates in this process. However, these are small hydrophilic molecules, and there has been a lack of analytical methods for the quantitation of *in vivo* levels of these metabolites. While methods are available for D-Ala-D-Lac quantitation using radiolabeled precursors, such methods are apparently limited to *in vitro* generated analytes [137-138]. Such methods are inadequate for detailed or *in vivo* studies of alanine branch metabolite changes in response to vancomycin in VRE, which are at the core of the vancomycin resistance mechanism.

Marfey's reagent is a chiral analog of Sanger's reagent used to derivatize chiral amino acid mixtures prior to separation on achiral media to determine stereochemical purity [106-107, 139]. In recent studies, we have developed a Marfey's reagent-based LC-MS/MS method to quantitate alanine branch intermediates – L-Ala, D-Ala, and D-Ala-D-Ala – in the standard bacterial cell wall biosynthesis pathway [105]. This method has been used to determine the mechanism of antibacterial activity of cycloserine and D-boroAlanine [140-141]. In this study, this method is extended to the detection and quantitation of D-Ala-D-Lac, the key intermediate for most types of vancomycin resistance, and demonstrated for determining the effect of vancomycin induction on alanine branch metabolites – including D-Ala-D-Lac – in VRE.

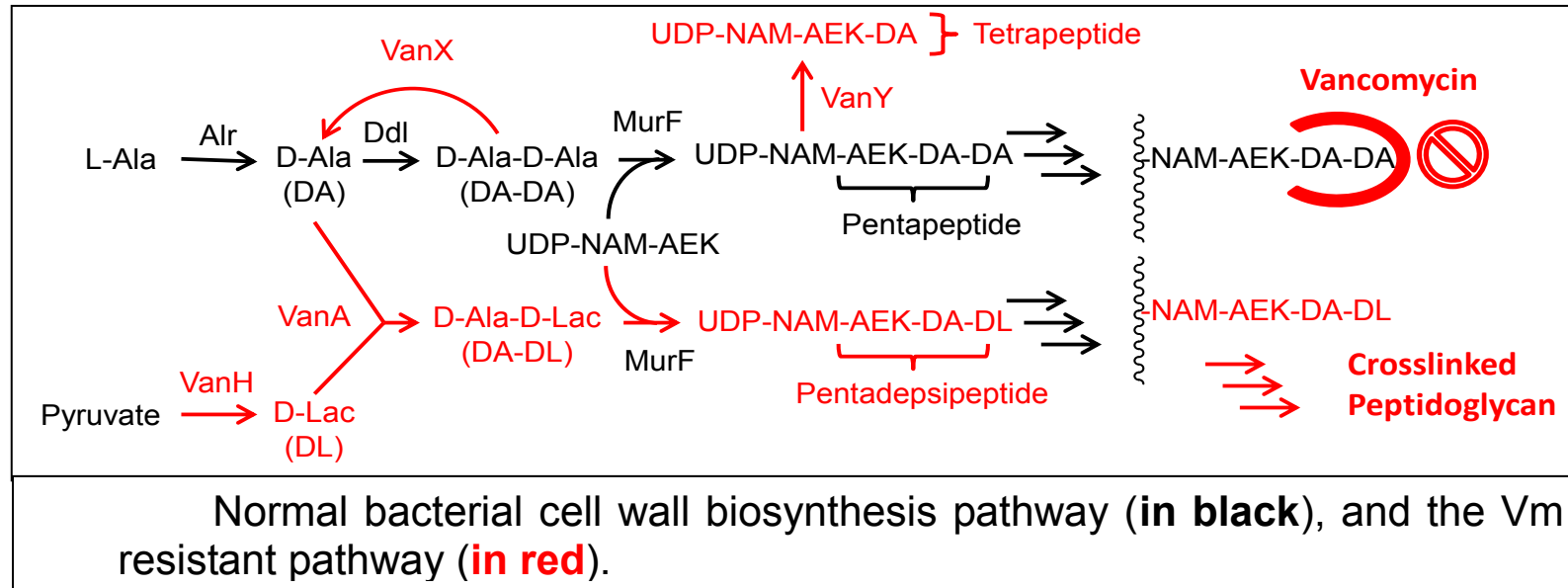


Figure 41. Cell wall intermediate biosynthesis pathway in VRE. Cell wall biosynthesis intermediates and enzymes specific to the vancomycin resistance pathway are shown in italicized bold text. NAM=N-acetylmuramic acid.

Materials and Methods

General: Vancomycin-resistant enterococcus (VRE) was a clinical isolate provided by Dr. Betty Herndon (University of Missouri-Kansas City, School of Medicine). D-Ala, L-Ala, D-Ala-D-Ala, $^{13}\text{C}_3$ -D-Ala, vancomycin, trifluoroacetic acid (TFA), hemin, and carbonyldiimidazole (CDI) were purchased from Sigma-Aldrich Corp (St. Louis, MO). Boc-D-Ala-OH and D-Lac-OtBu were purchased from Bachem Bioscience (King of Prussia, PA). C18-silica gel was from Sep-Pak Cartridges (Waters, Milford MA). Marfey's reagent (1-fluoro-2,4-dinitrophenyl-L-5-alanine amide) was purchased from Novabiochem (a division of EMD Chemicals, Gibbstown, NJ). Other reagents were from standard sources and were reagent grade or better. VRE growth media – consisting of brain heart infusion (37.5 g/L), NaCl (6.5 g/L), hemin (10 $\mu\text{g/mL}$), and NAD^+ (10 $\mu\text{g/mL}$) - was prepared following standard procedures. M9 minimal media – consisting of Na_2HPO_4 (6 g/L), KH_2PO_4 (3 g/L), NH_4Cl (1 g/L), NaCl (0.5 g/L), $\text{MgSO}_4 \cdot 7\text{H}_2\text{O}$ (1 mM), $\text{FeSO}_4 \cdot 7\text{H}_2\text{O}$ (3 $\mu\text{g/L}$), vitamin B1 (thiamine, 0.5 mg/L), and glycerol (20%, as carbon source) – was also prepared following standard procedures. LC-MS/MS was performed using electrospray ionization (ESI) in positive mode on an AB-Sciex 2000 QTrap LC-MS/MS mass spectrometer (Framingham, MA) equipped with an Agilent 1100 HPLC system (Santa Clara, CA). Data acquisition and processing were performed using the Analyst 1.4.2 software package (Applied Biosystems, Foster City CA). All chromatographic separations were performed on a Nucleodur 100-3 C8 125 x 2.0 mm column (Macherey–Nagel, Bethlehem PA). All centrifuge operations were performed on Sorvall RT6000 refrigerated Centrifuge.

Boc-D-Ala-D-Lac-OtBu: Boc-D-Ala-OH (1.1 eq, 3.8 mmol, 710 mg) was dissolved in anhydrous THF (10 mL), cooled to 0 °C, and carbonyldiimidazole (1.1 eq, 3.8 mmol, 610 mg) added. The reaction was allowed to proceed for 30 min to form the acyl imidazole intermediate. D-Lac-OtBu (1 eq, 3.4 mmol, 500 mg) was then added, and the mixture allowed to warm to room temperature. After 2 days, the reaction was quenched with 2M acetic acid (10 mL) and extracted three times with methylene chloride (3x15 mL), and the combined organic extracts back extracted with 1M HCl (1x5 mL), 1M NaHCO₃ (1x5 mL) and brine (1x5 mL). The organic extract was dried over anhydrous MgSO₄, filtered, and solvent removed by rotary evaporation. The product was obtained as a light clear oil. Yield 76%. LC-MS; expected [M+H]⁺ = 318.18 observed [M+H]⁺ = 318.20.

D-Ala-D-Lac: Boc-D-Ala-D-Lac-OtBu (1.6 mmol, 500 mg) was placed in a round bottom flask and treated with TFA (5 mL) for 1 hr. TFA was removed by evaporation using nitrogen gas stream, and then under vacuum (5 µmHg) for 2 hrs. The product was a clear oil, which was dissolved in water to yield a concentrated stock solution of D-Ala-D-Lac. LC-MS; expected [M+H]⁺ = 161.97 observed [M+H]⁺ = 162.10.

Preparation of standard solutions and quality control (QC) samples: 10 mM stock solutions of each analyte (D-Ala, L-Ala, D-Ala-D-Ala, and D-Ala-D-Lac) were prepared in water. An equimolar “standard mixture” was prepared by mixing aliquots of 60 µL of 10 mM stock solutions of L-Ala, D-Ala, D-Ala-D-Ala, and D-Ala-D-Lac with 760 µL of H₂O to give 1 mL of 0.6 mM of each. For method validation, QC samples of three concentrations of a mixture of all the analytes (400, 40 and 1 pmol) were

prepared in VRE extract. 20 μM $^{13}\text{C}_3\text{-D-Ala}$ was added to all samples as an internal standard. All solutions were stored at -20°C until use.

Marfey's Derivatization Reactions: To a 15 μL aliquot of the standard mixture was added 15 μL of 10 mM of Marfey's reagent (in acetone) and then 5 μL of 1 M triethylamine (in water). The contents were mixed well and kept in an incubator at 37°C for 150 minutes. The derivatization reaction was quenched and acidified by addition of 5 μL 1 M HCl, and the sample diluted up to 200 μL with 75% H_2O /25% acetonitrile + 0.1 % formic acid. This Marfey's derivatized "standard mixture" was used in initial experiments to optimize separation and quantitation parameters. Individual Marfey's adducts of L-Ala, D-Ala, D-Ala-D-Ala, and D-Ala-D-Lac were similarly prepared from 15 μL aliquots of 0.6 mM stocks following the same derivatization procedure.

MS and MS/MS optimization: Salts were observed to interfere with MS detection of Marfey's derivatives. To remove salts prior to MS and MS/MS optimization, a 50 μL sample of the Marfey's derivatized standard mixture of individual compound was loaded onto 100 mg of C18-silica in a 1 mL syringe prepared by first washing with MeOH (1 mL) and then pre-equilibrated with 1 mL of H_2O + 0.1% formic acid. After loading, the resin was washed with 100% H_2O + 0.1% formic acid and then 20% AcCN/ H_2O + 0.1% formic acid. Marfey's adducts were then eluted with 75% AcCN/25% H_2O + 0.1% formic acid to provide a sample of Marfey's adducts free of salts. MS, MS/MS and flow (LC-MS/MS) parameter optimization were performed using desalted Marfey's adduct samples using the

automated quantitative optimization routines in Analyst. Optimized detection and quantitation values were given in **Table 5**

Chromatographic conditions: Chromatography was performed at a flow rate of 300 μ L/min, with 75% solvent A (100% water and 0.1% formic acid) and 25% solvent B (70% acetonitrile/30% water + 0.1% formic acid) for the first minute, followed by a linear gradient to 50% solvent A/50% solvent B in 11 min, then a gradient to 100% solvent C (100% acetonitrile + 0.1% formic acid) in 1 min.

Bacterial Growth and Vancomycin Treatment: A saturated overnight culture of VRE was grown in an incubator-shaker at 35 °C in VRE media. Cells were harvested by centrifugation, and resuspended to the desired optical density (0.05 O.D at 600 nm) in fresh VRE media. 75 mL of this culture was placed into sterilized 250 mL baffled shaker flasks. Vancomycin was added to flasks at different concentrations (0, 0.032, 0.125, 1, 8, 32, and 128 μ g/mL) and the flasks were incubated with good agitation at 35 °C. Cell growth was monitored by absorbance at 600 nm. When the cultures reached 0.6 OD they were rapidly cooled in an ice-water bath, 4 samples of 10 mL each were removed from each flask to ice-cold 15 mL centrifuge tubes, and the cells pelleted by centrifuge at 3000 rpm for 10 min at 2 °C.

Cell Washing and Extraction: A sample of Marfey's derivatized VRE media was analyzed by LC-MS/MS and found to contain significant levels of L-Ala. To remove exogenous L-Ala from the bacterial cells, which would interfere with determination of endogenous L-Ala, we incorporated a step where VRE cells were washed with minimal media prior to metabolite extraction. Cell pellets (~50 μ L) were washed by resuspending in 300 μ L of ice-cold M9 minimal media, and the cells were

re-pelleted and wash media removed. To validate and monitor washing, 100 μM of γ -aminobutyric acid (GABA) was added as a marker to the VRE culture sample on ice prior to pelleting. After extraction as described below and derivatization with Marfey's reagent, the Marfey's adduct of GABA was quantitated. GABA analysis from cells washed one to four times was performed. Metabolites were extracted from VRE cell pellets by resuspending in 100 μL of ice-cold M9 minimal media, followed by addition of 200 μL ice-cold 80% acetone/water spiked with 20 μM of $^{13}\text{C}_3$ -D-Ala as internal standard. Tubes were kept on ice with occasional vortexing for 5-10 min. These tubes were again centrifuged to pellet cell debris and supernatants removed to fresh ice-cold microcentrifuge tubes. Samples (15 μL) were taken and subjected to Marfey's derivatization as described above.

Method Validation: Validation was done for selectivity, linearity, lower limit of quantification (LLOQ), limit of detection (LOD), accuracy, precision, recovery and stability as per recommendations for bioanalytical method validation by the Food and Drug Administration [142]. For linearity and LLOQ determination, serial dilutions of a 1:1:1:1 mixture of L-Ala:D-Ala:D-Ala-D-Ala:D-Ala-D-Lac in steps of two were prepared in water with 20 μM $^{13}\text{C}_3$ -D-Ala internal standard included. For LOD determination and to check for matrix (VRE extract) effect, an identical serial dilution was prepared in VRE culture extract. These serially diluted samples were derivatized with Marfey's reagent as described above, and LC-MS/MS analysis was performed on 10 μL injections. Calibration curves were constructed by plotting LC-MS/MS peak areas of the analyte (values from blank samples of VRE extract were subtracted from VRE extract values to correct for the endogenous concentration of

each analyte) versus the concentration of each analyte by linear regression. The LLOQ was defined as the concentration which gave a signal/noise ratio of 10. The LOD was defined as the concentration that gave a signal/noise ratio of 3. For inter- and intraday precision and accuracy determination, QC samples were used at low, mid, and high analyte levels (1, 40 and 400 pmol respectively, n=6). Analyte stability was performed on QC samples (1, 40 and 400 pmol, n=3). Freeze/thaw stability was determined after three freeze/thaw cycles. For long-term (pre-derivatization) stability determination – QC samples were stored at -20 °C for 90 days, and for post-derivatization stability determination – derivatized QC samples were kept at autosampler conditions (room temperature) for 48 hrs.

Results and Discussion

Washing method: Since VRE media was found to contain a significant level of L-Ala, a washing step with minimal media was necessary to remove exogenous L-Ala from VRE cells before extraction. GABA added to the cells immediately after cooling and prior to collection was used as a marker to assess washing efficiency. To determine the number of washing steps required, samples after one to four washings were prepared and analyzed for GABA using Marfey's derivatization and LC-MS/MS detection. After the third washing, the residual GABA level was undetectable **Figure 42**, and three washings were therefore used in all subsequent experiments.

LC-MS/MS method development: Marfey's derivatives of L-Ala, D-Ala, D-Ala-D-Ala, and D-Ala-D-Lac were prepared, and found to be well separated **Figure 43**. The standard Analyst quantitative optimization algorithms were run to optimize for

LC–MS/MS based quantitation of a desalted sample of Mar-D-Ala-D-Lac.

Fragmentation of the precursor ion revealed that the most intense product ion peak for Mar-D-Ala-D-Lac was the result of a neutral loss of 45 Da ($[M+H-45]^+$), analogous to the pattern observed for Mar-L-Ala, Mar-D-Ala, and Mar-D-Ala-D-Ala [140]. This - 45 Da product ion peak was selected for use in MRM detection and quantitation of Mar-D-Ala-D-Lac. The key parameters for Mar-D-Ala-D-Lac were the same as for the Mar-D-Ala-D-Ala [140].

Linearity and matrix effect: Linearity was confirmed by analysis of seven-point calibration curves for all four analytes (D-Ala, L-Ala, D-Ala-D-Ala, and D-Ala-D-Lac) over the range of 0-500 pmol **Figure 44**. All four analytes were included to ensure linearity and lack of matrix effects in VRE extract. Since these metabolites are endogenous, the calibration curve for serial dilutions in VRE extract was plotted after subtracting the blank values. This calibration range was found to be suitable for the determination of these analytes in VRE extracts, and sensitivity and linearity factors in both water and VRE extract are summarized in **Table 6**. All four analytes showed good linearity in this range with $R^2 > 0.99$, and without appreciable matrix effects. LLOQ and LOD for all four analytes were 1.2 pmol and 0.6 pmol respectively.

Accuracy, precision, and recovery: The only extraction step in this experimental protocol is the acetone extraction step, which is the earliest possible point for the addition of an internal standard. Amino acids and dipeptides (L-Ala, D-Ala, D-Ala-D-Ala and D-Ala-D-Lac) are highly soluble in acetone-water mixtures – with 100% recoveries expected in the cell extraction step, and a second extraction of the cell pellet revealed no detectable levels of these analytes – consistent with 100%

recoveries. In general, high-percentage recoveries are not a critical factor for a bioanalytical assay; reproducibility is the important factor [143]. The highly reproducible signals from the $^{13}\text{C}_3$ -D-Ala internal standard and analytes **Figure 45** demonstrate the reproducibility of this method. The intrarun and the interrune precisions were between 4 and 6%, and the intrarun and the interrune accuracies were between 3 and 5%.

Stability: In our previous study of Marfey's derivatization-based analysis of L-Ala, D-Ala and D-Ala-D-Ala, samples kept cold on ice before derivatization with Marfey's reagent were stable for at least 2 hrs, however, samples warmed to more than 10 °C demonstrated some conversion of $^{13}\text{C}_3$ -D-Ala to $^{13}\text{C}_3$ -L-Ala [140]. Similarly, samples containing underivatized D-Ala-D-Lac were stable for at least 2 hrs when stored on ice, and for at least 90 days when stored frozen at -20 °C. Derivatized samples containing Mar-D-Ala-D-Lac were stable for at least 48 hrs at room temperature, three cycles of freeze-thaw, and 3 months at -20 °C (changes of less than 4%).

Table 5. Summary of optimized parameters for MS/MS detection of Marfey's adducts

MS Parameters	
DP (V)	60
EP (V)	6
CEP (V)	Instrument Default
MS/MS Parameters	
CE (V)	20
CXP (V)	4
CAD (Arb)	5
ESI Parameters	
TEM (°C)	175
CUR (Arb)	30
GS1 (Arb)	40
GS2 (Arb)	50

Abbreviations; Arb=Arbitrary instrument based setting; DP=declustering potential; EP=entrance potential; CEP=collision cell exit potential; CE=collision energy; CXP=collision cell exit potential; CAD=collisionally activated dissociation; TEM=temperature; CUR=curtain gas setting; GS1 and GS2, gas spray 1 and 2 settings, respectively.

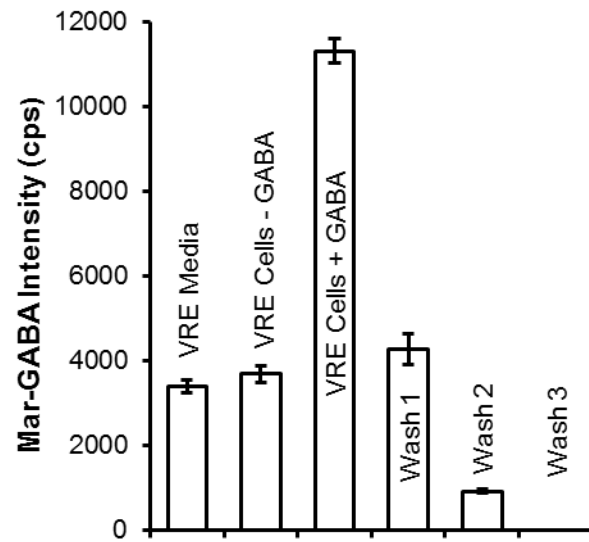


Figure 42. Measured levels of γ -aminobutyric acid (GABA) during washing. Error bars represent the standard error (n = 4) for each measurement.

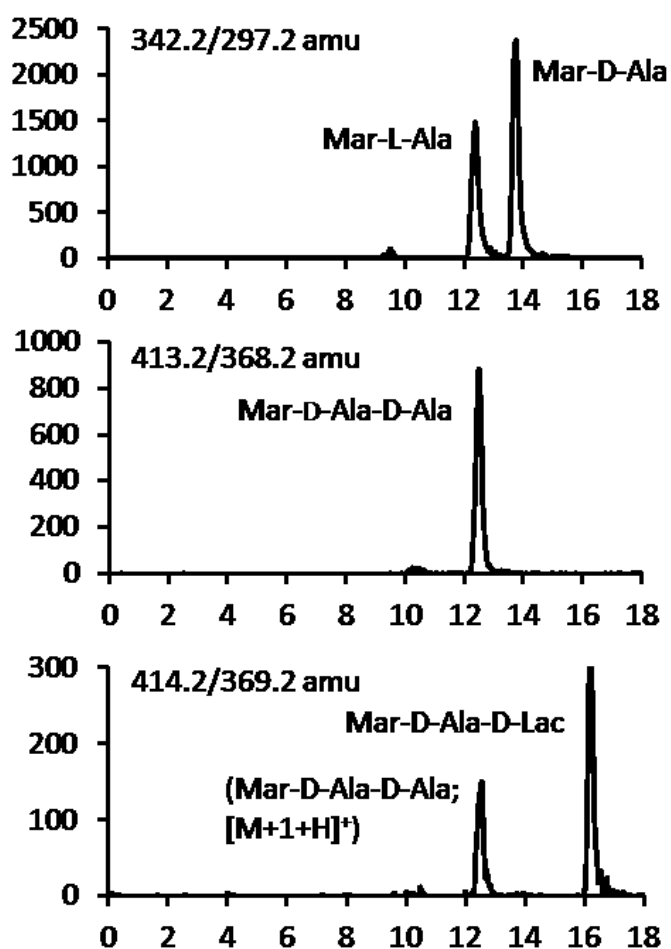


Figure 43. Representative LC–MS/MS chromatograms of Marfey’s derivatized metabolites extracted from VRE. Peak identities were verified using standards. Top panel: LC–MS/MS chromatogram detected at m/z 342.2/297.2 (Q1/Q3), which is specific for the Marfey’s adduct of L-Ala (12.4 min) and D-Ala (13.8 min). Middle panel: Analogous data for m/z 413.2/368.2, which is specific for the Marfey’s adduct of D-Ala-D-Ala (12.5 min). Bottom panel: Analogous data for m/z 414.2/369.2, which is specific for the Marfey’s adduct of D-Ala-D-Lac (peak at 16.2 min). A peak for the +1 isotopomer of D-Ala-D-Ala is also seen (12.5 min), but this peak is well resolved chromatographically from D-Ala-D-Lac (16.2 min) and does not interfere with quantitation of D-Ala-D-Lac.

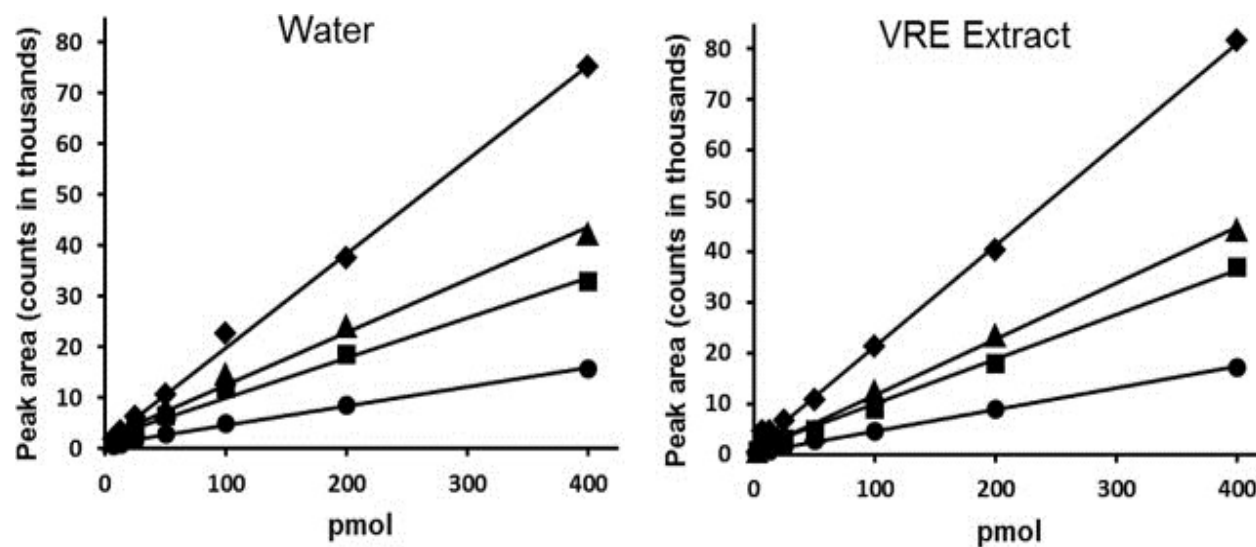


Figure 44. Standard curves for L-Ala, D-Ala, D-Ala-D-Ala, and D-Ala-D-Lac serially diluted in water (left panel) and VRE extract (right panel), derivatized with Marfey's reagent, and quantitated using the developed LC-MS/MS method. Because VRE has background levels of these metabolites, blank values were subtracted before plotting the values in the right panel. Each point represents the average of four determinations. Diamonds (♦), Mar-D-Ala; squares (■), Mar-L-Ala; triangles (▲), Mar-D-Ala-D-Ala; circles (●), Mar-D-Ala-D-Lac.

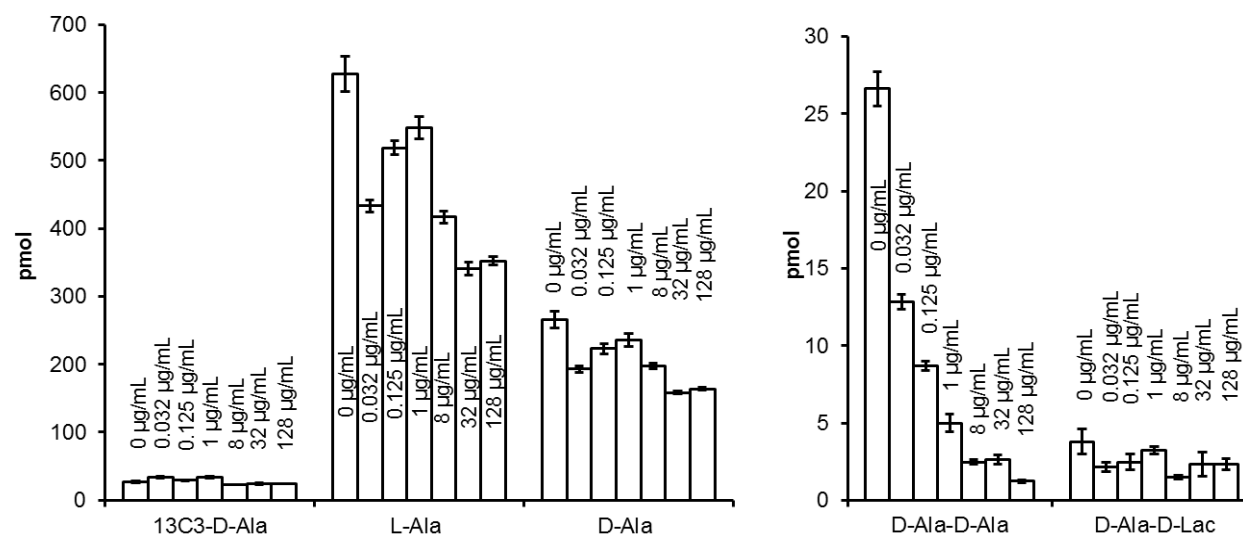


Figure 45. Measured levels of ¹³C₃-D-Ala (internal standard), L-Ala, D-Ala, D-Ala-D-Ala, and D-Ala-D-Lac from extracts of VRE grown at different levels of vancomycin. Each data point is from the extract of 7.0 µg dry cells.

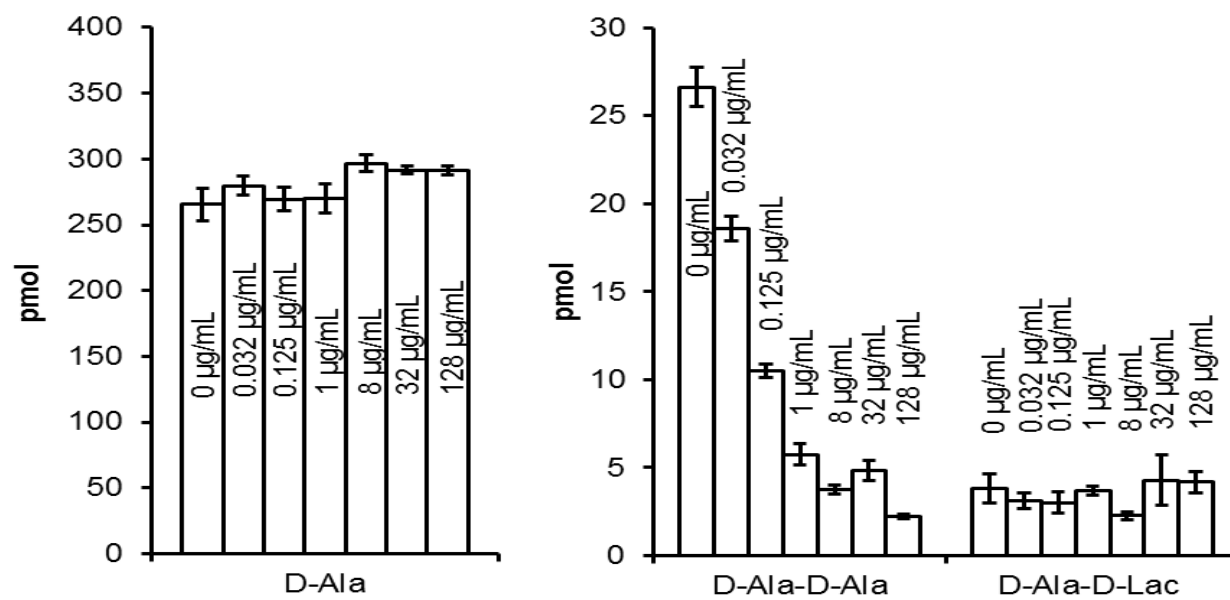


Figure 46. Data for D-Ala, D-Ala-D-Ala, and D-Ala-D-Lac in **Figure 45** normalized to corresponding levels of L-Ala in **Figure 45**.

Table 6. Analyte sensitivity and linearity characteristics in water and VRE extract (matrix).

Analytes	Slopes(AU/pmol) ± SE		R ²		Linear range (pmol)	LLOQ (pmol)	LOD (pmol)
	Water	VRE	Water	VRE			
Mar-D-Ala	185 ± 3	199 ± 4	0.999	0.998	400 - 1	1.17	0.59
Mar-L-Ala	79 ± 3	88 ± 3	0.994	0.996			
Mar-D-Ala-D-Ala	103 ± 2	111 ± 4	0.994	0.992			
Mar-D-Ala-D-Lac	38.3 ± 1.0	42.5 ± 0.6	0.999	0.997			

Selectivity: The selectivity of a Marfey's derivatization approach for the LC-MS/MS quantitation of L-Ala, D-Ala, and D-Ala-D-Ala has been demonstrated previously [140]. D-Ala-D-Lac is one mass unit higher in molecular mass than D-Ala-D-Ala. The +1 Da isotopomer of D-Ala-D-Ala will therefore have the same nominal molecular mass as D-Ala-D-Lac, which could pose a selectivity problem if these two analytes are not well separated chromatographically since the +1 Da isotopomer of D-Ala-D-Ala would also show up in the D-Ala-D-Lac MS/MS channel. A UV-vis monitored chromatogram demonstrated that Mar-D-Ala-D-Lac was well separated from Mar-D-Ala-D-Ala using our standard chromatographic conditions. After MRM optimization, Mar-D-Ala-D-Ala was only apparent in the D-Ala-D-Ala channel (**Figure 43**, middle panel), as expected. A +1 Da isotopomer signal was also observed in the D-Ala-D-Lac channel, also as expected (**Figure 43**, bottom panel), but chromatographic separation was very good and provided for analyte selectivity. D-Ala-D-Ala and D-Ala-D-Lac can therefore be quantitated independently using the Marfey's derivative-based method developed here. Further evidence of selectivity is that D-Ala-D-Lac was undetectable in vancomycin sensitive bacteria such as *Escherichia coli* and *Staphylococcus aureus* (data not shown).

Application of this method to quantitation of D-Ala-D-Ala and D-Ala-D-Lac in VRE: This method was then demonstrated for the quantitation of these key metabolites in VRE. Measured levels of the internal standard ($^{13}\text{C}_3$ -D-Ala) were highly reproducible **Figure 45**, demonstrating low experimental error in the extraction, derivatization, and LC-MS/MS steps. The variations observed in the raw L-Ala and D-Ala levels were strongly correlated (**Figure 45**, correlation

coefficient = 0.99), with only a weak correlation with vancomycin concentration (correlation coefficient = -0.60), indicating that variation in these metabolites was due to differences in cultures before the addition of the internal standard ($^{13}\text{C}_3\text{-D-Ala}$) and with only weak dependence on vancomycin concentration. The observed variation was also uncorrelated with the cell density (OD at 600 nm) at the time of harvesting (data not shown). Normalization of the D-Ala, D-Ala-D-Ala, and D-Ala-D-Lac levels using their L-Ala levels, with the L-Ala level at 0 $\mu\text{g/ml}$ vancomycin (70.7 pmol/ μg dry cells) as the reference value, was performed (Eq. (1)):

equation(1)

$$[\text{X}]_i \text{ (normalized)} = [\text{X}]_i \text{ (un-normalized)} \times [\text{LA}]_0 / [\text{LA}]_i,$$

where $[\text{X}]_i \text{ (normalized)}$ = normalized concentration of the X metabolite in the i th sample; $[\text{X}]_i \text{ (un-normalized)}$ = un-normalized concentration of the X metabolite in the i th sample; $[\text{LA}]_0$ = concentration of L-Ala in the control ([vancomycin] = 0) sample (70.7 pmol/ μg dry cells); and $[\text{LA}]_i$ = concentration of L-Ala in the i th sample. This normalization approach shows substantially reduced variation for the d-Ala data [$\sigma^2_{\text{d-Ala}}$ in **Figure 45** = 34 (pmol/ μg dry cells) 2 and $\sigma^2_{\text{D-Ala}}$ in **Figure 46** = 3.1 (pmol/ μg dry cells) 2]. The use of a core metabolite such as L-Ala as a reference, therefore, substantially corrects for variation between different culture flasks.

Exposure to vancomycin results in a concentration-dependent lowering of the D-Ala-D-Ala level **Figure 45**, with a midpoint around 0.06 $\mu\text{g/ml}$ vancomycin. This decrease in D-Ala-D-Ala level is consistent with induction of the VanX DD-dipeptidase activity with increasing vancomycin concentrations [144]. In contrast, D-

Ala-D-Lac levels were essentially constant from 0 to 128 µg/ml vancomycin **Figure 45**. The observation of flat D-Ala-D-Lac levels in response to increasing vancomycin concentrations is, however, somewhat surprising given that VanH and VanA—which encode for the D-Lac dehydrogenase and D-Ala-D-Lac ligase necessary for D-Ala-D-Lac synthesis—are part of the VanA gene cluster, which also encodes for VanX, the D-Ala-D-Ala dipeptidase necessary for D-Ala-D-Ala hydrolysis [145]. The general presumption is that the expression of these three genes would be coregulated in response to vancomycin [144]. However, the data in **Figure 45** clearly show a decrease in D-Ala-D-Ala concentration in response to vancomycin, demonstrating induction of VanX dipeptidase activity without a commensurate increase in D-Ala-D-Lac levels. To determine whether there was a separate non-VanA process that could produce the background levels of D-Ala-D-Lac observed, vancomycin-sensitive *Enterococcus faecium* (VSE, ATCC BAA-2127) was assayed for D-Ala-D-Lac. No detectible D-Ala-D-Lac was found. The LOD for D-Ala-D-Lac is 0.60 pmol, and the D-Ala-D-Lac level in VRE extracts was 4 pmol, so there is at least 7 times less D-Ala-D-Lac in VSE than in VRE. These observations suggest that the regulation of gene expression in the VanA gene cluster is more complex than anticipated previously.

This method was then demonstrated for the quantitation of these key metabolites in VRE. Measured levels of the internal standard (¹³C₃-D-Ala) were highly reproducible **Figure 45**, demonstrating low experimental error in the extraction, derivatization, and LC-MS/MS steps. The variation observed in the raw L-Ala and D-Ala levels appeared correlated **Figure 45**, which suggests that variation in these metabolites was due to differences in cultures before addition of the internal

standard ($^{13}\text{C}_3\text{-D-Ala}$). The observed variation was also uncorrelated with the cell density (OD at 600 nm) at the time of harvesting (data not shown). Normalization of the D-Ala, D-Ala-D-Ala, and D-Ala-D-Lac levels using L-Ala levels (a core metabolite) gives the results shown in **Figure 46**, which shows greatly reduced variation ($\sigma^2_{\text{D-Ala}}$ in panel A = 1290 pmol², and $\sigma^2_{\text{D-Ala}}$ in panel B = 140 pmol²). Exposure to vancomycin results in a concentration dependent lowering of the D-Ala-D-Ala level **Figure 45**, with a midpoint around 0.06 $\mu\text{g/mL}$ of vancomycin. This decrease in D-Ala-D-Ala levels is consistent with induction of the VanX DD-dipeptidase activity with increasing vancomycin concentration [144]. In contrast, D-Ala-D-Lac levels were essentially constant from 0 – 128 $\mu\text{g/mL}$ vancomycin **Figure 45**.

Summary: The analytical method described above extends the utility of a Marfey's reagent derivatization strategy for amino acid [140] and dipeptide [140, 146] quantitation, to the key depsipeptide intermediate in the most common types of vancomycin resistance [42-43]. This analytical method is demonstrated for characterizing the alanine branch metabolite profile in response to varied vancomycin concentration in VRE. The D-Ala-D-Ala level dropped substantially in response to increasing vancomycin concentration with a midpoint of $\sim 0.06 \mu\text{g/mL}$ **Figure 45**. In contrast, D-Ala-D-Lac was constant over the same vancomycin range, and present even in the absence of vancomycin/. This assay will be useful for studies of vancomycin-induced resistance, and for the discovery and development of new agents targeting vancomycin resistance in VRE.

CHAPTER 5

DESIGNER LINKERS: MODEL REACTIONS AND LINEAR FREE ENERGY RELATIONSHIPS IN THE REACTIVITY AND DESIGN OF SOLID-PHASE LINKERS

Introduction

The twentieth century has witnessed extraordinary developments in techniques for the synthesis of peptides and peptide mimetics. These techniques can be sub-divided into two main categories, “solution” and “solid-phase”. The various methods for synthesis in solution phase have been summarized in numerous monographs and reviews [147-149]. Unfortunately these methods are quite tedious and time consuming, and require considerable expertise, largely due to the unpredictable solubility characteristics of intermediates. In solution phase synthesis, purification and characterization are required after each step, and the solubility of the peptide worsens and becomes more unpredictable with increased chain length. Recognizing these limitations, R.B. Merrifield of Rockefeller University conceived the alternative solid-phase approach in 1959. In various publications Merrifield demonstrated the feasibility of the solid-phase approach for both manual and automated peptide synthesis [150-155]. Solid phase peptide synthesis (SPPS) has become a routine tool for the systematic exploration of biological and physical properties of peptides, and provided a basis for the development of combinatorial chemistry and solid-phase organic chemistry [103, 107, 156]. SPPS in the classical C-to-N direction is now a well-developed process. There is still considerable ongoing research in this area, with significant recent advances in the areas of protecting

groups (reviewed in [157-158]) coupling agents and methods (reviewed in [159]), strategies for assembling very large peptides from smaller building blocks using various ligation strategies (reviewed in [160]), strategies for attaching nascent peptide chain through the peptide backbone [161], and solid-phase methods for preparing C-terminally modified peptides [162].

Overview of Boc and Fmoc approaches

Two types of chemistry are commonly used for classical C-to-N SPPS, which differ based on the nature of the amine protecting group; Boc chemistry [163] and Fmoc chemistry [164-165] (Fig. 1). There are a number of common steps in traditional peptide synthesis: loading the first amine protected amino acid residue onto the resin through its carboxyl group, deprotection of the amine protecting group, and coupling with the next amine protected amino acid residue. Repeating the deprotection and coupling steps with the desired amino acid residues provides the final peptide fragment, with side chains protected, attached to the resin. The peptide-resin attachment and side chain protecting groups are then removed to provide the desired peptide cleaved from the resin. Boc chemistry uses moderately acidic trifluoroacetic acid (TFA) to remove the Boc protecting group, whereas Fmoc chemistry generally uses the weak secondary amine base piperidine to remove the Fmoc protecting group. The resin attachment and side chain protecting groups in standard Boc chemistry can be cleaved with anhydrous HF, trifluoromethanesulfonic acid/TFA (TFMSA/TFA) mixtures, or HBr/TFA mixtures, whereas with Fmoc chemistry more acid labile resins and side chain protecting groups are used which can be cleaved with TFA. Auxiliary reagents and different cleavage protocols are

often required to minimize side reactions, and to remove specific side chain protecting groups from the peptide (reviewed in [166]).

A number of variables affect the success of any SPPS effort and must be considered during its planning and execution. Important choices that influence the overall outcome of a synthesis include the nature of the solid support, coupling chemistries, protection scheme, cleavage conditions, and the linkage for anchoring the peptide to the support.

Resins for Boc SPPS (Figure 47)

Much of the original work in peptide synthesis was performed with Boc amino acids loaded onto hydroxymethyl (HM) polystyrene through an ester linkage (Fig. 2). After peptide synthesis is complete, the benzyl-O attachment bond is broken by use of relatively strong acid such as anhydrous HF, TFMSA/TFA, or HBr/TFA. Significant losses of peptide were observed on HM resins during repetitive deprotection of Boc groups with TFA, which led to the introduction of the more acid stable PAM (4-(oxymethyl)-phenylacetamidomethyl) resin [167]. The benzyl-O bond in PAM resin is stabilized to acid relative to HM polystyrene by the electron withdrawing CO-CH₂-group. In many applications it is desirable to prepare peptides with a C-terminal amide in place of a C-terminal carboxyl group, which led to the introduction of BHA (benzhydrylamine) resin [168]. The second benzene ring further stabilizes the benzyl cation generated during acidolysis, which is necessary since it is harder to acidically cleave the benzyl-N bond than the benzyl-O bond. After loading the first residue, peptide synthesis is performed following standard Boc protocols, and the peptide cleaved from the resin with a strong acid. Using BHA resin, it was observed that this

resin often gave low yields of product peptides due to inefficient cleavage of the benzyl-N bond. Substitution of this resin with the relatively weakly electron donating methyl group lead to the development of the more acid sensitive methylbenzhydrylamine (MBHA) resin [169], which is cleaved more efficiently with strong acids.

Resins for Fmoc SPPS

For Fmoc-based peptide synthesis, which uses the weak secondary amine base piperidine to remove the Fmoc protecting group, resins have been developed which allow the peptide to be cleaved from the resin with TFA, a considerably milder and easier to use reagent than HF or TFMSA/TFA. For carboxyl terminated peptides a *p*-alkoxybenzyl alcohol (Wang resin) is used [170], where the relatively strongly electron donating *p*-alkoxy substituent increases the acid sensitivity of the benzyl-O-peptide attachment relative to the analogous HM resin used in Boc chemistry **Figure 47**. For preparation of C-terminal amides, even more acid labile Rink amide [171] or PAL [172] resins can be used which allow the benzyl-N bond to be cleaved with TFA. Many other resins have been synthesized and tested for peptide synthesis and solid phase organic synthesis applications (reviewed in [173-174]).

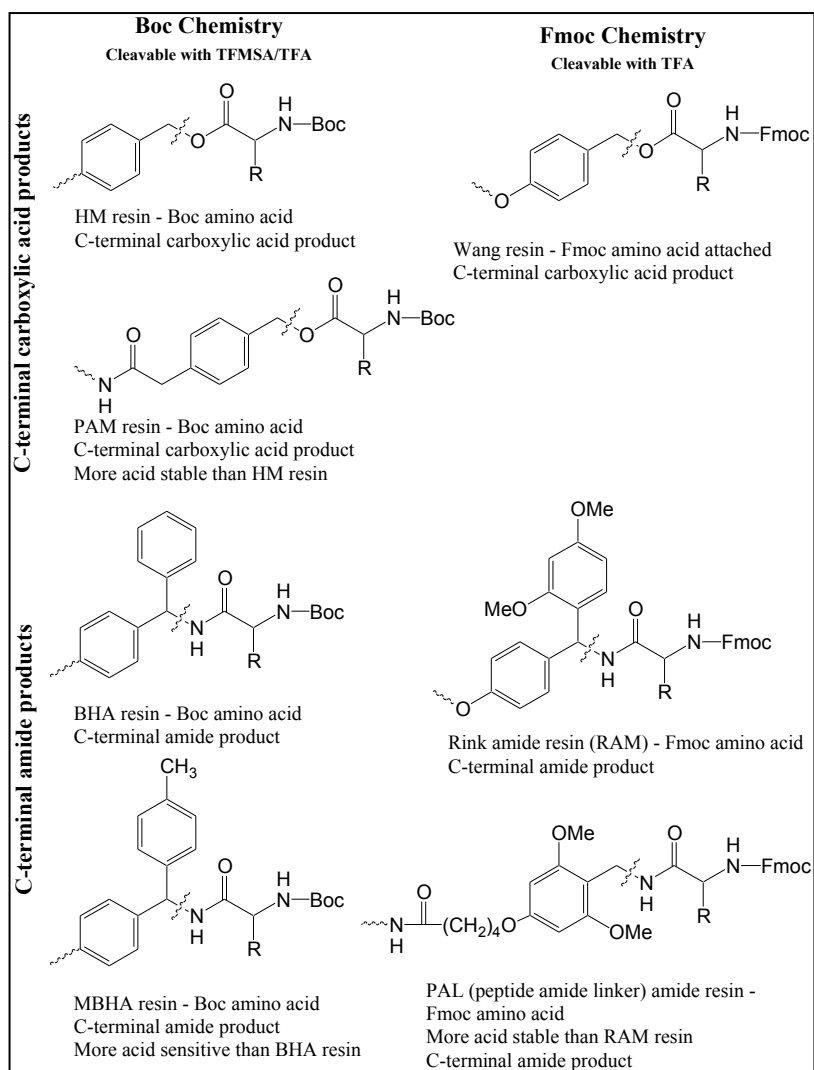


Figure 47. Standard resins for Boc and Fmoc SPPS.

Anchoring

Regardless of the structure and nature of the polymeric support chosen, it must contain appropriate functional groups, e.g., amino, hydroxyl, chloromethyl, or other functionality, onto which the first amino acid can be anchored. Nearly fifty functionalization methods have been developed [175]. Later, some advantages of the handle approaches for anchoring have been recognized [167, 176-177].

Handles are nothing but bifunctional spacers that on one end feature a smoothly cleavable protecting group, and on the other end allow coupling to a previously functionalized support. Thus, handles serve to link the first amino acid to the resin in two distinct steps [178-180] and thereby afford maximal control over this essential step of the synthesis.

Side chain protecting groups

Side protecting groups are an important aspect of solid phase peptide chemistry (reviewed in [157]). For Boc chemistry-based synthesis, where the peptide is cleaved from the resin with strong acids such as TFMSA/TFA, amine (Lys), carboxyl (Glu and Asp) groups, and hydroxyl (Ser, Thr, and Tyr) are generally protected with benzyl based protecting groups (Cbz, benzyl esters, and benzyl ethers respectively) which are simultaneously removed from the peptide during cleavage from the resin. Chlorine or Br substituted benzyl groups (Cl-Cbz; Br-Bzl) are more acid stable due to electron withdrawal by the halogen and are generally preferable as Lys and Tyr protecting groups respectively, especially for longer peptides. Alternatively, the more acid sensitive pMeO-Bzl or trityl protecting groups are preferred for Cys residues. Similarly strong acid (TFMSA/TFA) sensitive

protecting groups are used for other amino acids **Table 7**. Alternative selections of protecting groups are available if alternative HF, HBr, or TMSOTf cleavage protocols are to be employed. For Fmoc chemistry-based synthesis, where the peptide is cleaved from the resin with the moderately acidic TFA, amine and carboxylic acid functional groups are protected with t-butyl based protecting groups (Boc and t-butyl esters). Similarly moderate acid sensitive protecting groups are used for other functional groups. For both Boc and Fmoc-based syntheses, it is possible to cleave and deprotect simple (low amounts of side chain protecting groups) peptides from the resin using simple cleavage mixture, whereas more complex peptides often require additional scavengers or treatment to obtain good products.

Coupling reactions

The most important step in solid-phase peptide synthesis is the systematic elaboration of the growing peptide chain. This involves deprotection and coupling cycles. The temporary protecting group such as Boc or Fmoc is removed by acidolysis or base treatment to liberate the N^α -amine of the peptide resin. Then the α amine is neutralized with a tertiary amine such as diisopropylethylamine and the free amine of the resin-bound amino acid is ready to couple with a second protected amino acid. The latter must be activated for the reaction to occur. There are two major categories of activation. The first one is preactivation and the other one is in situ activation. In the former, the C^α - carboxyl of a protected amino acid is activated selectively to give a reasonably stable derivative, and in a separate step is reacted with an amine. In the later, an amine, carboxylic acid, and condensing agent are mixed together simultaneously to form an amide bond in situ. The

simplest and most often used procedure is activation with *N,N'*-dicyclohexylcarbodiimide (DCC). *N,N'*-diisopropylcarbodiimide (DIC or DIPCDI) is even more convenient to use because of handling considerations and the improved solubility of the corresponding urea. Several side reactions are possible when carbodiimides are used. The majority of these side reactions may be circumvented by the addition of additives (1-hydroxybenzotriazole (HOBt) [181] or 1-hydroxy-7-azabenzotriazole (3-hydroxy-3*H*-1,2,3-triazolo-[4,5-*b*] pyridine)(HOAt) [182], which react with the *O*-acylurea to form a less reactive but still effective acylating agent.

Table 7. Side chain protected amino acids suitable for Boc or Fmoc chemistry

Boc-AA TFMSA cleavage ^a	Fmoc-AA TFA cleavage ^b
Arg(Mts) ^c Asp(OBzl) Cys(pMeOBzl) Glu(OBzl) His(Bom) Lys(2-Cl-Cbz) Met(O) ^d Ser(Bzl) Thr(Bzl) Trp(For) ^d Tyr(2-Br-Bzl)	Arg(Pmc) Asp(OtBu) Cys(Trt) Glu(OtBu) His(Trt) Lys(Boc) Ser(tBu) Thr(tBu) Trp(Boc) Tyr(tBu)

^a For simple peptides 10% TFMSA in TFA can be used. To minimize side reactions in more complex peptides a scavenger cocktail can be used depending on the nature of the peptide. Typically, for 1x of resin, thioanisole/ethanedithiol (4x/2x), TFA (10x), and then TFMSA (2x) are added.

^b For standard cleavage reactions 95 % TFA, 2.5 % triisopropylsilane, 2.5 % H₂O can be used. To minimize side reactions a scavenger cocktail can be used depending on the nature of the peptide. Typically, for 1x of resin, add an 8-10 fold excess of 80% TFA, 5% thioanisole, 5% H₂O, 3% ethanedithiol, 1% triisopropylsilane.

^c Abbreviations: Mts - Mesitylene(2,4,6-trimethylbenzene)sulfonate; Pmc - 2,2,5,7,8-pentamethylchroman-6-sulfonate; Bom - benzyloxymethyl; Trt - trityl; For - formate. Other abbreviations are fairly standard.

^d Deprotected using a low-high TFMSA procedure.

Recently some *in situ* coupling reagents have gained popularity. These include phosphonium salts as well as uronium salts. The most widely used salts include *N*-[(1*H*-benzotriazol-1-yl)(dimethylamino)methylene]-*N*-methylmethanaminium hexafluorophosphate *N*-oxide (HBTU), *N*-[(dimethylamino)-1*H*-1,2,3-triazolo-[4,5*b*]pyridine-1-yl-methylene]-*N*-methylmethanaminium hexafluorophosphate *N*-oxide (HATU) [182]. These reagents react with the carboxylate of an amino acid to form an active ester intermediate. These phosphonium and uronium salts have low reactivity with amino groups and are therefore well suited to *in situ* coupling protocols. To extend the peptide chain, deprotection, neutralization and coupling steps need to be repeated until the desired sequence has been synthesized.

Cleavage from the resin

Once the desired sequence has been synthesized, the complete peptide is deprotected and cleaved from the resin. Multiple options are available to cleave the bond connecting the peptide to the handle. These include acid, base [183-185], fluoride ion, Pd⁰ [186], and light (*hν*) [175, 178, 180, 187-189]. Acid-labile handles are prevalent and can be divided further into those cleaved by strong acid (e.g., HF-scavengers), moderate acid (e.g., trifluoromethanesulfonic acid in TFA) [190], and mild acid (e.g., using very low percentage of TFA). The cleavage can be conducted to retain the permanent side chain protecting groups, and thus yield protected segments suitable for further condensation, or for later deblocking in solution [183, 191]. Most commonly the final deprotection of side chains is carried

out simultaneously with cleavage so that the released product is completely deprotected peptide [192].

Methods which allow for the synthesis of C-terminally modified peptides

Normal SPPS in the C-to-N direction allows N-terminally modified peptides to be synthesized, but does not in its standard format allow for modification of the chemically versatile C-terminus since it is attached to the resin. Substantial effort has been devoted to addressing this deficiency. Such efforts can be divided into three groups; efforts based on C-terminal functional group specific attachment, efforts to develop effective methods for inverse (N-to-C) SPPS (ISPPS), and efforts to attach the C-terminal residue through its backbone amide nitrogen (Backbone Amide Linker (BAL) strategy), thereby providing the C-terminal carboxyl group for further elaboration. A short description of each follows.

C-terminally modified peptide mimetics can be prepared through the use of functional group specific attachment strategies for the C-terminal residue which allows the C-terminal mimetic to be obtained upon cleavage from the resin. In this approach the peptide backbone is synthesized using classic C-to-N synthesis methods (Fmoc or Boc). Libraries with an aldehyde C-terminus have been prepared by an aldehyde-semicarbazone attachment strategy followed by traditional C-to-N peptide synthesis [193]. Specific attachment strategies have also been developed for peptide hydroxamic acids [194], and peptide alcohols [195]. Although suitable for a few C-terminal functional groups, the functional group specific attachment strategy lacks flexibility and generality.

It has long been recognized that a general approach for N-to-C solid-phase peptide synthesis (ISPPS) would be desirable, especially for the synthesis of C-terminally modified peptides [162]. ISPPS was first suggested by Letsinger & Kornet [196]. A number of investigations on strategies for ISPPS have been described, including based on the use of amino acid hydrazides [197], amino acid 9-fluorenylmethyl (Fm) esters [198], amino acid tri-tert-butyloxysilyl esters [199], and amino acid allyl esters [200]. These approaches all suffer from limitations, including the general lack of availability of suitable monomers. The strategy we have developed for ISPPS is based on amino acid t-butyl esters [201-203]. t-Butyl esters have many advantages for ISPPS, including that they are stable, commercially available, and the synthesis of commercially unavailable monomers is straightforward. The t-butyl ester strategy also has the benefit that this approach is exactly the reverse of the well-developed Boc strategy for normal C-to-N peptide synthesis, and the extensive knowledge of side chain protection and other chemical details can be transferred from Boc-based SPPS to t-butyl ester-based ISPPS.

Another approach to the preparation of C-terminally modified peptide mimetics is via a backbone amide linker (BAL) attachment strategy (reviewed in [204]). In this approach the first residue is attached to the resin through its amino group as a secondary amine, followed by Fmoc [205-207] or Boc [208-209] based synthesis of the peptide, selective protection/deprotection of the C-terminal carboxyl group, elaboration of the C-terminus into the desired functional group, and finally cleavage from the resin.

Overview of peptide derived agents (PDAs)

A wide variety of both naturally occurring and man-made PDAs are known. Many of these are useful drugs, and others are potent natural toxins. There is currently great interest in PDAs given their potential for the development of new drugs and bioactive agents [210-212]. There has also been increasing interest in PDAs as components for nanotechnology [210, 213-215]. There are a very large number of known PDAs agents, and a complete list cannot be presented here. A representative selection of cyclic natural PDAs is provided below. The agents included are agents for which a versatile ISPPS approach could be useful in improving or redirecting their biological activity.

Bacitracin is a group of at least 10 closely related peptides isolated from *Bacillus subtilis* **Figure 48**. The most active constituent is Bacitracin A. Bacitracin inhibits cell wall biosynthesis by binding to C55-isoprenyl pyrophosphate [216] reviewed in [217], an intermediate in bacterial cell wall biosynthesis. It is generally used topically, but can be administered parenterally to treat serious infections [218-219]. A solid-phase synthesis of bacitracin has not been reported to our knowledge, but could allow for the optimization of its antibacterial activity and minimization of its nephrotoxicity.

Capreomycin is a mixture of two closely related cyclic peptide antibiotics, which is used as a second line tuberculostatic agent **Figure 49**. It acts by inhibiting protein biosynthesis [220]. It is used as a second line agent due to toxicity, which mainly involves disturbances to electrolyte balance. Several solution phase syntheses of this antibiotic have been reported as a basis for structure function

studies [221] and references therein, the most recent of which provided the desired product in only 2% overall yield after 27 steps. A solid-phase synthesis of capreomycin has not been reported to our knowledge, but could be useful for the optimization of its anti-mycobacterial activity and minimization of toxicity.

Marine natural product peptides with anticancer activity. There have been a large number of peptide natural products derived from marine sources which have demonstrated anticancer activity, with a number having entered clinical trials including didemnin, hemiasterlin, dolastatins, cemadotin, soblidotin, aplidine, and kahalalide F [211-212]. These compounds have a diverse range of structures, and exert their effects through a variety of mechanisms. Kahalalide F is a representative example. It is cyclic peptide first identified in a marine mollusk [222], and later determined to be produced by an alga and taken up by the mollusk during feeding **Figure 50** [223]. A solid-phase synthesis of Kahalalide F has been reported [224].

Alpha-Amanitin. Alpha-amanitin is a highly toxic bicyclic octapeptide found in the *Amanita phalloides* (Death Cap) and Destroying Angel mushrooms **Figure 51** [225]. After ingestion it is absorbed, travels to the liver where it enters cells, and binds to and inhibits RNA polymerase II. This is often lethal, and is untreatable except with an emergency liver transplant. The structure of amanitin complexed with RNA polymerase II is known [226]. Amanitin is of interest as an example of a peptide agent which is orally available and which reaches an intercellular target. Redesigning this agent to be non-toxic, and to target other processes, offers potential for the development of novel peptide-based therapeutic agents.

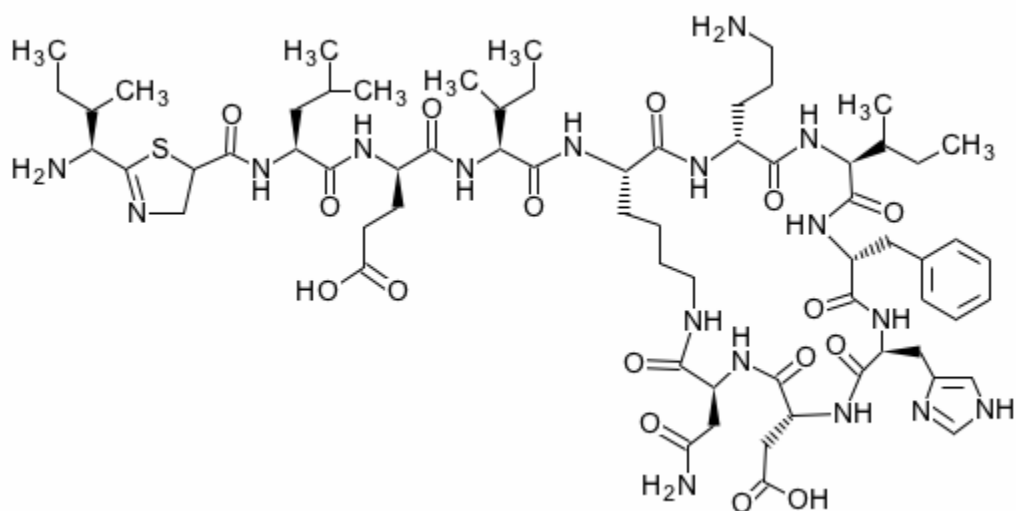


Figure 48. Structure of Bacitracin A. Adapted from Toscano et.al 1982.

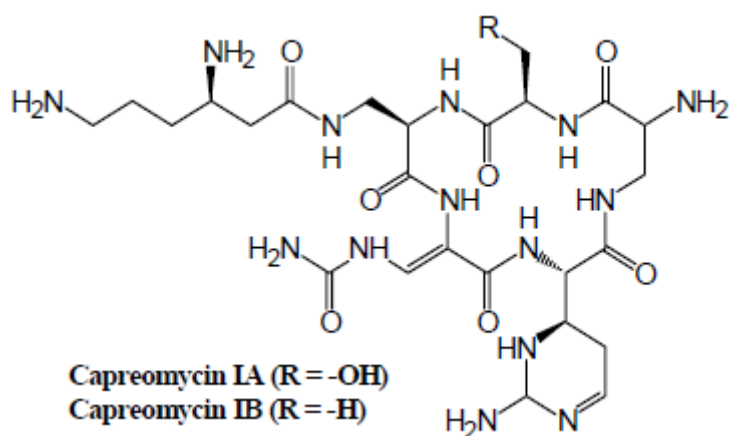


Figure 49. Structure of Capreomycin IA and IB. Adapted from DeMong D.E. et. al. 2003.

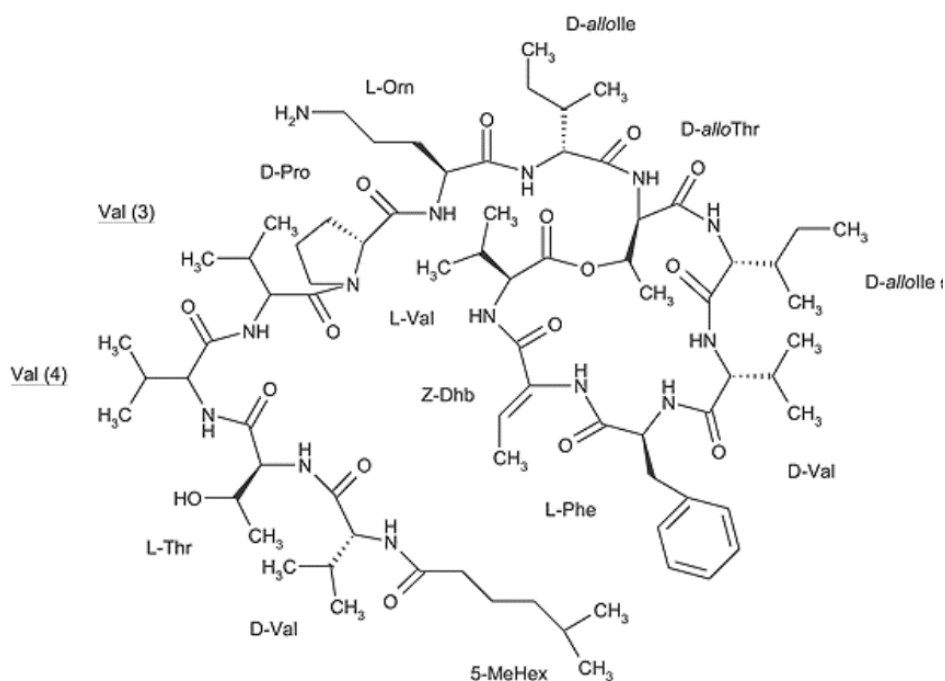


Figure 50. Structure of Kahalalide F. Adapted from Hamann M.T et. al. 2001.

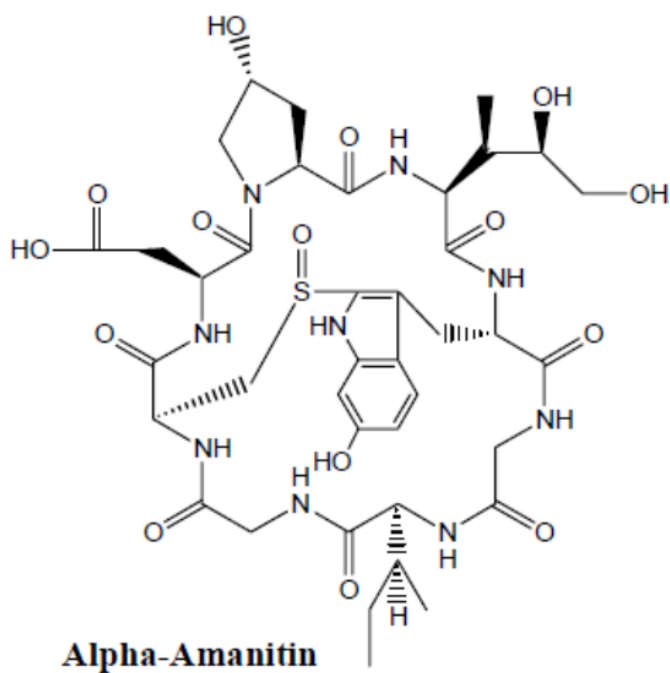


Figure 51. Structure of Alpha-Amanitin. Adapted from Bushnell D.A. et. al. 2002.

Hammett equation and constants

The Hammett equation was introduced by Hammett in 1937 and has been established as the most general and simplest approach to describe structure-reactivity relationships in organic reactions [227]. The Hammett equation is based on the ionization of benzoic acids in water at 25 °C **Figure 52** and is expressed as

$$\text{Log}(K_X/K_H) = \rho\sigma$$

Where K_X and K_H are the ionization constants of meta- or para- substituted and unsubstituted aromatic compounds, respectively, σ is the substituent constant, and ρ is the reaction constant.

When rate constants are involved the Hammett equation takes the form of

$$\text{Log}(k_X/k_H) = \rho\sigma$$

Where k_X and k_H are the rate constants of meta- or para- substituted and unsubstituted aromatic compounds, respectively.

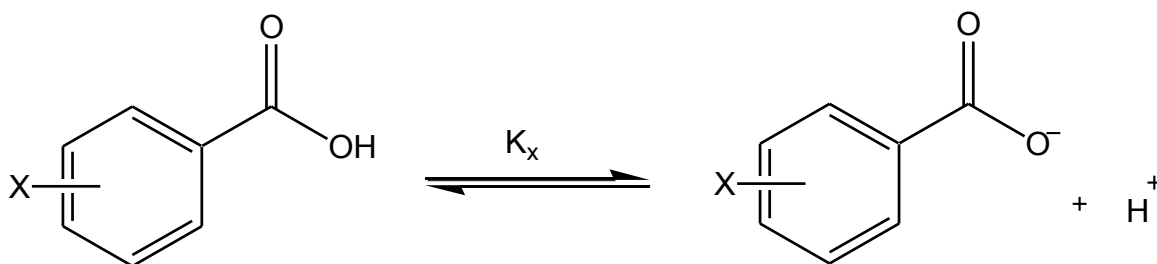


Figure 52. Ionization of benzoic acids.

σ constants obtained from the ionization of aromatic compounds in solution can successfully predict the ionization and rate constants for a wide variety of chemical reactions. Different reactions show different substituent sensitivities, which led to the use of alternative substituent constants (σ^+) were used for better correlated with reactions proceeding through benzyl cations. The σ^+ constants are determined using

the new standard reaction of hydrolysis of t-cumyl chlorides in 90 % aqueous acetone (90A) at 25 °C **Figure 53**.

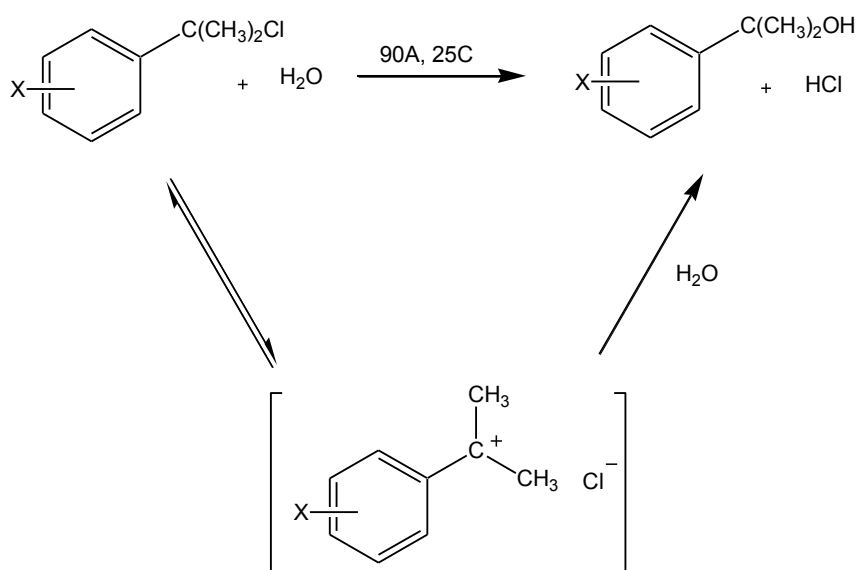


Figure 53. Hydrolysis of t-cumyl chlorides.

Table 8. Some Hammett σ_p^+ and σ_m constants from published standard tables.

Substituent	σ_p^+	σ_m
I	0.13	0.35
Br	0.15	0.39
Cl	0.11	0.37
F	-0.07	0.34
C ₆ H ₅	-0.21	0.05
CH ₃	-0.31	-0.06
SCH ₃	-0.6	0.15
OCH ₃	-0.65	0.11
OH	-0.92	0.13
NH ₂	-1.3	-0.16
N(CH ₃) ₂	-1.7	-0.15

Overall Rationale

It would be useful for solid-phase PDA synthesis to have a versatile and general solid-phase method for *bidirectional* solid-phase peptide synthesis (BSPPS). Several features would be desirable in such a technology. 1) Solid-phase attachment of the nascent peptide through a **backbone amide attachment**. This would allow for the attachment of nearly any amino acid residue (except for proline and other secondary amines), and provide maximum flexibility in designing syntheses. 2) Chain extension in the C-to-N direction (classical SPPS) and/or in the N-to-C direction (inverse SPPS (ISPPS)) (***bidirectional SPPS; BSPPS***). This would provide maximum flexibility in the design and execution of PDA syntheses. These two target features would provide a technology of wide application in areas including drug discovery, chemical biology, and nanotechnology. It was the goal of this study to develop and test backbone attachment strategies compatible with our t-butyl ester approach to ISPPS as the basis for such a general and flexible approach to PDA synthesis. The goal of the proposed effort will be to identify backbone amide attachment linkers with the appropriate chemical stability for BSPPS, and to then demonstrate an effective method for BSPPS using amino acid t-butyl esters for ISPPS, Fmoc amino acids for SPPS, and the use of the Dde group for N-terminal protection during ISPPS cycles. The experimental strategy for the overall rationale is as follows

- 1) Obtain commercially available 4-hydroxy benzaldehyde compounds
- 2) Do model reactions i.e loading of acetate or butyrate linker on the benzaldehyde compounds, loading of Phe-OtBu and capping the amine

group on Phe-OtBu with acetic anhydride. Deprotect the OtBu and purify the compounds.

- 3) Check the stability of the linker to deprotection of OtBu with 25%TFA/DCM and cleaving the Ac-Phe with 5% HBr/TFA. Determine the rate constant for this cleaving reaction.
- 4) Using the Hammett constants and the rate constants determine the reaction constant rho and also identify the linker with right stability for performing the ISPPS and be able to cleave using 5% HBr/TFA
- 5) Load the linker onto the resin and demonstrate the ISPPS using amino acid t-butyl esters.
- 6) Demonstrate SPPS using fmoc amino acids.

Experimental

Materials: Aminomethylated polystyrene (1.17 mmol/g, 70-90 mesh) was purchased from Novabiochem AG (Gibbstown, NJ), and amino acid t-butyl esters were purchased from Bachem AG (King of Prussia, PA). HATU (O-(7-azabenzotriazol-1-yl-N,N,N',N'-tetramethyluroniumhexafluorophosphate), DIPEA (N,N-Diisopropylethylamine), HBr (Hydrogen bromide, 33 wt.% solution in acetic acid), TMP (2,4,6-trimethylpyridine), TFA (trifluoroacetic acid) and TFMSA (trifluoromethane sulfonic acid), anhydrous DMF (N,N-dimethylformamide), and anhydrous DCM (dichloromethane) were purchased from Sigma-Aldrich (Milwaukee, WI). All chemicals purchased were of reagent grade.

Solvents: All the solvents used during solid phase synthesis are anhydrous and dried over 4A° molecular sieves.

Preparative HPLC: Preparative HPLC was performed on a Hewlett-Packard series 1050 system equipped with a diode array detector, fraction collector (Gilson Model 203) and a Econosil C18 column (22.0 x 250 mm, 10 µm particles). Chromatographic conditions used are gradient elution flow rate of 5.0 ml/min; 100% solvent A (0.1% TFA in water) for 5 min, then 0% to 100% of solvent B (0.1% TFA in 30:70 water:acetonitrile) in 55 min, and 0% to 100% of solvent C (0.1 % TFA in acetonitrile) in next 10 min and a linear gradient of 100% solvent A for 10 min. Eluting compounds were collected in fraction collector (Gilson Model 203). The fractions were analyzed by LC-MS and the pure fractions were lyophilized and used for further experiments.

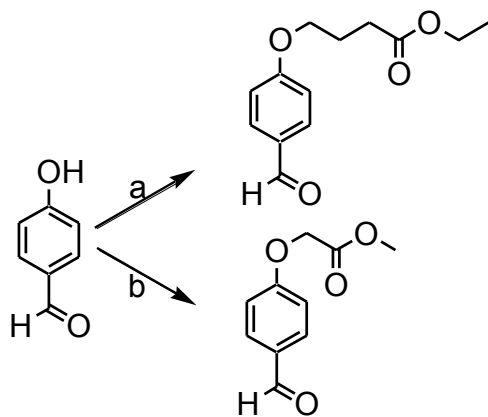
LC-MS Analysis: LC–MS analysis was carried out on an ABI 2000 Q-Trap mass spectrometer fitted with electro-spray ionization (ESI) source and interfaced to an Agilent 1100 series HPLC system equipped with a diode array detector. LC–MS was performed using a Nucleodur C8 column (2.0 x 125 mm, 5 μ m particles) and chromatographic conditions used are gradient elution with a flow rate of 0.3 ml/min; 100% solvent A (0.1% TFA in water) for 2 min, 0% to 100% of solvent B (0.1% TFA in 30:70 water:acetonitrile) in next 10 min, and 0% to 100% of solvent C (0.1 % TFA in acetonitrile) in next 3 min and then a linear gradient of 100% solvent A for 3 min.

Solution phase model reactions

The first set of model linkers were constructed as outlined in **Figure 54** and **Figure 55**. The substituents used on linkers were outlined in **Table 9**. These linkers were then tested for their acid stability using 25% TFA/DCM for 30 min. (OtBu deprotection conditions) and 5% HBr/TFA (peptide-resin cleavage conditions). The rate constants for the cleaving reaction with 5% HBr/TFA was determined for the linkers. The reaction constant ρ was determined using the rate constants and the Hammett constants of the linkers. Linkers with right acid stability i.e. stable during deprotection of OtBu with 25% TFA/DCM for 30 min. and which will be able to cleave the peptide with treatment of 5% HBr/TFA will be selected. These linkers will be loaded onto resin and ISPPS cycles performed to demonstrated their feasibility.

General synthesis procedure for butyrate and acetate connector based

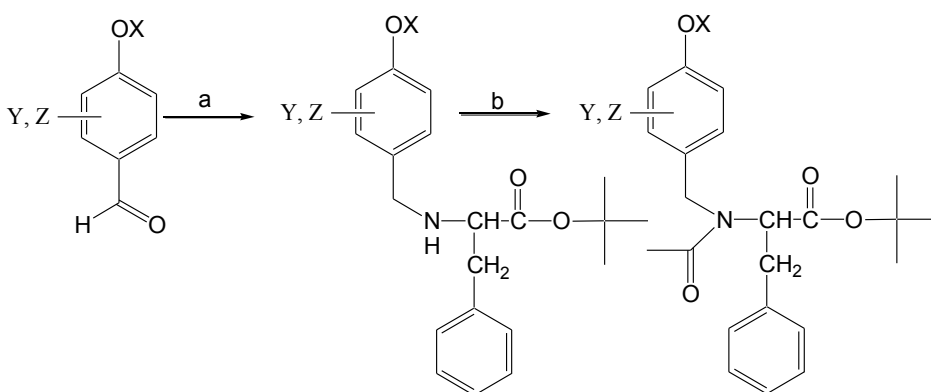
linkers:



(a) ethyl 4-bromobutyrate, K_2CO_3 , DMF; (b) methyl 2-bromoacetate, K_2CO_3 , DMF;

Figure 54. Scheme for loading acetate and butyrate linker onto benzaldehyde compounds

1 eq of 4-hydroxy benzaldehyde and 1.1 eq of linker (ethyl 4-bromobutyrate for attaching butyrate linker and methyl 2-bromoacetate for attaching acetate linker) were dissolved in DMF, 1.1 eq of K_2CO_3 was added and the mixture was stirred overnight at rt (**Figure 54**). The reaction mixture was quenched with 4 eq of 1M HCl, extracted 3 times with ethyl acetate and back extracted once with 1M $NaHCO_3$. The combined organic extracts were dried over $MgSO_4$ and evaporated to dryness in vacuo. This was sufficiently pure for further use. To attach butyrate or acetate linker to different benzaldehydes, their respective 4-hydroxy benzaldehydes were used.



(a) H-Phe-OtBu-HCl, DIPEA, NaCNBH₃, DMF; (b) acetic anhydride, DIPEA, DMF;

X,Y,Z substituents were outlined in **Table 9**.

Figure 55. Scheme for loading H-Phe-OtBu-HCl and capping with acetic anhydride.

Table 9. List of X,Y,Z substituents for the model compounds in **Figure 55**

Comp. No.	X	Y (ortho)	Z (ortho')
1	CH ₂ COOMe	H,H	H
2	(CH ₂) ₃ COOEt	H,H	H
3	CH ₃	H,H	H
4	CH ₃	CH ₃	H
5	(CH ₂) ₃ COOEt	CH ₃	H
6	CH ₂ COOMe	CH ₃	CH ₃
7	(CH ₂) ₃ COOEt	CH ₃	CH ₃
8	CH ₂ COOMe	OCH ₃	H
9	(CH ₂) ₃ COOEt	OCH ₃	H
10	CH ₃	OCH ₃	H
11	CH ₂ COOMe	OCH ₃	OCH ₃
12	(CH ₂) ₃ COOEt	OCH ₃	OCH ₃

General Procedure for loading Phe-OtBu on solution phase linkers: 1 eq. of benzaldehyde linker was dissolved in anhydrous DMF (dried over 4A° molecular sieves), 1 eq. of H-Phe-OtBu·HCl and 2 eq. of DIPEA (dried over 4A° molecular sieves) were added to the reaction mixture and stirred for 15 min. To this mixture was added 1.5 eq. of NaCNBH₃ and the mixture was stirred overnight at rt. The reaction mixture was diluted with water, 1M HCl added to pH 4, and the mixture was extracted 3 times with ethyl acetate the combined organic extracts back extracted 1x with NaOH, and with brine. The organic extract was dried over MgSO₄, and evaporated to dryness in vacuo.

Procedure for acetic anhydride capping on model compounds in solution phase: The Phe loaded model compound (1 eq.) was dissolved in anhydrous DMF (dried over 4A° molecular sieves), 3 eq. of DIPEA (dried over 4A° molecular sieves) and 3 eq. of acetic anhydride were added, and the reaction mixture was stirred overnight at rt **Figure 55**. The reaction mixture was quenched with 5 eq. of 1M NaHCO₃ and stirred for 30 min, extracted 3 times with ethyl acetate and the combined organic extracts was back extracted 1x with 1M HCl. The organic extract was dried over MgSO₄ and evaporated to dryness in vacuo.

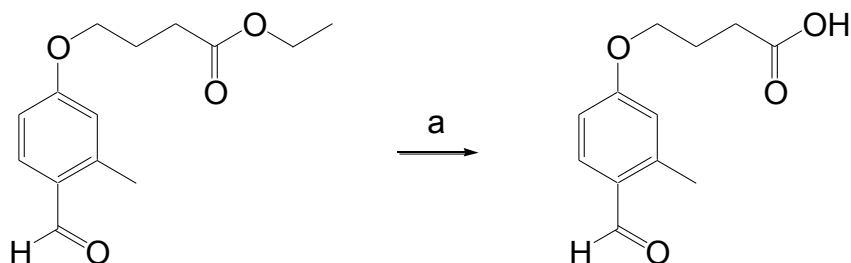
Deprotection of OtBu and cleaving AcPheCOOH: AcPheOtBu loaded model compound (40 mg) was treated with 25% TFA/DCM (2 mL) for 30 min and evaporated to dryness in vacuo to give AcPheCOOH loaded model compound **Figure 60**. This compound was purified on preparative HPLC. AcPheCOOH was cleaved from the model compound by treating with 5% HBr/TFA.

Rate constant determination: AcPheCOOH loaded benzaldehydes were treated with 5% HBr/TFA and samples were collected at 1, 5, 10, 30 mins, 1, 2, 4, 8, 12, 24 hrs. Since HBr/TFA is volatile this treatment was done in a vial sealed with rubber cap and kept in a bigger vial fitted with MININERT valve **Figure 56**. The samples collected were analyzed using LC-MS and the area of the AcPheCOOH peak was determined. Plots of $\ln(\text{area})$ vs time demonstrate first order kinetics and the rate constant k was determined from the slope of the plot.



Figure 56. Vial setup for performing kinetics on model compounds with 5%HBr/TFA.

Preparation of solid phase attached linker



a) K_2CO_3 , 1:1:1 mixture of H_2O :MeOH:acetonitrile

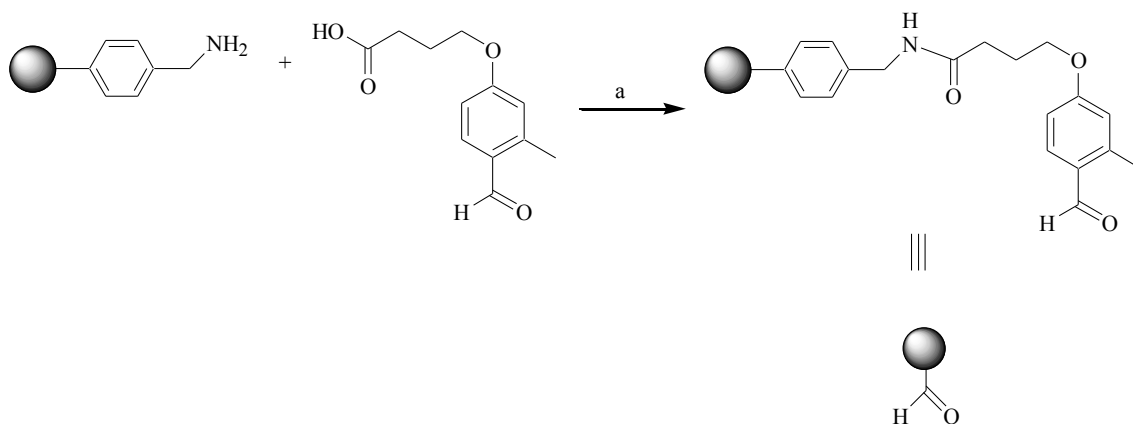
Figure 57. Scheme for saponification of ester group on the linker.

Synthesis of 2-methyl-4-(5-oxyvaleric acid)-benzaldehyde: 2-methyl-4-(5-oxyethylvalerate)-benzaldehyde linker 2 (919 mg, 3.67 mmol) and K_2CO_3 (1.52 g, 11.01 mmol) were dissolved in 1:1:1 mixture of H_2O :MeOH:acetonitrile and stirred overnight at rt. The reaction mixture was made neutral by adding 1M HCl and rotovaped to remove the solvents (MeOH and acetonitrile). The reaction mixtures was extracted once with ether, acidified to pH 4 with 1M HCl and extracted with ethyl acetate (3 X 30 mL). The combined organic extracts were dried over MgSO_4 and evaporated to dryness in vacuo yielding a yellow solid. Yield (653 mg, 80%).

Test conditions for acidolysis of Ac-Phe loaded 2-methyl-4-(5-oxyvaleric acid)-benzaldehyde model linker: 600 μL of 10 mM solution of 2-methyl-4-(5-oxyvaleric acid)-benzaldehyde was subjected to various test treatments; 25% TFA/DCM, 37.5% TFA/DCM, 50% TFA/DCM, 75% TFA/DCM, 100% TFA/DCM, 95% TFA/ H_2O , 10% TFMSA/TFA, 5% HBr/TFA. Samples (10 μL) were collected at regular time intervals (15 min, 30 min, 1 hr, 2 hr, 4 hr, 8 hr, 12 hr and 20 hr), diluted

in 90 μL of $\text{ACN}:\text{H}_2\text{O}$, and analyzed on LC/MS. The rate constants and half-life's of each testing condition were determined and tabulated in **Table 15**.

Loading of linker onto resin and demonstration of ISPPS



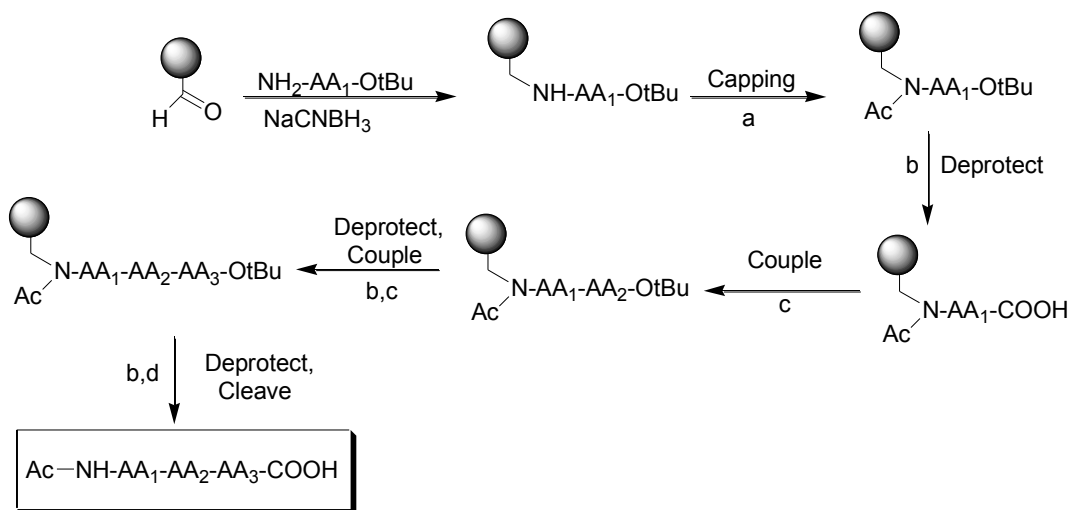
(a) HATU, DIPEA, DMF;

Figure 58. Scheme for loading 2-methyl-4-(5-oxo-5-oxopentanoic acid)benzaldehyde linker onto the amino methyl polystyrene resin.

2-methyl-4-(5-oxo-5-oxopentanoic acid)benzaldehyde linker attachment onto resin:

Aminomethylated polystyrene resin (loading 0.78 mmol g⁻¹, 100-200 mesh) was swollen in DMF for 2 hrs and then washed with DMF. 2-methyl-4-(5-oxo-5-oxopentanoic acid)benzaldehyde linker (86.7 mg, 0.39 mmol) and O-(7-azabenzotriazol-1-yl)-N,N,N',N'-tetramethyluronium hexafluorophosphate (HATU) (148.3 mg, 0.39 mmol) were dissolved in DMF (1 mL), DIPEA (140 μL , 0.78 mmol) was added, and the clear solution was immediately added to resin (100 mg, 0.078 mmol). The suspension was shaken for 16 hrs at rt. The resin was washed with 3 X DCM (700 μL), 3 X DMF (700 μL) and vacuum dried. A solution of acetic anhydride (22.1 μL , 0.23 mmol) and DIPEA (40.7 μL , 0.23 mmol) in DMF was stirred with resin for 12 hrs

to cap unreacted amino groups. The resin was washed 3 x DCM (700 μ L), 3 x DMF (700 μ L) and vacuum dried. The anchored 2-methyl-4-(5-oxyvalericacid)-benzaldehyde linker can be seen in **Figure 58**.



(a) Ac_2O , DIPEA, DMF; (b) 25% TFA/DCM; (c) HATU, amino acid, TMP, DMF;
(d) 5% HBr/TFA

Figure 59. Scheme for amino acid t-butyl ester based ISPPS.

Table 10. Amino acid t-butyl ester based ISPPS protocol.

Description	Reagent	Repetition and Duration
OtBu Deprotection	10% TFA/DCM	1 × 5 s
	25% TFA/DCM	1 × 30 min
Washes	DCM	3 × 5 s
	NMP	2 × 5 s
	DCM	3 × 5 s
Activation /Coupling	5 eq. HATU	12 h
	5 eq. AA-OtBu·HCl	
	10 eq. TMP in DMF	
Washes	DCM	3 × 5 s
	DMF	3 × 5 s

Loading of the first amino acid by reductive amination: The overall synthesis strategy is outlined in **Figure 59**. To load the first amino acid (Phe), a solution of H-Phe-OtBu-HCl (80.2 mg, 0.31 mmol) and DIPEA (108.7 μ L, 0.62 mmol) in DMF (750 μ L) was added to the resin (100 mg, 0.078 mmol). After shaking for 15 min, NaBH₃CN (29.4 mg, 0.47 mmol) was added and shaken for 16 Hrs at rt. The resin was washed with 3 X DCM (700 μ L) and 3 X DMF (700 μ L) and vacuum dried.

Capping: It was desirable to test the chemical sensitivity of different capping groups on sensitivity to cleavage (25% TFA/DCM and 5% HBr/TFA). After loading, the secondary amine of the resin attached HPhe-OtBu was capped with different capping reagents such as acetic anhydride, toluoyl chloride, isovaleryl chloride and benzoyl chloride. To cap the first amino acid (Phe), a solution of capping reagent (3 eq.) and DIPEA (7.5 eq.) in 750 μ L DCM was added to the resin and shaken for 12 Hrs at rt. The resin was washed with 3 X DCM and 3 X DMF and vacuum dried.

Amino Acid t-Butyl Ester-Based ISPPS: After loading, the t-butyl ester of the first residue was deprotected with 25% TFA/DCM, and synthesis cycles were performed as outlined in **Table 10**.

Cleavage of peptides from resin: Peptide loaded resin sample (10 mg) was treated with 5% HBr/TFA for 8 Hr. The cleavage solution was sampled and analyzed by HPLC and LC/MS. Four tripeptides with acetic anhydride as capping group and Phe capped with different capping groups were synthesized **Table 16** and **Table 17**. These peptides were analyzed by LC-MS for purity and yield and for amino acid racemization using Marfey's reagent.

Amino acid racemization: The amount of racemization of amino acids in product peptides was determined by derivitization with Marfey's reagent [107, 139]. A 2 μL aliquot of a 50 mM aqueous solution of the sample was hydrolyzed with 100 μL 6 N HCl for 4 hours at 110 $^{\circ}\text{C}$ in sealed vials, and the hydrolyzed mixture dried under vacuum. To this was added 14.3 μL (5 eq per amino acid) of a 1% solution of Marfey's reagent (1-fluoro-2,4-dinitrophenyl-5-L-alanine amide) in acetone, 4 μL of 1 M NaHCO_3 and 6 μL of water, and the mixture was kept at 35-40 $^{\circ}\text{C}$ for 90 min. The reaction was quenched by the addition of 4 μL of 1 M HCl. Solvent was removed under vacuum and the residue was dissolved in 400 μL of 1:1 acetonitrile and water containing 0.1% of TFA. A 10 μL injection was made for HPLC analysis.

Results and Discussion

Importance of solution phase model reactions: Several commercial resins were tried for the development of this approach but these resins were not stable to treatment of acids either for deprotection of OtBu with 25% TFA/DCM or cleaving of peptide with 5% HBr treatment. During treatments with these acid, part of the resin would cleave off or the peptide itself would come off it can be very difficult to determine exactly what is happening in a solid-phase reaction, especially when the resin attachment is involved, since a portion of the reaction products are solid-phase attached. Inability to characterize some of the fragments that we see after acid treatment complicates a full understanding of what is happening. To circumvent this limitation, model solution phase reactions were used to characterize different potential linker moieties as a prelude to performing the analogous reactions on the solid-phase. With an aim to develop a linker that would be stable to 25% TFA/DCM

treatment and cleave the peptide when treated with 5% HBr/TFA, several substituted benzaldehyde linkers were investigated for their acid stability using model solution phase reactions.

Scheme of model cleaving reaction on solution phase: OtBu was deprotected from N-Acetyl-[2-methyl-4-(5-oxy-ethylvalerate)benzyl]-L-phenylalanine-OtBu by treating with 25% TFA/DCM for 30 mins. The resulting N-Acetyl-[2-methyl-4-(5-oxyvalericacid)benzyl]-L-phenylalanine was then treated with 5% HBr/TFA for 24 hrs and samples were collected at 1, 5, 10, 30 mins, 1, 2, 4, 8, 12, 24 hrs and analyzed using LC-MS. The area of AcPheCOOH formed was determined. The rate constant of this reaction was obtained by plotting $\ln(\text{area of AcPhe formed})$ vs time. Rate constants and $t_{1/2}$ of the linkers were reported in **Table 12**.

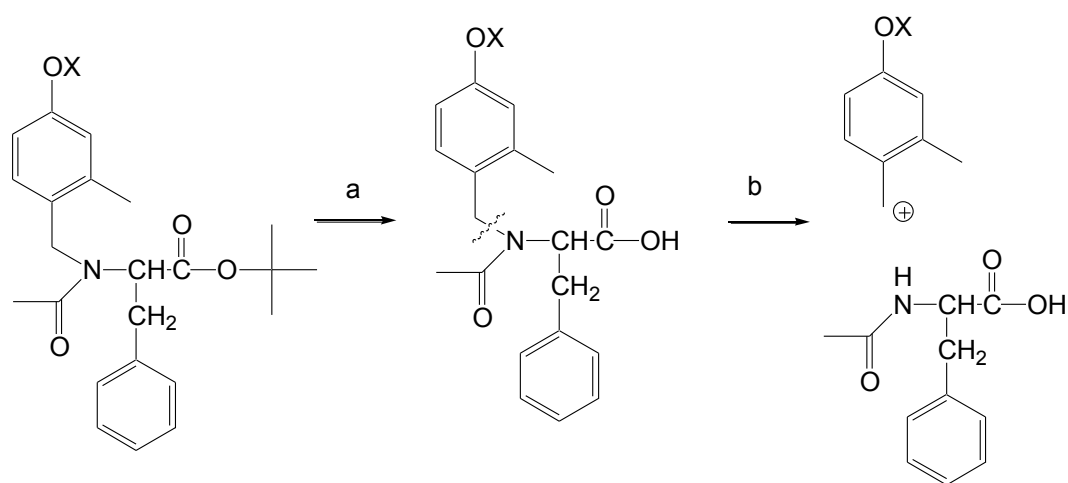


Figure 60. Scheme of solution phase model cleaving reaction

Table 11. Molecular weight confirmation and yields of linkers synthesized.

Comp. No.	Compound Name	Mol Wt [M+H] ⁺		Yield (%)	Mass Spectrum	HPLC Chromatogram
		Calcd	Found			
1	N-Acetyl-[4-(5-oxy-methylbutyrate)benzyl]-L-phenylalanine	442.5	442.1	53	Figure 63	Figure 64
2	N-Acetyl-[4-(5-oxy-ethylvalerate)benzyl]-L-phenylalanine	484.6	484.2	59	Figure 65	Figure 66
3	N-Acetyl-[4-methoxybenzyl]-L-phenylalanine	384.5	384.2	49	Figure 67	Figure 68
4	N-Acetyl-[2-methyl-4-methoxybenzyl]-L-phenylalanine	398.5	398.3	54	Figure 69	Figure 70
5	N-Acetyl-[2-methyl-4-(5-oxy-ethylvalerate)benzyl]-L-phenylalanine	498.6	498.2	57	Figure 71	Figure 72
6	N-Acetyl-[2,6-dimethyl-4-(5-oxy-methylbutyrate)benzyl]-L-phenylalanine	470.6	470.2	47	Figure 73	Figure 74
7	N-Acetyl-[2,6-dimethyl-4-(5-oxy-ethylvalerate)benzyl]-L-phenylalanine	512.7	512.2	57	Figure 75	Figure 76
8	N-Acetyl-[2-methoxy-4-(5-oxy-methylbutyrate)benzyl]-L-phenylalanine	472.5	472.4	54	Figure 77	Figure 78
9	N-Acetyl-[2-methoxy-4-(5-oxy-ethylvalerate)benzyl]-L-phenylalanine	514.6	514.2	58	Figure 79	Figure 80
10	N-Acetyl-[2-methoxy-4-methoxybenzyl]-L-phenylalanine	414.5	414.2	51	Figure 81	Figure 82
11	N-Acetyl-[2,6-dimethoxy-4-(5-oxy-methylbutyrate)benzyl]-L-phenylalanine	502.6	502.0	59	Figure 83	Figure 84
12	N-Acetyl-[2,6-dimethoxy-4-(5-oxy-ethylvalerate)benzyl]-L-phenylalanine	544.7	543.4	49	Figure 85	Figure 86
13	N-Acetyl-[4-(5-oxy-methylbutyrate)naphthyl]-L-phenylalanine	492.6	492.1	53	Figure 87	Figure 88
14	N-Acetyl-[4-(5-oxy-ethylvalerate)naphthyl]-L-phenylalanine	534.7	534.2	52	Figure 89	Figure 90

Table 12. Half-lives and rate constants of the linkers under 5% HBr/TFA treatment.

Cmp.No.		OR	o,o'	$t_{1/2}$ (hr)	k (hr ⁻¹)	SE
1	Bz	CH ₂ COOMe	H,H	n/a	n/a	n/a
2		(CH ₂) ₃ COOEt	H,H	4.56	0.15	0.38
3		CH ₃	H,H	5.41	0.13	0.01
4		CH ₃	CH ₃	2.75	0.25	0.02
5		(CH ₂) ₃ COOEt	CH ₃	1.86	0.37	0
6		CH ₂ COOMe	CH ₃ ,CH ₃	1.55	0.45	0.01
7		(CH ₂) ₃ COOEt	CH ₃ ,CH ₃	0.68	1.02	0.11
8		CH ₂ COOMe	OCH ₃	1.76	0.39	0.03
9		(CH ₂) ₃ COOEt	OCH ₃	0.07	9.59	0.66
10		CH ₃	OCH ₃	0.07	9.6	0.4
11		CH ₂ COOMe	OCH ₃ , OCH ₃	0.3	2.32	0.12
12		(CH ₂) ₃ COOEt	OCH ₃ , OCH ₃	0.31	2.2	0.12
13	Nap	CH ₂ COOMe	H,H	2.64	0.26	0.01
14		(CH ₂) ₃ COOEt	H,H	0.19	3.62	0.2

Bz=Benzaldehyde; Nap=Napthaldehyde;

Calculation of σ^+ values for different linkers: The σ^+ values of individual substituent Me and OMe were obtained from published tables [228] and listed in **Table 13**. The σ^+ values of individual substituent OAc and OBu were obtained by least squares. For substituents with unknown σ^+ values, σ^+ values were obtained by minimizing the sum of squares of the difference between observed k value and the best fit line for other compounds with known k values. The obtained σ^+ values are reported in **Table 13**. A plot between observed k value and predicted k value is shown in **Figure 61**. The σ^+ values for synthesized linkers were calculated by

summing up the individual σ^+ values (**Table 13**) of all the substituents on the linker.

The final σ^+ values of the linkers were summarized in **Table 14**.

Table 13. σ^+ values of individual substituents

Substituent	σ^+
Me	-0.256 Lit.
OMe	-0.648 Lit.
OCH ₂ COOMe	-0.305 Calc.
O(CH ₂) ₃ COOEt	-0.86 Calc.

Lit.=Literature; Calc.=Calculated;

Table 14. σ^+ values for different benzaldehyde linkers synthesized

S.No.		OR	o,o'	σ^+
1	Bz	CH ₂ COOMe	H,H	-0.305
2		(CH ₂) ₃ COOEt	H,H	-0.86
3		CH ₃	H,H	-0.648
4		CH ₃	CH ₃	-0.904
5		(CH ₂) ₃ COOEt	CH ₃	-1.116
6		CH ₂ COOMe	CH ₃ ,CH ₃	-0.817
7		(CH ₂) ₃ COOEt	CH ₃ ,CH ₃	-1.372
8		CH ₂ COOMe	OCH ₃	-0.953
9		(CH ₂) ₃ COOEt	OCH ₃	-1.508
10		CH ₃	OCH ₃	-1.296
11		CH ₂ COOMe	OCH ₃ , OCH ₃	-1.601
12		(CH ₂) ₃ COOEt	OCH ₃ , OCH ₃	-2.156

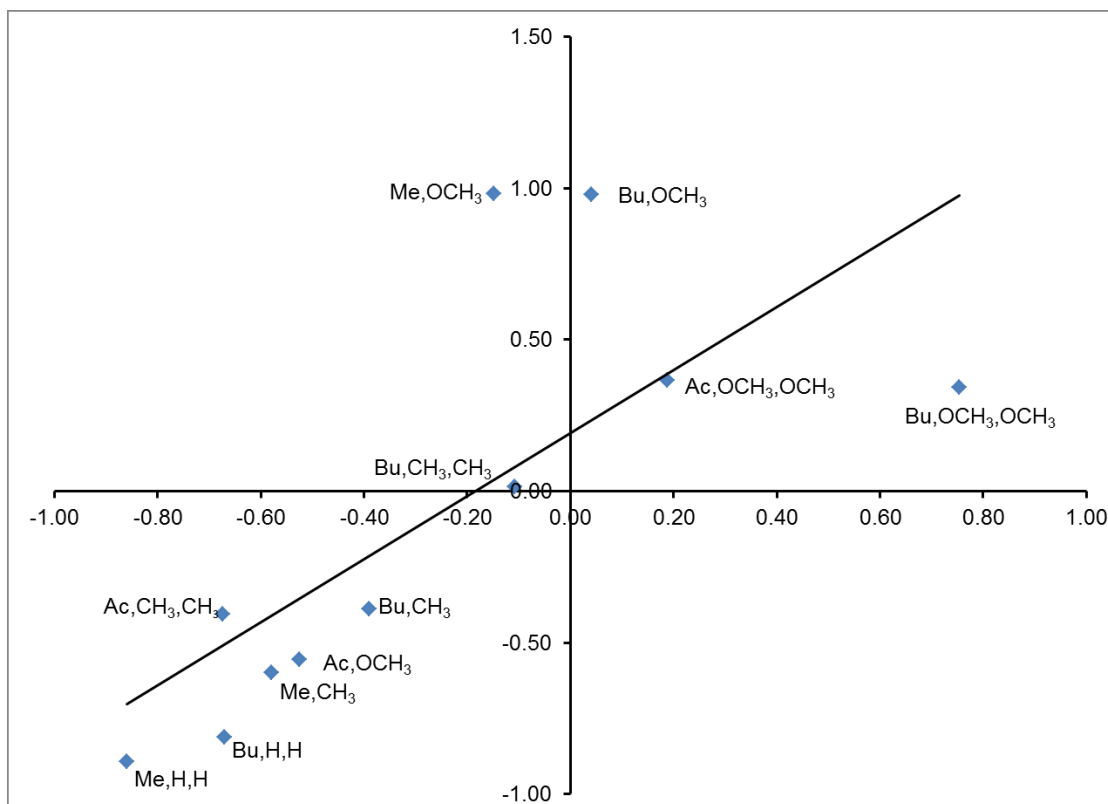


Figure 61. Plot between observed k value and predicted k value for different linkers, and consensus best line.

Plot showing Rho Calculation: linkers which fell on the straight line in **Figure 61** were chosen for calculating the ρ value. In other words linkers that fell on the consensus line for observed and predicted rate constants were chosen for calculating ρ value. The reaction constant ρ was obtained from the slope of the plot between the $\log(\text{observed rate constant of the reaction with substituent})$ vs the σ^+ of the substituents **Figure 62**. The reaction constant ρ obtained was -1.1.

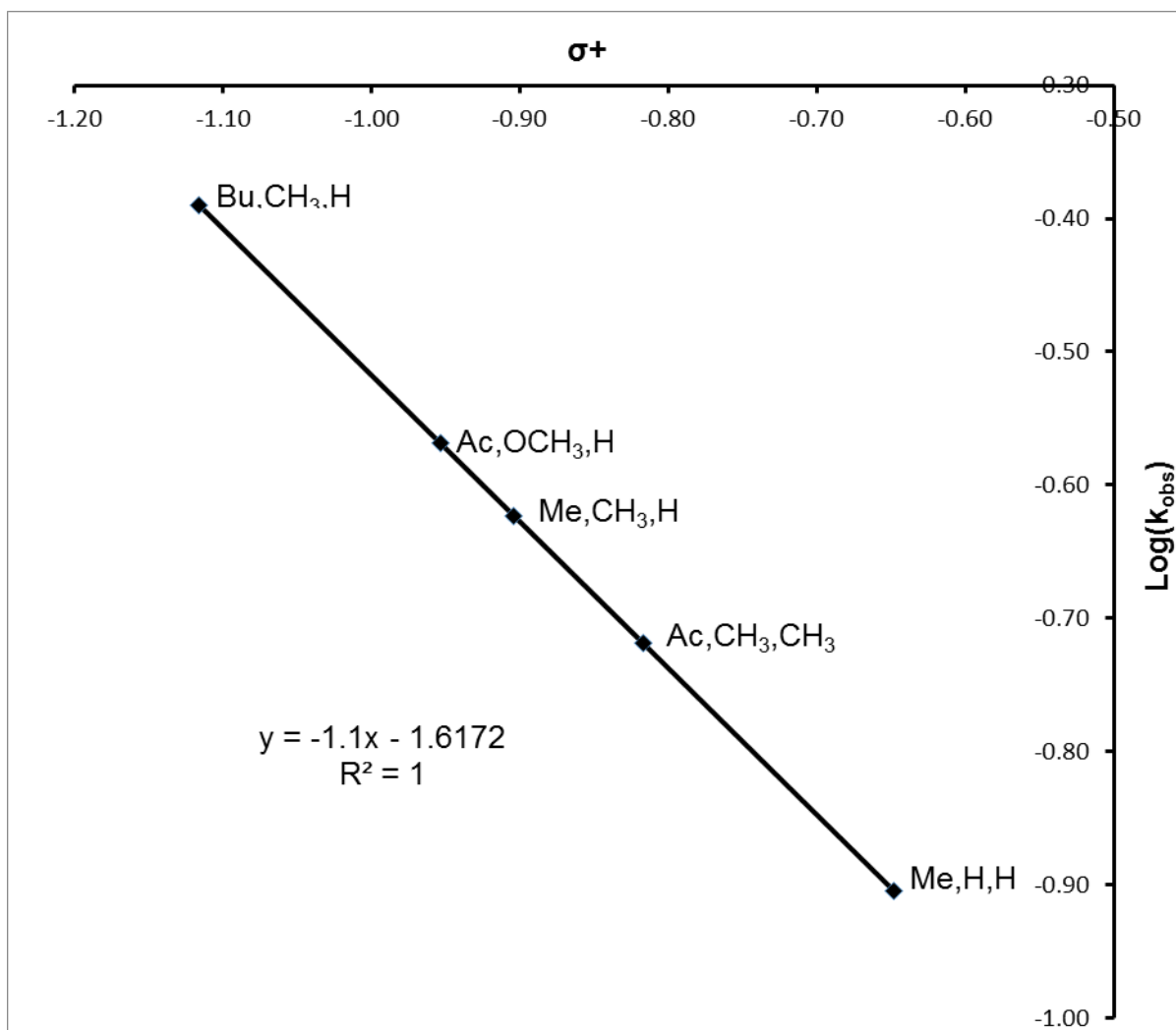


Figure 62. Plot between σ^+ and $\log(k_{\text{obs}})$ for calculating Rho value.

Selection of final particular linker: To provide a suitable linker for BSPPS using our t-butyl ester strategy for ISPPS (N-to-C) and an Fmoc strategy for SPPS (C-to-N), it is necessary for the attachment to be stable to the TFA/DCM conditions used to deprotect t-butyl esters, and stable to the condition necessary to deprotect Fmoc and Dde groups. The attachment must also be cleavable using standard strong acid conditions such as TFMSA/TFA or HBr/TFA. All the possible benzaldehyde linkers that are commercially available and which could provide the acid stability required for the envisioned application were procured and model solution phase reactions were done as shown in **Figure 60**. Half-life and rate constants for the cleaving step with 5% HBr/TFA were determined for the linkers and tableted in **Table 12**. During model solution phase reactions we have observed that the 4-methoxy benzaldehyde based linker (compound number 3 in **Table 11**) was too stable to acid treatment with 5% HBr/TFA and gave poor yields and incomplete cleavage. In contrast, 2, 4-dimethoxy-benzaldehyde based linker (compound number 10 in **Table 11**) was too easily cleaved even with the 25% TFA/DCM treatment that is needed to deprotect t-butyl esters. Among other linkers N-Acetyl-[2-methyl-4-(5-oxy-ethylvalerate)benzyl]-L-phenylalanine (compound number 5 in **Table 11**) seemed to be the perfect linker with the right kind of acid stability. When treated with 25% TFA/DCM for 30 min. a small amount (less than 2%) of the Ac-Phe cleavage product was detected. This loss (cleavage) is small and indicates that the analogous 2-methyl-4-(5-oxyvalericacid)benzaldehyde based resin would be suitable for up to 12 synthesis cycles with greater than a 80% yield of the product peptide.

90% of the peptide cleavage can be done with 5% HBr/TFA in 6.2 Hrs and 99% of the peptide can be cleaved in 12.5 Hrs. The chemical reactivity of this linker was further examined with various concentrations of TFA in DCM and their rate constants and half-life's were determined **Table 15**. The ability of this linker to be cleaved by an extended treatment with 100% TFA may provide a useful means to prepare protected peptide fragments (with a unprotected C-terminus) from the analogous resin, since Boc chemistry compatible side chain protecting groups should be stable to this treatment.

Table 15. N-Acetyl-[2-methyl-4-(5-oxy-ethylvalerate)benzyl]-L-phenylalanine linker's cleavage rate for different acid treatments.

Test Condition	k (hr ⁻¹)	t _{1/2} (Hrs)
25% TFA/DCM	0.073	9.56
37.5% TFA/DCM	0.076	9.17
50% TFA/DCM	0.082	8.49
75% TFA/DCM	0.094	7.39
100% TFA/DCM	0.144	4.81
95% TFA/H ₂ O	0.122	5.67
10% TFMSA/TFA	0.422	1.64
5% HBr/TFA	0.435	1.59

Loading of linker onto resin: To load the 2-methyl-4-(5-oxyethylvalerate)-benzaldehyde linker onto resin, the ethyl ester was saponified by K_2CO_3 in a 1:1:1 mixture of $H_2O:EtOH:acetonitrile$ **Figure 57**. The deprotected linker was coupled to the α -amine of the aminomethyl polystyrene resin using HATU **Figure 58**. Any residual free amino groups was capped with acetic anhydride.

Loading of first amino acid onto resin: The first amino acid was loaded onto the resin by reductive amination, followed by N-acylation **Figure 59**. The above outlined procedure was followed with Phe as the loaded residue and capped with acetic anhydride. Cleavage using 5% HBr/TFA and quantitation of Ac-Phe by HPLC with UV-Vis detection at of 260 nm demonstrated greater than 90% loading efficiency.

Demonstration of ISPPS cycles: To demonstrate this linker for ISPPS, four acetic anhydride capped tripeptides were synthesized. All these peptides were identified by LC-MS and were obtained in good yield and purity **Table 16**. Peptides were analyzed for the degree of amino acid racemization using Marfey's reagent. No detectable levels of racemization was observed using this approach. This solution phase model reaction linker was capped with only acetic anhydride. Effect of different capping groups on the stability of the linker was checked on the solid phase by capping the first amino acid (Phe) with acetic anhydride, toluoyl chloride, isovaleryl chloride and benzoyl chloride. OtBu was deprotected by treating with 25% TFA/DCM for 30 min. and the capped Phe was cleaved by treating with 5% HBr/TFA and analyzed by LC-MS **Table 17**. Tolyoyl and benzoyl capping groups made the

linker more acid liable and during the deprotection of OtBu, indicative higher acid sensitivity with these capping groups.

Table 16. Molecular weight confirmation, purities, and yields of the synthesized peptides.

Product	Mol Wt [M+H] ⁺		Purity ^a %	Yield ^b %
	Calcd	Found		
1 AcPheAlaGly	335.4	336.2	98	88
2 AcPheLeuVal	419.5	420.4	95	80
3 AcPheGlyVal	363.4	364.2	95	85
4 AcPheAlaVal	377.4	377.0	88	81

^a Determined by HPLC of cleaved peptide

^b Determined by amount of peptide obtained after cleavage

Table 17. Molecular weight confirmation of different capping groups and % cleavage during deprotection step.

Product	Mol Wt [M+H] ⁺		% Cleaved during 25% TFA/DCM treatment
	Calcd	Found	
1 Ac-Phe	207.2	208.2	1
2 Tolyoyl-Phe	283.3	284.2	9
3 Isovaleryl L-Phe	249.3	250.2	1
4 Benzoyl-Phe	269.3	270.2	6

Attempt to demonstrate BSPPS: To achieve maximum flexibility for PDA synthesis, it would be desirable to be able to perform chain extension reactions also in the C-to-N direction (SPPS). This will provide a common central core for the subsequent SPPS and ISPPS extension cycles. The linker was attached to the resin by backbone amide link and then first amino acid Phe-OtBu was loaded by reductive amination. Then we tried to acylate the secondary amino group either with Fmoc-Ala or Dde-Ala. No acylation was observed with Fmoc-Ala and only very low percentage (20%) acylation was achieved with Dde-Ala, even after a second acylation. It has been published previously that acylation of the secondary amine of backbone attached amino acids was difficult by Jensen et. al. [38], who suggested some variations in standard acylation reaction conditions. We have tried the suggested variations like use of high ratio of DCM to DMF (9:1) and using acyl chloride as the acylating agent (Fmoc-Ala-Cl) but still no change was observed in acylation. Later the acylation was carried in a microwave reactor with optimized condition of prespin for 5 min., temperature of 150 °C for 1 Hr. No acylation was observed with Fmoc-Ala, but with Dde-Ala 85% acylation found. This dipeptide Dde-Ala-Phe-OtBu provides a common central core for ISPPS and SPPS extension cycles.

Deprotection of OtBu with 25% TFA/DCM for 30 min was tested. This deprotection solution was analyzed by LC-MS, and it was found that around 40% of the central core Dde-Ala-Phe was cleaved. To determine if this change in the acid sensitivity of the linker is due to the Dde group or not, the following steps were followed. The Dde group was deprotected with 5% Hydrazine for 1 hr, capped with acetic anhydride, and OtBu deprotected with 25% TFA/DCM. Analysis by LC-MS found that 40% of

Ac-Ala-Phe was cleaved. Acylation of the secondary amino group with an amino acid made the linker more acid liable than with simple acylation (with acetyl or isovarleryl capping groups) and this linker 2-methyl-4-(5-oxyethylvalerate)-benzaldehyde couldn't be used for the demonstration of BSPPS. The most stable among the linkers in **Table 12**, 4-(5-oxy-methylbutyrate)benzaldehyde, was chosen and tried for demonstrating BSPPS. Deprotection of OtBu with 25% TFA/DCM still significantly cleaved the nascent peptide from the resin. BSPPS demonstration with the linkers that were studied in this project was not possible due to the fact that the linker became more acid sensitive with the acylation of the secondary amino group and the central core dipeptide was getting cleaved during the deprotection of OtBu.

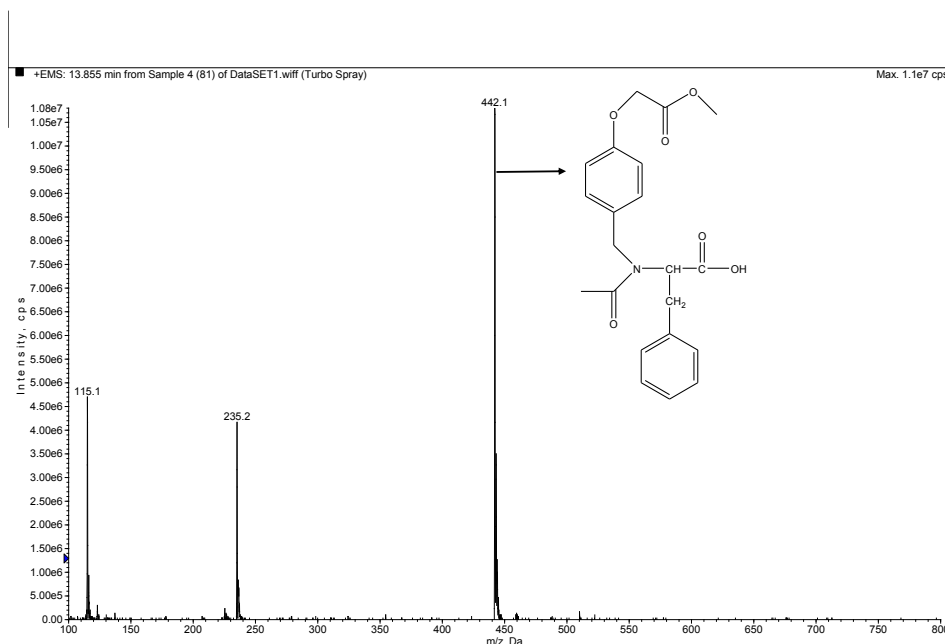


Figure 63. Mass spectrum of N-Acetyl-[4-(5-oxy-methylbutyrate)benzyl]-L-phenylalanine (Cmp. No. 1).

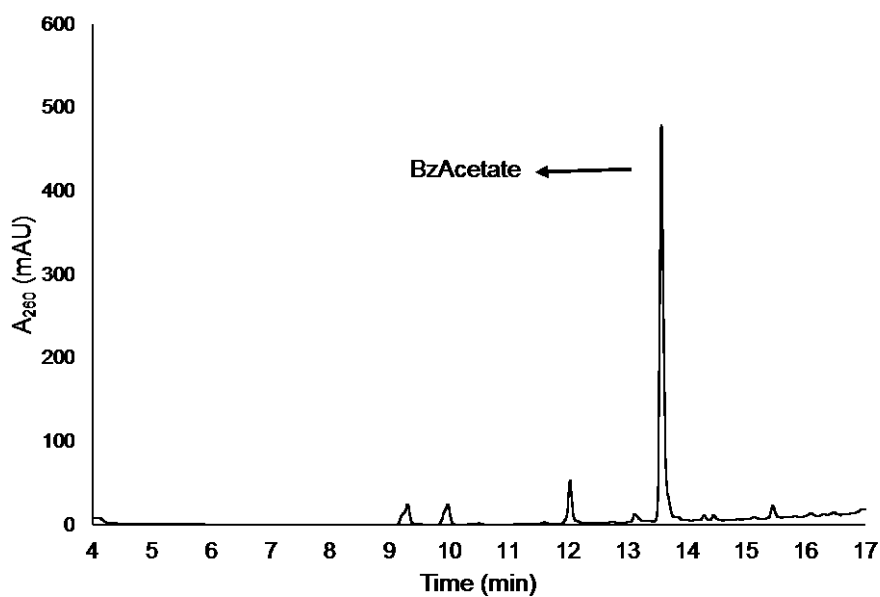


Figure 64. HPLC chromatogram of N-Acetyl-[4-(5-oxy-methylbutyrate)benzyl]-L-phenylalanine (Cmp. No. 1).

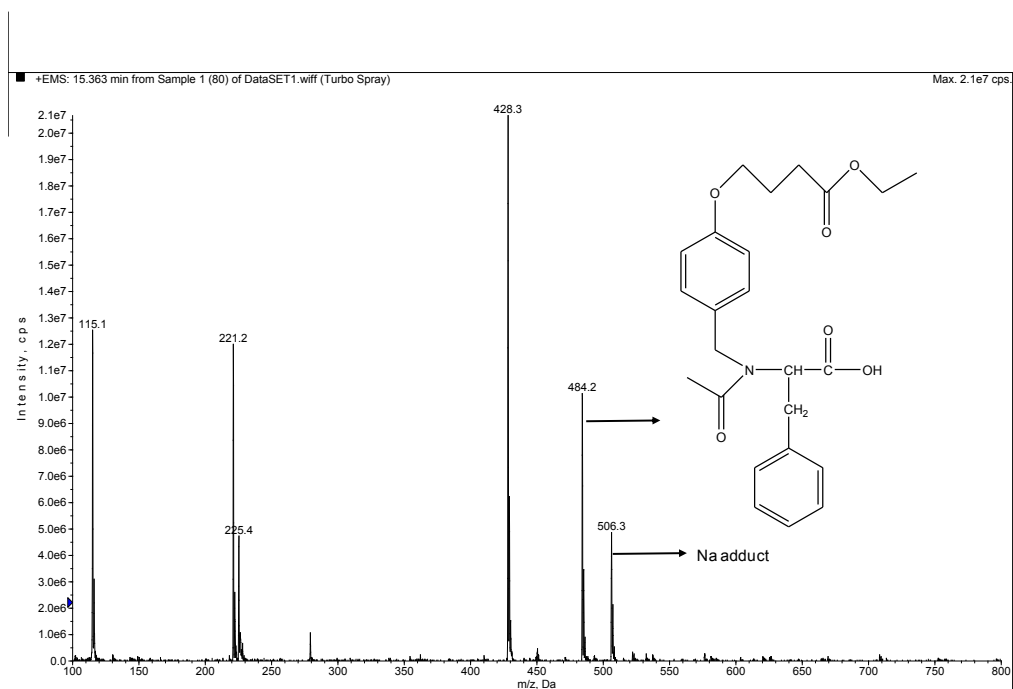


Figure 65. Mass spectrum of N-Acetyl-[4-(5-oxy-ethylvalerate)benzyl]-L-phenylalanine (Cmp. No. 2).

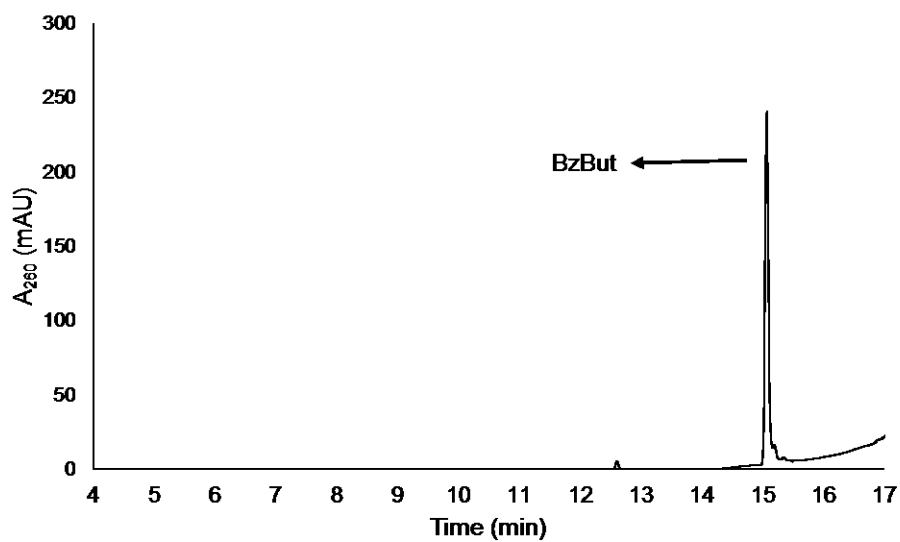


Figure 66. HPLC chromatogram of N-Acetyl-[4-(5-oxy-ethylvalerate)benzyl]-L-phenylalanine (Cmp. No. 2).

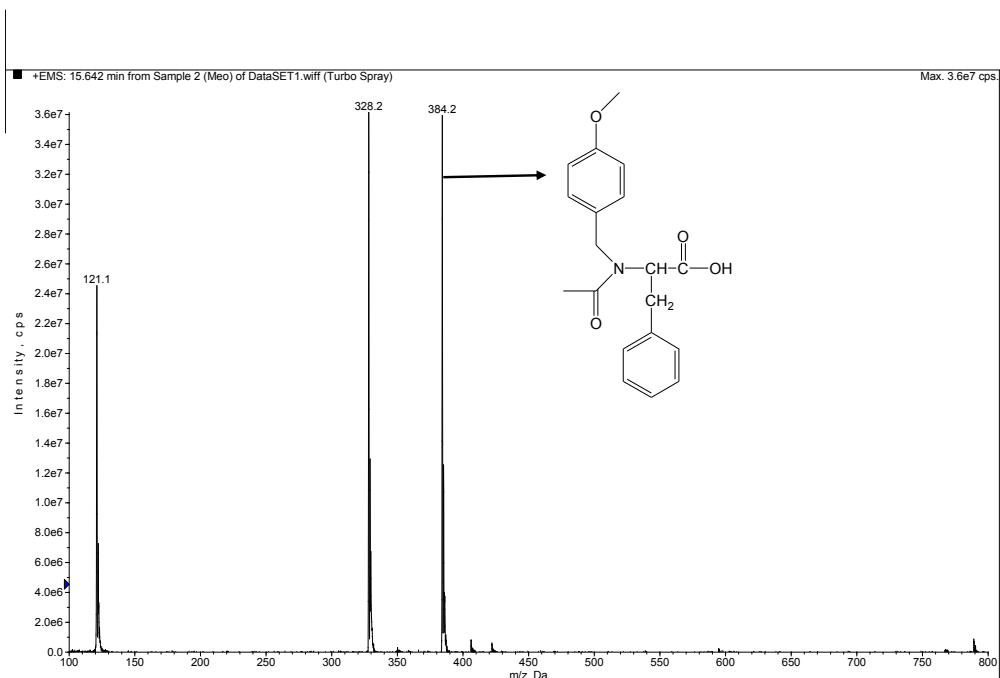


Figure 67. Mass spectrum of N-Acetyl-[4-methoxybenzyl]-L-phenylalanine (Cmp. No. 3).

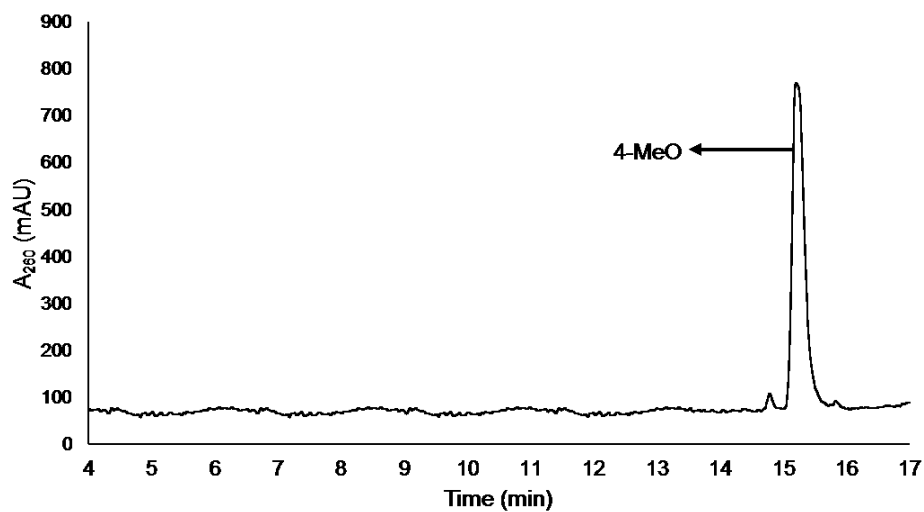


Figure 68. HPLC chromatogram of N-Acetyl-[4-methoxybenzyl]-L-phenylalanine (Cmp. No. 3).

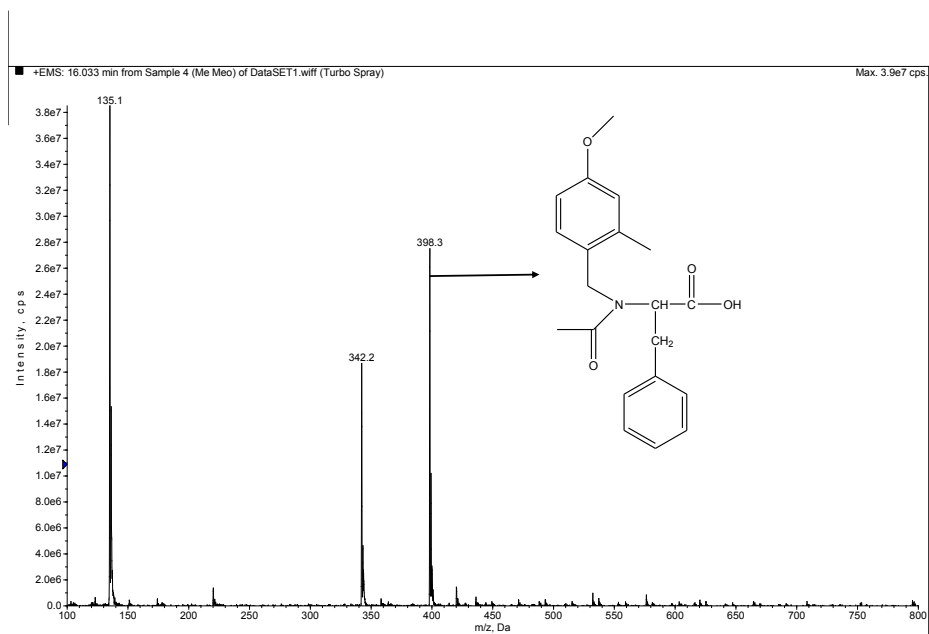


Figure 69. Mass spectrum of N-Acetyl-[2-methyl-4-methoxybenzyl]-L-phenylalanine (Cmp. No. 4).

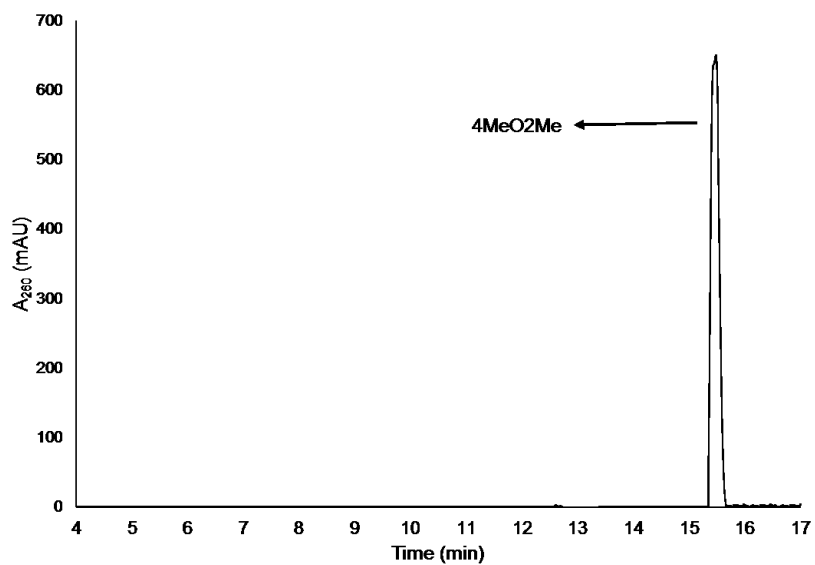


Figure 70. HPLC chromatogram of N-Acetyl-[2-methyl-4-methoxybenzyl]-L-phenylalanine (Cmp. No. 4).

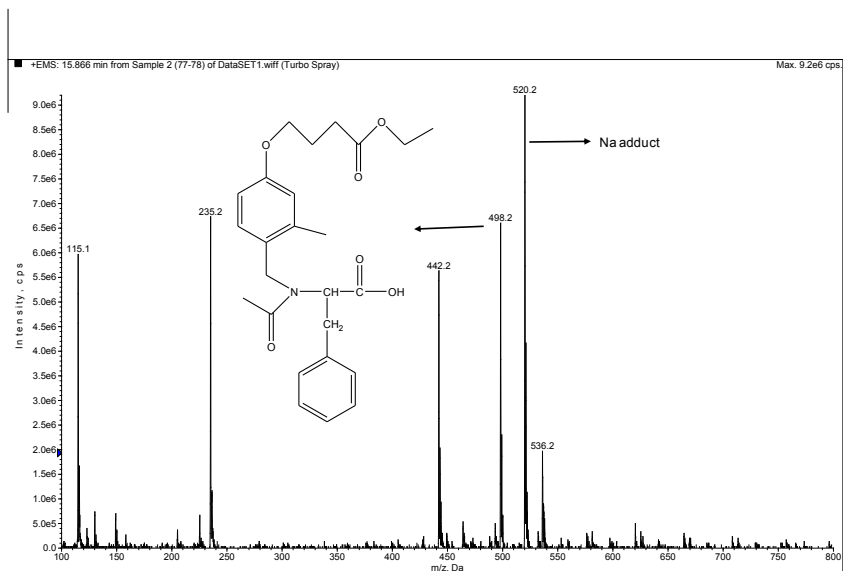


Figure 71. Mass spectrum of N-Acetyl-[2-methyl-4-(5-oxy-ethylvalerate)benzyl]-L-phenylalanine (Cmp. No. 5).

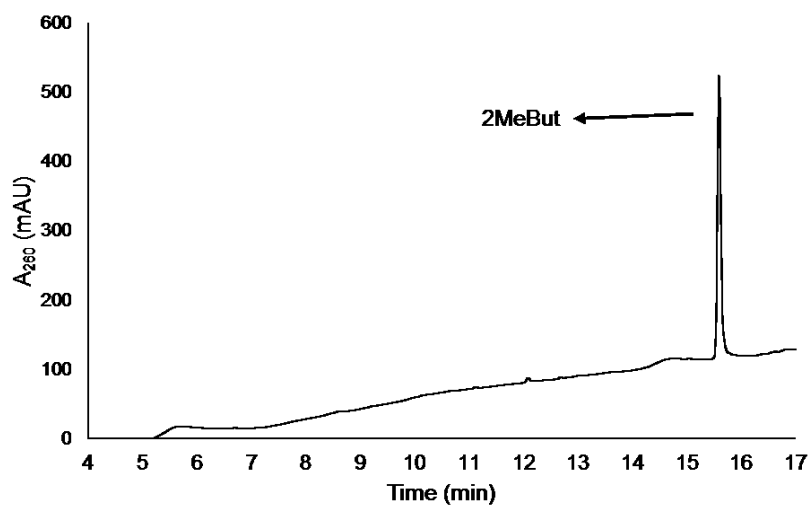


Figure 72. HPLC chromatogram of N-Acetyl-[2-methyl-4-(5-oxy-ethylvalerate)benzyl]-L-phenylalanine (Cmp. No. 5).

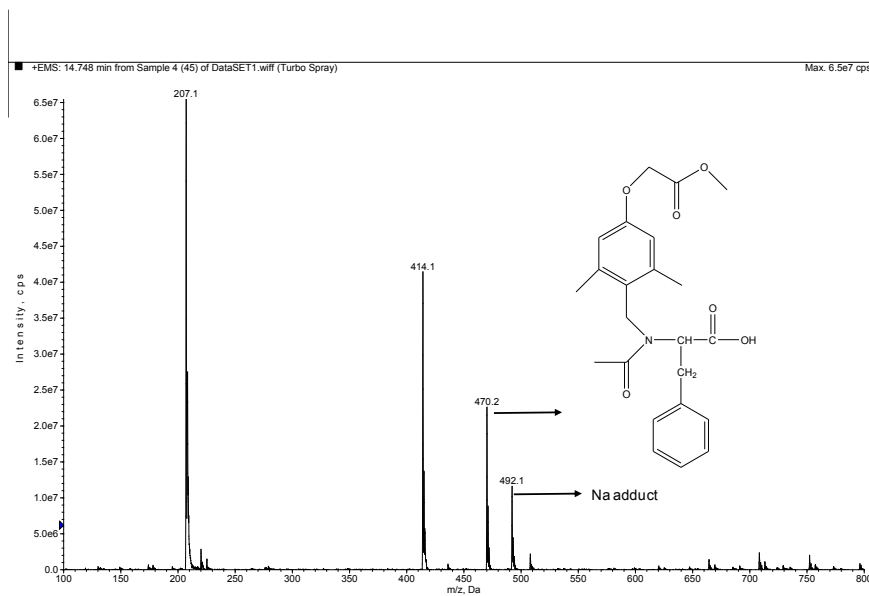


Figure 73. Mass spectrum of N-Acetyl-[2,6-dimethyl-4-(5-oxy-methylbutyrate)benzyl]-L-phenylalanine (Cmp. No. 6).

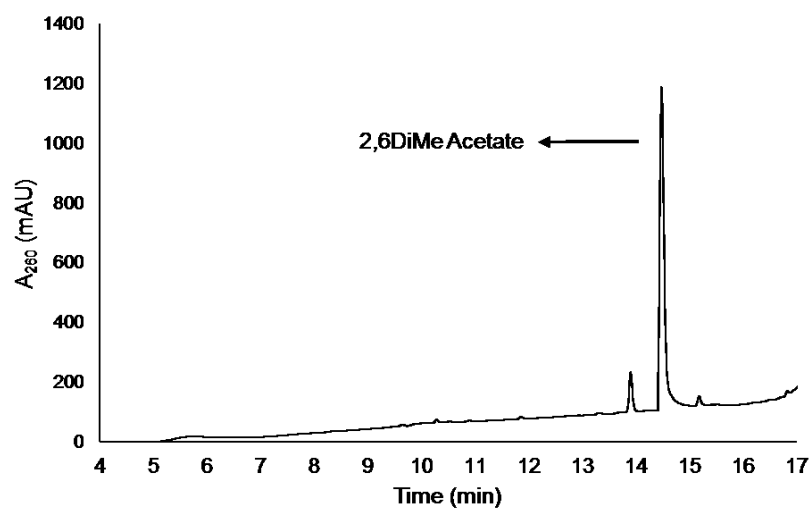


Figure 74. HPLC chromatogram of N-Acetyl-[2,6-dimethyl-4-(5-oxy-methylbutyrate)benzyl]-L-phenylalanine (Cmp. No. 6).

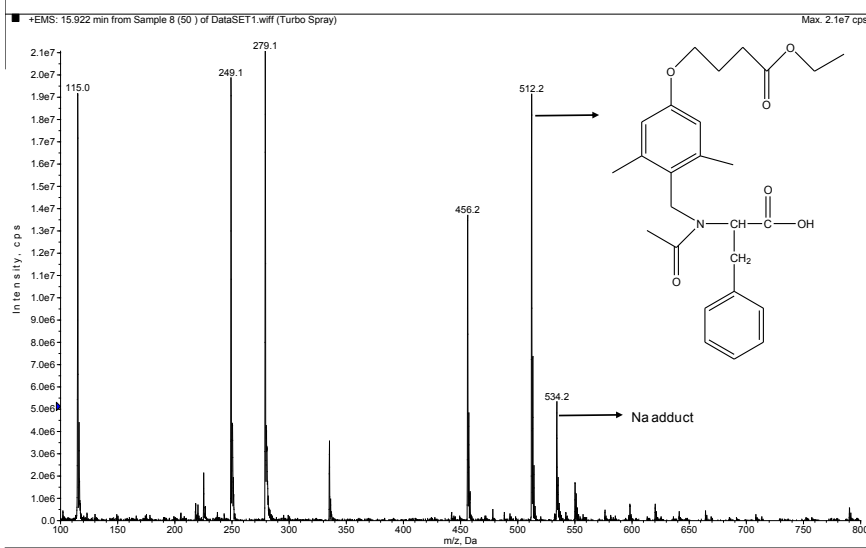


Figure 75. Mass spectrum of N-Acetyl-[2,6-dimethyl-4-(5-oxy-ethylvalerate)benzyl]-L-phenylalanine (Cmp. No. 7).

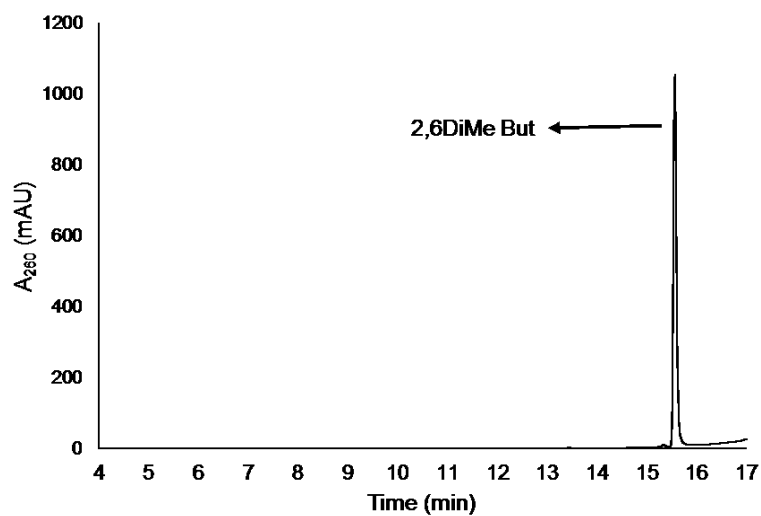


Figure 76. HPLC chromatogram of N-Acetyl-[2,6-dimethyl-4-(5-oxy-ethylvalerate)benzyl]-L-phenylalanine (Cmp. No. 7).

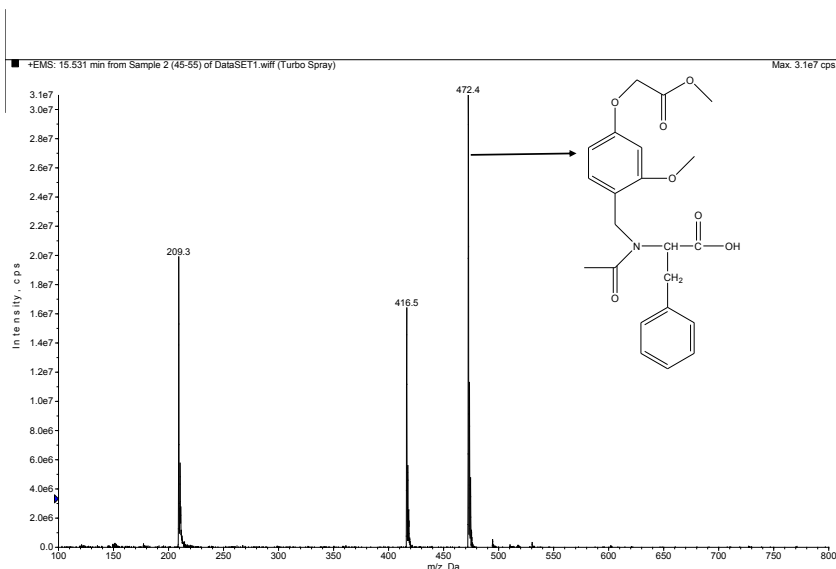


Figure 77. Mass spectrum of N-Acetyl-[2-methoxy-4-(5-oxy-methylbutyrate)benzyl]-L-phenylalanine (Cmp. No. 8).

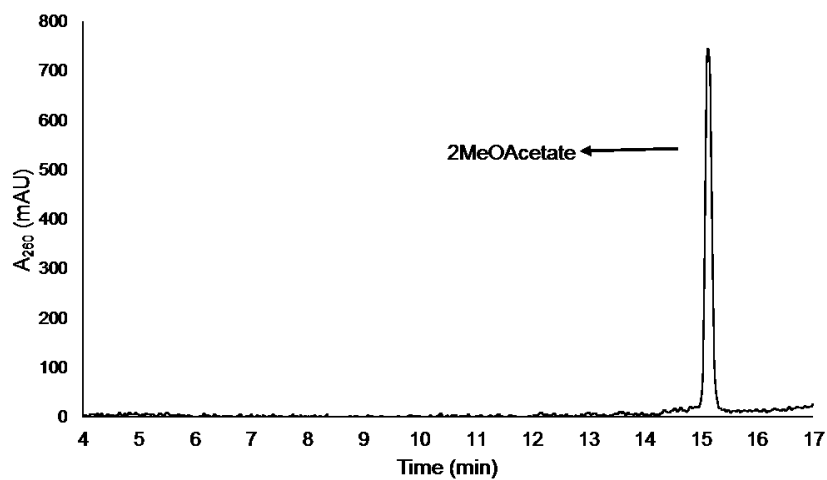


Figure 78. HPLC chromatogram of N-Acetyl-[2-methoxy-4-(5-oxy-methylbutyrate)benzyl]-L-phenylalanine (Cmp. No. 8).

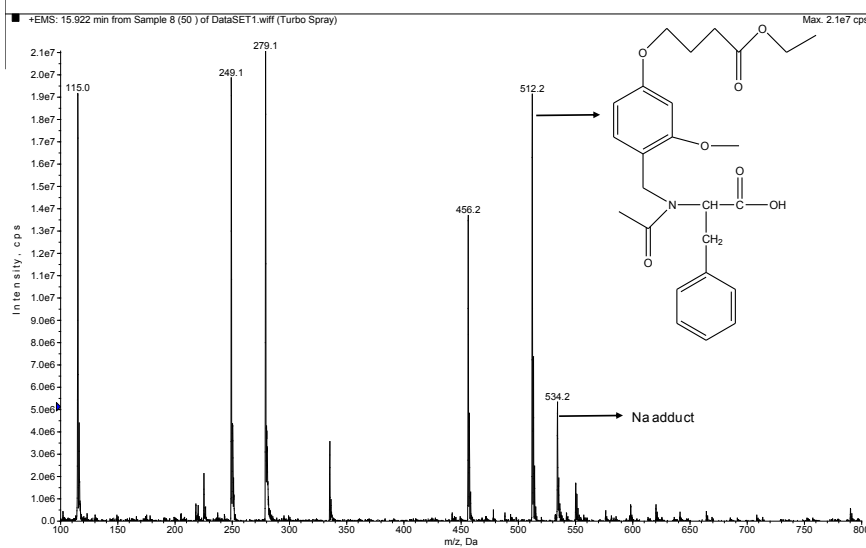


Figure 79. Mass spectrum of N-Acetyl-[2-methoxy-4-(5-oxy-ethylvalerate)benzyl]-L-phenylalanine (Cmp. No. 9).

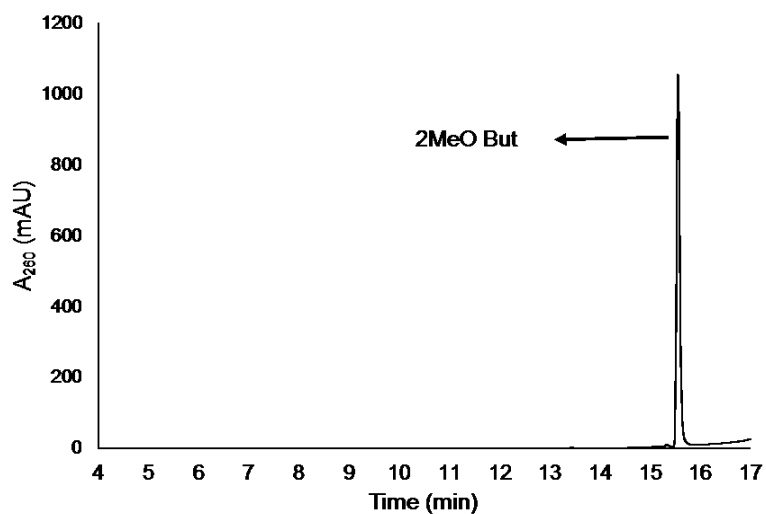


Figure 80. HPLC chromatogram of N-Acetyl-[2-methoxy-4-(5-oxy-ethylvalerate)benzyl]-L-phenylalanine (Cmp. No. 9).

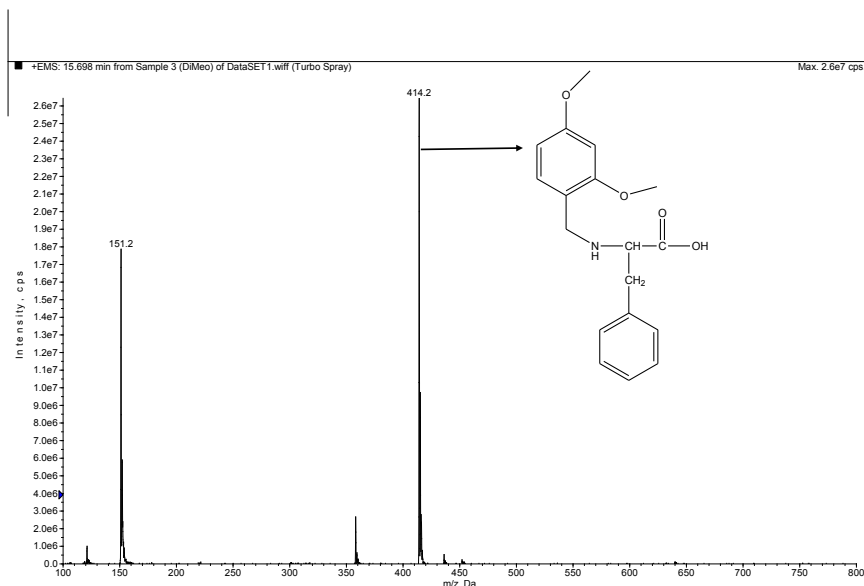


Figure 81. Mass spectrum of N-Acetyl-[2-methoxy-4-methoxybenzyl]-L-phenylalanine (Cmp. No. **10**).

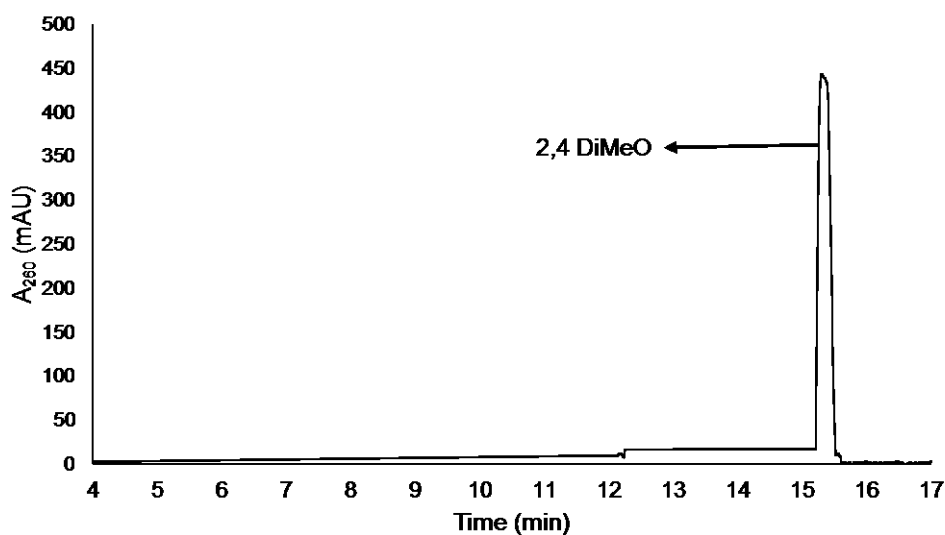


Figure 82. HPLC chromatogram of N-Acetyl-[2-methoxy-4-methoxybenzyl]-L-phenylalanine (Cmp. No. **10**).

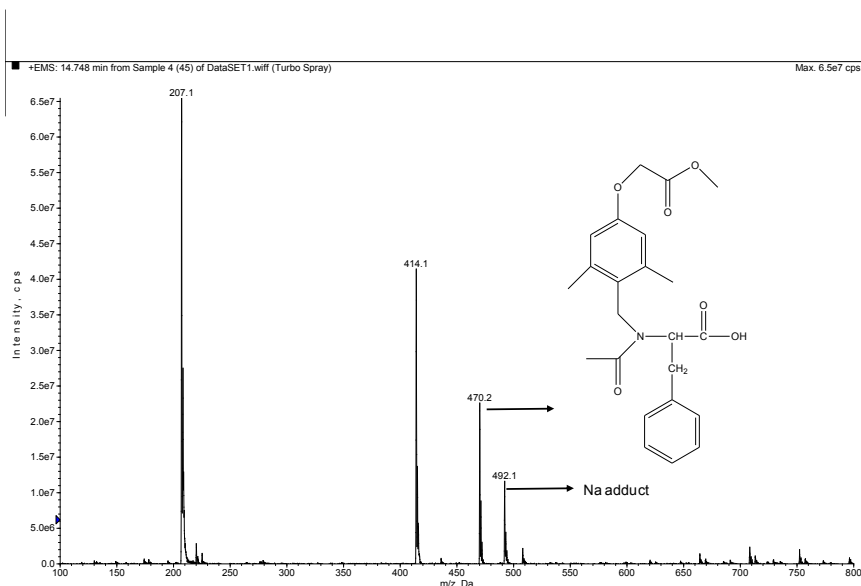


Figure 83. Mass spectrum of N-Acetyl-[2,6-dimethoxy-4-(5-oxy-methylbutyrate)benzyl]-L-phenylalanine (Cmp. No. 11).

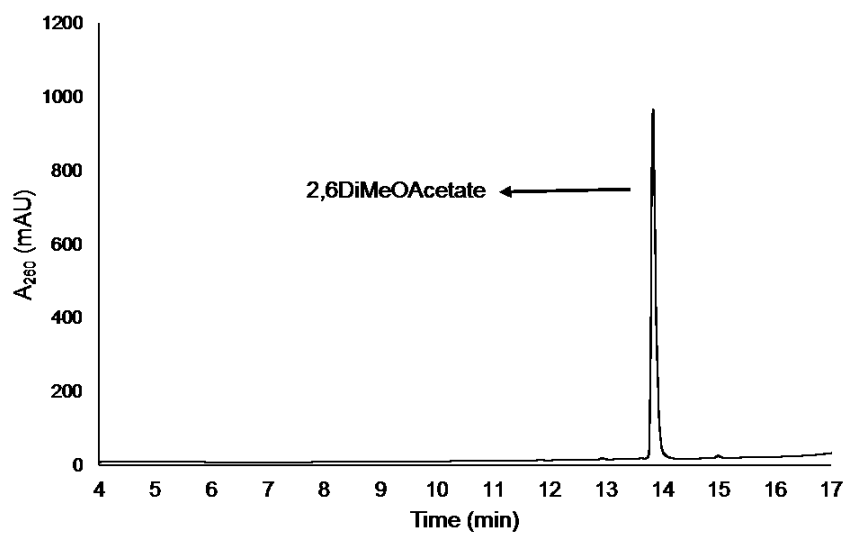


Figure 84. HPLC chromatogram of N-Acetyl-[2,6-dimethoxy-4-(5-oxy-methylbutyrate)benzyl]-L-phenylalanine (Cmp. No. 11).

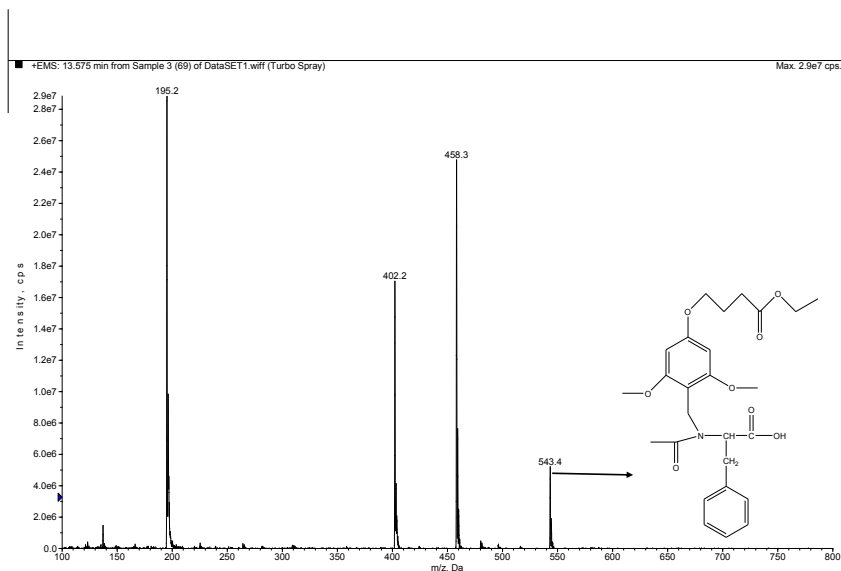


Figure 85. Mass spectrum of N-Acetyl-[2,6-dimethoxy-4-(5-oxy-ethylvalerate)benzyl]-L-phenylalanine (Cmp. No. 12).

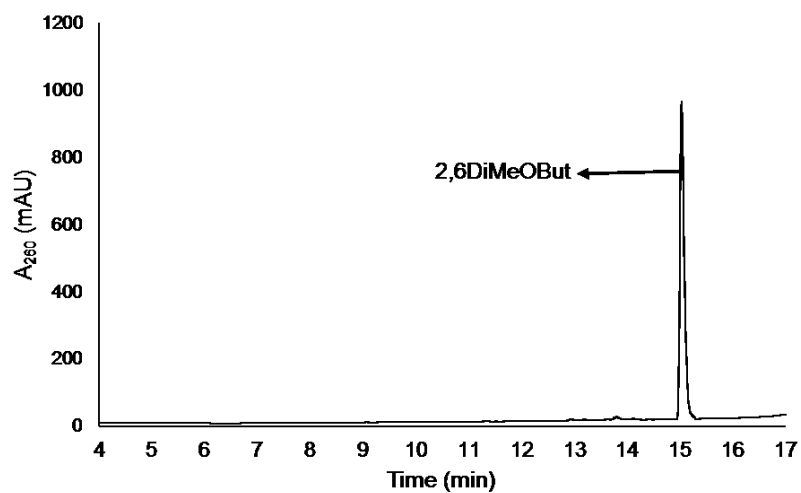


Figure 86. HPLC chromatogram of N-Acetyl-[2,6-dimethoxy-4-(5-oxy-ethylvalerate)benzyl]-L-phenylalanine (Cmp. No. 12).

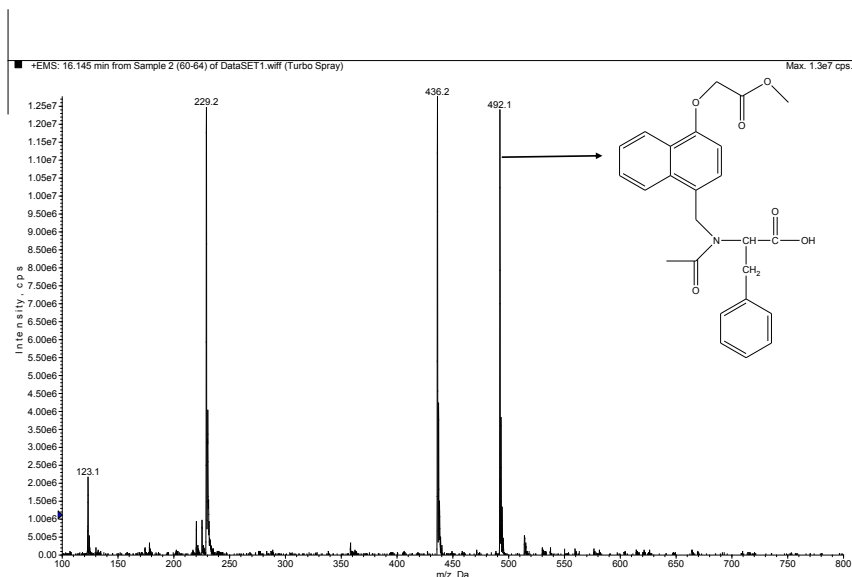


Figure 87. Mass spectrum of N-Acetyl-[4-(5-oxy-methylbutyrate)naphthyl]-L-phenylalanine (Cmp. No. 13).

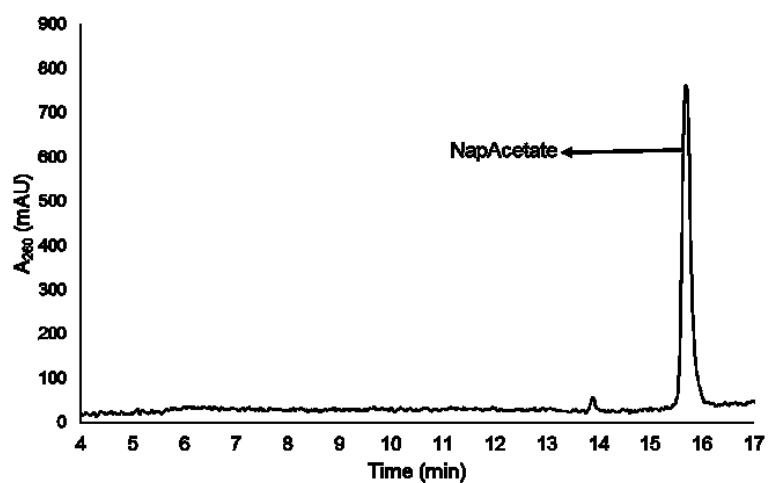


Figure 88. HPLC chromatogram of N-Acetyl-[4-(5-oxy-methylbutyrate)naphthyl]-L-phenylalanine (Cmp. No. 13).

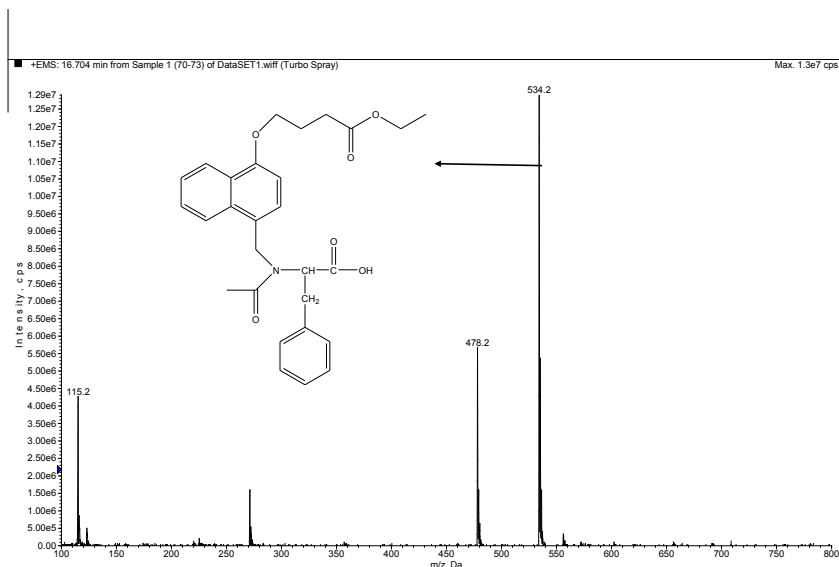


Figure 89. Mass spectrum of N-Acetyl-[4-(5-oxy-ethylvalerate)naphthyl]-L-phenylalanine (Cmp. No. **14**).

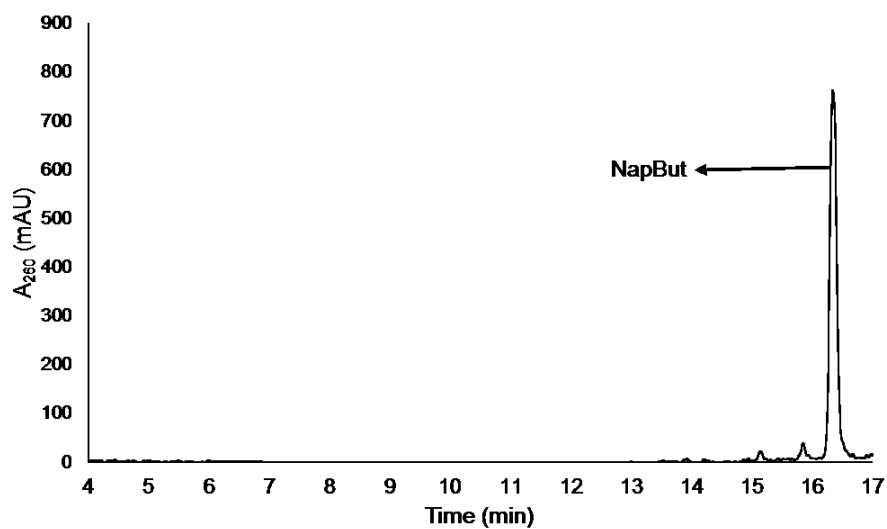


Figure 90. HPLC chromatogram of N-Acetyl-[4-(5-oxy-ethylvalerate)naphthyl]-L-phenylalanine (Cmp. No. **14**).

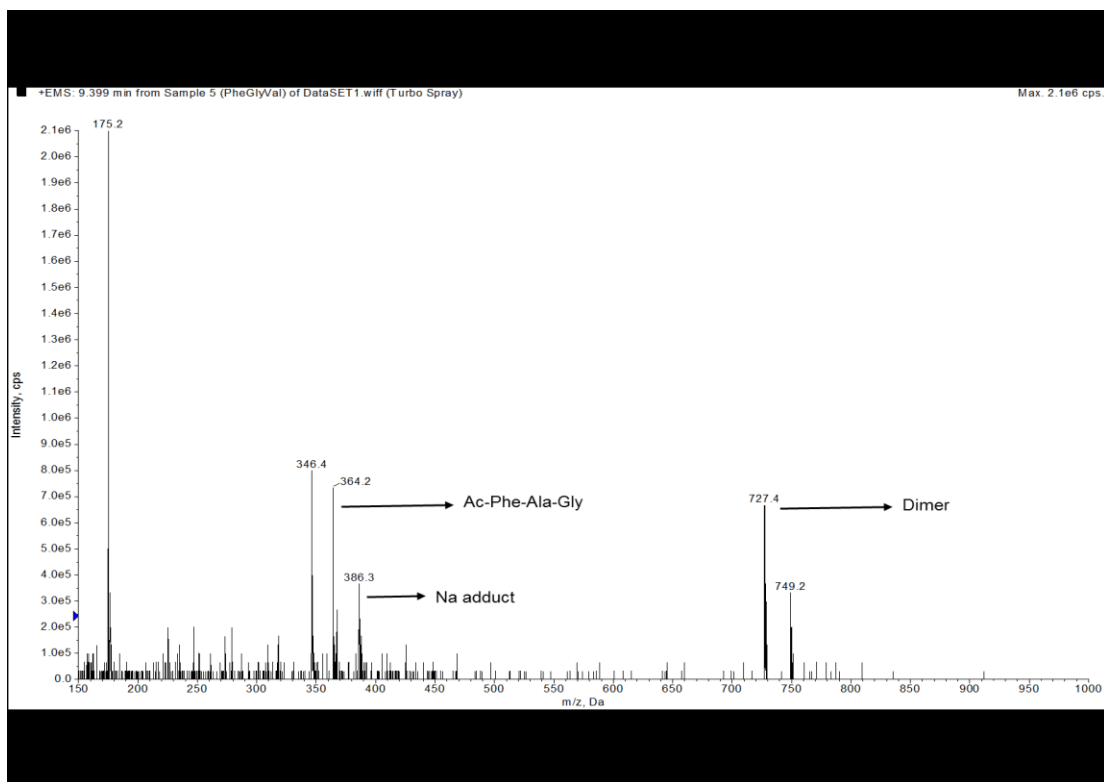


Figure 91. Mass spectrum of Ac-Phe-Ala-Gly.

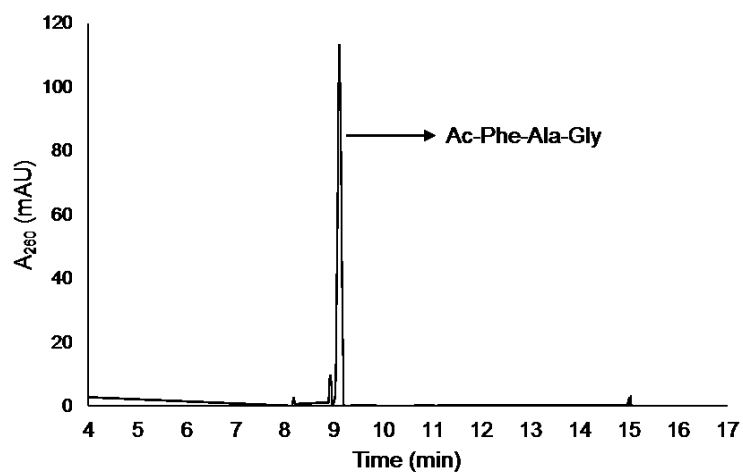


Figure 92. HPLC chromatogram of Ac-Phe-Ala-Gly.

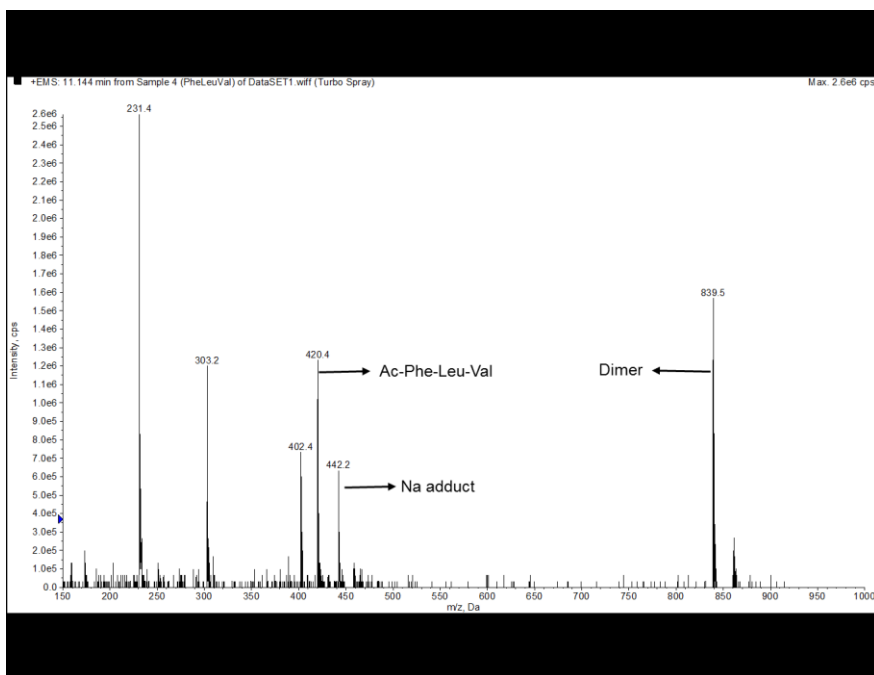


Figure 93. Mass spectrum of Ac-Phe-Leu-Val.

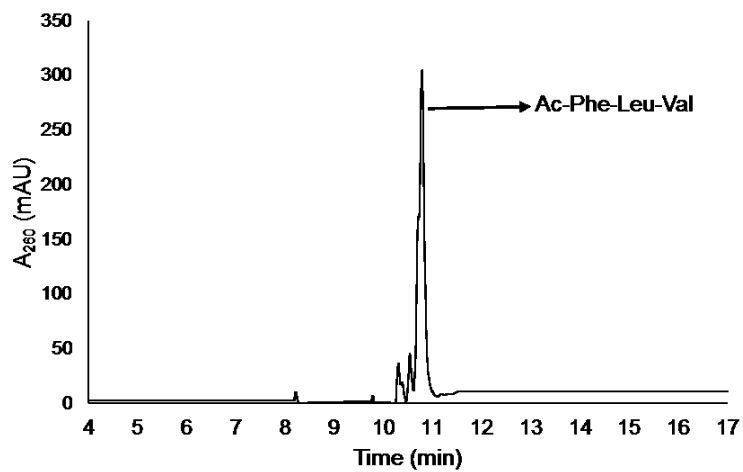


Figure 94. HPLC chromatogram of Ac-Phe-Leu-Val.

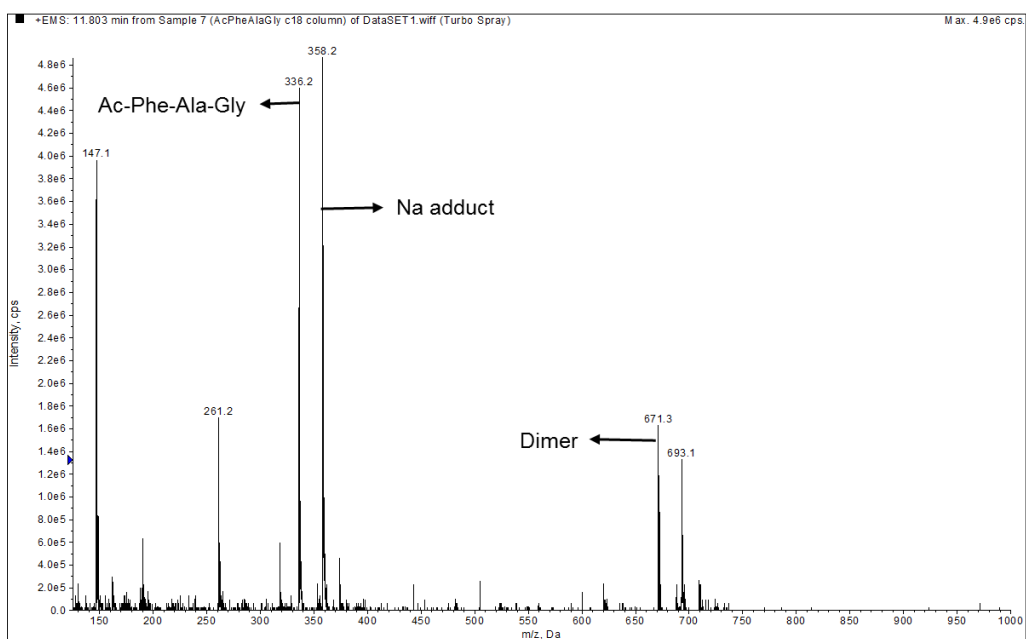


Figure 95. Mass spectrum of Ac-Phe-Ala-Gly.

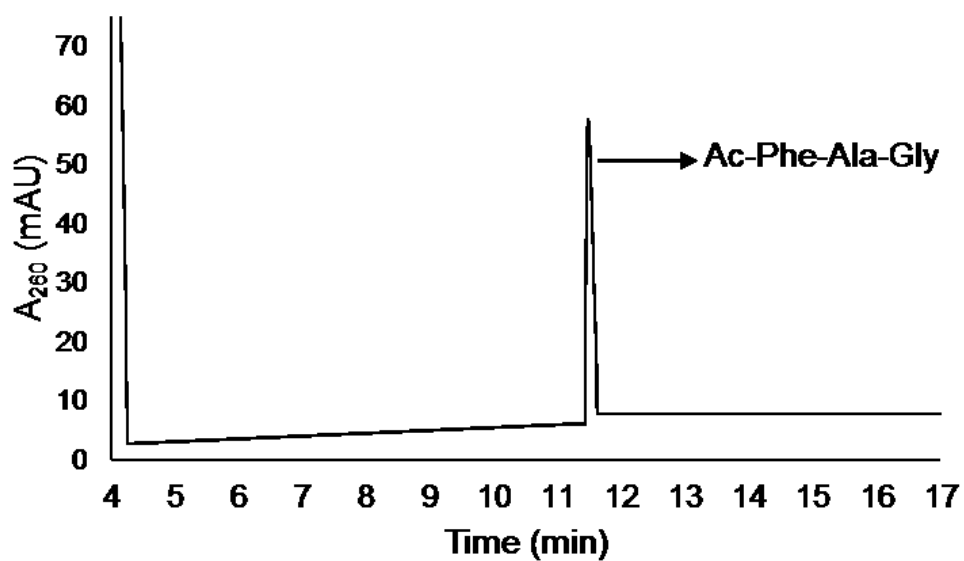


Figure 96. HPLC chromatogram of Ac-Phe-Ala-Gly.

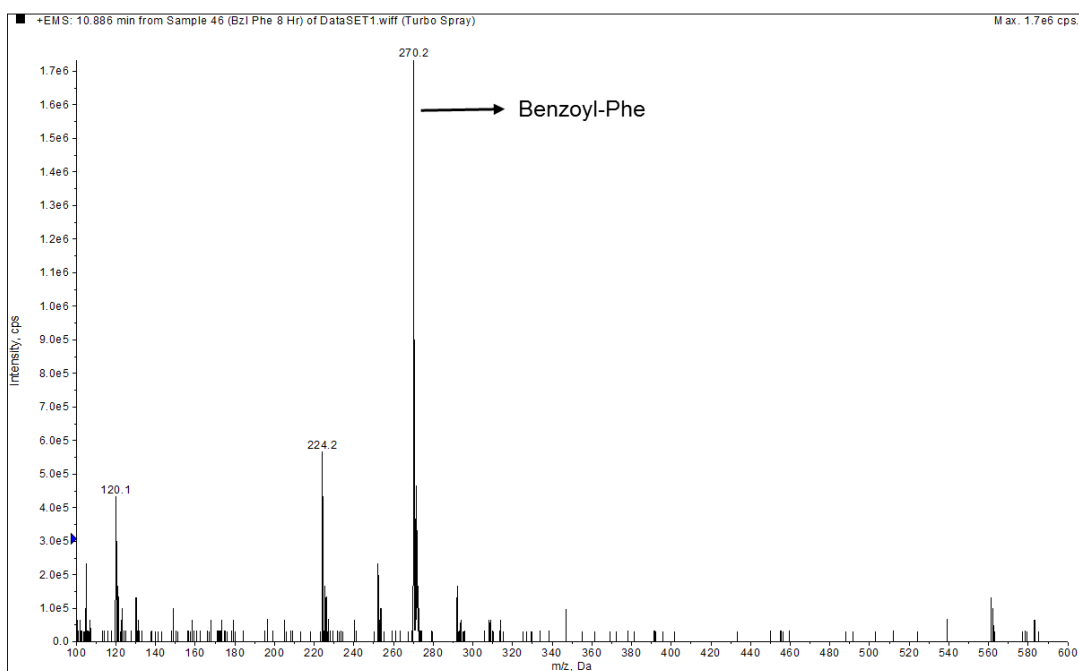


Figure 97. Mass spectrum of Benzoyl-Phe.

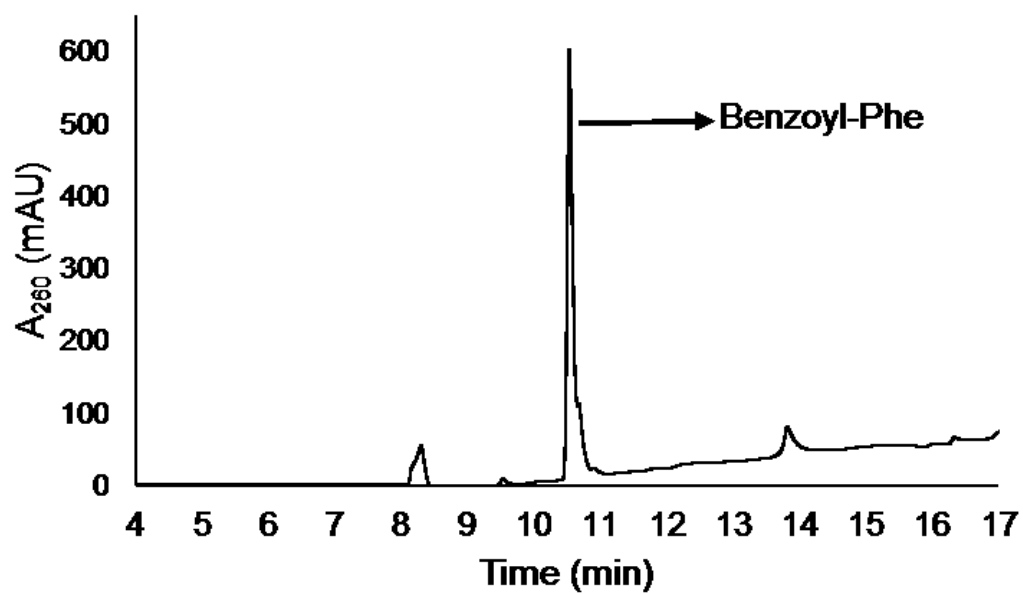


Figure 98. HPLC chromatogram of Benzoyl-Phe.

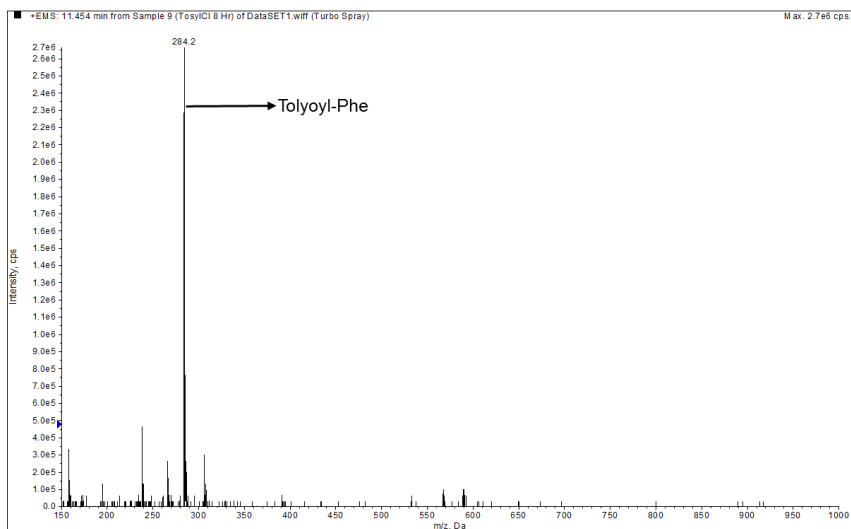


Figure 99. Mass spectrum of Tolyoyl-Phe.

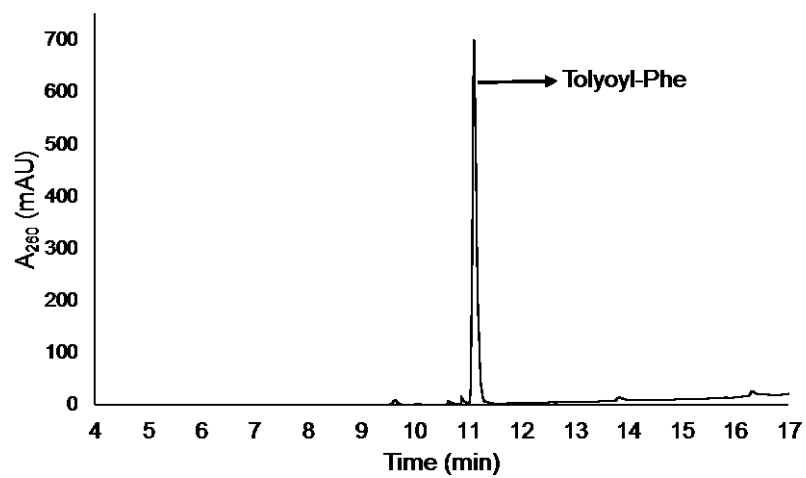


Figure 100. HPLC chromatogram of Tolyoyl-Phe.

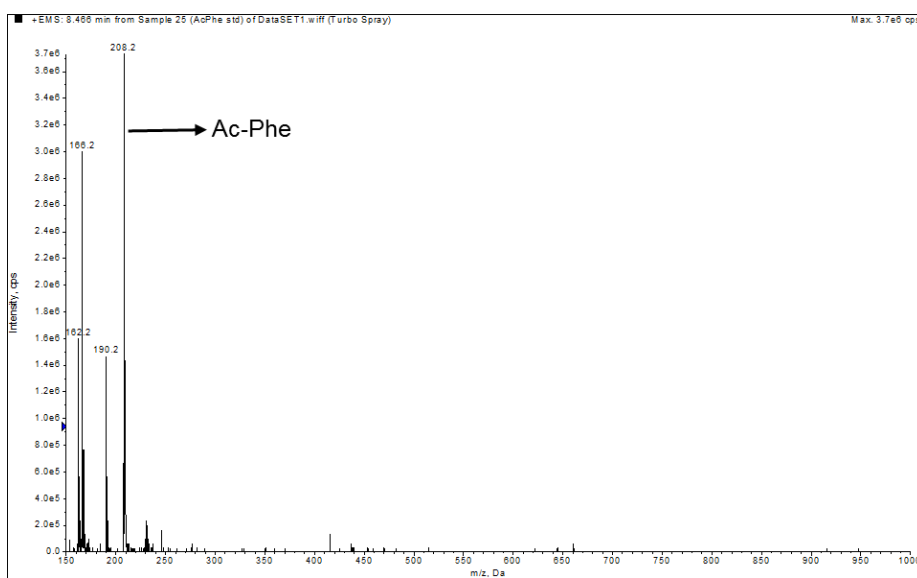


Figure 101. Mass spectrum of Ac-Phe.

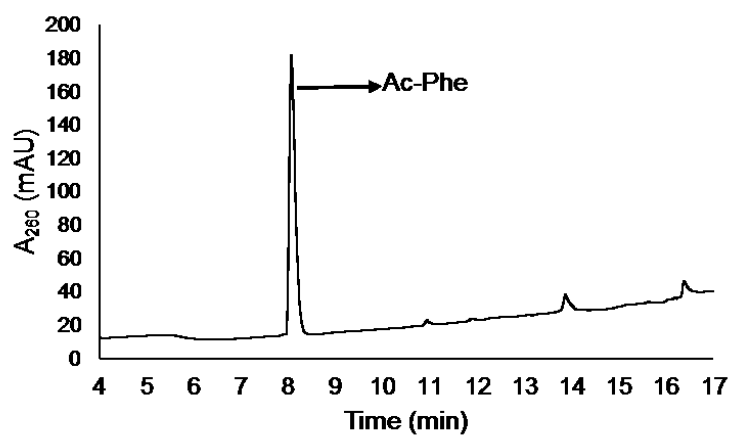


Figure 102. HPLC chromatogram of Ac-Phe.

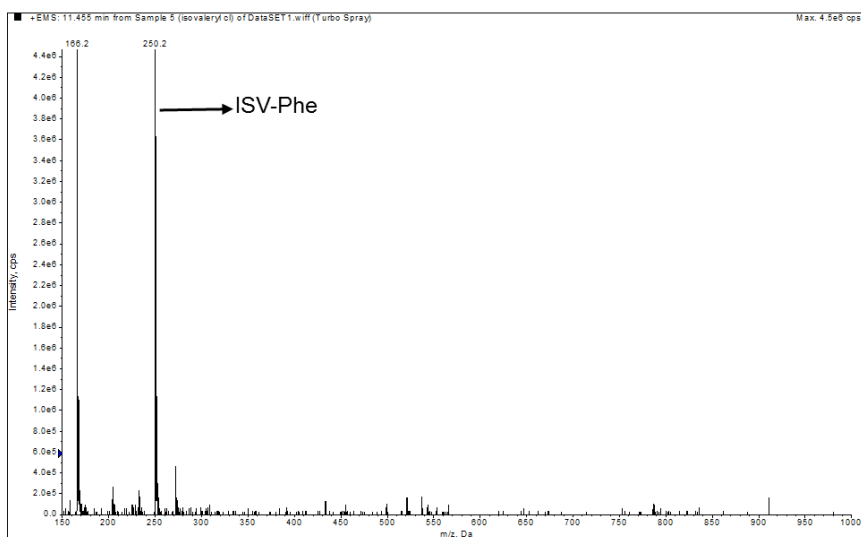


Figure 103. Mass spectrum of Isovaleryl -Phe.

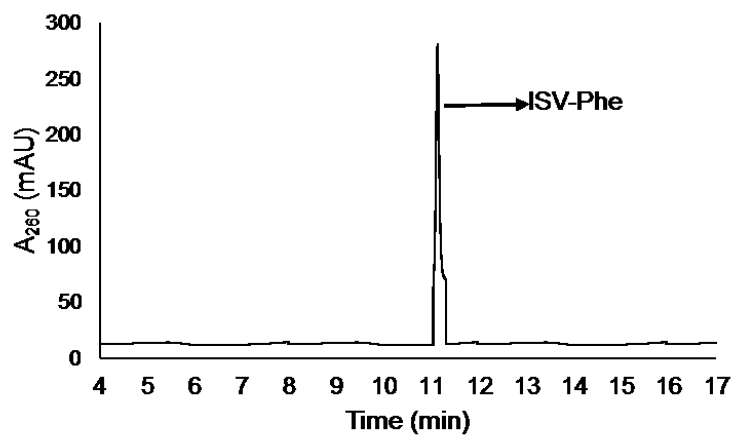


Figure 104. HPLC chromatogram of Isovaleryl -Phe.

SUMMARY

In the first part of dissertation, D-boroAla was identified and characterized as an antibacterial agent. D-boroAla has activity against both Gram-positive and Gram-negative organisms, with minimal inhibitory concentrations down to 8 µg/mL. A structure-function study on the alkyl side chain revealed that D-boroAla is the most effective agent in a series including boroGly, D-boroHomoAla, and D-boroVal. L-boroAla was much less active, and N-acetylation completely abolished activity. An LC-MS/MS assay was used to demonstrate that D-boroAla exerts its antibacterial activity by inhibition of D-Ala-D-Ala ligase. D-boroAla is bactericidal at 1x minimal inhibitory concentration against *Staphylococcus aureus* and *Bacillus subtilis*, which each encode one copy of D-Ala-D-Ala, and at 4x minimal inhibitory concentration against *Escherichia coli* and *Salmonella enterica serovar Typhimurium*, which each encode two copies of D-Ala-D-Ala ligase. D-boroAla demonstrated a frequency of resistance of 8×10^{-8} at 4x minimal inhibitory concentration in *S. aureus*. These results demonstrate that D-boroAla has promising antibacterial activity and could serve as the lead agent in a new class of D-Ala-D-Ala ligase targeted antibacterial agents. This study also demonstrates D-boroAla as a possible probe for D-Ala-D-Ala ligase function.

Vancomycin exerts its antibacterial activity by binding to D-Ala-D-Ala in bacterial cell wall precursors. Vancomycin resistance in vancomycin-resistant enterococci (VRE) is due to an alternative cell wall biosynthesis pathway in which D-Ala-D-Ala is replaced, most commonly by D-Ala-D-Lac. In the middle part of dissertation, we extend our recently developed Marfey's derivatization-based liquid

chromatography-tandem mass spectrometry (LC-MS/MS) assay for L-Ala, D-Ala, and D-Ala-D-Ala to D-Ala-D-Lac and apply it to the quantitation of these metabolites in VRE. The first step in this effort was the development of an effective washing method for removing medium components from VRE cells. Mar-D-Ala-D-Lac was well resolved chromatographically from Mar-D-Ala-D-Ala, a prerequisite for MS/MS quantitation of D-Ala-D-Ala and D-Ala-D-Lac. Mar- D-Ala-D-Lac gave similar detection parameters, sensitivity, and linearity as Mar-D-Ala-D-Ala. L-Ala, D-Ala, D-Ala-D-Ala, and D-Ala-D-Lac levels in VRE were then determined in the presence of variable vancomycin levels. Exposure to vancomycin resulted in a dramatic reduction of D-Ala-D-Ala, with a response midpoint at approximately 0.06 $\mu\text{g/ml}$ vancomycin and with a broad response profile up to 128 $\mu\text{g/ml}$ vancomycin. In contrast, D-Ala-D-Lac was present in the absence of vancomycin, with its level constant up to 128 $\mu\text{g/ml}$ vancomycin. This method will be useful for the discovery, characterization, and refinement of agents targeting vancomycin resistance in VRE.

Peptide-based agents are of considerable interest as bioactive agents and drugs. Considerable research has been done to synthesize peptides and peptide mimetics using classical solid-phase peptide synthesis (SPPS) in the C-to-N direction. However, this strategy is not generally useful for preparing C-terminally modified peptide derivatives. On the other hand, SPPS in the N-to-C direction (Inverse SPPS) would provide the synthetically versatile C-terminal carboxyl group for further elaboration. In the last part of the dissertation, several benzaldehyde linkers were studied for use in this application. Using model reactions, rate constants of all the linkers were determined and the reaction constant ρ was determined as -

1.1. The linker with right stability i.e. stable to 25% TFA/DCM treatment for 30 min. and should be able cleave the peptide with treatment by 5% HBr/TFA was selected 2-methyl-4-(5-oxy-ethylvalerate)benzaldehyde and backbone amide linker (BAL) strategy for use with amino acid t-butyl ester based ISPPS was developed. The stability of the linker was demonstrated by synthesizing and characterization of several acetyl capped peptides. This approach provided acetyl capped peptides in high yield and purity, without detectable levels of racemization. However, an effort to use this and similar linkers for Bidirection SPPS was unsuccessful, since the linker with suitable acid stability for OtBu deprotection were unreactive for amino acid acylation of the secondary amine intermediate. This approach will be helpful in synthesizing several peptide mimetic classes by using already available starting materials. This approach is also suited for use with combinatorial chemistry based strategies for drug and bioactive agents discovery and optimization.

APPENDIX

This is a License Agreement between Sandeep Putty ("You") and John Wiley and Sons ("John Wiley and Sons") provided by Copyright Clearance Center ("CCC"). The license consists of your order details, the terms and conditions provided by John Wiley and Sons, and the payment terms and conditions.

All payments must be made in full to CCC. For payment instructions, please see information listed at the bottom of this form.

License Number	3318891330389
License date	Jan 30, 2014
Licensed content publisher	John Wiley and Sons
Licensed content publication	Chemical Biology & Drug Design
Licensed content title	Characterization of d-boroAla as a Novel Broad-Spectrum Antibacterial Agent Targeting d-Ala-d-Ala Ligase
Licensed copyright line	© 2011 John Wiley & Sons A/S
Licensed content author	Sandeep Putty,Aman Rai,Darshan Jamindar,Paul Pagano,Cheryl L. Quinn,Takehiko Mima,Herbert P. Schweizer,William G. Gutheil
Licensed content date	Sep 21, 2011
Start page	757
End page	763
Type of use	Dissertation/Thesis
Requestor type	Author of this Wiley article
Format	Print and electronic
Portion	Full article
Will you be translating?	No
Title of your thesis / dissertation	Characterization of D-boroAla as a novel broad spectrum antibacterial agent and confirmation of D-Ala-D-Ala ligase as the target in Escherichia coli using LC-MS/MS
Expected completion date	May 2014
Expected size (number of pages)	200
Total	0.00 USD

This is a License Agreement between Sandeep Putty ("You") and Elsevier ("Elsevier") provided by Copyright Clearance Center ("CCC"). The license consists of your order details, the terms and conditions provided by Elsevier, and the payment terms and conditions.

All payments must be made in full to CCC. For payment instructions, please see information listed at the bottom of this form.

Supplier	Elsevier Limited The Boulevard, Langford Lane Kidlington, Oxford, OX5 1GB, UK
Registered Company Number	1982084
Customer name	Sandeep Putty
Customer address	2464 Charlotte St KANSAS CITY, MO 64112
License number	3318891049492
License date	Jan 30, 2014
Licensed content publisher	Elsevier
Licensed content publication	Analytical Biochemistry
Licensed content title	A liquid chromatography–tandem mass spectrometry assay for D-Ala-D-Lac: A key intermediate for vancomycin resistance in vancomycin-resistant enterococci
Licensed content author	Sandeep Putty, Harika Vemula, Sudheer Bobba, William G. Gutheil
Licensed content date	15 November 2013
Licensed content volume number	442
Licensed content issue number	2
Number of pages	6
Start Page	166
End Page	171
Type of Use	reuse in a thesis/dissertation
Portion	full article
Format	both print and electronic
Are you the author of this Elsevier article?	Yes
Will you be translating?	No
Title of your thesis/dissertation	Characterization of D-boroAla as a novel broad spectrum antibacterial agent and confirmation of D-Ala-D-Ala ligase as the target in Escherichia coli.

This is a License Agreement between Sandeep Putty ("You") and Elsevier ("Elsevier") provided by Copyright Clearance Center ("CCC"). The license consists of your order details, the terms and conditions provided by Elsevier, and the payment terms and conditions.

All payments must be made in full to CCC. For payment instructions, please see information listed at the bottom of this form.

Supplier	Elsevier Limited The Boulevard, Langford Lane Kidlington, Oxford, OX5 1GB, UK
Registered Company Number	1982084
Customer name	Sandeep Putty
Customer address	2464 Charlotte St KANSAS CITY, MO 64112
License number	3323210174761
License date	Feb 06, 2014
Licensed content publisher	Elsevier
Licensed content publication	The International Journal of Biochemistry & Cell Biology
Licensed content title	Multivariate geometrical analysis of catalytic residues in the penicillin- binding proteins
Licensed content author	Sudheer Bobba, William G. Gutheil
Licensed content date	October 2011
Licensed content volume number	43
Licensed content issue number	10
Number of pages	10
Start Page	1490
End Page	1499
Type of Use	reuse in a thesis/dissertation
Intended publisher of new work	other
Portion	figures/tables/illustrations
Number of figures/tables/illustrations	1
Format	both print and electronic
Are you the author of this Elsevier article?	No
Will you be translating?	No

This is a License Agreement between Sandeep Putty ("You") and Elsevier ("Elsevier") provided by Copyright Clearance Center ("CCC"). The license consists of your order details, the terms and conditions provided by Elsevier, and the payment terms and conditions.

All payments must be made in full to CCC. For payment instructions, please see information listed at the bottom of this form.

Supplier	Elsevier Limited The Boulevard, Langford Lane Kidlington, Oxford, OX5 1GB, UK
Registered Company Number	1982084
Customer name	Sandeep Putty
Customer address	2464 Charlotte St KANSAS CITY, MO 64112
License number	3323210085665
License date	Feb 06, 2014
Licensed content publisher	Elsevier
Licensed content publication	Analytical Biochemistry
Licensed content title	A liquid chromatography–tandem mass spectrometry assay for Marfey's derivatives of L-Ala, D-Ala, and D-Ala-D-Ala: Application to the in vivo confirmation of alanine racemase as the target of cycloserine in <i>Escherichia coli</i>
Licensed content author	Darshan Jamindar, William G. Gutheil
Licensed content date	1 January 2010
Licensed content volume number	396
Licensed content issue number	1
Number of pages	7
Start Page	1
End Page	7
Type of Use	reuse in a thesis/dissertation
Intended publisher of new work	other
Portion	figures/tables/illustrations
Number of figures/tables/illustrations	3
Format	both print and electronic
Are you the author of this Elsevier article?	No

This is a License Agreement between Sandeep Putty ("You") and John Wiley and Sons ("John Wiley and Sons") provided by Copyright Clearance Center ("CCC"). The license consists of your order details, the terms and conditions provided by John Wiley and Sons, and the payment terms and conditions.

All payments must be made in full to CCC. For payment instructions, please see information listed at the bottom of this form.

License Number	3362520351435
License date	Apr 05, 2014
Licensed content publisher	John Wiley and Sons
Licensed content publication	British Journal of Pharmacology
Licensed content title	Novel classes of antibiotics or more of the same?
Licensed copyright line	© 2011 The Authors. British Journal of Pharmacology © 2011 The British Pharmacological Society
Licensed content author	Anthony RM Coates, Gerry Halls, Yanmin Hu
Licensed content date	Apr 6, 2011
Start page	184
End page	194
Type of use	Dissertation/Thesis
Requestor type	University/Academic
Format	Print and electronic
Portion	Figure/table
Number of figures/tables	3
Original Wiley figure/table number(s)	Figure 1 Table 1
Will you be translating?	No
Title of your thesis / dissertation	Characterization of D-boroAla as a novel broad spectrum antibacterial agent and confirmation of D-Ala-D-Ala ligase as the target in Escherichia coli using LC-MS/MS
Expected completion date	May 2014

REFERENCES

1. Leclercq, R., et al., *Plasmid-mediated resistance to vancomycin and teicoplanin in Enterococcus faecium*. The New England journal of medicine, 1988. **319**(3): p. 157-61.
2. Werner, G., et al., *Emergence and spread of vancomycin resistance among enterococci in Europe*. Euro surveillance : bulletin europeen sur les maladies transmissibles = European communicable disease bulletin, 2008. **13**(47).
3. Driscoll, J.A., S.L. Brody, and M.H. Kollef, *The epidemiology, pathogenesis and treatment of Pseudomonas aeruginosa infections*. Drugs, 2007. **67**(3): p. 351-68.
4. Van Delden, C. and B.H. Iglewski, *Cell-to-cell signaling and Pseudomonas aeruginosa infections*. Emerg Infect Dis, 1998. **4**(4): p. 551-60.
5. Schleifer, K.H., *Classification of Bacteria and Archaea: past, present and future*. Syst Appl Microbiol, 2009. **32**(8): p. 533-42.
6. Yarza, P., et al., *The All-Species Living Tree project: a 16S rRNA-based phylogenetic tree of all sequenced type strains*. Syst Appl Microbiol, 2008. **31**(4): p. 241-50.
7. Stackebrandt, E., et al., *Report of the ad hoc committee for the re-evaluation of the species definition in bacteriology*. Int J Syst Evol Microbiol, 2002. **52**(Pt 3): p. 1043-7.
8. Woese, C.R., *Bacterial evolution*. Microbiol Rev, 1987. **51**(2): p. 221-71.
9. *Peptidoglycan types of bacterial cell walls and their taxonomic implications*. Bacteriol Rev, 1973. **37**(2): p. 258.

10. Schleifer, K.H. and O. Kandler, *Peptidoglycan types of bacterial cell walls and their taxonomic implications*. Bacteriol Rev, 1972. **36**(4): p. 407-77.
11. Buchanan, R.E., *Taxonomy*. Annu Rev Microbiol, 1955. **9**: p. 1-20.
12. Leboffe, M.J. and B.E. Pierce, *Microbiology Laboratory Theory and Application: Brief*. 2010: Morton Publishing Company.
13. L.Patrick, G., ed. *An Introduction to Medicinal Chemistry* 1995, Oxford University Press.
14. Newman, D.J. and G.M. Cragg, *Natural products as sources of new drugs over the 30 years from 1981 to 2010*. J Nat Prod, 2012. **75**(3): p. 311-35.
15. Hair, P.I. and S.J. Keam, *Daptomycin: a review of its use in the management of complicated skin and soft-tissue infections and Staphylococcus aureus bacteraemia*. Drugs, 2007. **67**(10): p. 1483-512.
16. Zappia, G., et al., *The contribution of oxazolidinone frame to the biological activity of pharmaceutical drugs and natural products*. Mini Rev Med Chem, 2007. **7**(4): p. 389-409.
17. Butler, M.S. and A.D. Buss, *Natural products--the future scaffolds for novel antibiotics?* Biochem Pharmacol, 2006. **71**(7): p. 919-29.
18. Powers, J.H., *Antimicrobial drug development--the past, the present, and the future*. Clin Microbiol Infect, 2004. **10 Suppl 4**: p. 23-31.
19. Coates, A., et al., *The future challenges facing the development of new antimicrobial drugs*. Nat Rev Drug Discov, 2002. **1**(11): p. 895-910.
20. Coates, A.R., G. Halls, and Y. Hu, *Novel classes of antibiotics or more of the same?* Br J Pharmacol, 2011. **163**(1): p. 184-94.

21. Fischbach, M.A. and C.T. Walsh, *Antibiotics for emerging pathogens*. Science, 2009. **325**(5944): p. 1089-93.
22. McManus, M.C., *Mechanisms of bacterial resistance to antimicrobial agents*. Am J Health Syst Pharm, 1997. **54**(12): p. 1420-33; quiz 1444-6.
23. Neu, H.C., *The crisis in antibiotic resistance*. Science, 1992. **257**(5073): p. 1064-73.
24. Tenover, F.C., *Mechanisms of antimicrobial resistance in bacteria*. Am J Infect Control, 2006. **34**(5 Suppl 1): p. S3-10; discussion S64-73.
25. Drlica, K. and X. Zhao, *DNA gyrase, topoisomerase IV, and the 4-quinolones*. Microbiol Mol Biol Rev, 1997. **61**(3): p. 377-92.
26. Campbell, E.A., et al., *Structural mechanism for rifampicin inhibition of bacterial rna polymerase*. Cell, 2001. **104**(6): p. 901-12.
27. Calvori, C., et al., *Effect of rifamycin on protein synthesis*. Nature, 1965. **207**(995): p. 417-8.
28. Yao, J., Moellering, R.J. , ed. *Antibacterial agents*. 8th Edition ed. Manual of Clinical Microbiology ed. E.J.B. P.R. Murray, J.H. Jorgensen, M.A. Pfaller, R.H. Tenover (Eds.). 2003, ASM Press: Washington, DC. 1039-1073.
29. Petri, W.A.J., ed. *Antimicrobial agents: sulfonamides, trimethoprim-sulfamethoxazole, quinolones, and agents for urinary tract infections*. 11th Edition ed. Goodman & Gilman's The Pharmacological Basis of Therapeutics, ed. J.S.L. L.L. Brunton, K.L. Parker (Eds.). 2006, McGraw-Hill: New York 1111–1126.

30. Storm, D.R., K.S. Rosenthal, and P.E. Swanson, *Polymyxin and related peptide antibiotics*. Annu Rev Biochem, 1977. **46**: p. 723-63.
31. Carpenter, C.F. and H.F. Chambers, *Daptomycin: another novel agent for treating infections due to drug-resistant gram-positive pathogens*. Clinical infectious diseases, 2004. **38**(7): p. 994-1000.
32. Noguchi, J.K. and M.A. Gill, *Sulbactam: a beta-lactamase inhibitor*. Clin Pharm, 1988. **7**(1): p. 37-51.
33. Fisher, J., et al., *Beta-lactamase inactivation by mechanism-based reagents*. Philos Trans R Soc Lond B Biol Sci, 1980. **289**(1036): p. 309-19.
34. Neu, H.C. and K.P. Fu, *Clavulanic acid, a novel inhibitor of beta-lactamases*. Antimicrob Agents Chemother, 1978. **14**(5): p. 650-5.
35. Rivera, M.J., et al., *Aminoglycoside-phosphotransferases APH(3')-IV and APH(3'') synthesized by a strain of Campylobacter coli*. J Antimicrob Chemother, 1986. **18**(2): p. 153-8.
36. Phillips, I. and K. Shannon, *Aminoglycoside resistance*. Br Med Bull, 1984. **40**(1): p. 28-35.
37. Davies, J. and D.I. Smith, *Plasmid-determined resistance to antimicrobial agents*. Annu Rev Microbiol, 1978. **32**: p. 469-518.
38. Courvalin, P. and J. Davies, *Plasmid-mediated aminoglycoside phosphotransferase of broad substrate range that phosphorylates amikacin*. Antimicrob Agents Chemother, 1977. **11**(4): p. 619-24.

39. Smith, M.D. and M.C. Kelsey, *Demonstration of a functional variant of chloramphenicol acetyltransferase in Haemophilus influenzae*. J Med Microbiol, 1989. **29**(4): p. 263-8.
40. Leslie, A.G., P.C. Moody, and W.V. Shaw, *Structure of chloramphenicol acetyltransferase at 1.75-A resolution*. Proc Natl Acad Sci U S A, 1988. **85**(12): p. 4133-7.
41. Shaw, W.V., D.W. Bentley, and L. Sands, *Mechanism of Chloramphenicol Resistance in Staphylococcus epidermidis*. J Bacteriol, 1970. **104**(3): p. 1095-105.
42. Courvalin, P., *Vancomycin resistance in gram-positive cocci*. Clinical infectious diseases, 2006. **42 Suppl 1**: p. S25-34.
43. Pootoolal, J., J. Neu, and G.D. Wright, *Glycopeptide antibiotic resistance*. Annu Rev Pharmacol Toxicol, 2002. **42**: p. 381-408.
44. Burns, J.L., D.M. Lien, and L.A. Hedin, *Isolation and characterization of dihydrofolate reductase from trimethoprim-susceptible and trimethoprim-resistant Pseudomonas cepacia*. Antimicrob Agents Chemother, 1989. **33**(8): p. 1247-51.
45. Wylie, B.A., et al., *Identification of a novel plasmid-encoded dihydrofolate reductase mediating high-level resistance to trimethoprim*. J Antimicrob Chemother, 1988. **22**(4): p. 429-35.
46. Flensburg, J. and O. Skold, *Massive overproduction of dihydrofolate reductase in bacteria as a response to the use of trimethoprim*. Eur J Biochem, 1987. **162**(3): p. 473-6.

47. Young, H.K. and S.G. Amyes, *A new mechanism of plasmid trimethoprim resistance. Characterization of an inducible dihydrofolate reductase*. J Biol Chem, 1986. **261**(6): p. 2503-5.
48. Then, R.L., *Mechanisms of resistance to trimethoprim, the sulfonamides, and trimethoprim-sulfamethoxazole*. Rev Infect Dis, 1982. **4**(2): p. 261-9.
49. Ahmad, M.H., A. Rechenmacher, and A. Bock, *Interaction between aminoglycoside uptake and ribosomal resistance mutations*. Antimicrob Agents Chemother, 1980. **18**(5): p. 798-806.
50. Davis, B.D., *Mechanism of bactericidal action of aminoglycosides*. Microbiol Rev, 1987. **51**(3): p. 341-50.
51. Smith, J.T. and S.G. Amyes, *Bacterial resistance to antifolate chemotherapeutic agents mediated by plasmids*. Br Med Bull, 1984. **40**(1): p. 42-6.
52. Courvalin, P., H. Ounissi, and M. Arthur, *Multiplicity of macrolide-lincosamide-streptogramin antibiotic resistance determinants*. J Antimicrob Chemother, 1985. **16 Suppl A**: p. 91-100.
53. Weisblum, B., *Inducible resistance to macrolides, lincosamides and streptogramin type B antibiotics: the resistance phenotype, its biological diversity, and structural elements that regulate expression--a review*. J Antimicrob Chemother, 1985. **16 Suppl A**: p. 63-90.
54. Speer, B.S. and A.A. Salyers, *Novel aerobic tetracycline resistance gene that chemically modifies tetracycline*. J Bacteriol, 1989. **171**(1): p. 148-53.

55. Park, B.H. and S.B. Levy, *The cryptic tetracycline resistance determinant on Tn4400 mediates tetracycline degradation as well as tetracycline efflux.* Antimicrob Agents Chemother, 1988. **32**(12): p. 1797-800.
56. Speer, B.S. and A.A. Salyers, *Characterization of a novel tetracycline resistance that functions only in aerobically grown Escherichia coli.* J Bacteriol, 1988. **170**(4): p. 1423-9.
57. Nikaido, H., *Multidrug resistance in bacteria.* Annu Rev Biochem, 2009. **78**: p. 119-46.
58. Pitout, J.D. and K.B. Laupland, *Extended-spectrum beta-lactamase-producing Enterobacteriaceae: an emerging public-health concern.* Lancet Infect Dis, 2008. **8**(3): p. 159-66.
59. Bonomo, R.A. and D. Szabo, *Mechanisms of multidrug resistance in Acinetobacter species and Pseudomonas aeruginosa.* Clinical infectious diseases, 2006. **43 Suppl 2**: p. S49-56.
60. McGowan, J.E., Jr., *Resistance in nonfermenting gram-negative bacteria: multidrug resistance to the maximum.* Am J Med, 2006. **119**(6 Suppl 1): p. S29-36; discussion S62-70.
61. Waxman, D.J. and J.L. Strominger, *Penicillin-binding proteins and the mechanism of action of beta-lactam antibiotics.* Annu Rev Biochem, 1983. **52**: p. 825-69.
62. Ghuysen, J.M., *Serine beta-lactamases and penicillin-binding proteins.* Annu Rev Microbiol, 1991. **45**: p. 37-67.

63. Goffin, C. and J.M. Ghuysen, *Multimodular penicillin-binding proteins: an enigmatic family of orthologs and paralog*s. Microbiol Mol Biol Rev, 1998. **62**(4): p. 1079-93.
64. Holtje, J.V., *Growth of the stress-bearing and shape-maintaining murein sacculus of Escherichia coli*. Microbiol Mol Biol Rev, 1998. **62**(1): p. 181-203.
65. Frere, J.M., et al., *Occurrence of a serine residue in the penicillin-binding site of the exocellular DD-carboxy-peptidase-transpeptidase from Streptomyces R61*. FEBS Lett, 1976. **70**(1): p. 257-60.
66. Georgopapadakou, N., S. Hammarstrom, and J.L. Strominger, *Isolation of the penicillin-binding peptide from D-alanine carboxypeptidase of Bacillus subtilis*. Proc Natl Acad Sci U S A, 1977. **74**(3): p. 1009-12.
67. Tipper, D.J. and J.L. Strominger, *Mechanism of action of penicillins: a proposal based on their structural similarity to acyl-D-alanyl-D-alanine*. Proc Natl Acad Sci U S A, 1965. **54**(4): p. 1133-41.
68. Bradford, P.A., *Extended-spectrum beta-lactamases in the 21st century: characterization, epidemiology, and detection of this important resistance threat*. Clin Microbiol Rev, 2001. **14**(4): p. 933-51, table of contents.
69. Spratt, B.G., *Resistance to antibiotics mediated by target alterations*. Science, 1994. **264**(5157): p. 388-93.
70. Schramm, V.L., *Enzymatic transition states and transition state analog design*. Annu Rev Biochem, 1998. **67**: p. 693-720.
71. Radzicka, A. and R. Wolfenden, *Transition state and multisubstrate analog inhibitors*. Methods Enzymol, 1995. **249**: p. 284-312.

72. Poulos, T.L., et al., *Polypeptide halomethyl ketones bind to serine proteases as analogs of the tetrahedral intermediate. X-ray crystallographic comparison of lysine- and phenylalanine-polypeptide chloromethyl ketone-inhibited subtilisin*. J Biol Chem, 1976. **251**(4): p. 1097-103.
73. Schoellmann, G. and E. Shaw, *Direct evidence for the presence of histidine in the active center of chymotrypsin*. Biochemistry, 1963. **2**: p. 252-5.
74. Bachovchin, W.W., et al., *Nitrogen-15 NMR spectroscopy of the catalytic-triad histidine of a serine protease in peptide boronic acid inhibitor complexes*. Biochemistry, 1988. **27**(20): p. 7689-97.
75. Kettner, C.A. and A.B. Shenvi, *Inhibition of the serine proteases leukocyte elastase, pancreatic elastase, cathepsin G, and chymotrypsin by peptide boronic acids*. J Biol Chem, 1984. **259**(24): p. 15106-14.
76. Thompson, R.C., *Peptide aldehydes: potent inhibitors of serine and cysteine proteases*. Methods Enzymol, 1977. **46**: p. 220-5.
77. Dunlap, R.P., P.J. Stone, and R.H. Abeles, *Reversible, slow, tight-binding inhibition of human leukocyte elastase*. Biochem Biophys Res Commun, 1987. **145**(1): p. 509-13.
78. Imperiali, B. and R.H. Abeles, *Inhibition of serine proteases by peptidyl fluoromethyl ketones*. Biochemistry, 1986. **25**(13): p. 3760-7.
79. Ness, S., et al., *Structure-based design guides the improved efficacy of deacylation transition state analogue inhibitors of TEM-1 beta-Lactamase(,)*. Biochemistry, 2000. **39**(18): p. 5312-21.

80. Powers, R.A., et al., *The complexed structure and antimicrobial activity of a non-beta-lactam inhibitor of AmpC beta-lactamase*. Protein Sci, 1999. **8**(11): p. 2330-7.
81. Crompton, I.E., et al., *Beta-lactamase inhibitors. The inhibition of serine beta-lactamases by specific boronic acids*. Biochem J, 1988. **251**(2): p. 453-9.
82. Beesley, T., et al., *The inhibition of class C beta-lactamases by boronic acids*. Biochem J, 1983. **209**(1): p. 229-33.
83. Kiener, P.A. and S.G. Waley, *Reversible inhibitors of penicillinases*. Biochem J, 1978. **169**(1): p. 197-204.
84. Kaur, K., M.J. Lan, and R.F. Pratt, *Mechanism of inhibition of the class C beta-lactamase of Enterobacter cloacae P99 by cyclic acyl phosph(on)ates: rescue by return*. J Am Chem Soc, 2001. **123**(43): p. 10436-43.
85. Rahil, J. and R.F. Pratt, *Phosphonate monoester inhibitors of class A beta-lactamases*. Biochem J, 1991. **275 (Pt 3)**: p. 793-5.
86. Pratt, R.F., *Inhibition of a class C beta-lactamase by a specific phosphonate monoester*. Science, 1989. **246**(4932): p. 917-9.
87. Li, N., et al., *Structure-activity studies of the inhibition of serine beta-lactamases by phosphonate monoesters*. Bioorg Med Chem, 1997. **5**(9): p. 1783-8.
88. Pechenov, A., et al., *Potential transition state analogue inhibitors for the penicillin-binding proteins*. Biochemistry, 2003. **42**(2): p. 579-88.
89. Kluytmans, J. and M. Struelens, *Meticillin resistant Staphylococcus aureus in the hospital*. BMJ, 2009. **338**: p. b364.

90. Taubes, G., *The bacteria fight back*. Science, 2008. **321**(5887): p. 356-61.
91. O'Neill, A.J., *New antibacterial agents for treating infections caused by multi-drug resistant Gram-negative bacteria*. Expert Opin Investig Drugs, 2008. **17**(3): p. 297-302.
92. Dijkshoorn, L., A. Nemec, and H. Seifert, *An increasing threat in hospitals: multidrug-resistant Acinetobacter baumannii*. Nat Rev Microbiol, 2007. **5**(12): p. 939-51.
93. Klevens, R.M., et al., *Invasive methicillin-resistant Staphylococcus aureus infections in the United States*. JAMA, 2007. **298**(15): p. 1763-71.
94. Appelbaum, P.C., *Reduced glycopeptide susceptibility in methicillin-resistant Staphylococcus aureus (MRSA)*. Int J Antimicrob Agents, 2007. **30**(5): p. 398-408.
95. Barrett, C.T. and J.F. Barrett, *Antibacterials: are the new entries enough to deal with the emerging resistance problems?* Curr Opin Biotechnol, 2003. **14**(6): p. 621-6.
96. Baltz, R.H., *Daptomycin: mechanisms of action and resistance, and biosynthetic engineering*. Curr Opin Chem Biol, 2009. **13**(2): p. 144-51.
97. Abbanat, D., M. Macielag, and K. Bush, *Novel antibacterial agents for the treatment of serious Gram-positive infections*. Expert Opin Investig Drugs, 2003. **12**(3): p. 379-99.
98. Nicola, G., et al., *Crystal structure of Escherichia coli penicillin-binding protein 5 bound to a tripeptide boronic acid inhibitor: a role for Ser-110 in deacylation*. Biochemistry, 2005. **44**(23): p. 8207-17.

99. Duncan, K., et al., *(1-Aminoethyl)boronic acid: a novel inhibitor for Bacillus stearothermophilus alanine racemase and Salmonella typhimurium D-alanine:D-alanine ligase (ADP-forming)*. Biochemistry, 1989. **28**(8): p. 3541-9.
100. Matteson D.S., J.P.K., Sadhu K.M., *Synthesis and properties of pinanediol α -amido boronic esters*. Organometallics, 1984. **3**: p. 1284-1288.
101. Amiri, P., et al., *Benzamidomethaneboronic acid: synthesis and inhibition of chymotrypsin*. Arch Biochem Biophys, 1984. **234**(2): p. 531-6.
102. Venkatraman, S., et al., *Potent inhibitors of HCV-NS3 protease derived from boronic acids*. Bioorg Med Chem Lett, 2009. **19**(1): p. 180-3.
103. Martichonok, V. and J.B. Jones, *Cysteine proteases such as papain are not inhibited by substrate analogue peptidyl boronic acids*. Bioorg Med Chem, 1997. **5**(4): p. 679-84.
104. *Clinical and Laboratory Standards Institute. Performance Standards for Antimicrobial Susceptibility Testing TIS*. Vol. Vol 30. January 2010 Wayne, Pa. M100-S20.
105. Jamindar, D. and W.G. Gutheil, *A liquid chromatography-tandem mass spectrometry assay for Marfey's derivatives of L-Ala, D-Ala, and D-Ala-D-Ala: application to the in vivo confirmation of alanine racemase as the target of cycloserine in Escherichia coli*. Anal Biochem, 2010. **396**(1): p. 1-7.
106. Bhushan, R. and H. Bruckner, *Marfey's reagent for chiral amino acid analysis: a review*. Amino Acids, 2004. **27**(3-4): p. 231-47.

107. Adamson, J.G., et al., *Use of Marfey's reagent to quantitate racemization upon anchoring of amino acids to solid supports for peptide synthesis*. Anal Biochem, 1992. **202**(1): p. 210-4.
108. Lambert, M.P. and F.C. Neuhaus, *Mechanism of D-cycloserine action: alanine racemase from Escherichia coli W*. J Bacteriol, 1972. **110**(3): p. 978-87.
109. Bhushan, R. and H. Bruckner, *Use of Marfey's reagent and analogs for chiral amino acid analysis: assessment and applications to natural products and biological systems*. J Chromatogr B Analyt Technol Biomed Life Sci, 2011. **879**(29): p. 3148-61.
110. Matteson, D.S. and K.M. Sadhu, *Boronic ester homologation with 99% chiral selectivity and its use in syntheses of the insect pheromones (3S,4S)-4-methyl-3-heptanol and exo-brevicomin*. J Am Chem Soc, 1983. **105**: p. 2077-8.
111. Matteson, D.S., P.K. Jesthi, and K.M. Sadhu, *Synthesis and properties of pinanediol α -amido boronic esters*. Organometallics, 1984. **3**: p. 1284-8.
112. Pachon-Ibanez, M.E., et al., *Prevention of rifampicin resistance in Acinetobacter baumannii in an experimental pneumonia murine model, using rifampicin associated with imipenem or sulbactam*. J Antimicrob Chemother, 2006. **58**(3): p. 689-92.
113. Bjorkholm, B., et al., *Mutation frequency and biological cost of antibiotic resistance in Helicobacter pylori*. Proc Natl Acad Sci U S A, 2001. **98**(25): p. 14607-12.

114. Hanninen, M.L. and M. Hannula, *Spontaneous mutation frequency and emergence of ciprofloxacin resistance in Campylobacter jejuni and Campylobacter coli*. J Antimicrob Chemother, 2007. **60**(6): p. 1251-7.
115. Baquero, M.R., et al., *Polymorphic mutation frequencies in Escherichia coli: emergence of weak mutators in clinical isolates*. J Bacteriol, 2004. **186**(16): p. 5538-42.
116. Zygmunt, W.A., *REVERSAL OF d-CYCLOSERINE INHIBITION OF BACTERIAL GROWTH BY ALANINE*. J Bacteriol, 1962. **84**(1): p. 154-6.
117. Bondi, A., J. Kornblum, and C. Forte, *Inhibition of antibacterial activity of cycloserine by alpha-alanine*. Proc Soc Exp Biol Med, 1957. **96**(1): p. 270-2.
118. Tytgat, I., et al., *DD-ligases as a potential target for antibiotics: past, present and future*. Curr Med Chem, 2009. **16**(20): p. 2566-80.
119. Tannock, G.W., and G. Cook, *Enterococci as members of the intestinal microflora of humans*. The enterococci: pathogenesis, molecular biology, and antibiotic resistance, ed. I.M.S.G. (ed.). 2002, Washington, DC: ASM Press.
120. Arias, C.A. and B.E. Murray, *The rise of the Enterococcus: beyond vancomycin resistance*. Nat Rev Microbiol, 2012. **10**(4): p. 266-78.
121. Wang, J.L. and P.R. Hsueh, *Therapeutic options for infections due to vancomycin-resistant enterococci*. Expert Opin Pharmacother, 2009. **10**(5): p. 785-96.
122. Koomanachai, P., J.L. Crandon, and D.P. Nicolau, *Newer developments in the treatment of Gram-positive infections*. Expert Opin Pharmacother, 2009. **10**(17): p. 2829-43.

123. Rivera, A.M. and H.W. Boucher, *Current concepts in antimicrobial therapy against select gram-positive organisms: methicillin-resistant Staphylococcus aureus, penicillin-resistant pneumococci, and vancomycin-resistant enterococci*. Mayo Clin Proc, 2011. **86**(12): p. 1230-43.
124. Wang, J.L. and P.R. Hsueh, *Therapeutic options for infections due to vancomycin-resistant enterococci*. Expert opinion on pharmacotherapy, 2009. **10**(5): p. 785-96.
125. Schleifer, K.H. and O. Kandler, *Peptidoglycan types of bacterial cell walls and their taxonomic implications*. Bacteriol Rev, 1972. **36**: p. 407-77.
126. Vollmer, W., D. Blanot, and M.A. de Pedro, *Peptidoglycan structure and architecture*. FEMS Microbiol Rev, 2008. **32**(2): p. 149-67.
127. Bouhss, A., et al., *The biosynthesis of peptidoglycan lipid-linked intermediates*. FEMS Microbiol Rev, 2008. **32**(2): p. 208-33.
128. van Heijenoort, J., *Lipid intermediates in the biosynthesis of bacterial peptidoglycan*. Microbiol Mol Biol Rev, 2007. **71**(4): p. 620-35.
129. van Heijenoort, J., *Recent advances in the formation of the bacterial peptidoglycan monomer unit*. Nat Prod Rep, 2001. **18**(5): p. 503-19.
130. Sauvage, E., et al., *The penicillin-binding proteins: structure and role in peptidoglycan biosynthesis*. FEMS Microbiol Rev, 2008. **32**(2): p. 234-58.
131. Barreteau, H., et al., *Cytoplasmic steps of peptidoglycan biosynthesis*. FEMS Microbiol Rev, 2008. **32**(2): p. 168-207.
132. van Heijenoort, J., *Formation of the glycan chains in the synthesis of bacterial peptidoglycan*. Glycobiology, 2001. **11**(3): p. 25R-36R.

133. Nieto, M. and H.R. Perkins, *Physicochemical properties of vancomycin and iodovancomycin and their complexes with diacetyl-L-lysyl-D-alanyl-D-alanine*. Biochem J, 1971. **123**(5): p. 773-87.
134. Barna, J.C. and D.H. Williams, *The structure and mode of action of glycopeptide antibiotics of the vancomycin group*. Annu Rev Microbiol, 1984. **38**: p. 339-57.
135. Healy, V.L., et al., *Vancomycin resistance in enterococci: reprogramming of the D-ala-D-Ala ligases in bacterial peptidoglycan biosynthesis*. Chem Biol, 2000. **7**(5): p. R109-19.
136. Mainardi, J.L., et al., *Evolution of peptidoglycan biosynthesis under the selective pressure of antibiotics in Gram-positive bacteria*. FEMS Microbiol Rev, 2008. **32**(2): p. 386-408.
137. Park, I.S., C.H. Lin, and C.T. Walsh, *Gain of D-alanyl-D-lactate or D-lactyl-D-alanine synthetase activities in three active-site mutants of the Escherichia coli D-alanyl-D-alanine ligase B*. Biochemistry, 1996. **35**(32): p. 10464-71.
138. Park, I.S. and C.T. Walsh, *D-Alanyl-D-lactate and D-alanyl-D-alanine synthesis by D-alanyl-D-alanine ligase from vancomycin-resistant Leuconostoc mesenteroides. Effects of a phenylalanine 261 to tyrosine mutation*. J Biol Chem, 1997. **272**(14): p. 9210-4.
139. Marfey, P., *Determination of D-amino acids. II. Use of a bifunctional reagent, 1,5-difluoro-2,4-dinitrobenzene*. Calsberg Res Commun, 1984. **49**: p. 591-6.
140. Jamindar, D. and W.G. Gutheil, *A liquid chromatography-tandem mass spectrometry assay for Marfey's derivatives of L-Ala, D-Ala, and D-Ala-D-Ala:*

- application to the in vivo confirmation of alanine racemase as the target of cycloserine in Escherichia coli*. Analytical biochemistry, 2010. **396**(1): p. 1-7.
141. Putty, S., et al., *Characterization of d-boroAla as a novel broad-spectrum antibacterial agent targeting d-Ala-d-Ala ligase*. Chemical biology & drug design, 2011. **78**(5): p. 757-63.
 142. *Food and Drug Administration Center for Drug Evaluation and Research (CDER) Guidance for Industry: Bioanalytical Method Validation*, D.o.H.a.H. Services, Editor. 2001: US.
 143. Bansal, S. and A. DeStefano, *Key elements of bioanalytical method validation for small molecules*. The AAPS journal, 2007. **9**(1): p. E109-14.
 144. Baptista, M., et al., *Specificity of induction of glycopeptide resistance genes in Enterococcus faecalis*. Antimicrob Agents Chemother, 1996. **40**(10): p. 2291-5.
 145. Courvalin, P., *Vancomycin resistance in gram-positive cocci*. Clin Infect Dis, 2006. **42 Suppl 1**: p. S25-34.
 146. Bobba, S., G.E. Resch, and W.G. Gutheil, *A liquid chromatography-tandem mass spectrometry assay for detection and quantitation of the dipeptide Gly-Gln in rat brain*. Analytical biochemistry, 2012. **425**(2): p. 145-50.
 147. Bodanszky, M., *In search of new methods in peptide synthesis. A review of the last three decades*. Int J Pept Protein Res, 1985. **25**(5): p. 449-74.
 148. Bodanszky, M., *Peptide chemistry: A practical textbook*. Second, revised ed. 1993, Berlin, Heidelberg: Springer-Verlag. 217.

149. Bodanszky, M. and A. Bodanzsky, *The practice of peptide synthesis*. Second, revised ed. 1994, Berlin, Heidelberg: Springer-Verlag. 217.
150. Merrifield, R.B., *Solid phase peptide synthesis.1. Synthesis of a tetrapeptide*. J Am Chem Soc, 1963. **85**: p. 2149-2154.
151. Merrifield, R.B., *Solid-Phase Peptide Synthesis.3. An Improved Synthesis of Bradykinin*. Biochemistry, 1964. **14**: p. 1385-90.
152. Gutte, B. and R.B. Merrifield, *The total synthesis of an enzyme with ribonuclease A activity*. J Am Chem Soc, 1969. **91**(2): p. 501-2.
153. Gutte, B. and R.B. Merrifield, *The synthesis of ribonuclease A*. J Biol Chem, 1971. **246**(6): p. 1922-41.
154. Merrifield, R.B. and J.M. Stewart, *Automated peptide synthesis*. Nature, 1965. **207**(996): p. 522-3.
155. Merrifield, R.B., J.M. Stewart, and N. Jernberg, *Instrument for automated synthesis of peptides*. Anal Chem, 1966. **38**(13): p. 1905-14.
156. Czarnik, A.W., ed. *Solid-phase organic syntheses*. 2001, John Wiley & Sons, Inc.: New York.
157. Doherty-Kirby, A.L.a.G.A.L., ed. *Side-chain protecting groups*. in Solid-phase synthesis : a practical guide, ed. S.A. Kates and F. Albericio. 2000, Marcel Dekker: New York. 129-195.
158. Albericio, F., *Orthogonal protecting groups for N(alpha)-amino and C-terminal carboxyl functions in solid-phase peptide synthesis*. Biopolymers, 2000. **55**(2): p. 123-39.

159. Albericio, F.a.S.A.K., ed. *Coupling methods:Solid-phase formation of amide and ester bonds*. in Solid-phase synthesis : a practical guide, ed. S.A.K.a.F. Albericio. 2000, Marcel Dekker: New York. 275-330.
160. Lloyd-Williams, P.a.E.G., ed. *Solid-phase convergent approaches to the synthesis of native peptides and proteins*. in Solid-phase synthesis : a practical guide, ed. S.A.K.a.F. Albericio. 2000, Marcel Dekker: New York. 377-418.
161. Alsina, J., et al., *Backbone amide linker strategies for the solid-phase synthesis of C-terminal modified peptides*. Methods Mol Biol, 2005. **298**: p. 195-208.
162. Alsina, J. and F. Albericio, *Solid-phase synthesis of C-terminal modified peptides*. Biopolymers, 2003. **71**(4): p. 454-77.
163. Merrifield, R.B., *Solid-Phase Peptide Synthesis. 3. An Improved Synthesis of Bradykinin*. Biochemistry, 1964. **3**: p. 1385-90.
164. Carpino, L.A. and G.Y. Han, *9-Fluorenylmethoxycarbonyl function, a new base-sensitive amino-protecting group*. J Am Chem Soc, 1970. **92**(19): p. 5748-5749.
165. Carpino, L.A. and G.Y. Han, *9-Fluorenylmethoxycarbonyl amino-protecting group*. The Journal of Organic Chemistry, 1972. **37**(22): p. 3404-3409.
166. Atherton, E.a.R.C.S., ed. *Solid phase peptide synthesis : a practical approach. The Practical approach series*. ix ed. 1989, IRL Press at at Oxford University Press: Oxford, England 203.

167. Mitchell, A.R., et al., *Tert-butoxycarbonylaminoacyl-4-(oxymethyl)-phenylacetamidomethyl-resin, a more acid-resistant support for solid-phase peptide synthesis*. J Am Chem Soc, 1976. **98**(23): p. 7357-62.
168. Pietta, P.G.a.G.R.M., *Amide protection and amide supports in solid-phase peptide synthesis*. Chemical Communications, 1970: p. 650-651.
169. Matsueda, G.R. and J.M. Stewart, *A p-methylbenzhydrylamine resin for improved solid-phase synthesis of peptide amides*. Peptides, 1981. **2**(1): p. 45-50.
170. Wang, S.S., *p-alkoxybenzyl alcohol resin and p-alkoxybenzyloxycarbonylhydrazide resin for solid phase synthesis of protected peptide fragments*. J Am Chem Soc, 1973. **95**(4): p. 1328-33.
171. Rink, H., *Solid-phase synthesis of protected peptide fragments using a trialkoxy-diphenyl-methylester resin*. Tetrahedron Letters, 1987. **28**(33): p. 3787-3790.
172. Albericio, F., R. van Abel, and G. Barany, *Solid-phase synthesis of peptides with C-terminal asparagine or glutamine. An effective, mild procedure based on N alpha-fluorenylmethyloxycarbonyl (Fmoc) protection and side-chain anchoring to a tris(alkoxy)benzylamide (PAL) handle*. Int J Pept Protein Res, 1990. **35**(3): p. 284-6.
173. Forns, P.a.G.B.F., , , ed. *The solid support*. in Solid-phase synthesis : a practical guide., ed. S.A. Kates and F. Albericio. 2000, Marcel Dekker: New York. 1-77.

174. Blackburn, C., ed. *Solid supports for the synthesis of peptides and small molecules*. in *Solid-phase synthesis : a practical guide*, ed. S.A.K.a.F. Albericio. 2000, Marcel Dekker: New York. 197-273.
175. Barany, G.a.M., R. B., *In: E Gross, J Meiehnhofer, eds. Vol 2. The Peptides: Analysis, Synthesis, Biology: Special methods in Peptide Synthesis*. New York Academic Press, 1979: p. 1-284.
176. Albericio, F. and G. Barany, *An acid-labile anchoring linkage for solid-phase synthesis of C-terminal peptide amides under mild conditions*. *Int J Pept Protein Res*, 1987. **30**(2): p. 206-16.
177. Albericio, F. and G. Barany, *Improved approach for anchoring N alpha-9-fluorenylmethyloxycarbonylamino acids as p-alkoxybenzyl esters in solid-phase peptide synthesis*. *Int J Pept Protein Res*, 1985. **26**(1): p. 92-7.
178. Fields, G., Tian, Z. and Barany, G., *In: Ga Grant, Ed. Synthetic peptides. A User's Guide*. New York: WH Freeman, 1992: p. pp 77-183.
179. Barany, G., N. Kneib-Cordonier, and D.G. Mullen, *Solid-phase peptide synthesis: a silver anniversary report*. *Int J Pept Protein Res*, 1987. **30**(6): p. 705-39.
180. Songster, M.F. and G. Barany, *Handles for solid-phase peptide synthesis*. *Methods Enzymol*, 1997. **289**: p. 126-74.
181. Konig, W. and R. Geiger, *[A new method for synthesis of peptides: activation of the carboxyl group with dicyclohexylcarbodiimide using 1-hydroxybenzotriazoles as additives]*. *Chem Ber*, 1970. **103**(3): p. 788-98.

182. Carpino, L., Han, GY., *The 9-fluorenylmethoxycarbonyl amino-protecting group*. J Org Chem, 1972. **37**: p. 3404-3409.
183. Manning, M., E. Coy, and W.H. Sawyer, *Solid-phase synthesis of (4-threonine)-oxytocin. A more potent and specific oxytocic agent than oxytocin*. Biochemistry, 1970. **9**(20): p. 3925-30.
184. Barton, M.A., R.U. Lemieux, and J.Y. Savoie, *Solid-phase synthesis of selectively protected peptides for use as building units in the solid-phase synthesis of large molecules*. J Am Chem Soc, 1973. **95**(14): p. 4501-6.
185. Stewart, J.M.a.Y., J. D., *Solid Phase Peptide Synthesis. 2nd Edn. Rockford, Illinois*. Pierce Chemical Company, 1984.
186. Schlatter, J.M., Mazur, R. H. and Goodmoson, O., *Hydrogenation in solid phase peptide synthesis. I. Removal of product from resin*. Tetrahedron Lett, 1977. **18**(33): p. 2851-2852.
187. Tam, J.P., R.D. Dimarchi, and R.B. Merrifield, *Photolabile multi-detachable p-alkoxybenzyl alcohol resin supports for peptide fragment or semi-synthesis*. Int J Pept Protein Res, 1980. **16**(5): p. 412-25.
188. Rich, D.H. and S.K. Gurwara, *Preparation of a new o-nitrobenzyl resin for solid-phase synthesis of tert-butyloxycarbonyl-protected peptide acids*. J Am Chem Soc, 1975. **97**(6): p. 1575-9.
189. Blackburn, C. and S.A. Kates, *Solid-phase synthesis of cyclic homodetic peptides*. Methods Enzymol, 1997. **289**: p. 175-98.

190. Heavner, G.A., Doyle, D. L. and Riexinger, D., *Cleavage of peptides from benzhydrylamine resins using trifluoromethanesulfonic acid*. Tetrahedron Lett, 1985. **26**(38): p. 4583-4586.
191. Manning, M., *Synthesis by the Merrifield method of a protected nonapeptide amide with the amino acid sequence of oxytocin*. J Am Chem Soc, 1968. **90**(5): p. 1348-9.
192. Clark-Lewis, I., et al., *Automated chemical synthesis of a protein growth factor for hemopoietic cells, interleukin-3*. Science, 1986. **231**(4734): p. 134-9.
193. Siev, D.V. and J.E. Semple, *Novel hydrazino-carbonyl-amino-methylated polystyrene (HCAM) resin methodology for the synthesis of P1-aldehyde protease inhibitor candidates*. Org Lett, 2000. **2**(1): p. 19-22.
194. Ngu, K. and D.V. Patel, *Preparation of acid-labile resins with halide linkers and their utility in solid phase organic synthesis*. Tetrahedron Letters, 1997. **38**(6): p. 973-976.
195. Hsieh, H.P., Y.T. Wu, S.T. Chen, and K.T. Wang, , *Dihydropyran-2-carboxylic acid, a novel bifunctional linker for the solid-phase synthesis of peptides containing a C-terminal alcohol*. Chemical Communications, 1998. **6**: p. 649-650.
196. Letsinger, R.L.a.M.J.K., *Popcorn polymer as a support in multistep synthesis*. J Am Chem Soc, 1963(85): p. 3045-3046.
197. Felix, A.M. and R.B. Merrifield, *Azide solid phase peptide synthesis*. J Am Chem Soc, 1970. **92**(5): p. 1385-91.

198. Henkel, B., L.S. Zhang, and E. Bayer, , *Investigations on solid-phase peptide synthesis in N-to-C direction (inverse synthesis)*. Liebigs Annalen-Recueil, 1997. **10**: p. 2161-2168.
199. Johansson, A., et al., *An improved procedure for N- to C-directed (Inverse) solid-phase peptide synthesis*. J Comb Chem, 2000. **2**(5): p. 496-507.
200. Thieriet, N., F. Guibe, and F. Albericio, *Solid-phase peptide synthesis in the reverse (N --> C) direction*. Org Lett, 2000. **2**(13): p. 1815-7.
201. Rai, A. and W.G. Gutheil, *A Dde resin based strategy for inverse solid-phase synthesis of amino terminated peptides, peptide mimetics and protected peptide intermediates*. J Pept Sci, 2005. **11**(2): p. 69-73.
202. Sasubilli, R. and W.G. Gutheil, *General inverse solid-phase synthesis method for C-terminally modified peptide mimetics*. J Comb Chem, 2004. **6**(6): p. 911-5.
203. Gutheil, W.G. and Q. Xu, *N-to-C solid-phase peptide and peptide trifluoromethylketone synthesis using amino acid tert-butyl esters*. Chem Pharm Bull (Tokyo), 2002. **50**(5): p. 688-91.
204. Alsina, J., S.A. Kates, G. Barany, and F. Albericio, , *Backbone amide linker strategies for the solid-phase synthesis of C-terminal modified peptides*. Methods Mol Biol, 2005. **298**: p. 195-208.
205. Jensen, K.J., et al., *Backbone Amide Linker (BAL) Strategy for Solid-Phase Synthesis of C-Terminal-Modified and Cyclic Peptides^{1,2,3}*. J Am Chem Soc, 1998. **120**(22): p. 5441-5452.

206. Boas, U., et al., *The ortho backbone amide linker (o-BAL) is an easily prepared and highly acid-labile handle for solid-phase synthesis*. J Comb Chem, 2002. **4**(3): p. 223-8.
207. Alsina, J., et al., *Backbone Amide Linker (BAL) Strategy for N(alpha)-9-Fluorenylmethoxycarbonyl (Fmoc) Solid-Phase Synthesis of Unprotected Peptide p-Nitroanilides and Thioesters(1)*. J Org Chem, 1999. **64**(24): p. 8761-8769.
208. Bourne, G.T., W.D.F. Meutermans, and M.L. Smythe, *The development of solid phase protocols for a backbone amide linker and its application to the Boc-based assembly of linear peptides*. Tetrahedron Letters, 1999. **40**(40): p. 7271-7274.
209. Bourne, G.T., et al., *A Backbone Linker for BOC-Based Peptide Synthesis and On-Resin Cyclization: Synthesis of Stylostatin 1(,)*. J Org Chem, 1999. **64**(9): p. 3095-3101.
210. Gentilucci, L., A. Tolomelli, and F. Squassabia, *Peptides and peptidomimetics in medicine, surgery and biotechnology*. Curr Med Chem, 2006. **13**(20): p. 2449-66.
211. Rawat, D.S., et al., *Marine peptides and related compounds in clinical trial*. Anticancer Agents Med Chem, 2006. **6**(1): p. 33-40.
212. Simmons, T.L., et al., *Marine natural products as anticancer drugs*. Mol Cancer Ther, 2005. **4**(2): p. 333-42.
213. Banta, S., et al., *Engineering protein and peptide building blocks for nanotechnology*. J Nanosci Nanotechnol, 2007. **7**(2): p. 387-401.

214. Colombo, G., P. Soto, and E. Gazit, *Peptide self-assembly at the nanoscale: a challenging target for computational and experimental biotechnology*. Trends Biotechnol, 2007. **25**(5): p. 211-8.
215. Singh, Y., et al., *Synthetic Peptide templates for molecular recognition: recent advances and applications*. Chembiochem, 2006. **7**(9): p. 1298-314.
216. Storm, D.R., *Mechanism of bacitracin action: a specific lipid-peptide interaction*. Ann N Y Acad Sci, 1974. **235**(0): p. 387-98.
217. Toscano, W.A., Jr. and D.R. Storm, *Bacitracin*. Pharmacol Ther, 1982. **16**(2): p. 199-210.
218. Hendrick, E.B., E.H. Botterell, and P.H. Greey, *Acute staphylococcal septicaemia cured with systemic bacitracin*. Can Med Assoc J, 1952. **67**(6): p. 669-71.
219. Meleney, F.L., P. Shambaugh, and R.S. Millen, *Systemic bacitracin in the treatment of progressive bacterial synergistic gangrene*. Ann Surg, 1950. **131**(2): p. 129-44.
220. Yamada, T., et al., *Altered ribosomes in antibiotic-resistant mutants of Mycobacterium smegmatis*. Antimicrob Agents Chemother, 1976. **9**(5): p. 817-23.
221. DeMong, D.E. and R.M. Williams, *Asymmetric synthesis of (2S,3R)-capreomycin and the total synthesis of capreomycin IB*. J Am Chem Soc, 2003. **125**(28): p. 8561-5.

222. Hamann, M.T., et al., *Kahalalides: Bioactive Peptides from a Marine Mollusk Elysia rufescens and Its Algal Diet Bryopsis sp.(1)*. J Org Chem, 1996. **61**(19): p. 6594-6600.
223. Becerro, M.A., et al., *Chemical defenses of the sacoglossan mollusk Elysia rufescens and its host Alga bryopsis sp.* J Chem Ecol, 2001. **27**(11): p. 2287-99.
224. Bourel-Bonnet, L., et al., *Solid-phase total synthesis of kahalalide A and related analogues*. J Med Chem, 2005. **48**(5): p. 1330-5.
225. Wieland, T. and H. Faulstich, *Amatoxins, phallotoxins, phallolysin, and antamanide: the biologically active components of poisonous Amanita mushrooms*. CRC Crit Rev Biochem, 1978. **5**(3): p. 185-260.
226. Bushnell, D.A., P. Cramer, and R.D. Kornberg, *Structural basis of transcription: alpha-amanitin-RNA polymerase II cocrystal at 2.8 Å resolution*. Proc Natl Acad Sci U S A, 2002. **99**(3): p. 1218-22.
227. L.P., H., J. Am. chem. Soc., 1937. **59**: p. 96.
228. Brown, H.C. and Y. Okamoto, *Electrophilic Substituent Constants*. J Am Chem Soc, 1958. **80**(18): p. 4979-4987.

VITA

Sandeep Putty was born on August 31, 1982, in the town of Guntur, Andhra Pradesh, India. He completed his primary education from St. Ignatius English Medium School, Guntur in 1997. He completed his intermediate education from Wisdom Junior College, Guntur in 1999. He obtained his Bachelor of Pharmacy (Honors) degree from Birla Institute of Technology & Science, Pilani, India in 2003.

In spring 2004, he graduated with a M.S. in chemistry degree from Western Illinois University, Macomb. During his M.S. he worked under the guidance of Prof. Netkal Made Gowda on “Synthesis and characterization of zinc (II) iodide-phenothiazine complexes” and presented his work at various conferences.

Sandeep Putty joined University of Missouri-Kansas City in Fall-2005 in pursuit of an interdisciplinary doctorate degree in Pharmaceutical Sciences and Pharmacology. During his PhD program he worked under the guidance of Dr. William Gutheil on “Characterization of D-boroAla as a novel broad spectrum antibacterial agent” and “Modeling reactivity and linear free energy relationships in the design of solid-phase linkers”. He has authored/co-authored several peer reviewed research articles in reputed international journals.